ANS&A

eotechnical Centrifuge Technology

EARTHQUAKE-INDUCED LIQUEFACTION OF CONFINED SOIL ZONES: A CENTRIFUGE STUDY

FINAL TECHNICAL REPORT

By

R.S.Steedman and S.P.Gopal Madabhushi

9th December 1993

Principal Investigator	**Dr. R S Steedman**
Research Associate	**Dr. S P Gopal Madabhushi**
Contractor	**Andrew N Schofield and Associates Ltd. 9 Little St Mary's Lane, Cambridge**
Contract Number	**DAJA45-93-C-0029**
ANS&A Report Number	**26-04-R-05**
Monitoring Agency Number	**[redacted]**

United States Army

EUROPEAN RESEARCH OFFICE OF THE U.S.ARMY

Approved for Public Release; distribution unlimited

Andrew N Schofield & Associates Limited, 9 Little Saint Mary's Lane, Cambridge, CB2 1RR
Telephone (0223) 460555, Facsimile (0223) 460777
Reg. in England No. 1866438, VAT No. 393 15 7827

DISCLAIMER NOTICE

THIS DOCUMENT IS BEST QUALITY AVAILABLE. THE COPY FURNISHED TO DTIC CONTAINED A SIGNIFICANT NUMBER OF COLOR PAGES WHICH DO NOT REPRODUCE LEGIBLY ON BLACK AND WHITE MICROFICHE.

Synopsis

Reported here are data from four dynamic centrifuge tests conducted on model embankments with confined liquefiable soil layers. The model embankments were constructed with a steeper slope on one side to give a factor of safety similar to that of the down stream slope of an equivalent embankment with outward seepage. These liquefiable zones were inclined and were located on the steeper slope side of the model embankment.

In the first centrifuge test LEG-1 the liquefiable layer of sand was inclined but the excess pore pressures dissipated rapidly. There was some settlement of the crest and slipping of the down stream slope. In the subsequent centrifuge tests LEG-2 to LEG-4 the loose layer was confined by placing a thin impermeable rock flour layer at its interface with denser sections. In these tests the excess pore pressures were sustained for much longer time. The acceleration traces recorded on the down stream slope showed significant peak accelerations in one direction indicating slipping of this slope. Large suctions were recorded in the dense sections of the embankment and significant excess pore pressures were observed in the loose zone.

The post test profiles measured after the centrifuge tests clearly showed the slipping of the down stream slope. In all of the centrifuge tests the up stream slope was more or less intact. The origin of the slip almost always coincided with the top of the loose confined zone. Using the post test profiles the quantity of soil movement before and after the earthquake loading was estimated for each centrifuge test. By comparing these results for the first two centrifuge tests with similar geometry indicated that the presence of confined liquefiable zone may increase the quantity of soil movement. In the third and fourth tests the movement of soil was larger than the first test with unconfined loose zone but was smaller than in the second test.

EARTHQUAKE-INDUCED LIQUEFACTION OF CONFINED SOIL ZONES: A CENTRIFUGE STUDY

Contract Number: DAJA45-93-C-0029

ANS&A Reprot Number : 26-04-R-05

1.0 Introduction

Embankments constitute a significant portion of the civil engineering structures concerning with flood control and regulation of water. Construction of an embankment is carried out by compacting layers of soil excavated from close by borrow pits. The construction methods employed in the field may sometimes result in a small loose pocket to be present within a densely compacted embankment. If the water table is shallow, the embankment may be under saturated conditions. The seismic behaviour of such an embankment is a major concern especially when the failure of the embankment may lead to loss of human lives or damage important structures in the vicinity.

During an earthquake the saturated soil is subjected to a rapid cyclic shear stress variation. This leads to densification of an initially loose soil element causing the pore pressure to increase. If undrained conditions are assumed during the earthquake loading the increase in pore pressure is translated into a lowering of the effective stress. This results in liquefaction conditions when the excess pore pressure equals the total stress. Hence a loose layer of sand present in a saturated embankment may liquefy under the seismic loading and can result in the slipping of embankment slopes. In the first series of dynamic centrifuge tests reported by Steedman and Madabhushi (1992), the methods of construction of loose sections of sand within the model embankment were investigated. The loose sections were horizontal and were situated on the down stream side of the embankment. The results from these tests showed a lateral spreading of the embankment during the earthquake loading but did not reveal any distinct slip surface along the slopes.

In the present series of centrifuge tests the liquefiable loose section of the embankment was inclined and was situated on the down stream slope side of the embankment. A schematic diagram of the embankment is shown in Fig.1. In order to study the seismic behaviour of such an embankment we need to consider

1. Generation of excess pore pressures within the confined loose layer.

2. Retaining the excess pore pressures in the loose zone long enough without dissipation for the crest to react to the De Alembert's inertial forces induced by the earthquake.

2.0 Design of the embankment section

The following aspects were considered in designing the embankment section used in the present centrifuge models.

2.1 Selection of sands

The choice of sands and their initial stress states in Zones A, B and C shown in Fig.1 is very important. As explained earlier the sand in Zone B needs to be in an 'initially' loose state so that when it is subjected to earthquake loading it moves towards a denser state resulting in the generation of excess pore pressures. Also the magnitude of the excess pore pressures must be large enough so that it is equal to the total stress in this zone due to self weight and the overburden pressure due to sand in Zone A leading to a near zero effective stress.

The sand in Zones A and C must be in an 'initially' dense state so that the cyclic loading of the earthquake results in the dilatation of these zones. Suction pressures will be generated in these zones and the effective stress increases and the zones A and C will act as rigid blocks.

If both the conditions outlined above are satisfied the crest of the embankment will suffer a slipping and the liquefied zone B will offer a slip plane. In the present tests the Zone B soil will constitute of very fine Leighton Buzzard 100/170 sand. For Zones A and C coarse Leighton Buzzard 14/25 sand will be used.

2.2 Up Stream and Down Stream slopes

Many of the embankments encountered in the field which are used for retaining water will have a differential water head across them. In a centrifuge test same level of fluid is present on each side of the embankment. A steeper down stream slope was used to achieve a factor of safety for the down stream slope which would be similar to the factor of safety for an equivalent prototype embankment with a differential water head across its section. Such a prototype has a phreatic surface which may intersect the lower section of the down stream slope. The factor of safety of the down stream slope in the presence of outward seepage will be different from that of the up stream slope which will be subjected to inward seepage. The difference in the degree of strength mobilisation beneath the upstream and down stream slopes in the prototype is simulated by making the down stream slope steeper in the centrifuge models.

2.3 Parametric variation in different centrifuge tests

In figure 2 an embankment with a steeper downstream slope and a flatter up stream slope is shown. The down stream slope angle is given as α and the up stream slope is given as γ. The confined loose zone is inclined to the base at an angle β. In the four different centrifuge tests it is envisaged to vary these three slope angles. Further the thickness of the loose layer 'd' and its location in the embankment will be varied. The parameters that will be used in all the tests are listed below:

Table 1 Slope angles for model embankments in centrifuge tests LEG-1 to LEG-4

Test	Angle α	Angle β	Angle γ	Thickness d (mm)	Zone B confinement
LEG-1	35°	30°	20.8°	15.0	Unconfined
LEG-2	35°	30°	23.5°	20.0	Confined
LEG-3	35°	18.2°	23.5°	20.0	Confined
LEG-4	35°	10.3°	23.5°	10.0	Confined

3.0 Facilities

3.1 Cambridge Geotechnical Centrifuge Centre

The beam centrifuge at the Cambridge Geotechnical Centrifuge Centre has an effective radius of about 4.0 metres and a maximum testing gravity of 155 g and is a 150 g-ton machine. The centrifuge chamber has a diameter of 10 metres. The beam centrifuge was commissioned in 1975 and over 1100 model tests were carried out using this facility. The operation of the beam centrifuge has been described by Schofield (1980).

3.2 Bumpy Road Earthquake Actuator

The model earthquakes in the centrifuge tests conducted in this series were generated by the Bumpy Road Actuator. The details of the earthquake actuating system were described by Kutter (1982). The schematic diagram of the actuator is presented in Fig.4. A duraluminium box which holds the model embankment is suspended on a pair of flexible straps which enable the lateral movement during a model earthquake. There is a toothed rack fixed to the base of the strong box which engages with a counter part on the bumpy road actuator. A sinusoidal track on which 10 cycles are machined is fixed firmly to the wall of the centrifuge chamber. An earthquake can be triggered at the desired time by controlling the pressures across a double acting piston which makes a wheel on the actuator to come into contact with the sinusoidal track (see Fig.4). The radial movement of the wheel is translated into lateral movement of the base of strong box by a bell-crank mechanism. Since the earthquake actuator was put into operation in 1981 about 1400 earthquakes events have been recorded on a wide range of models.

3.3 Strong box

The model container is a strong and stiff box made of duraluminium. The inside dimensions of the box are 0.9 m × 0.48 m × 0.22 m and for an 80g centrifuge test these dimensions correspond to dimensions of a soil body of 72 m × 38.4 m × 19.6 m. The maximum pay load allowed for a dynamic test is just below 300 kg for a 80g test. This corresponds to a soil weight of about 100,000 tons in the prototype.

4.0 Instrumentation

4.1 Accelerometers (ACC)

In the centrifuge tests reported here miniature piezoelectric accelerometers manufactured by D.J.Birchall were used to measure the accelerations in the soil as well as the input acceleration of the strong box. The device has a resonant frequency of about 50 kHz and a maximum error of 5%. The weight of the transducer is about 20 grams. Fig.5a shows the dimensions of the accelerometer. The accelerometers embedded in the soil were sealed with silicone rubber.

The accelerometers were calibrated before each test by subjecting them to a saturated '2g' acceleration and measuring the output generated on a cathode ray oscilloscope. The calibration constant for each accelerometer was expressed in the units of 'V/g'.

4.2 Pore pressure transducers (PPT)

Pore pressures in the saturated soil were monitored by Druck PDCR 81 pore pressure transducers. This type of pore pressure transducers have a linear range up to 300 kPa and weigh about 10 grams. The corner frequency of the dynamic response of the transducer is 15 kHz. The maximum error is 0.2 %. In the centrifuge tests reported here, the active diaphragm of the PPT is covered with a porous brass stone. The dimensions of the PPT are presented in Fig.5b.

All the pore pressure transducers were calibrated by applying standard water pressures on the active diaphragm. The output generated by the device was measured using a digital voltmeter and calibration constant was obtained in the units of 'kPa/mV'.

5.0 Materials

5.1 Sand

Two grades of sand were used in the centrifuge tests reported here.

5.1.1 LB 14/25 sand

Leighton Buzzard 14/25 medium dense sand was used to construct the dense section of the embankment of all the centrifuge models. The nominal size of this sand is 0.89 mm. The specific gravity of the sand is 2.65 and the maximum and minimum void ratio's are 0.965 and 0.425 respectively. The maximum and minimum void ratio's were determined experimentally before the centrifuge models were constructed. This sand was supplied by D.J.Ball and Co., Colworth and was employed in many a centrifuge tests conducted in Cambridge.

5.1.2 LB 100/170 sand

Leighton Buzzard 100/170 medium dense sand was used to construct the loose section of the embankment of all the centrifuge models. The nominal size of this sand is 0.12 mm. The specific gravity of the sand is 2.65 and the maximum and minimum void ratio's are 1.025 and 0.585 respectively. The maximum and minimum void ratio's were determined experimentally before the entrifuge models were constructed This sand was also supplied by D.J.Ball and Co., Colworth and was employed in many a centrifuge tests conducted in Cambridge.

5.2 Silicone oil

The pore fluid used in all the centrifuge tests was silicone oil. The viscosity of this oil was 80 centiStokes in these centrifuge tests. A centrifuge model saturated with high viscosity pore fluid satisfies the dynamic time scale relationship and the consolidation time rate effects simultaneously.

6.0 Model Preparation and testing procedure

A standard procedure was adopted for the preparation of the model embankments and for conducting the centrifuge tests. As explained in section 2 the model embankment had a steeper down stream slope. Hence it was critical that the model preparation and especially the saturation of the model is carried out very carefully.

The model embankment was constructed in three stages. The first stage involved in the construction of the dense section shown as zone A in Fig.6. LB 14/25 coarse sand was rained from a sand hopper at a predetermined rate. Miniature accelerometers (ACC's) and pore pressure transducers (PPT's) were placed at the desired locations (see Plate

9.4). After the desired profile is achieved approximately both the up stream and down stream slopes were vacuum levelled to the exact profile (see Plate 9.1). In the case of the centrifuge tests LEG-2 to LEG-4 a thin, impermeable layer of rock flour was constructed on the down stream slope side after the end of zone A construction. (see Plate 9.2.)

The loose section indicated by zone B in Fig.6 is constructed by 'slumping' LB 100/170 sand from a plastic container. The slumping method places the sand in a very loose state. In Plate 9.3 a view of the loose zone deposited by this method is shown. After the desired profile is achieved the surface of this sand layer is vacuum levelled. In case of the centrifuge tests LEG-2 to LEG-4 a thin, impermeable layer of rock flour was constructed on the down stream slope side.

Finally the dense section constituting the crest of the embankment shown as zone C in Fig.6 is constructed by raining LB 14/25 sand. After the final profile of the embankment was achieved the model was vacuum levelled. The strong box is then covered with a lid and is subjected to a vacuum pressure of -30 cm of Mercury. After evacuating the model under this pressure for about 1 hour the blended silicone oil with a viscosity of 80 centiStokes is admitted at the base of the embankment and the saturation is carried out very slowly until the level of silicone oil coincided with the crest of the embankment. Care was exercised to see that the silicone oil level on both the slopes of the embankment are the same through out the saturation process. The whole process of saturation took about 15 hours for each model.

After the saturation was completed the centrifuge model was transported very carefully onto the centrifuge arm. Immediately after the loading procedure was complete the strong box was fixed using wooden wedges to make the centrifuge model level. Pre flight checks were completed at this stage. Just before starting up the centrifuge motor, the strong box was released to hang freely at the end of the arm.

The centrifuge acceleration was increased in steps of 20g, 40g, 60g and 80g. At each stage the pore pressures within the model were monitored using a DVM. After the testing acceleration of 80g was achieved at the centroid of the model the steady acceleration was maintained for 20 minutes before any earthquake was fired. The pore pressures were monitored again after the 20 minutes. An earthquake was fired and the data was plotted. The strength of the subsequent earthquakes was gradually increased. When the test was finished the centrifuge was showed down and stopped. The model was recovered from the pit carefully and the post test profile of the embankment was

measured. In Fig.7 the schematic diagram of the centrifuge model in flight is shown. The surface of the fluid is curved and the radius of curvature is about 3.875 m.

7.0 Presentation of the data

A new software package called 'Global Lab' supplied by Data Translation Inc., was used to digitise the data recorded on the two 14 channel Racal tape recorders. Also the faster A/D converter cards compatible with Global Lab software made it possible to acquire 16 channels of data in real time. Data from the important transducers was backed up by acquiring it in real time as well as recording it on the Racal tapes.

Several macros were developed with Global Lakes. It is possible to estimate the quantity of the soil movement resulting when the model embankment is subjected to the earthquake loading. In order to estimate the quantity of soil moved during the earthquakes, the difference of the embankment profiles before and after the earthquakes is plotted. This graph is presented in Fig.10.33. Using the numerical integration procedure given by Simpson's rule, the area under the curve shown in Fig.10.33 is estimated. Using this area the volume of the soil movement presented in the units of kPa and are shown with the transducer number. Each of these traces contains 1024 data points collected in a time of 200 ms giving a data point spacing of 1.95×10^{-4} seconds. The Nyquist frequency of the data is 2.56 kHz. However the data presented in the earlier report was processed using 2 smoothing passes to reduce the high frequency electrical noise in the signals. In the present data report the data is processed using a low pass Bessel filter. This filter was designed especially to match the filtering characteristics of the FLY14 smoothing passes. In Fig.8 the attenuation characteristics of the Bessel filter used in processing all of the present data are shown. These may be compared with the attenuation characteristics of the old 2 pass smoothing filter presented in Fig.9. Comparing these two figures it can be seen that the present test data is subjected to a very similar filtering as the data reported for the earlier centrifuge tests. This makes it possible to compare the results from these two test series without reprocessing the old data.

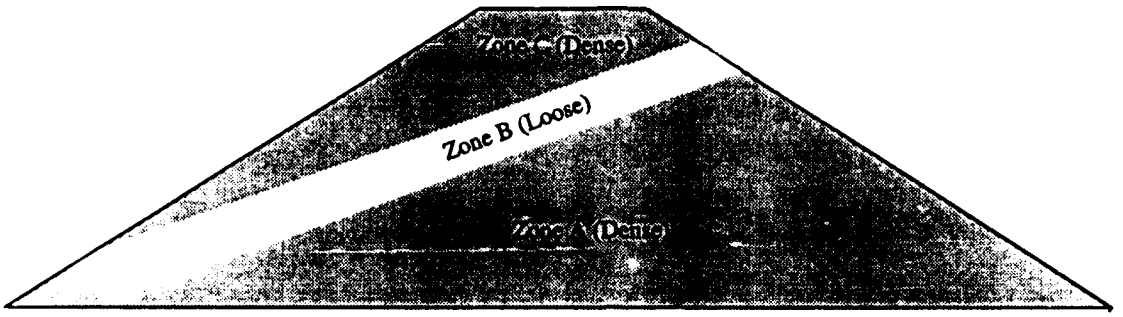

Fig.1 Embankment with a loose embedded zone

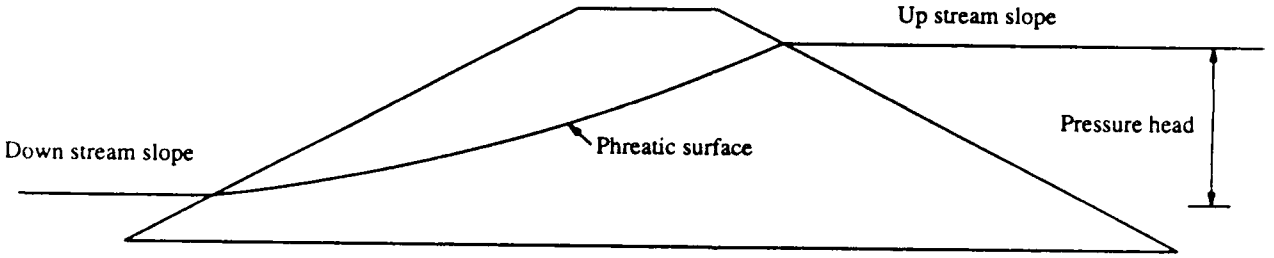

Fig.2 Water retaining embankment

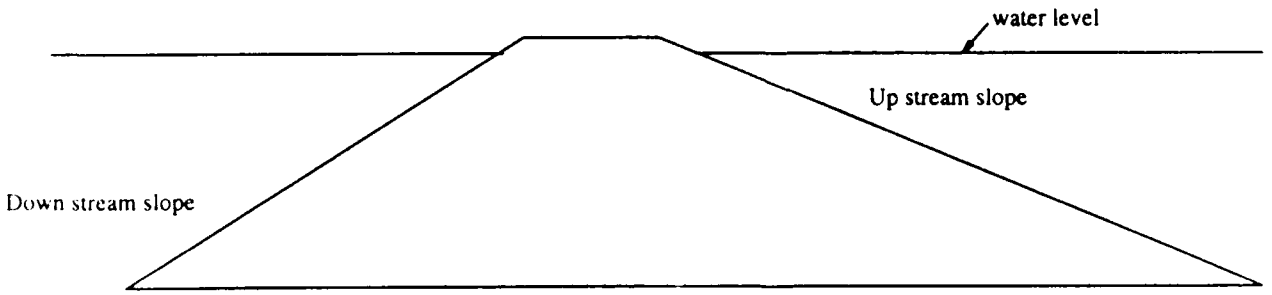

Fig.3 Centrifuge test with a steeper down stream slope

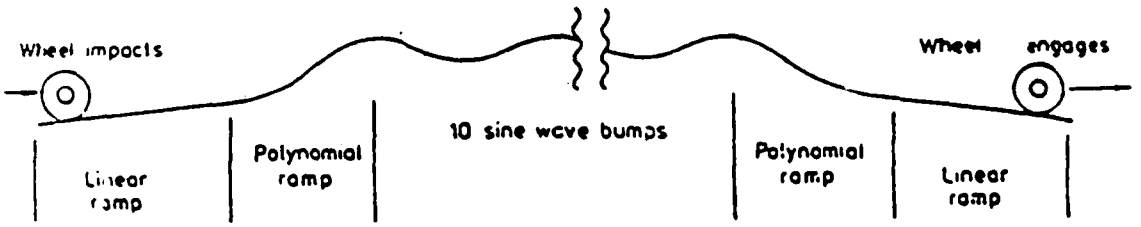

Schematic diagram showing the transitional curves before and after the sinusoidal wave track

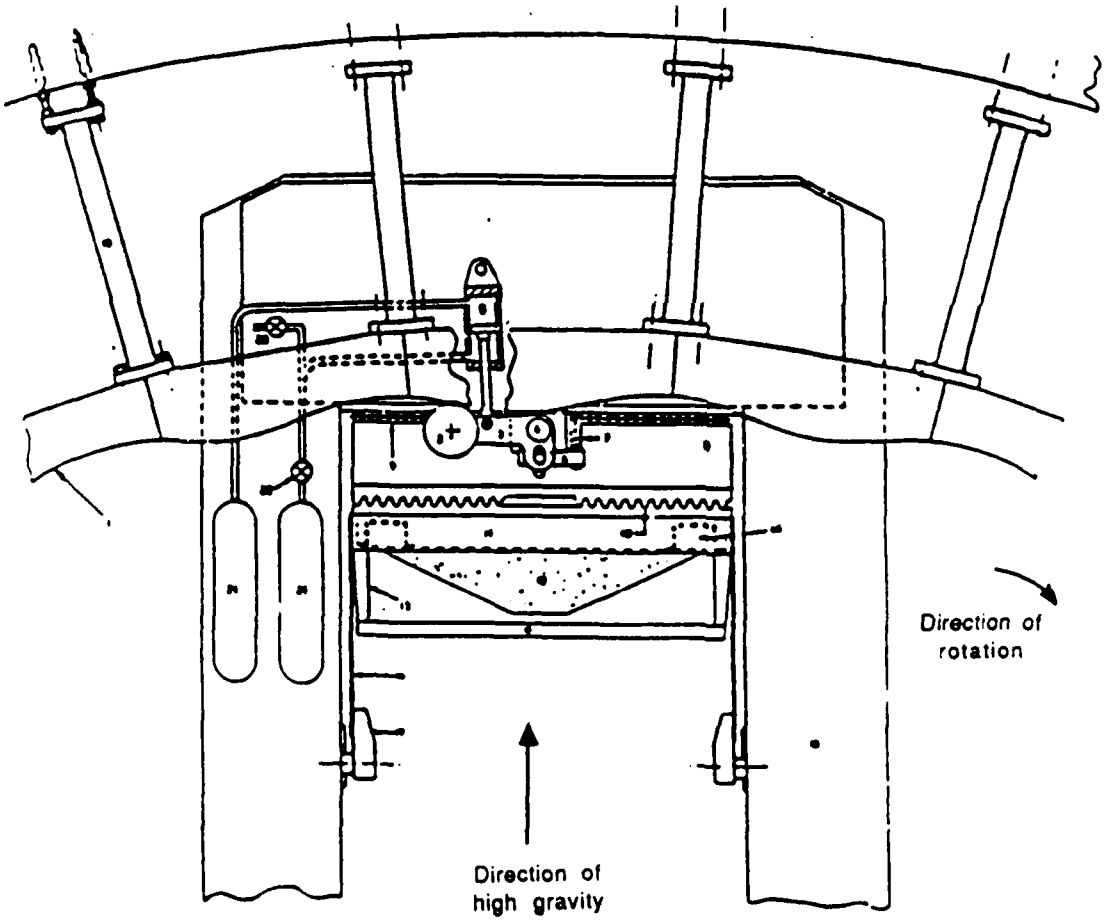

Fig.4 Schematic view of Bumpy road shaking system with the strong box in swung up position (after Kutter, 1982)

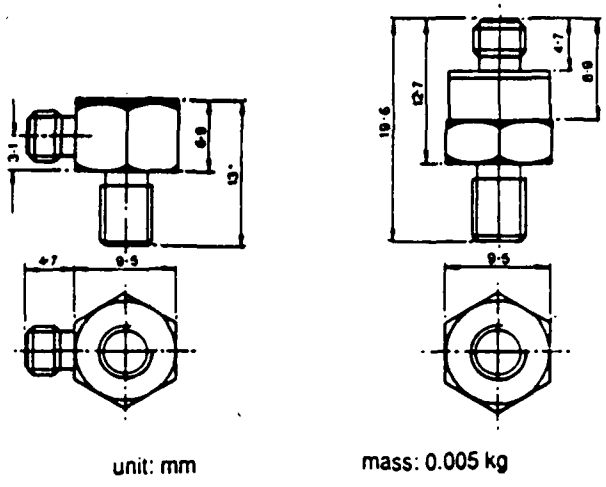

Fig.5a Typical dimensions of an accelerometer

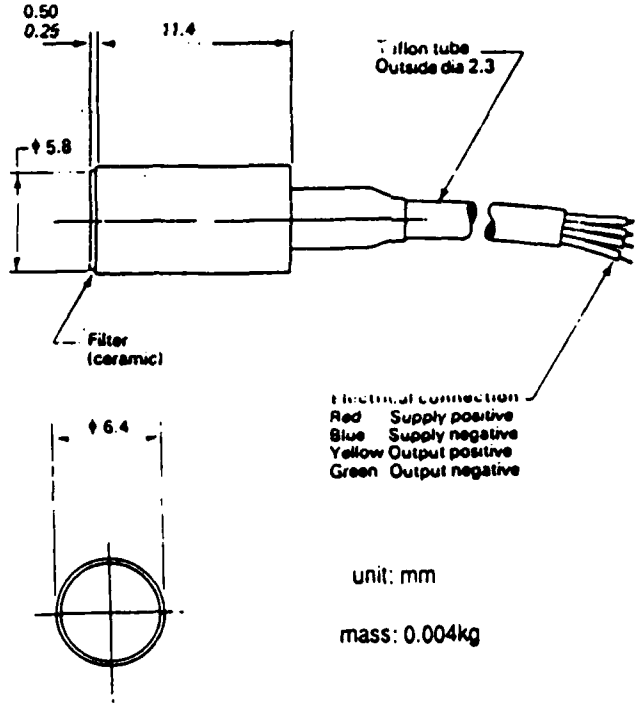

Fig.5b Typical dimensions of a pore pressure transducer

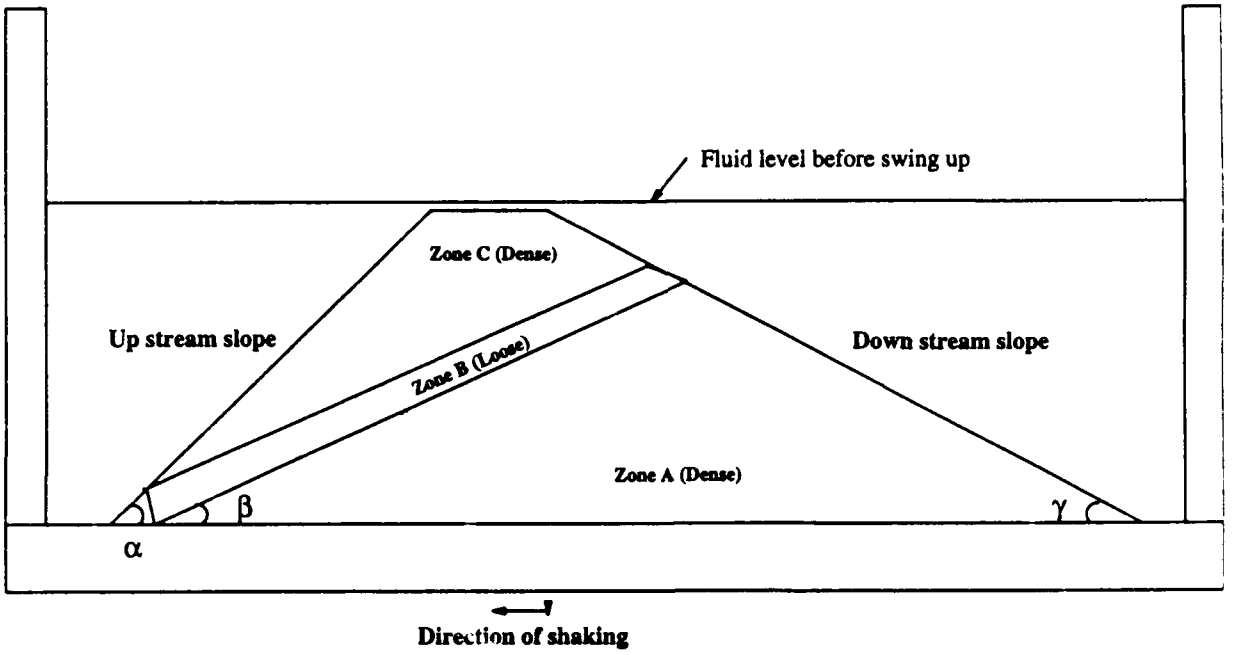

Fig.6 Schematic section showing the embankment before swing up

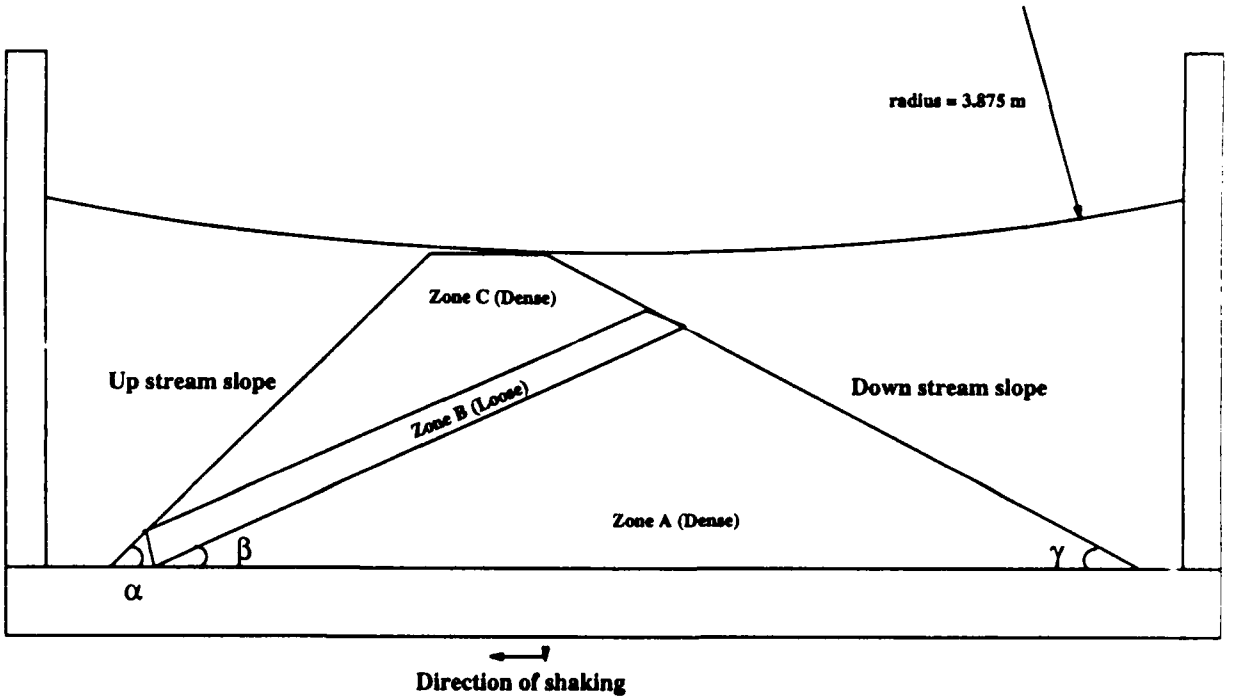

Fig.7 Schematic section showing the embankment during flight

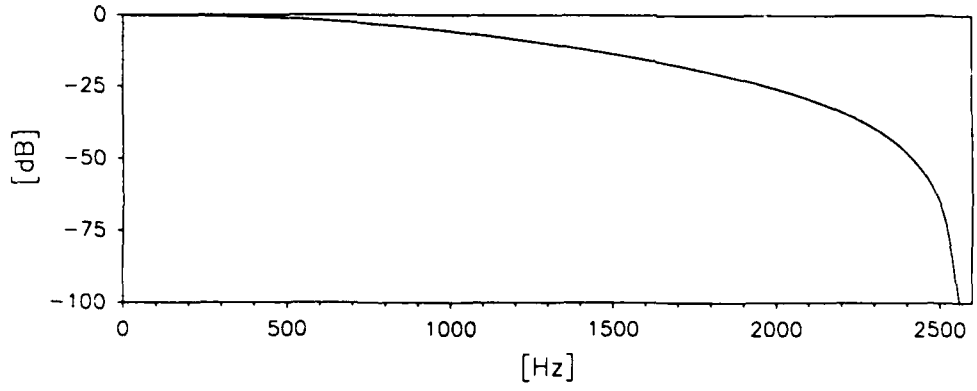

Fig.8 Attenuation characterstics of the new software filter

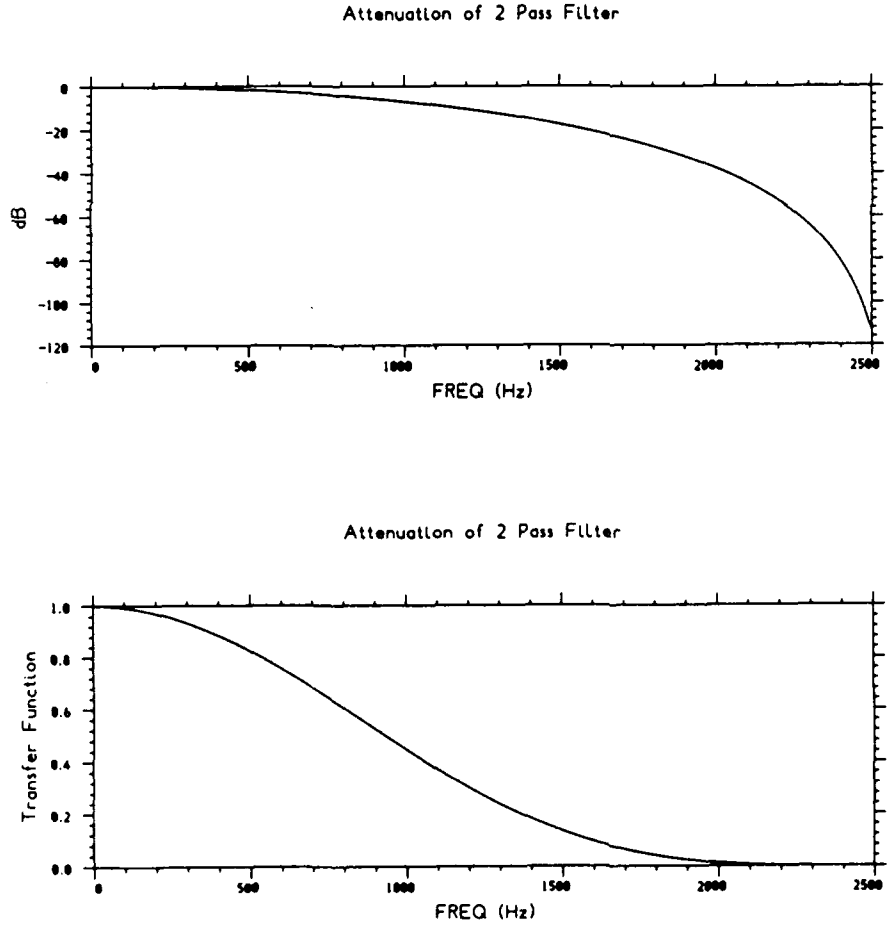

Fig.9 Attenuation characterstics of the old software filter

8.0 Centrifuge Test LEG-1

8.1 Configuration of the test

In the first centrifuge test LEG-1 the down stream slope was 35^{o} and the up stream slope was 21^{o} .The loose layer of sand was inclined at an angle of 30^{o} and had a thickness of 15 mm. The dense section of the embankment was constructed using coarse Leighton Buzzard 14/25 sand and the loose section of the embankment was constructed using fine Leighton Buzzard 100/170 sand as explained in section 6.0. The schematic diagram showing the cross section of the model is presented in Fig.8.1. The placement of transducers is shown in Fig.8.2.

8.2 Test Data

In this test the down stream slope suffered a slip resulting in the movement of the crest towards the down stream toe of the embankment. The slip surface was along the loose section of the sand as shown in Fig.8.1 (zone B). The dry densities of each of the zones in Fig.8.1 together with the void ratio and relative densities for this centrifuge model are presented in Table 8.1. The hydrostatic pore pressures recorded during the swing up of the centrifuge and increase of the centrifugal acceleration to 80g and after each earthquake are presented in Table 8.2. The data recorded during this test are presented in Figs.8.3 to 8.21. The accelerometer 1926 placed in the crest of the embankment registered strong acceleration in one direction suggesting the slipping of the crest in one direction. This is supported by the accelerometer traces 3457 and 3466 which are also in this region. ACC 3441 and 3466 have flat top peaks suggesting the slipping of the down stream slope. The traces recorded by the accelerometers in the up stream slope were more or less uniform suggesting no movement of this slope. The post test profile measured after the test confirmed this.

The pore pressure traces recorded in the crest section by PPT 3139 showed strong suctions. Similarly the pore pressures recorded in the lower dense section (shown in Fig.8.2) by PPT 5406 and 6266 showed strong suction pressures. This shows that the dense zones were dilating and under the suction pressures they would behave almost like rigid blocks. In the loose section there was small excess pore pressure which was dissipated rapidly. However during the model earthquake the loose section was the slip plane available for the down stream slope as there was no suction pressure in this zone

and it was at a relatively higher pore pressure than the other two zones. During this test the pore pressure transducer 6514 has floated partially as seen in Plate 8.1. Also accelerometer 3466 was exposed.

8.3 Post test profile

The post test profile measured after the centrifuge test is presented in Fig.8.22 together with the original profile of the embankment. The post test profile is measured at various longitudinal sections and the average profile is shown in this figure. Also the cross sectional profile is shown in Fig.8.23 which suggests that the slip is more or less uniform across the model embankment. From the post test profiles it can be clearly seen that there is a slip on the down stream slope side of the embankment. In Plate 8.2 a section of this centrifuge model during the post test investigation is presented. In this Plate the curvilinear shape of the initially straight loose sand layer may be observed. Also the sand from the crest region is deposited on the top of this layer. The up stream slope is relatively unchanged before and after the earthquakes. It is possible to estimate the quantity of the soil movement resulting when the model embankment is subjected to the earthquake loading. In order to estimate the quantity of soil moved during the earthquakes, the difference of the embankment profiles before and after the earthquakes is plotted. This graph is presented in Fig.8.24. Performing numerical integration using the Simpson's rule, the area under the curve shown in Fig.8.24 is estimated. Using this area the volume of the soil movement resulting from the earthquake loading is estimated. The quantity of soil which slipped from the crest of the embankment was 1.525×10^{-3} m^3 and the quantity of soil deposited at the toe of the embankment is 1.143×10^{-3} m^3. In prototype terms these quantities are 780.8 m^3 and 585.32 m^3 respectively. The differential volume which may indicate the error in measurement of the post test profile is 1.47 % of the total volume of the embankment.

Table 8.1 Dry density of sand in different zones of the embankment in centrifuge test LEG-1

Zone*	γ_d (kg/m^3)	void ratio (e)	Relative Density (%)
A	1749.36	0.515	83.3
B	1368.49	0.936	20.2
C	1780.00	0.490	87.9

* see Fig.8.1 for zone specification

Table 8.2 Hydrostatic pore pressures recorded in centrifuge test LEG-1

Device	kPa/V	20-G kPa	40-G kPa	60-G kPa	80-G kPa	EQ-1 kPa	EQ-2 kPa	EQ-3 kPa	EQ-4 kPa
PPT6266	440.55	20.12	39.78	61.26	84.43	83.72	83.28	83.06	83.11
PPT3139	379.53	3.61	7.85	12.18	17.20	18.45	19.14	19.63	20.08
PPT6260	365.81	2.19	4.48	6.78	9.33	9.12	8.93	8.79	8.71
PPT3965	-405.50	17.44	16.63	17.44	27.17	94.48	95.29	91.64	89.62
PPT6270	385.84	0.74	1.60	2.40	3.26	3.20	3.17	3.08	3.03
PPT6514	350.88	7.30	15.71	23.59	32.38	34.24	36.38	37.85	39.68
PPT6263	365.27	2.60	5.52	8.19	11.28	11.28	11.02	10.95	10.91
PPT2540	361.77	18.43	39.85	59.22	81.89	80.55	80.40	80.15	80.00
PPT5406	393.98	23.41	50.99	75.50	104.34	102.45	102.29	101.78	101.70

Plate 8.1 Pore pressure transducer 6514 suffered a floatation during the centrifuge test LEG-1

Plate 8.2 Section of centrifuge model LEG-1 during post test investigation note the curvilinear shape of the loose sand zone due to slipping of soil from the crest

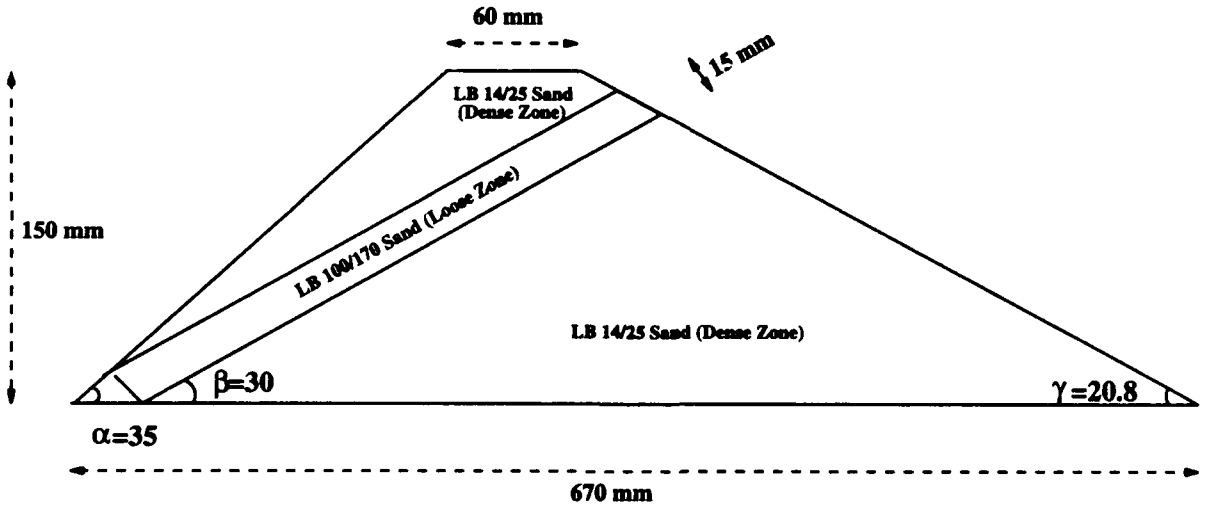

Fig.8.1 Cross section of the centrifuge model LEG-1

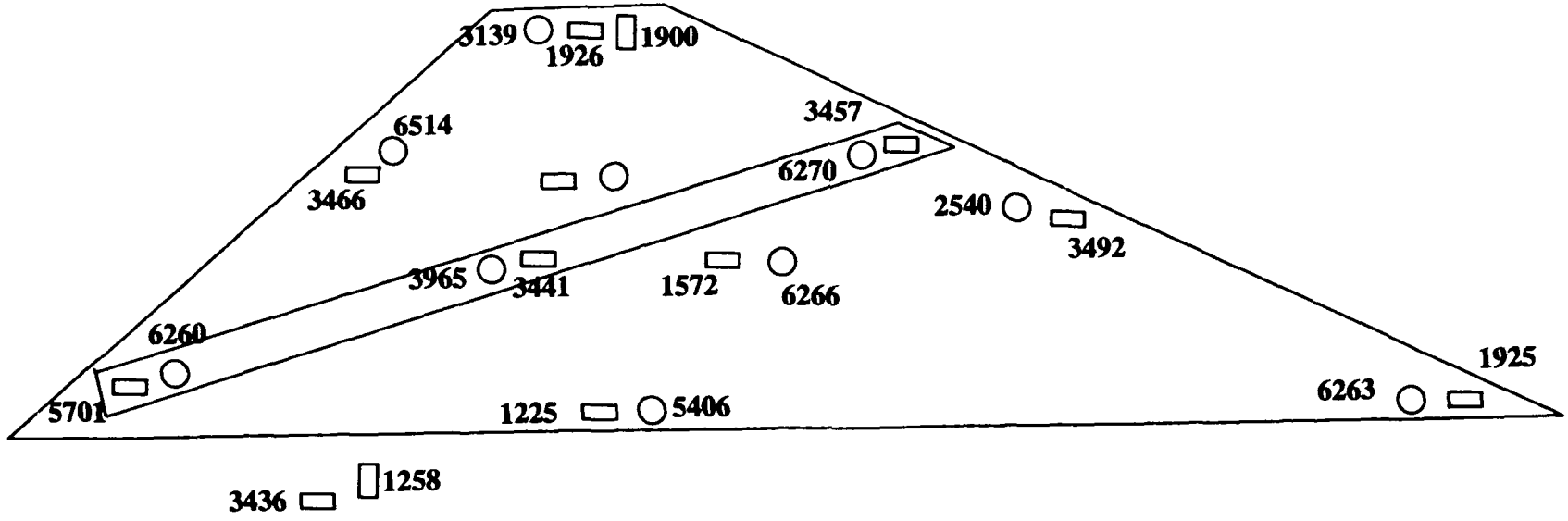

Fig.8.2 Placement of transducers in centrifuge test LEG-1

840 datapoints plotted per complete transducer record

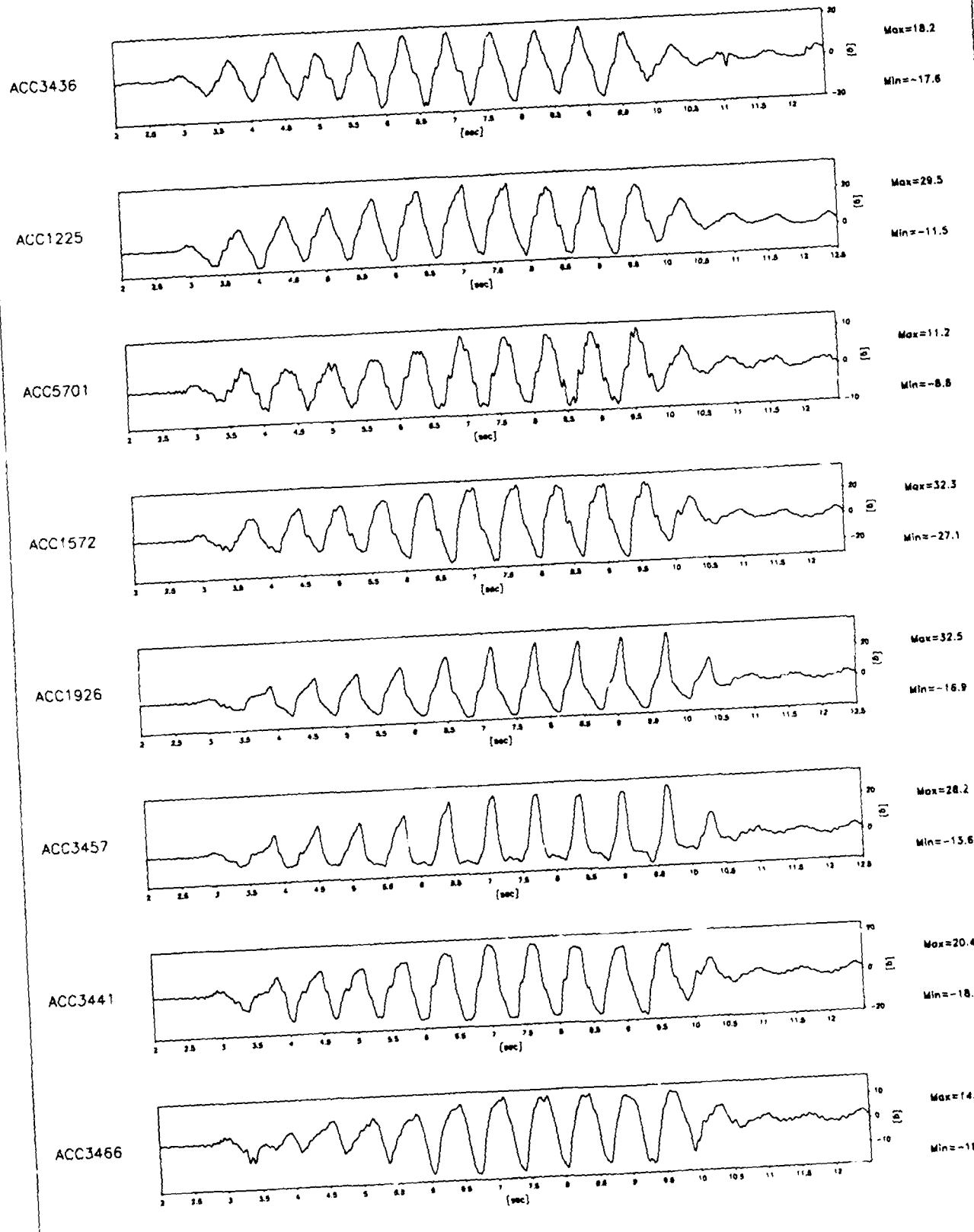

Scales : Prototype

TEST LEG-1 MODEL SAT FLIGHT -1	EQ-1	SHORT TERM TIME RECORDS	G Level 80	FIG.NO. **8.3**

840 datapoints plotted per complete transducer record

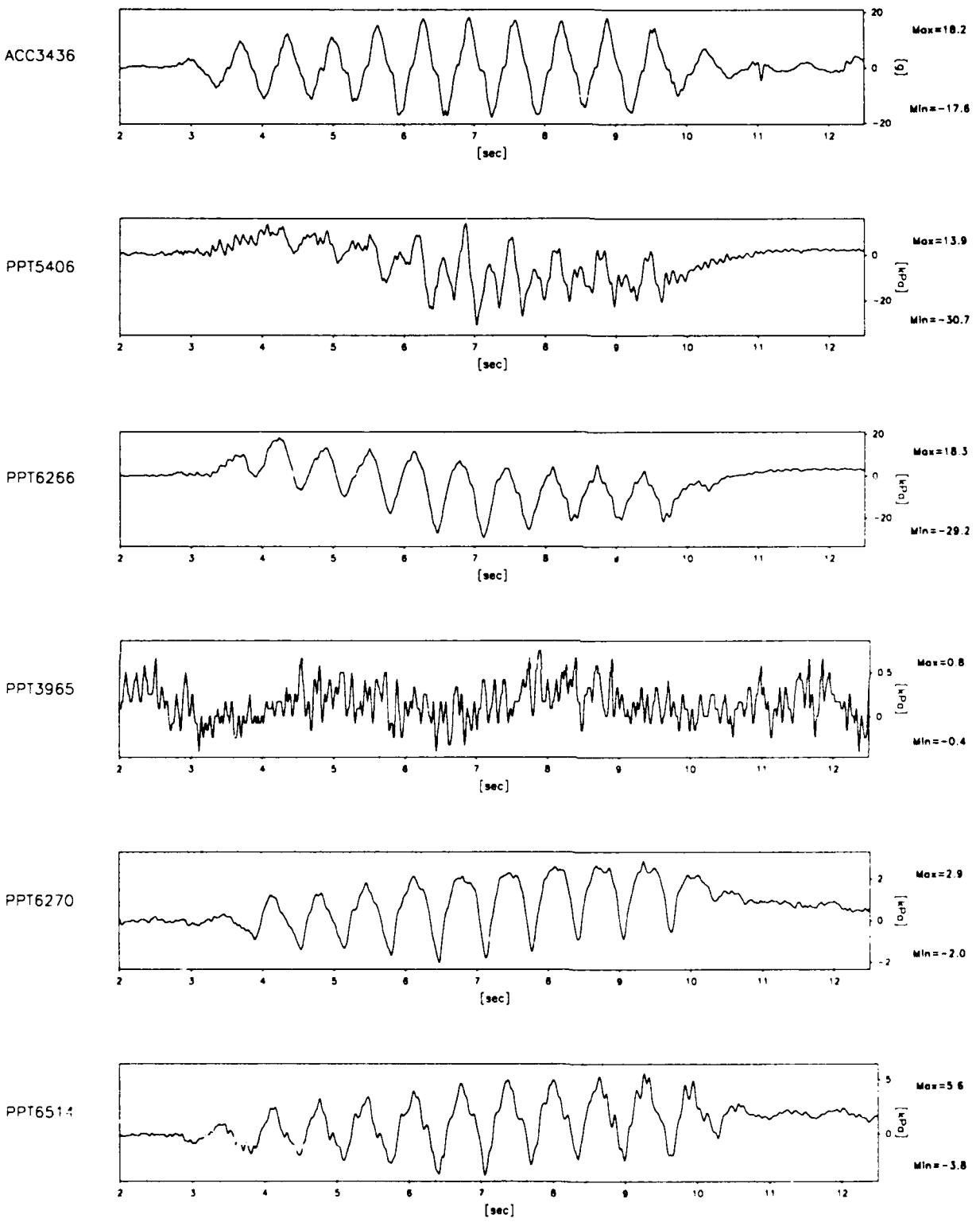

Scales : Prototype

TEST LEG-1 MODEL SAT FLIGHT -1	EQ-1	SHORT TERM TIME RECORDS	G Level 80	FIG.NO. **8.4**

840 datapoints plotted per complete transducer record

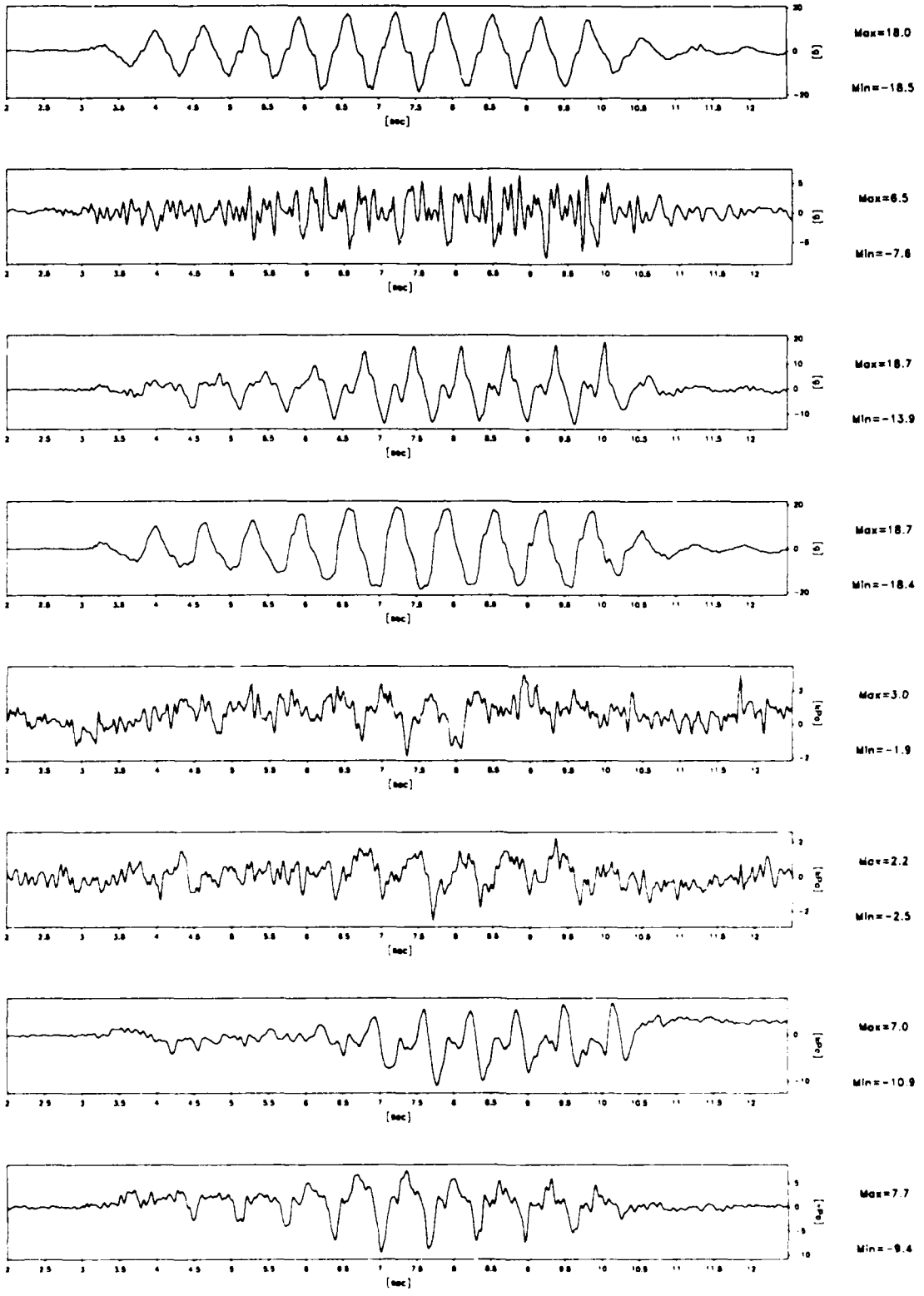

Scales : Prototype

TEST LEG-1 MODEL SAT FLIGHT -1	EQ-1	SHORT TERM TIME RECORDS	G Level 80	FIG.NO. 8.5

750 datapoints plotted per complete transducer record

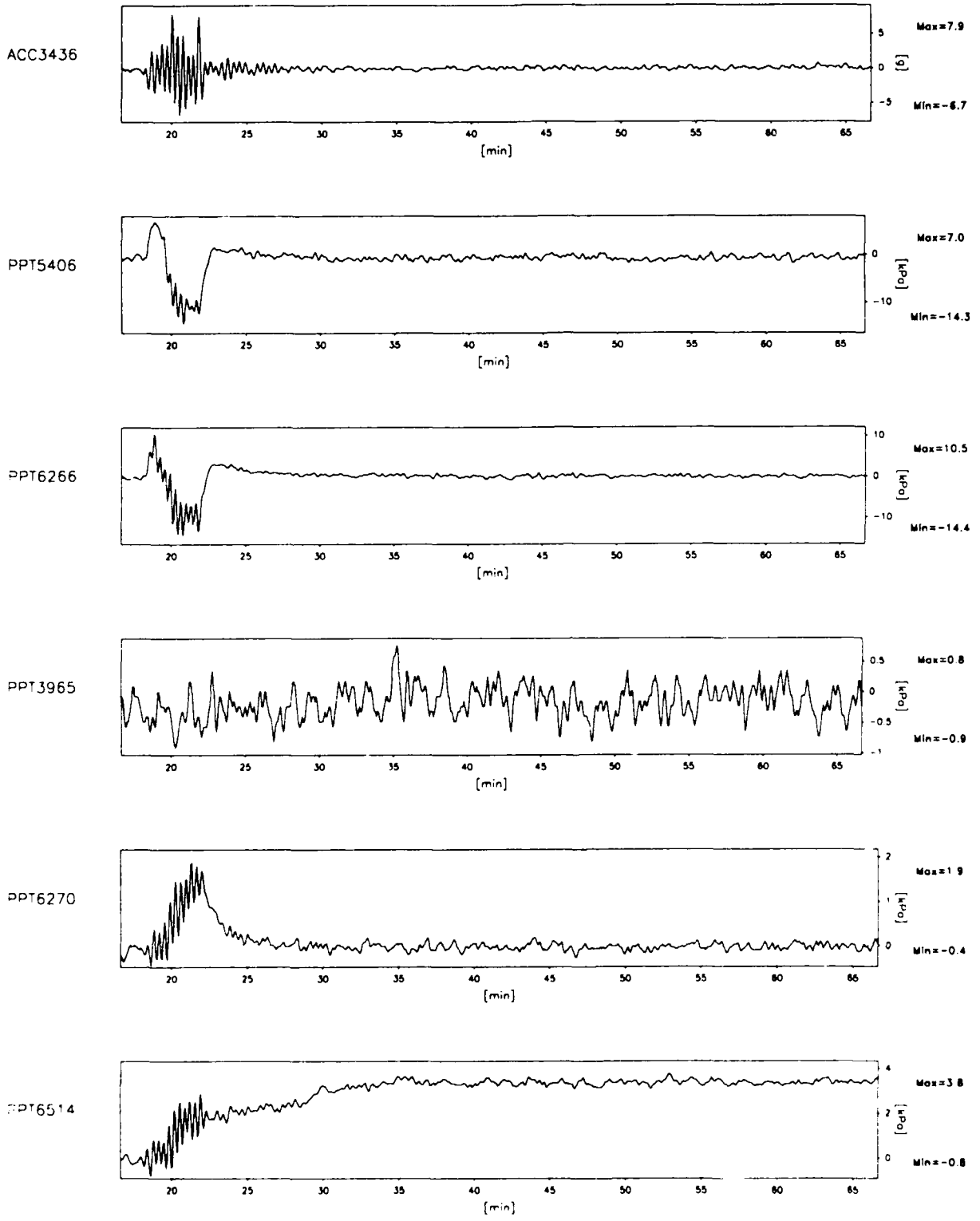

Scales : Prototype

TEST LEG-1 MODEL SAT FLIGHT -1	EQ-1	LONG TERM TIME RECORDS	G Level 80	FIG.NO. **8.6**

955 datapoints plotted per complete transducer record

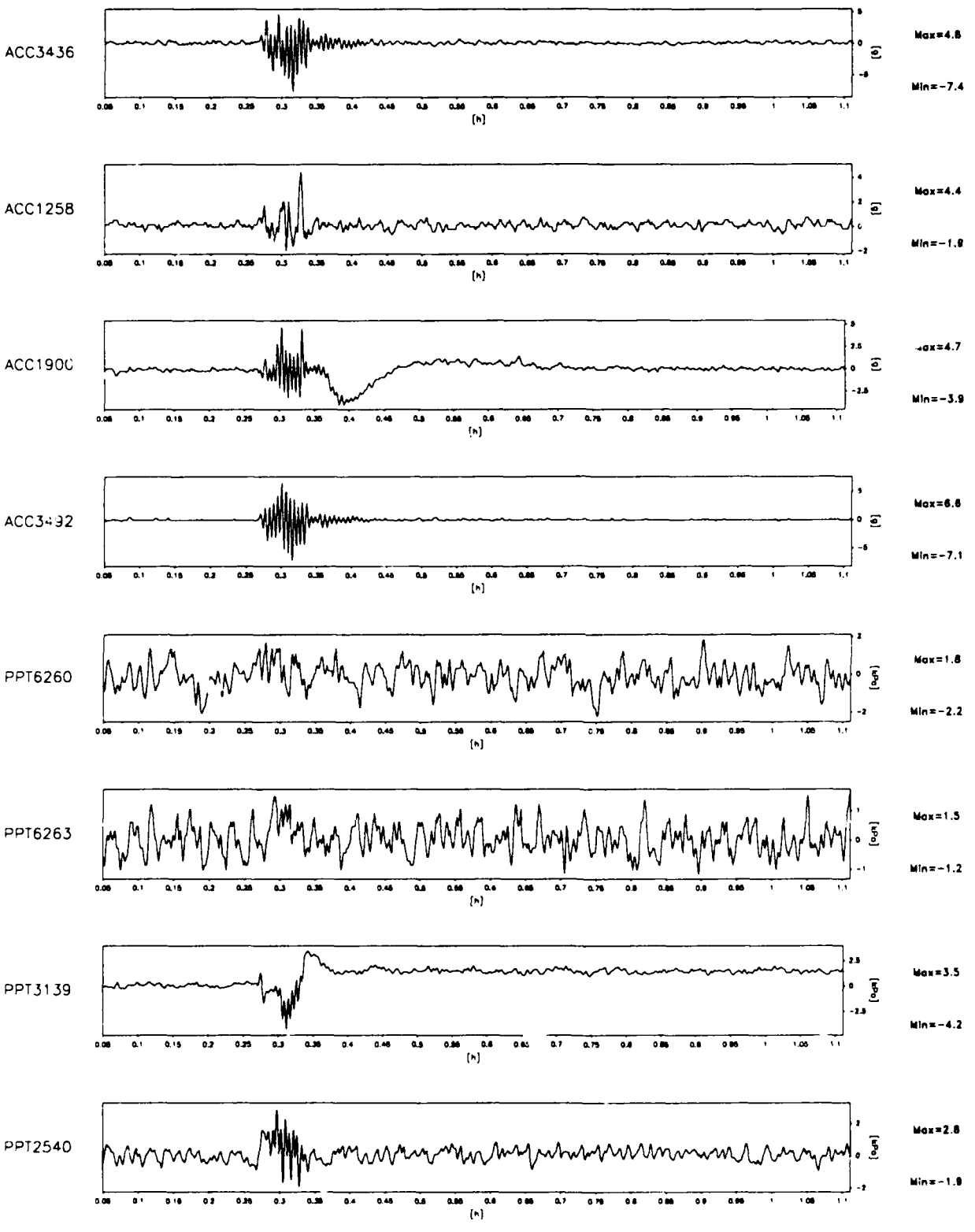

Scales : Prototype

TEST LEG-1 MODEL SAT FLIGHT -1	EQ-1	LONG TERM TIME RECORDS	G Level 80	FIG.NO. 8.7

840 datapoints plotted per complete transducer record

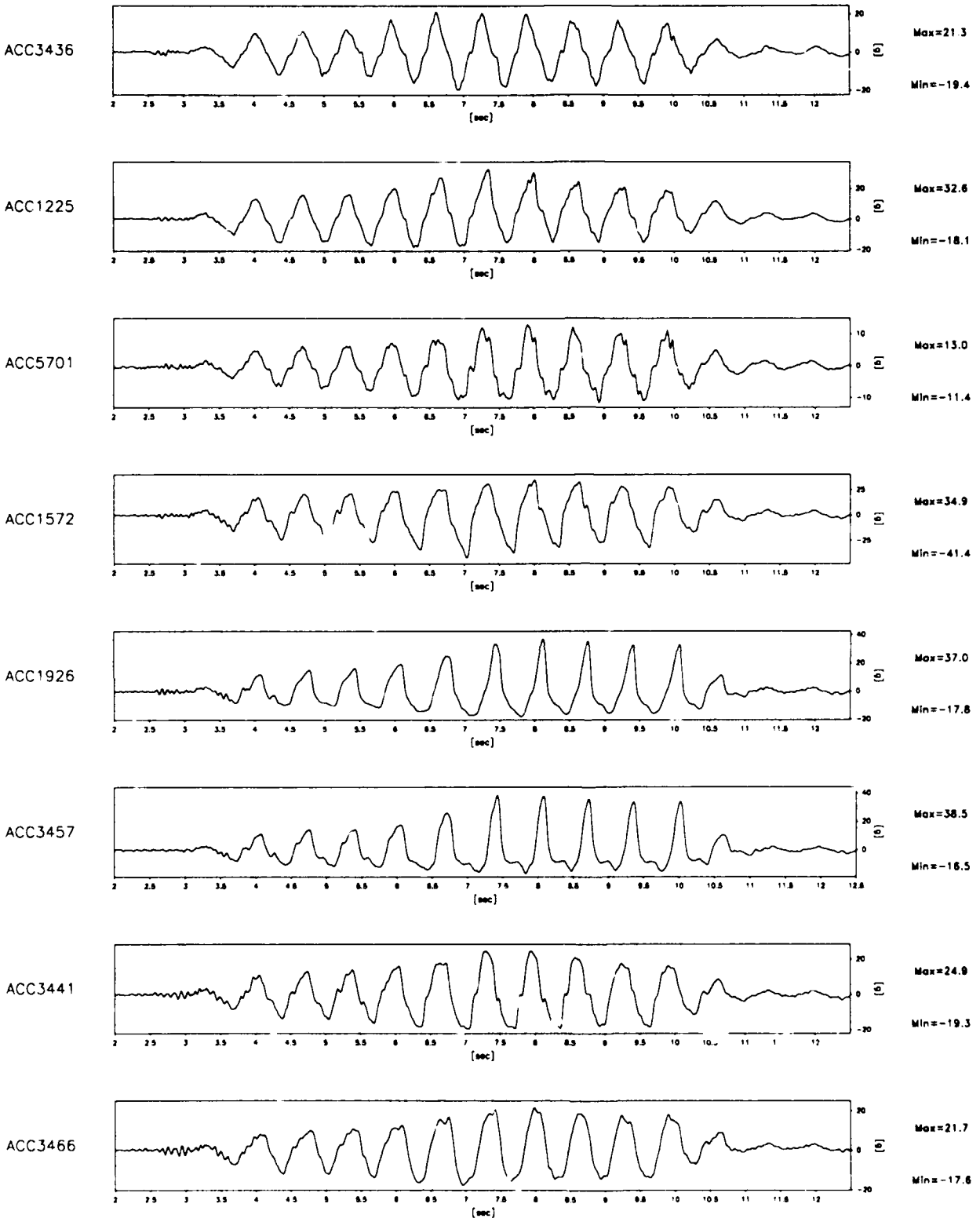

Scales : Prototype

TEST LEG-1 MODEL SAT FLIGHT -1	EQ-2	SHORT TERM TIME RECORDS	G Level 80	FIG.NO. **8.8**

840 datapoints plotted per complete transducer record

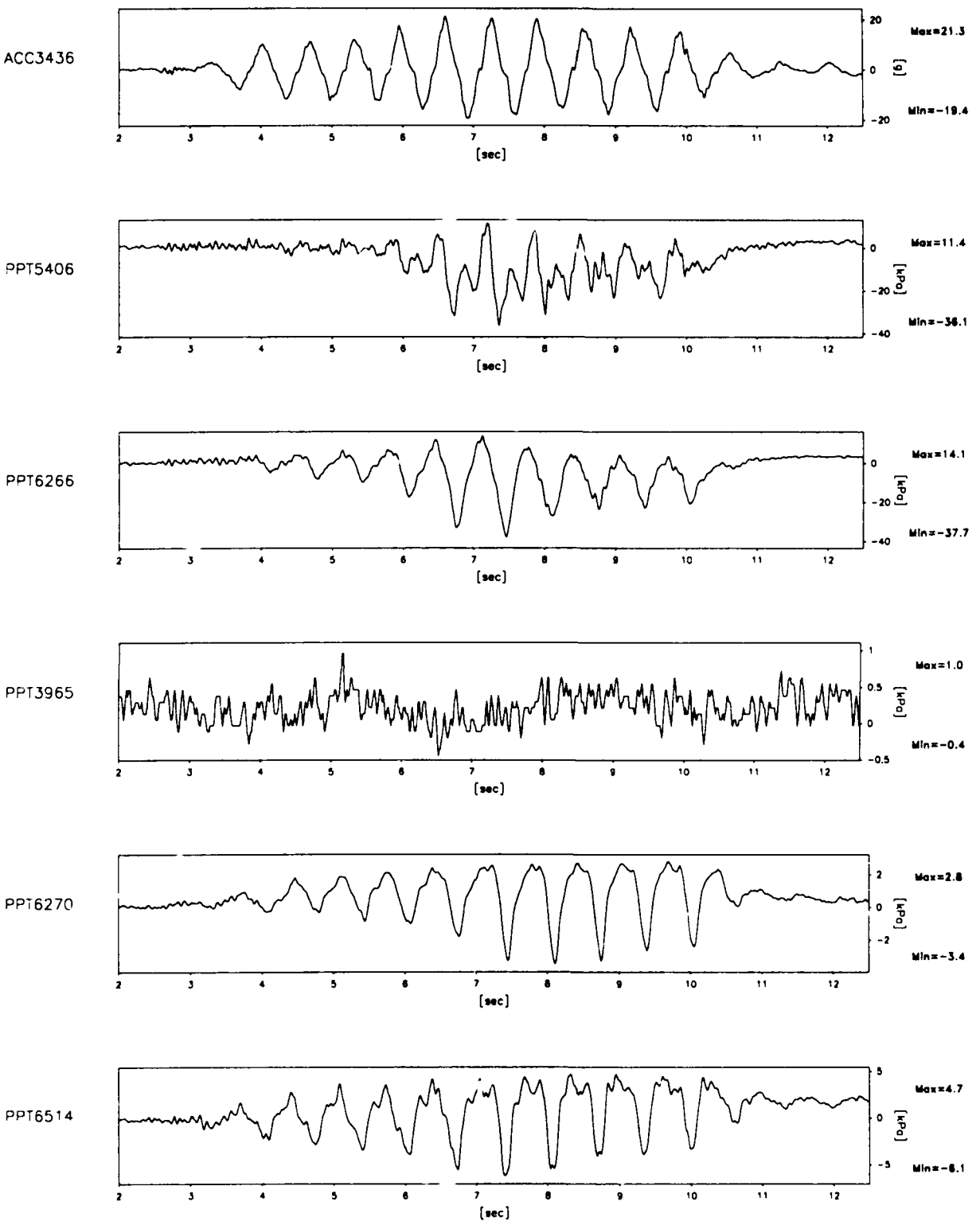

Scales : Prototype

TEST LEG-1 MODEL SAT FLIGHT -1	EQ-2	SHORT TERM TIME RECORDS	G Level 80	FIG.NO. 8.9

840 datapoints plotted per complete transducer record

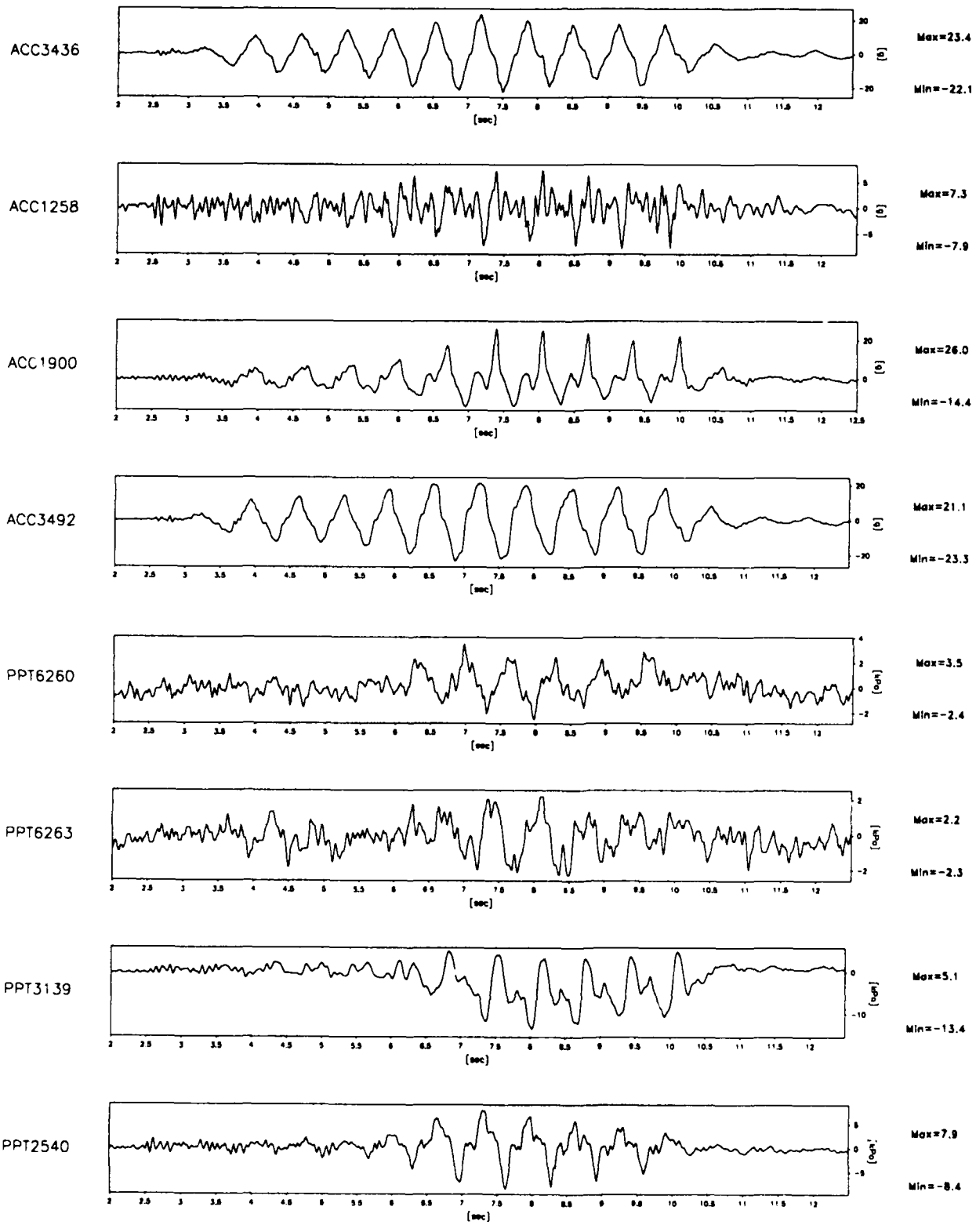

Scales : Prototype

TEST LEG-1 MODEL SAT FLIGHT -1	EQ-2	SHORT TERM TIME RECORDS	G Level 80	FIG.NO. 8.10

608 datapoints plotted per complete transducer record

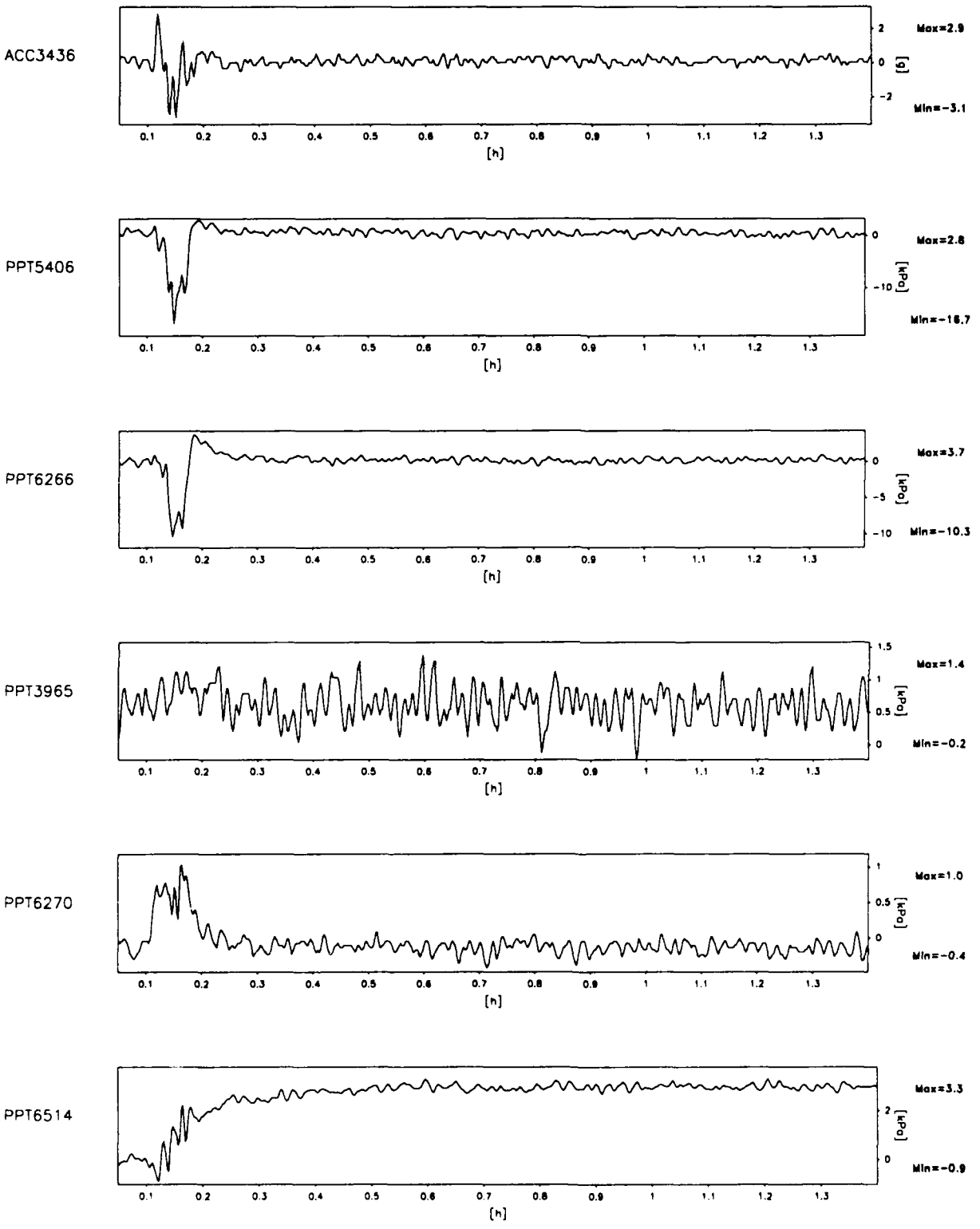

Scales : Prototype

TEST LEG-1 MODEL SAT FLIGHT -1	EQ-2	LONG TERM TIME RECORDS	G Level 80	FIG.NO. **8.11**

955 datapoints plotted per complete transducer record

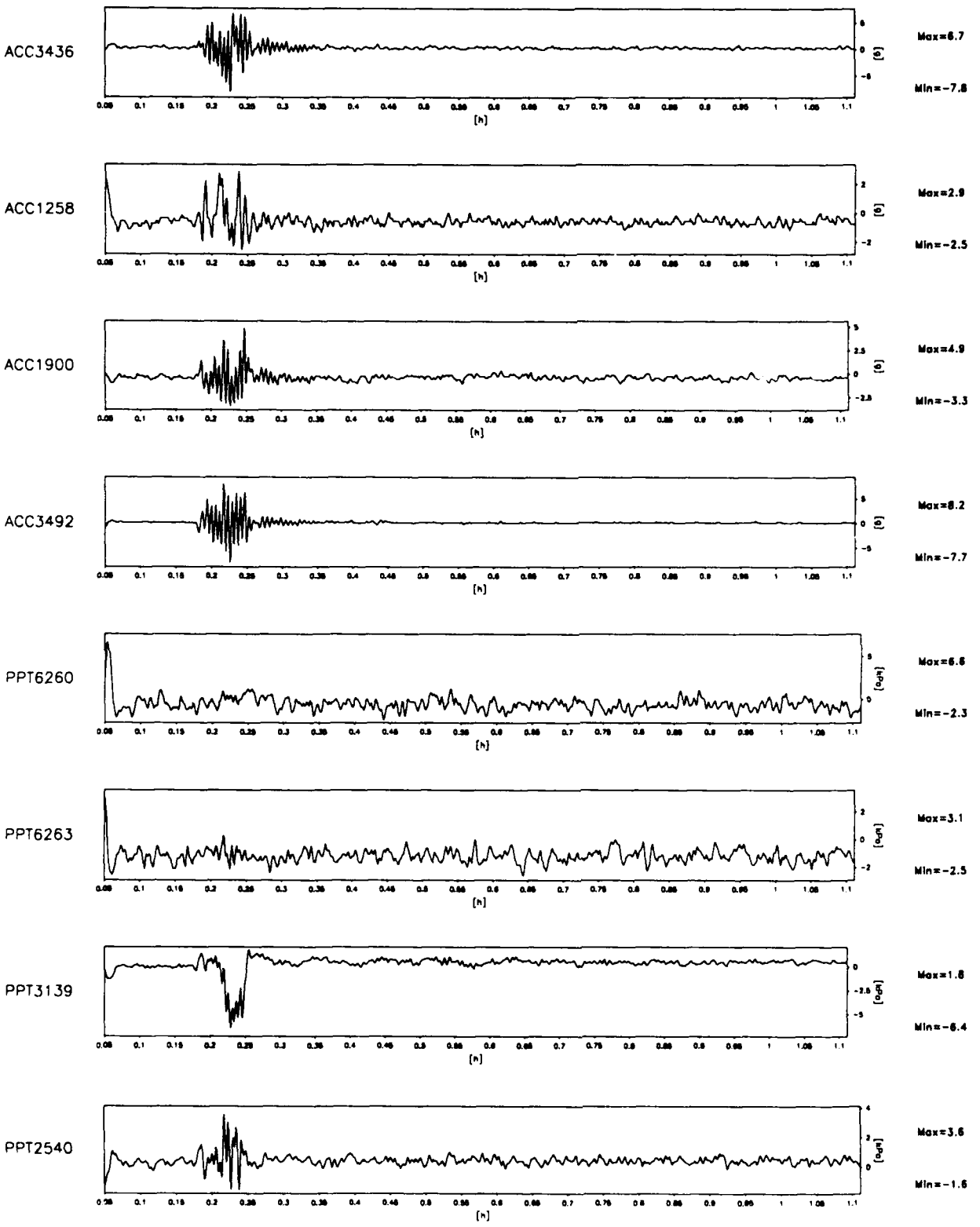

Scales : Prototype

TEST LEG-1 MODEL SAT FLIGHT -1	EQ-2	LONG TERM TIME RECORDS	G Level 80	FIG.NO. **8.12**

840 datapoints plotted per complete transducer record

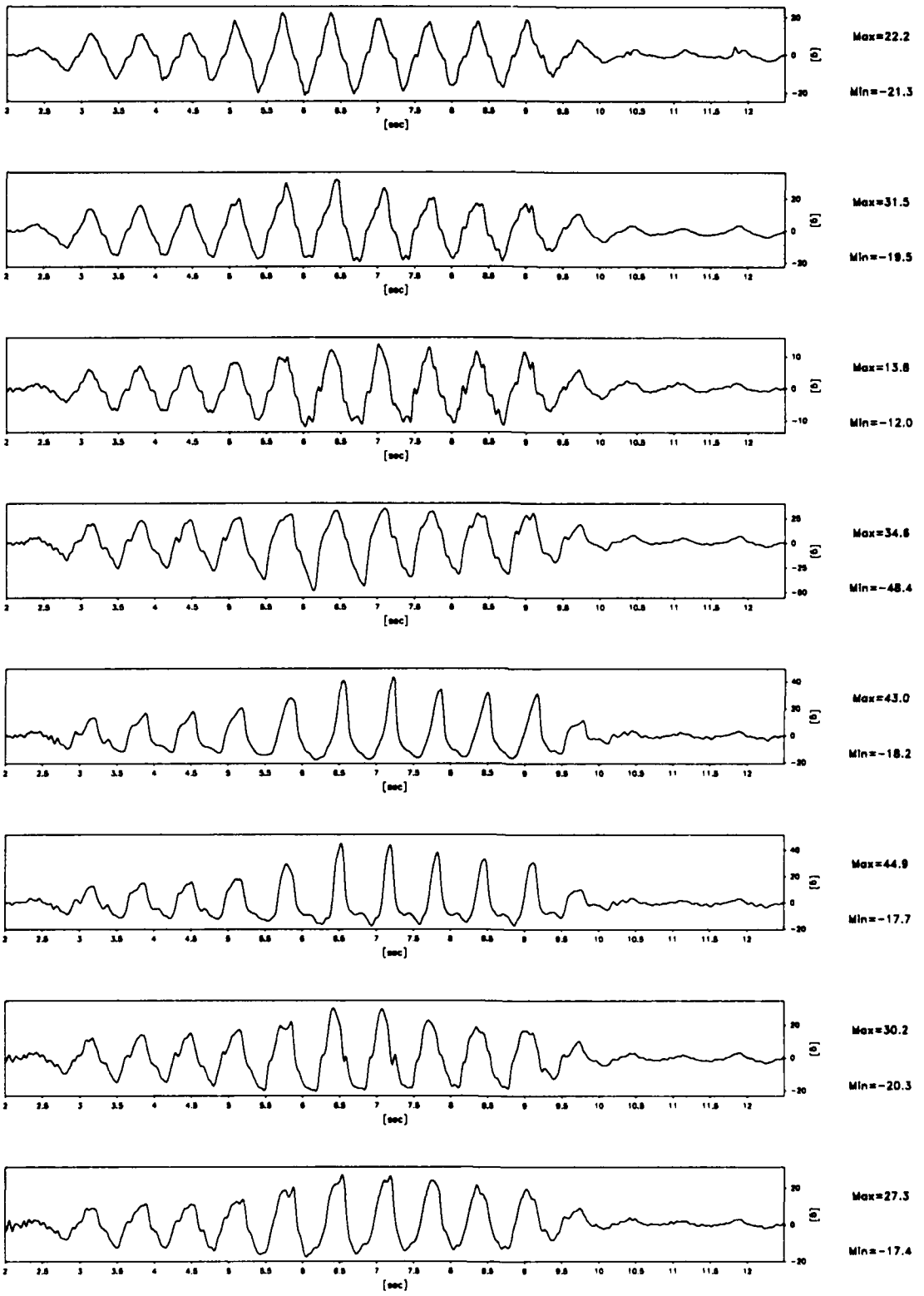

Scales : Prototype

TEST LEG-1 MODEL SAT FLIGHT -1	EQ-3	SHORT TERM TIME RECORDS	G Level 80	FIG.NO. **8.13**

840 datapoints plotted per complete transducer record

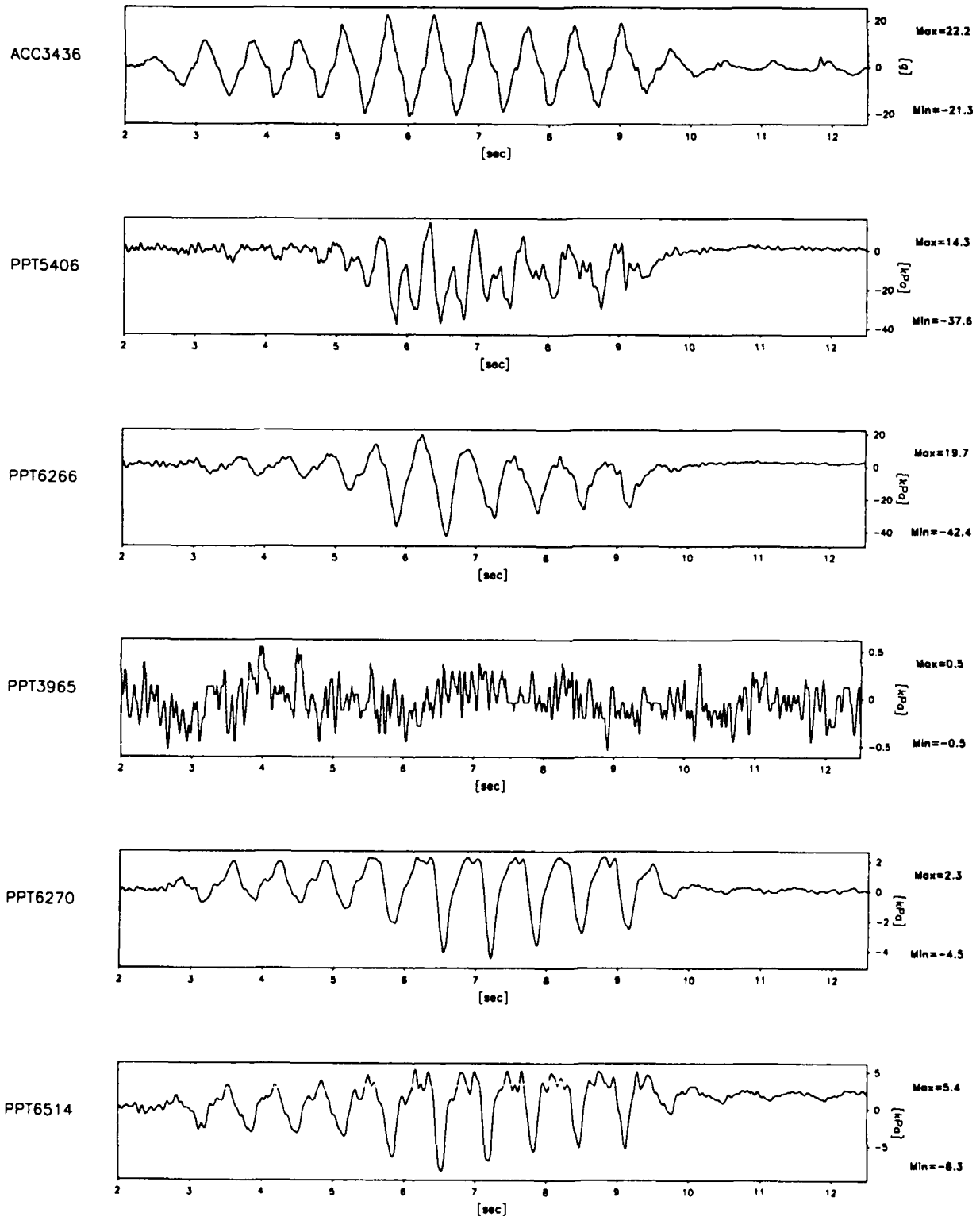

Scales : Prototype

TEST LEG-1 MODEL SAT FLIGHT -1	EQ-3	SHORT TERM TIME RECORDS	G Level 80	FIG.NO. **8.14**

840 datapoints plotted per complete transducer record

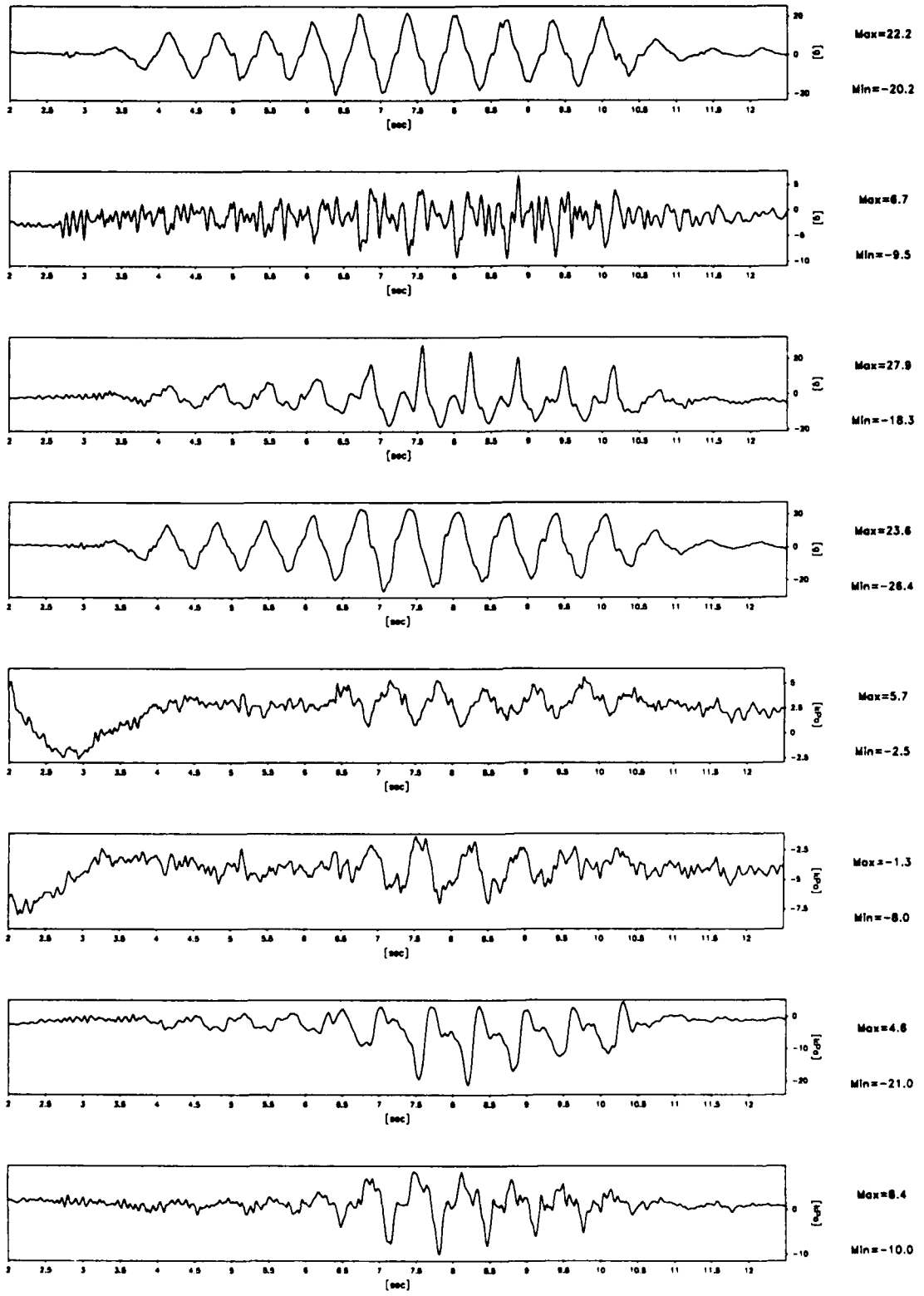

Scales : Prototype

TEST LEG-1 MODEL SAT FLIGHT -1	EQ-3	SHORT TERM TIME RECORDS	G Level 80	FIG.NO. **8.15**

900 datapoints plotted per complete transducer record

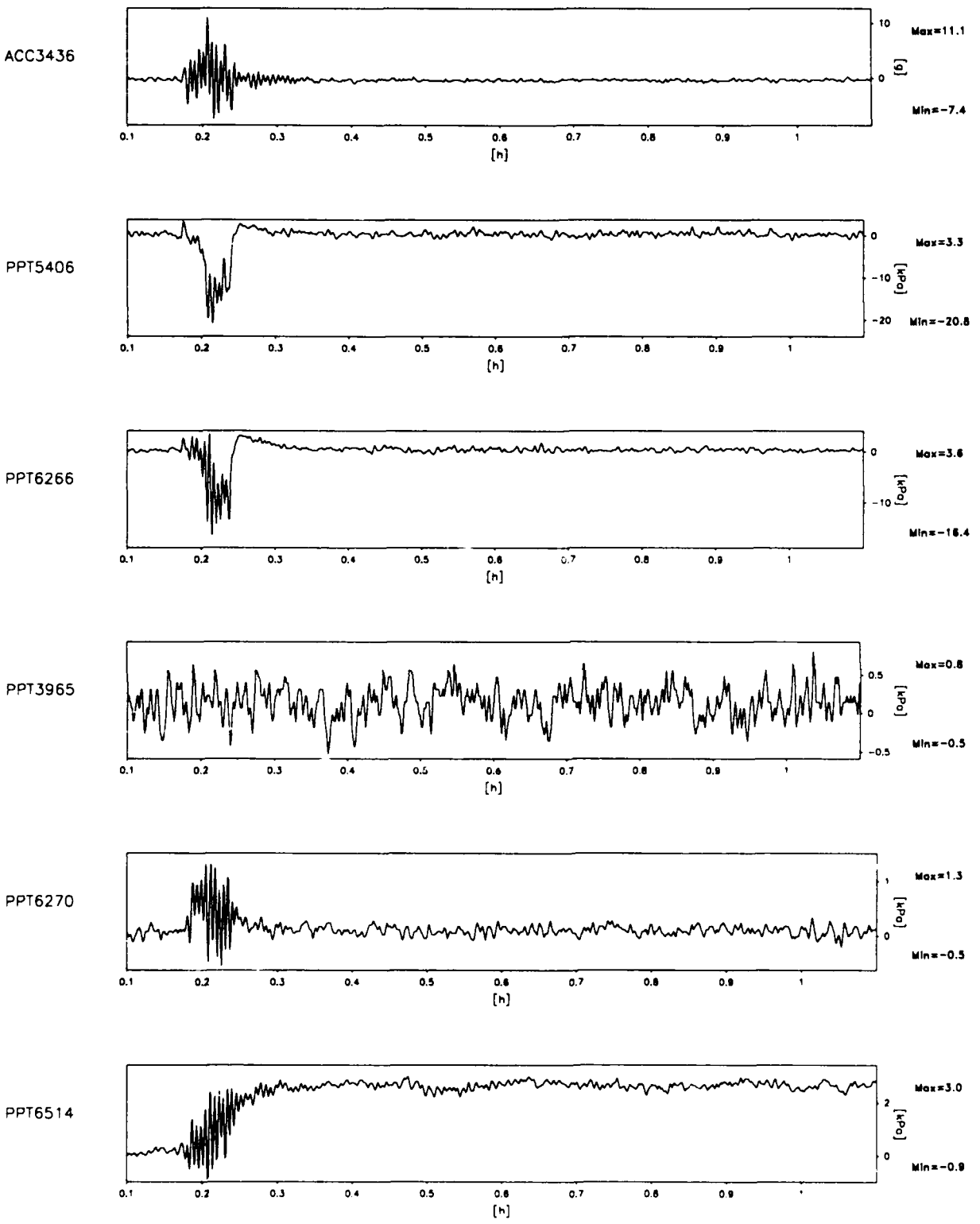

Scales : Prototype

TEST LEG-1 MODEL SAT FLIGHT -1	EQ-3	LONG TERM TIME RECORDS	G Level 80	FIG.NO. 8.1€

955 datapoints plotted per complete transducer record

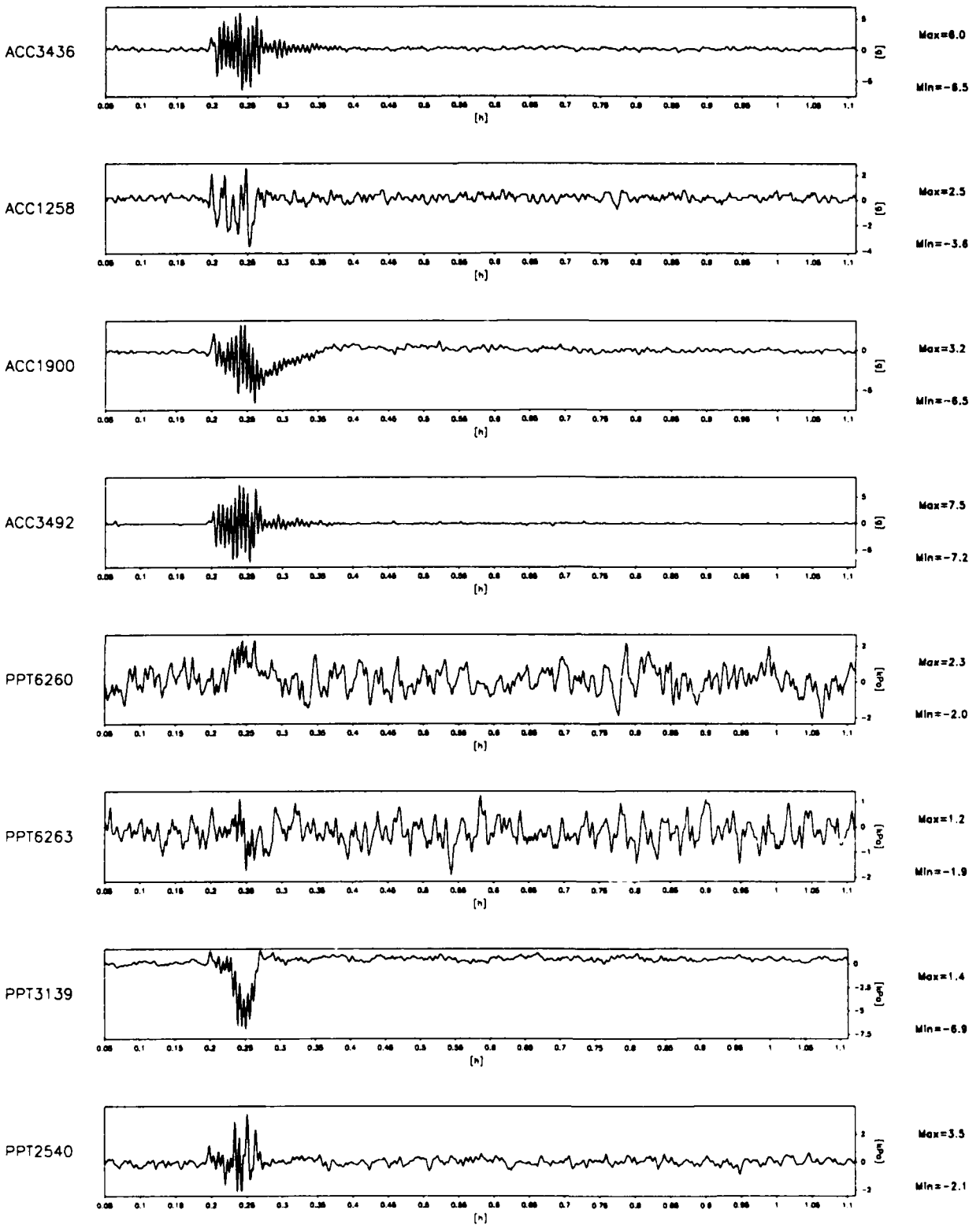

Scales : Prototype

TEST LEG-1 MODEL SAT FLIGHT -1	EQ-3	LONG TERM TIME RECORDS	G Level 80	FIG.NO. 8.17

840 datapoints plotted per complete transducer record

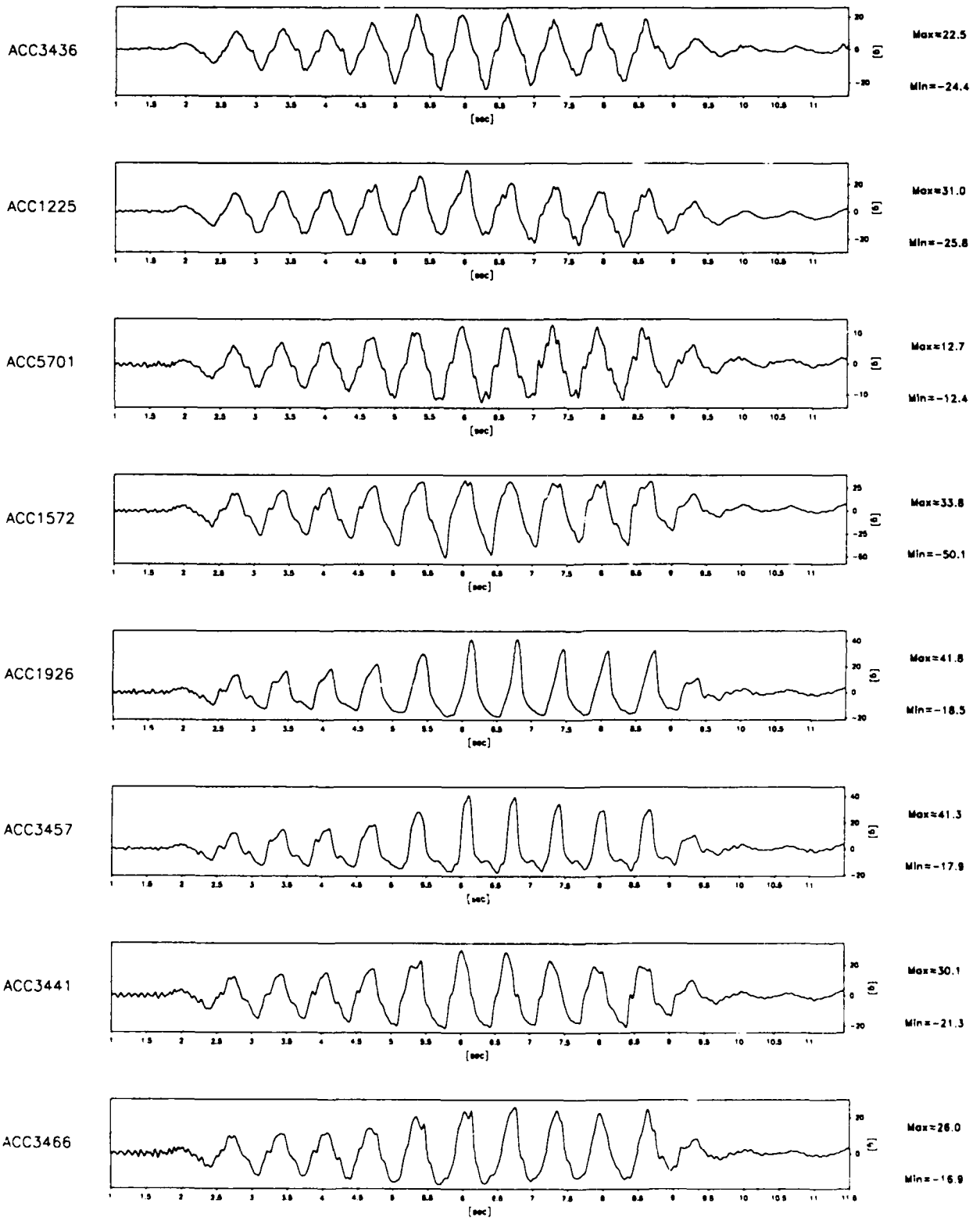

Scales : Prototype

TEST LEG-1 MODEL SAT FLIGHT -1	EQ-4	SHORT TERM TIME RECORDS	G Level 80	FIG.NO. 8.18

840 datapoints plotted per complete transducer record

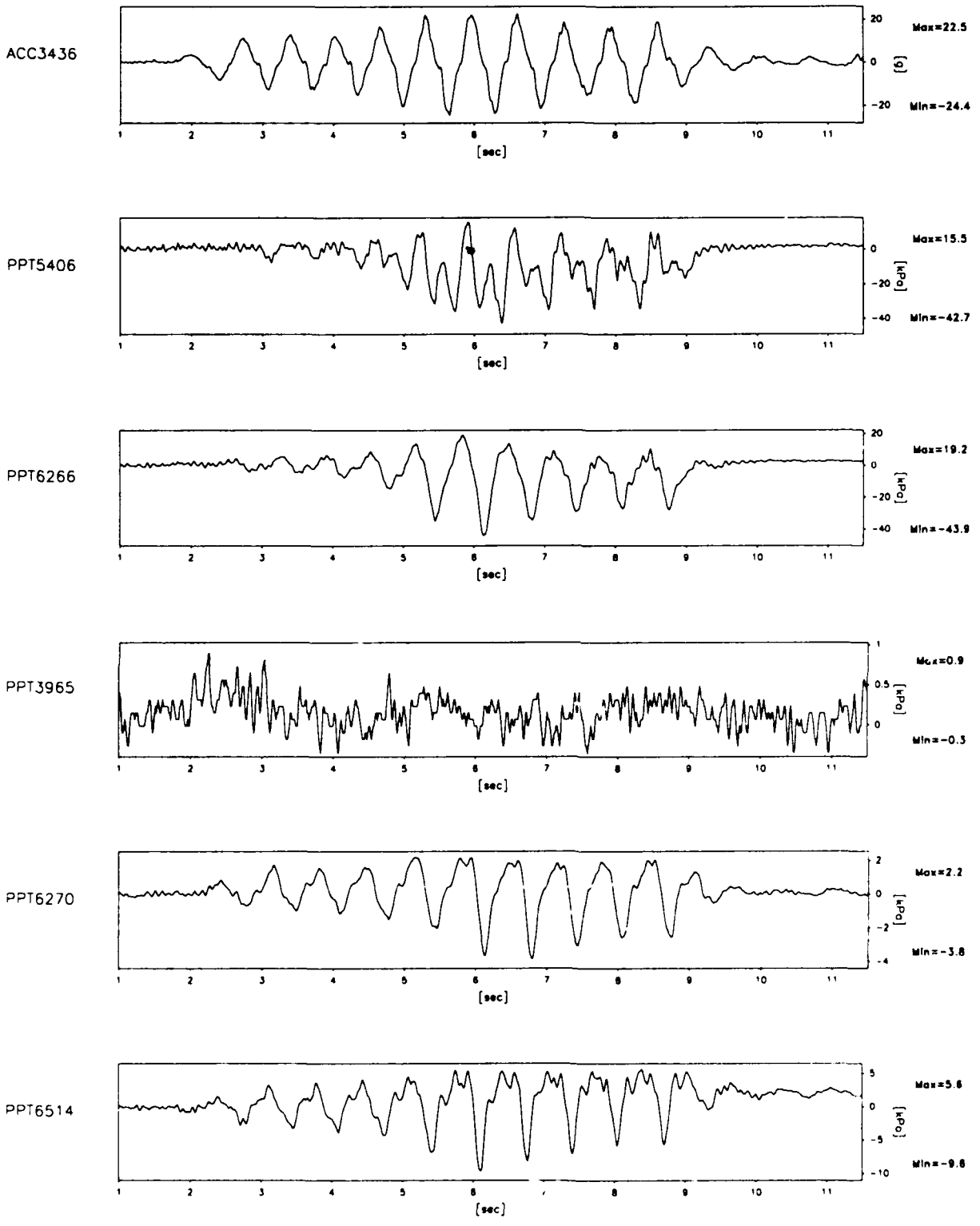

Scales : Prototype

TEST LEG-1 MODEL SAT FLIGHT -1	EQ-4	SHORT TERM TIME RECORDS	G Level 80	FIG.NO. **8.19**

840 datapoints plotted per complete transducer record

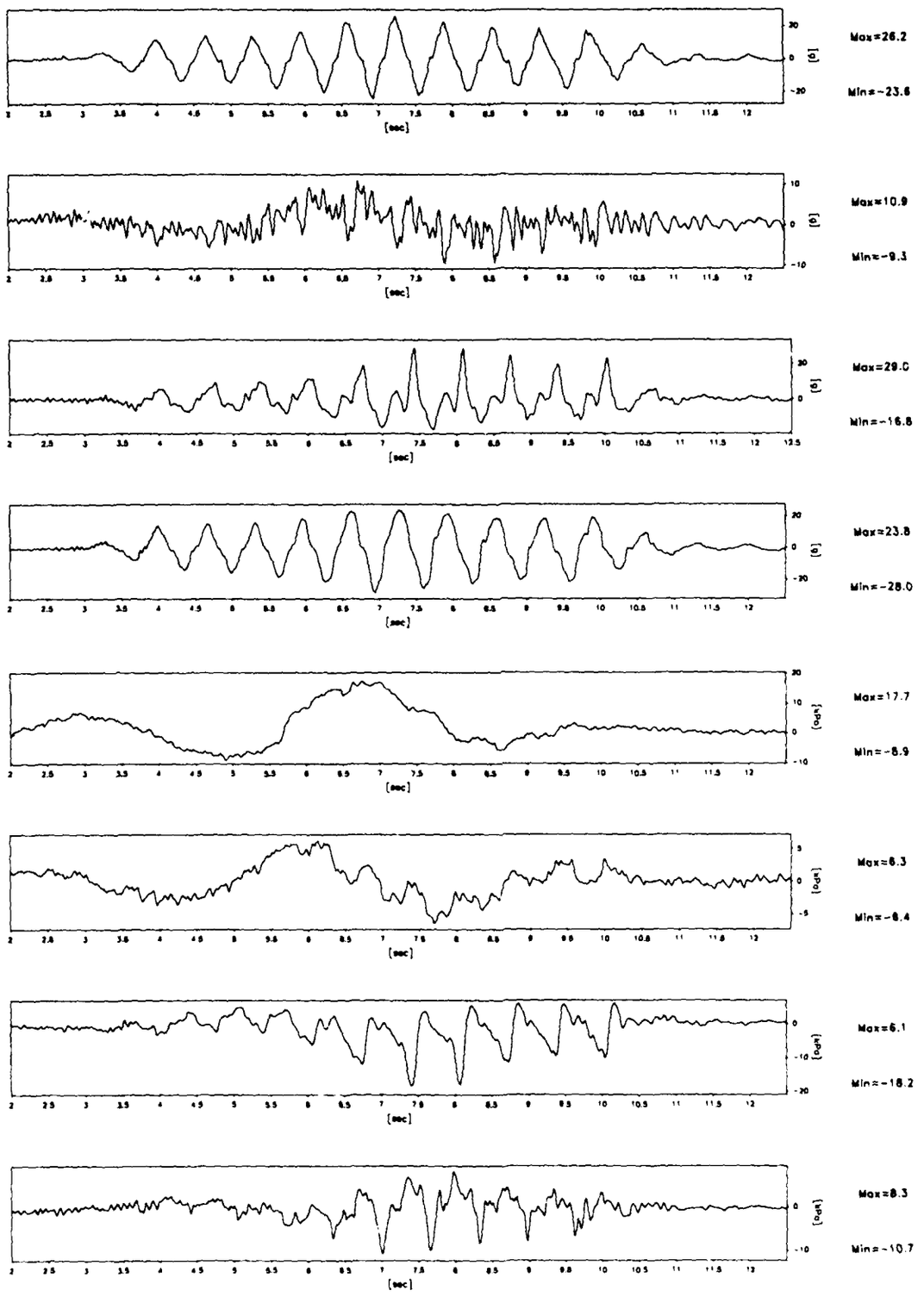

Scales : Prototype

TEST LEG-1 MODEL SAT FLIGHT -1	EQ-4	SHORT TERM TIME RECORDS	G Level 80	FIG.NO. 8.20

955 datapoints plotted per complete transducer record

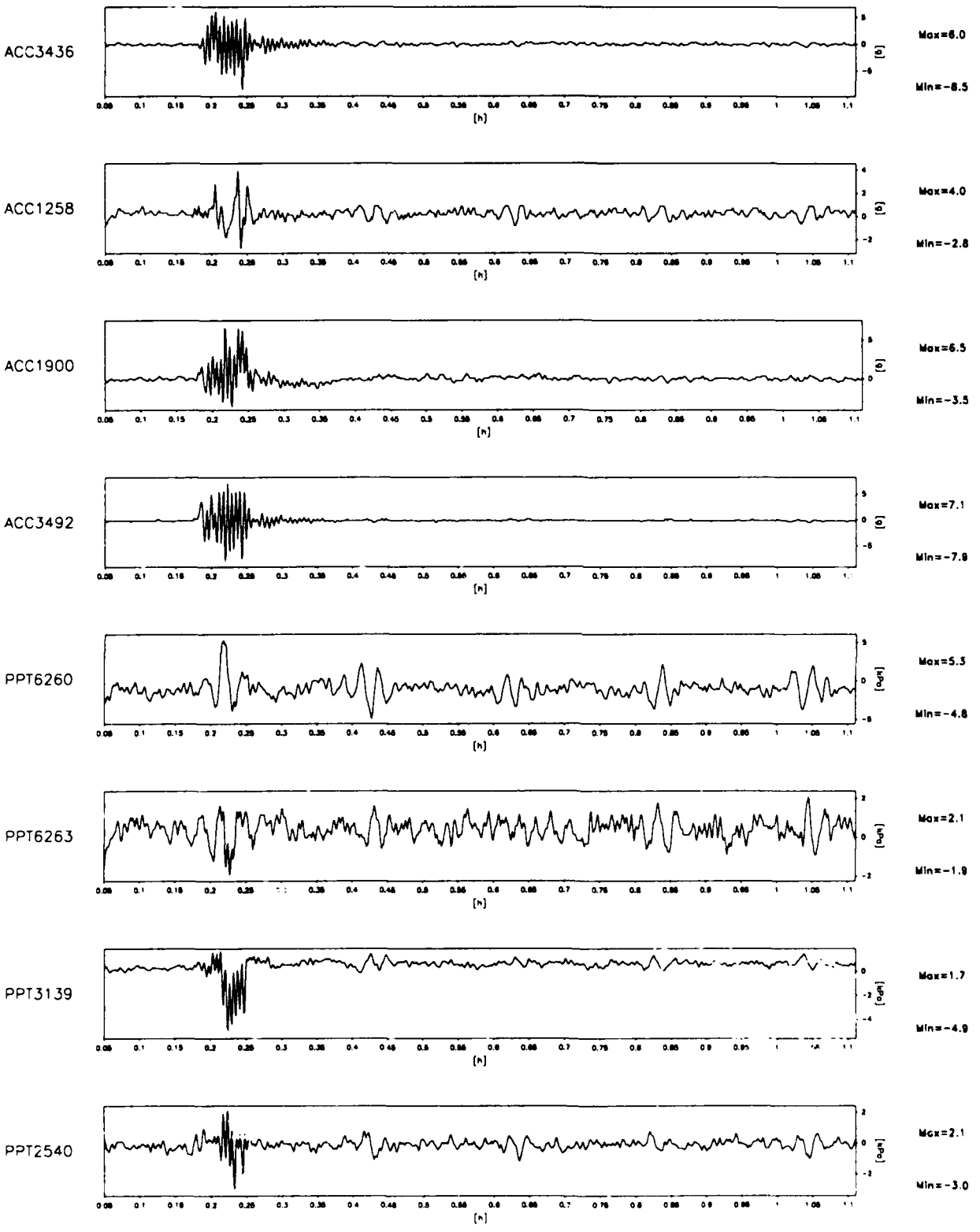

Scales : Prototype

TEST LEG-1 MODEL SAT FLIGHT -1	EQ-4	LONG TERM TIME RECORDS	G Level 80	FIG.NO. **8.21**

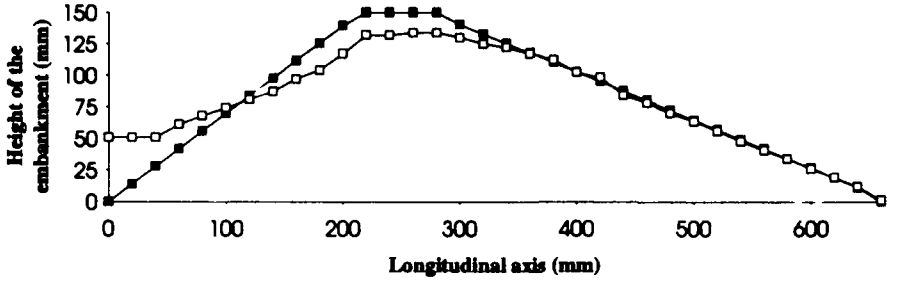

Fig. 8.22 Post test profile of centrifuge model LEG-1

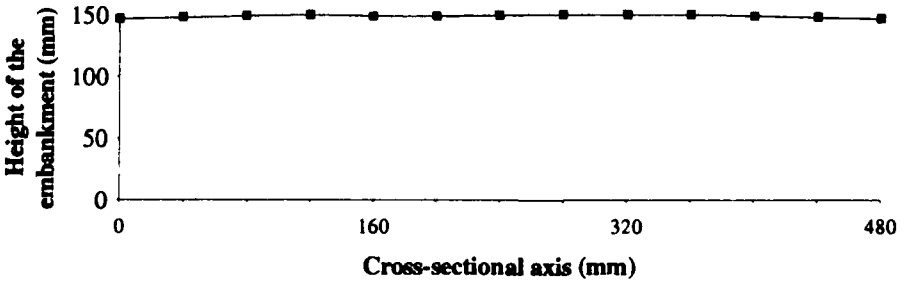

Fig.8.23 Post test profile along the cross section of centrifuge model LEG-1

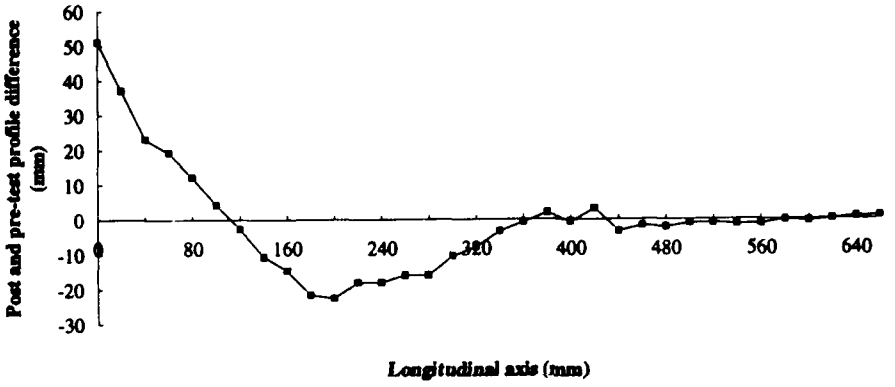

Fig.8.24 Difference of post and pre-test profiles along the longitudinal axis in centrifuge test LEG-1

9.0 Centrifuge Test LEG-2

9.1 Configuration of the test

In the second centrifuge test LEG-2 the down stream slope was 35^{o} and the up stream slope was 24^{o} .The loose layer of sand was inclined at an angle of 30^{o} and had a thickness of 20 mm. The dense section of the embankment was constructed using coarse Leighton Buzzard 14/25 sand and the loose section of the embankment was constructed using fine Leighton Buzzard 100/170 sand as explained in section 6.0. The schematic diagram showing the cross section of the model is presented in Fig.9.1. The placement of the transducers is shown in Fig.9.2. In this test it was decided to confine the loose section of the embankment using very fine rock flour to sustain the excess pore pressure built up during the earthquake loading for a longer time. Accordingly a thin layer of rock flour was introduced at the top and bottom interfaces between the loose section and the dense sections of the embankment. The various stages of construction of this embankment can be seen in Plates 9.1 to 9.4

9.2 Test data

In this test the down stream slope suffered a slip resulting in the movement of the crest towards the down stream toe of the embankment. The slip surface was along the loose section of the sand as shown in Fig.9.1 (zone B). The dry densities of each of the zones in Fig.9.1 together with the void ratio and relative densities for this centrifuge model are presented in Table 9.1. The hydrostatic pore pressures recorded during the swing up of the centrifuge and increase of the centrifugal acceleration to 80g and after each earthquake are presented in Table 9.2. The data recorded during this test are presented in Figs.9.3 to 9.17. The accelerometer 1926 placed in the crest of the embankment have suffered a rotation due to the strong motion and registered the vertical acceleration. However the vertical accelerometer 1900 also suffered a rotation and recorded the horizontal acceleration. The trace recorded by ACC 1900 showed strong peak acceleration in one direction suggesting the movement of the crest. This is supported by the accelerometer traces 3457 and 3466 which are also in this region. ACC 3441 and 3466 have flat top peaks suggesting the slipping of the down stream slope. The traces recorded by the accelerometers in the up stream slope were more or less uniform suggesting no movement of this slope. The post test profile measured after the test confirmed this.

The pore pressure traces recorded in the crest section by PPT 3139 showed strong suctions. Similarly the pore pressures recorded in the lower dense section (shown in Fig.1) by PPT 5406 and 6266 showed strong suction pressures. This shows that the dense zones were dilating and under the suction pressures they would behave almost like rigid blocks. In the loose section there was a much larger excess pore pressure which was retained for a very long time due to the impermeable rock flour interface between the loose and dense sections. During the model earthquake the loose section was the slip plane available for the down stream slope as there were excess pore pressures in this zone and it was at a higher pore pressure than the other two zones. The slow dissipation of the excess pore pressure in the loose zone is revealed in the long term traces. During this test ACC 1926 has partially floated and moved by about 20 mm towards the down stream slope. ACC 1900 has moved by about 32 mm in the same direction. Also the accelerometer 3466 has suffered partial floatation and was exposed. These transducers can be seen in Plate 9.5. PPT 6514 has floated completely while PPT 3139 suffered a movement of about 14 mm towards the down stream slope. A section of this model during the post test investigation is presented in Plate 9.6. The extent of soil movement can observed in this plate by comparing the original profile on the longitudinal wall of the strong box with the post test profile. Also the rock flour interface and the loose sand zone can be seen in this plate.

9.3 Post test profile

The post test profile measured after the centrifuge test is presented in Fig.9.18 together with the original profile of the embankment. The post test profile is measured at various longitudinal sections and the average profile is shown in this figure. Also the cross sectional profile is shown in Fig.9.19 which suggests that the slip is more or less uniform across the model embankment. From the post test profiles it can be clearly seen that there is a slip on the down stream slope side of the embankment. The up stream slope is relatively unchanged before and after the earthquakes. It is possible to estimate the quantity of the soil movement resulting when the model embankment is subjected to the earthquake loading. In order to estimate the quantity of soil moved during the earthquakes, the difference of the embankment profiles before and after the earthquakes is plotted. This graph is presented in Fig.9.20. Performing numerical integration using the Simpson's rule, the area under the curve shown in Fig.9.20 is estimated. Using this area the volume of the soil movement resulting from the earthquake loading is estimated. The quantity of soil which slipped from the crest of

the embankment was 2.312×10^{-3} m^3 and the quantity of soil deposited at the toe of the embankment is 1.754×10^{-3} m^3. In prototype terms these quantities are 1183.76 m^3 and 898.05 m^3 respectively. The differential volume which may indicate the error in measurement of the post test profile is 2.28 % of the total volume of the embankment.

Table 9.1 Dry density of sand in different zones of the embankment in centrifuge test LEG-2

Zone*	γ_d (kg/m^3)	void ratio (e)	Relative Density (%)
A	1681.40	0.576	72.03
B	1375.59	0.926	22.5
C	1710.7	0.549	77.04

* see Fig.9.1 for zone specification

Table 9.2 Hydrostatic pore pressures recorded in centrifuge test LEG-2

Device	kPa/V	20-G kPa	40-G kPa	60-G kPa	80-G kPa	EQ-1 kPa	EQ-2 kPa	EQ-3 kPa
PPT2540	361.77	11.90	27.05	38.42	53.23	50.62	51.07	51.05
PPT3139	379.53	11.23	24.77	35.30	48.88	47.46	48.63	49.52
PPT6514	350.88	2.28	5.06	8.27	11.76	11.13	11.09	11.01
PPT6260	365.88	26.90	57.50	83.88	114.35	106.85	106.38	105.35
PPT6263	365.27	1.70	3.61	5.29	7.18	6.82	6.85	6.89
PPT6270	385.84	4.20	9.53	14.35	19.79	18.60	19.06	19.18
PPT6266	440.55	1.61	3.49	5.32	7.18	6.70	6.78	6.78
PPT3965	-405.50	226.27	207.21	147.20	165.44	193.30	191.96	192.49
PPT5406	393.98	25.82	51.93	81.14	109.59	102.61	102.50	102.18

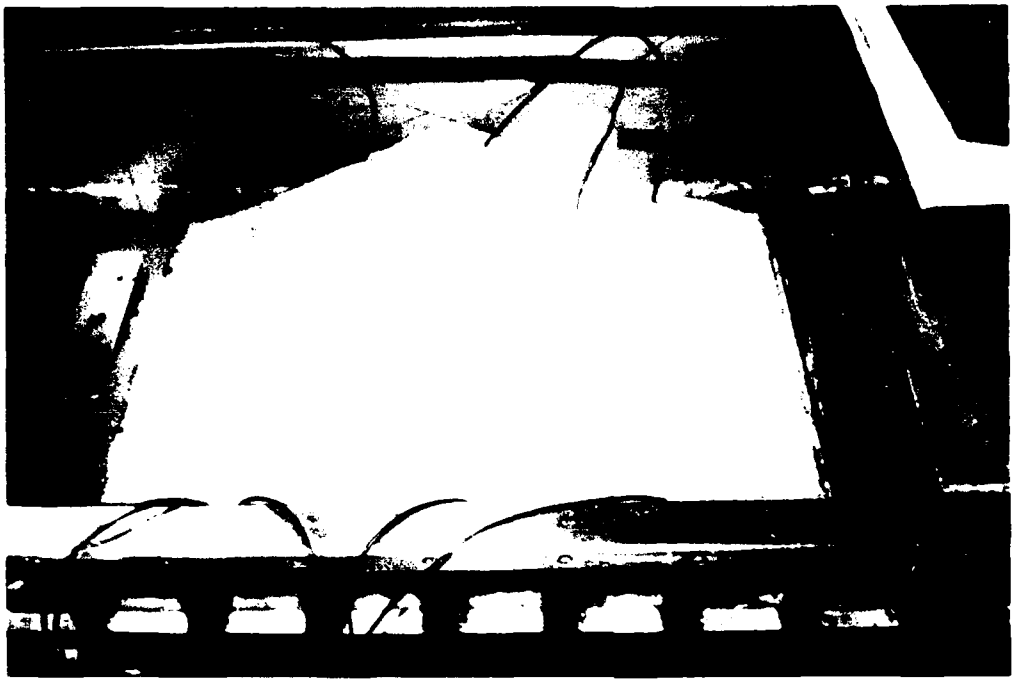

Plate 9.1 A view of the model embankment at the end of Zone A construction

Plate 9.2 Impermeable rock flour layer spreaded at the interface between loose and dense zones

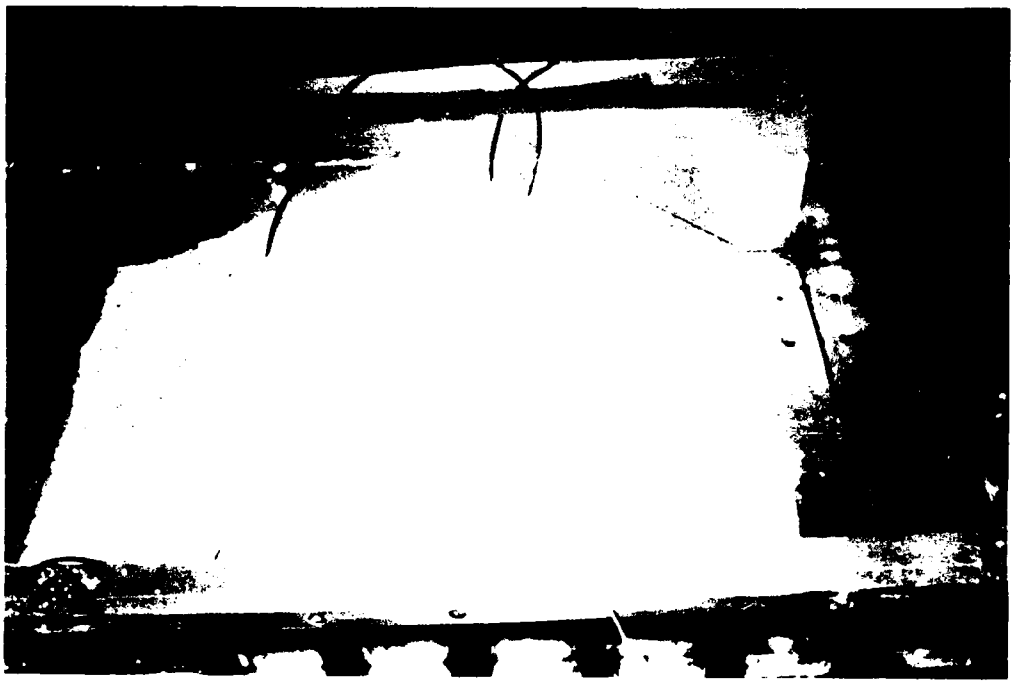

Plate 9.3 A view of the loose sand zone constructed by slumping method

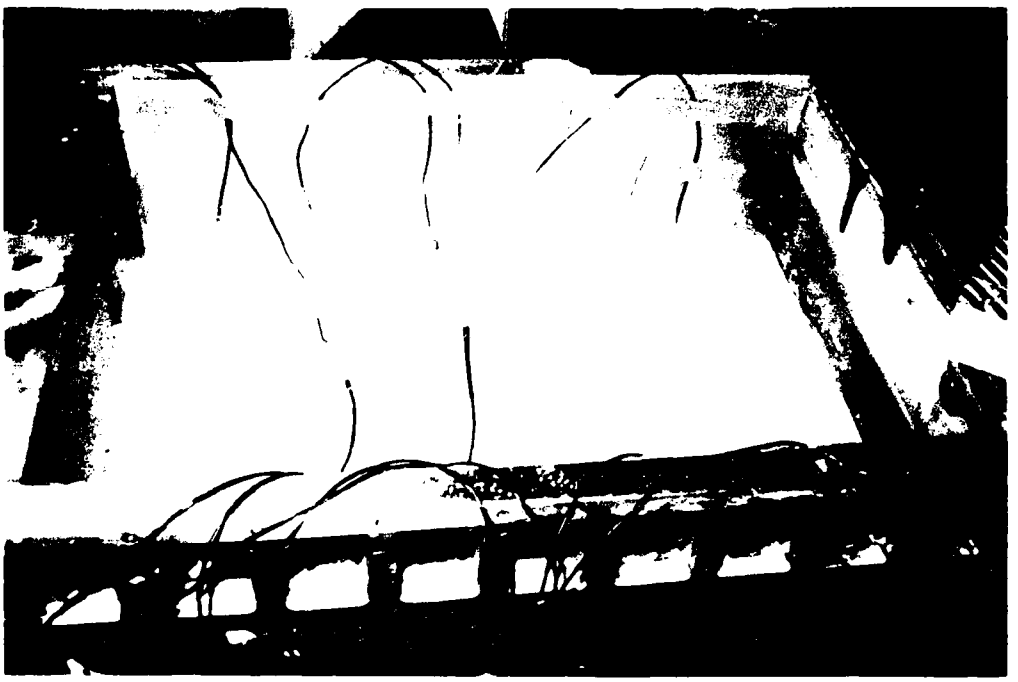

Plate 9.4 Placement of instruments in the crest and down stream slope of the model embankment

Plate 9.5 A view of the model embankment after centrifuge test LEG-2 (Note the complete slipping of down stream slope. ACC 1926 and ACC 3466 (black lead) have floated in this test)

Plate 9.6 Section of centrifuge model LEG 2 during the post test investigation

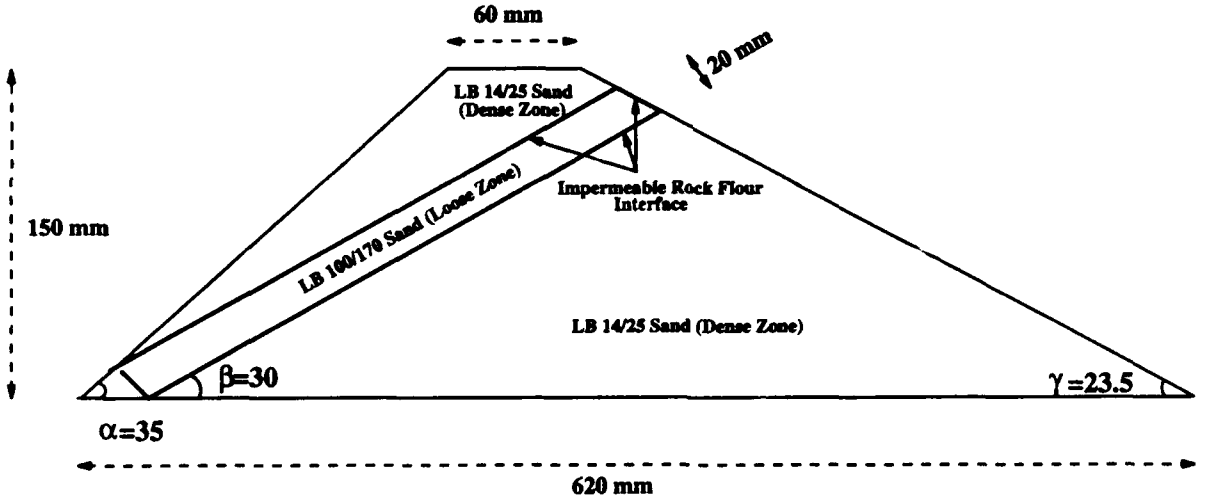

Fig.9.1 Cross section of the centrifuge model LEG-2

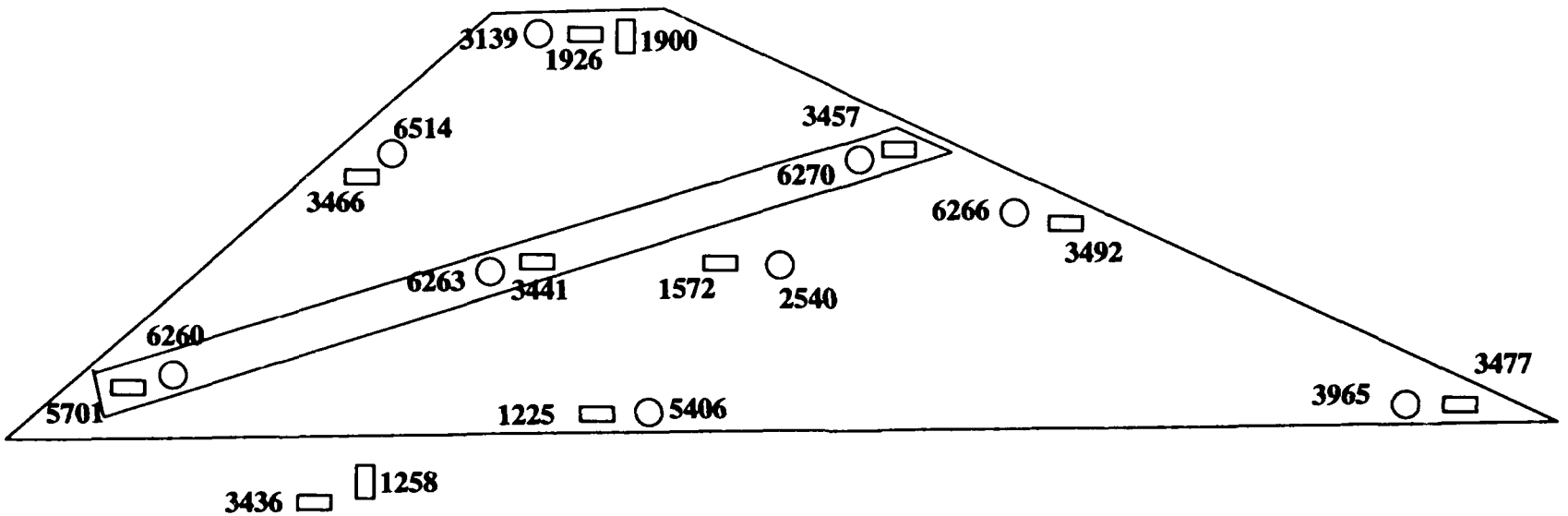

Fig.9.2 Placement of transducers in centrifuge test LEG-2

920 datapoints plotted per complete transducer record

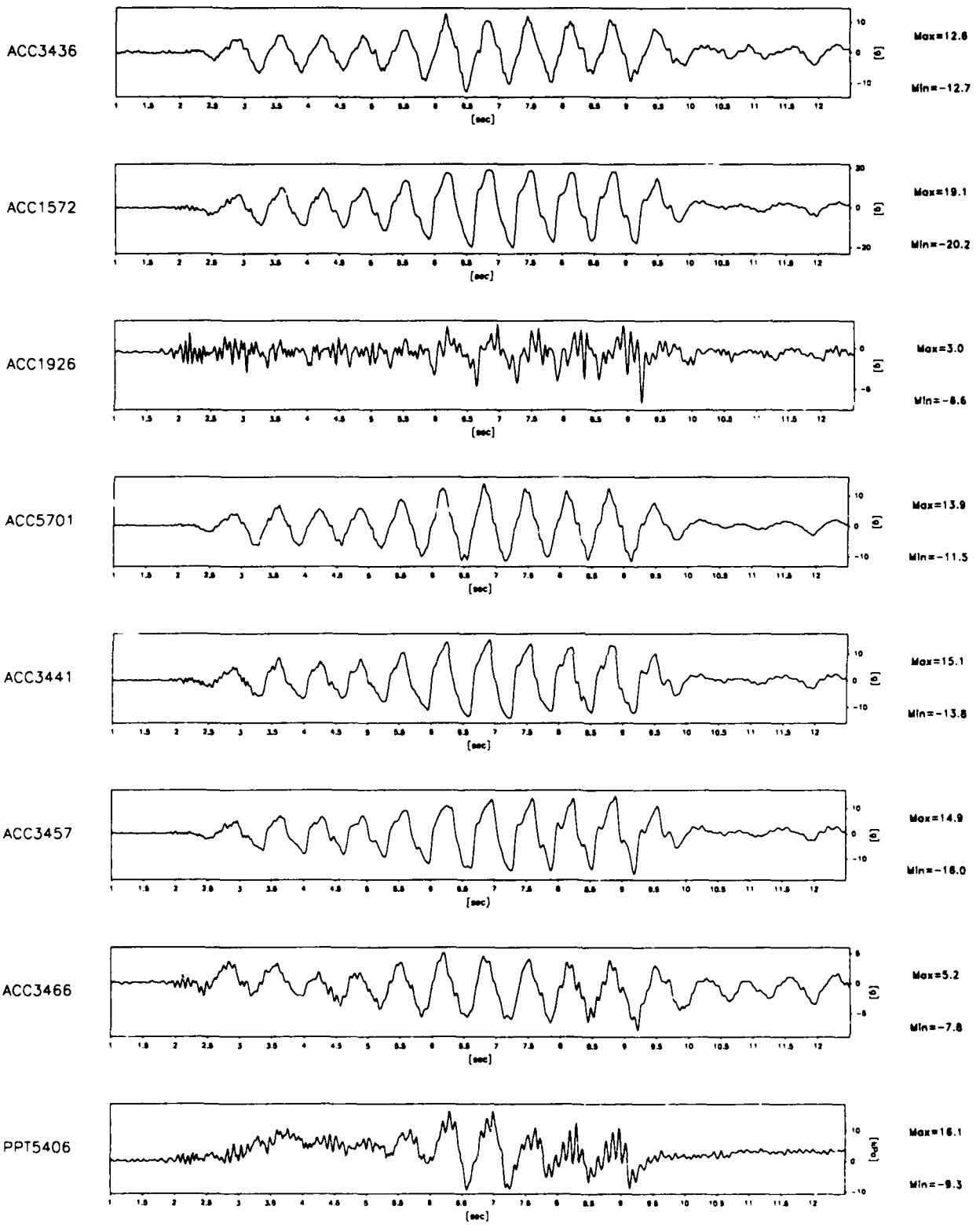

Scales : Prototype

TEST LEG-2 MODEL SAT FLIGHT -1	EQ-1	SHORT TERM TIME RECORDS	G Level 80	FIG.NO. 9.3

920 datapoints plotted per complete transducer record

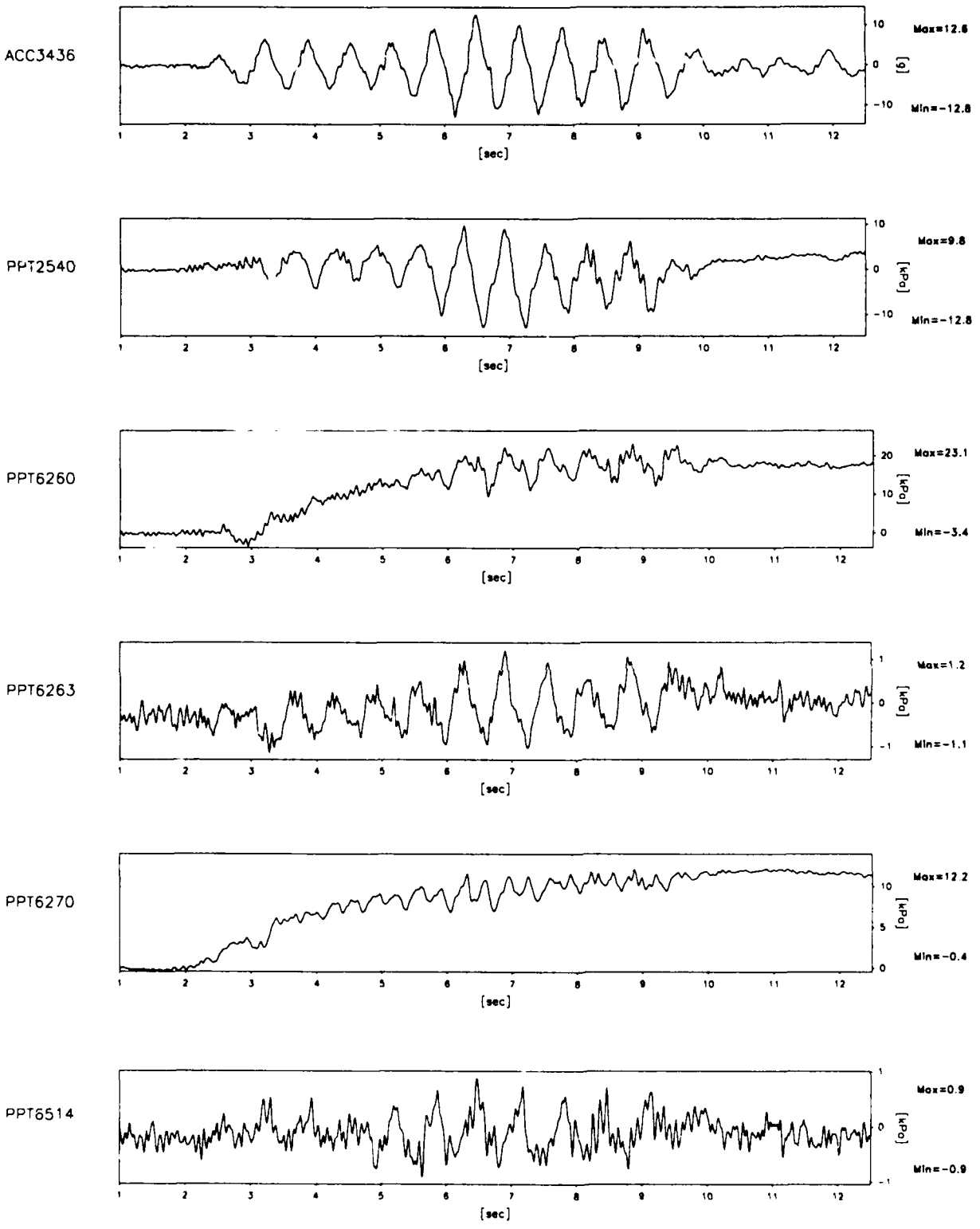

Scales : Prototype

TEST LEG-2 MODEL SAT FLIGHT -1	EQ-1	SHORT TERM TIME RECORDS	G Level 80	FIG.NO. 9.4

921 datapoints plotted per complete transducer record

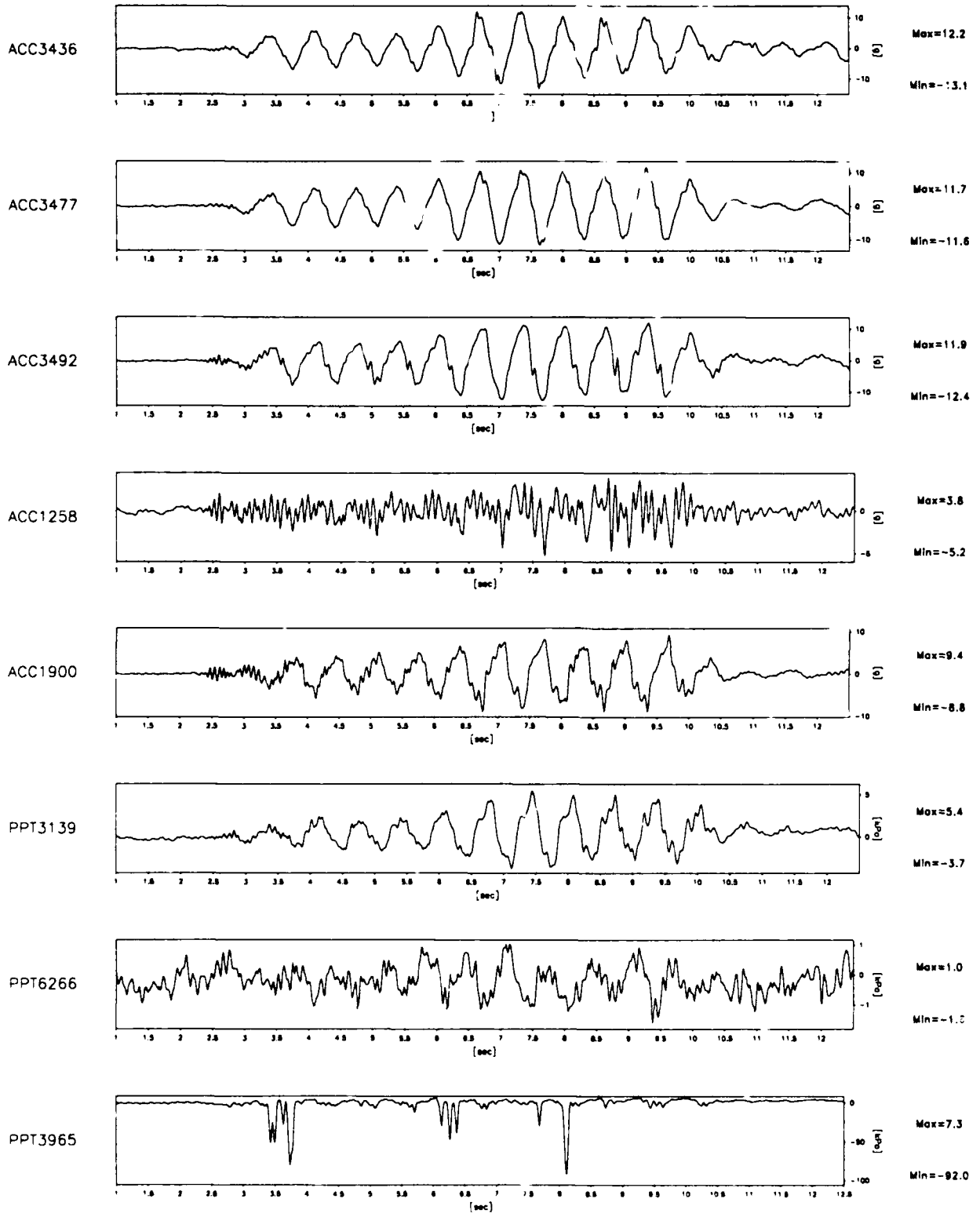

Scales : Prototype

TEST LEG-2 MODEL SAT FLIGHT -1	EQ-1	SHORT TERM TIME RECORDS	G Level 80	FIG.NO. 9.5

930 datapoints plotted per complete transducer record

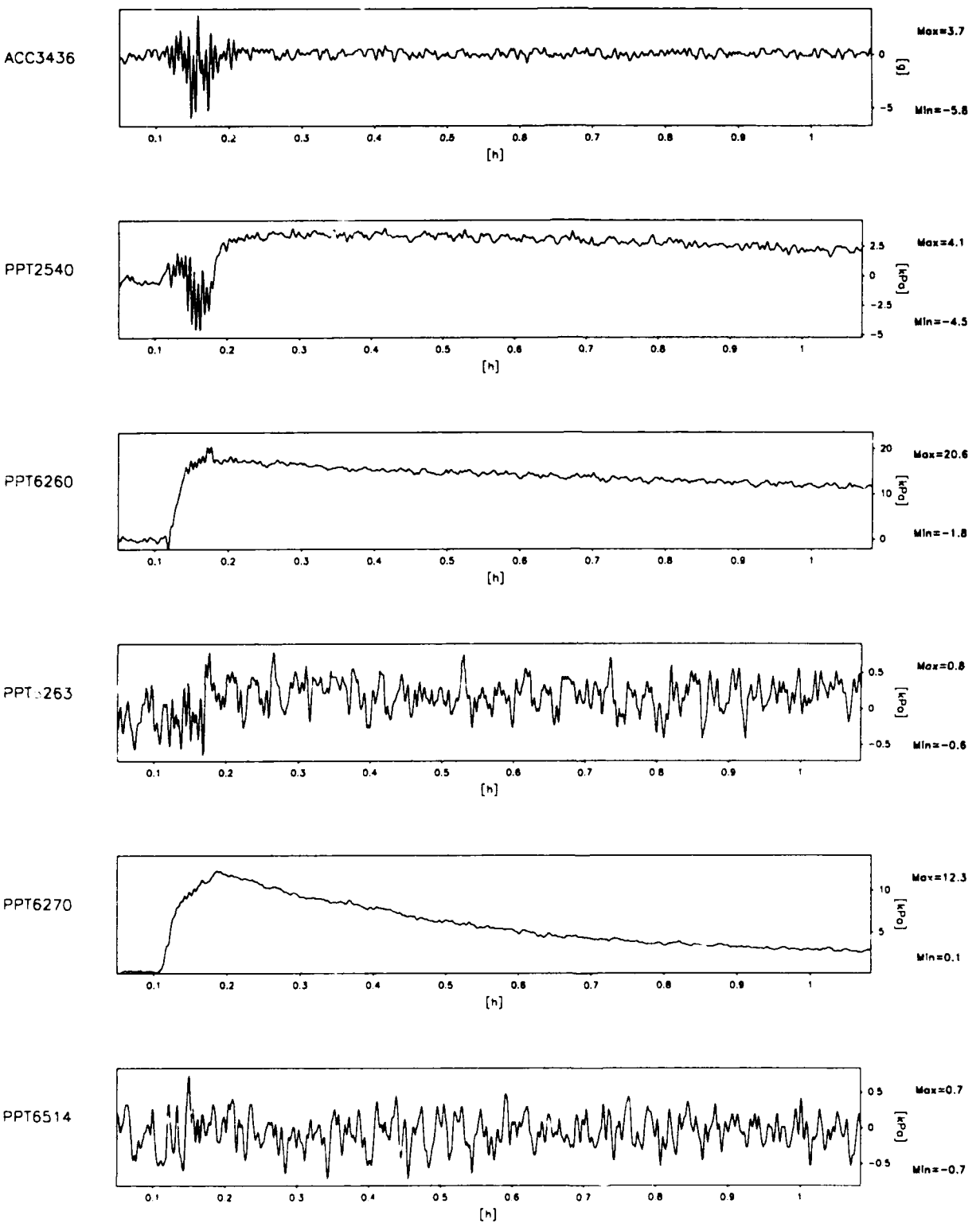

Scales : Prototype

TEST LEG-2 MODEL SAT FLIGHT -1	EQ-1	LONG TERM TIME RECORDS	G Level 80	FIG.NO. **9.6**

931 datapoints plotted per complete transducer record

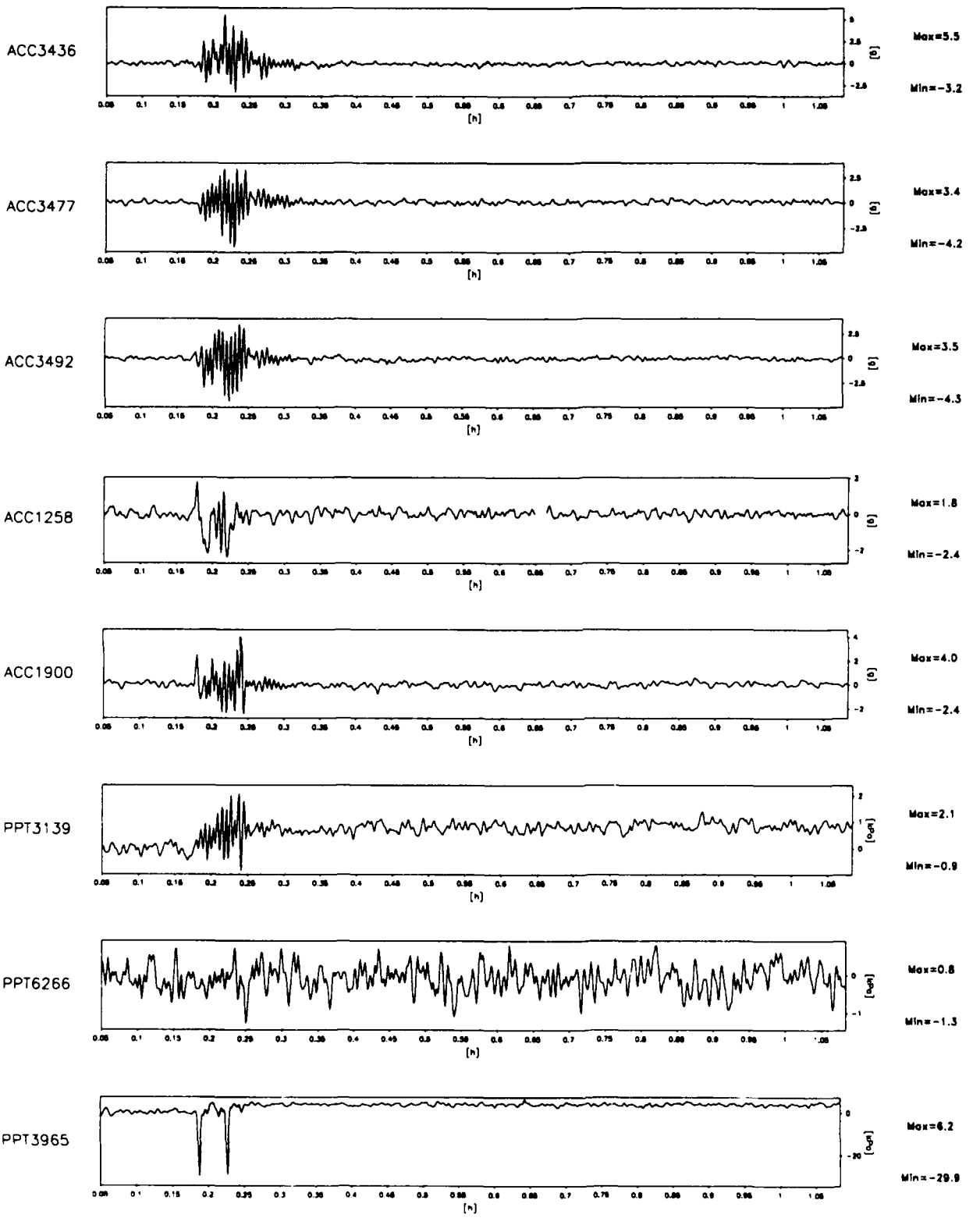

Scales : Prototype

TEST LEG-2 MODEL SAT FLIGHT -1	EQ-1	LONG TERM TIME RECORDS	G Level 80	FIG.NO. 9.7

920 datapoints plotted per complete transducer record

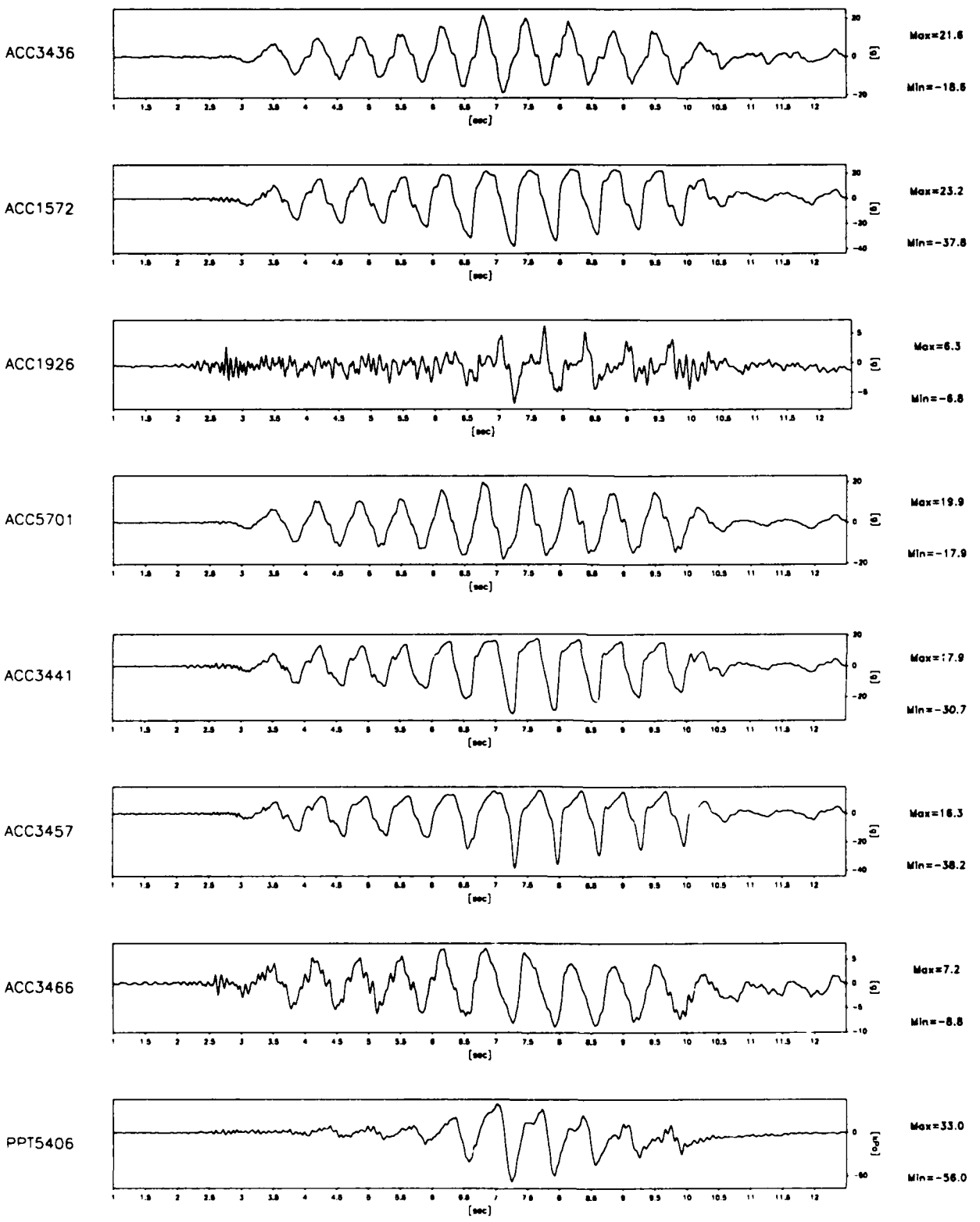

Scales : Prototype

TEST LEG-2 MODEL SAT FLIGHT -1	EQ-2	SHORT TERM TIME RECORDS	G Level 80	FIG.NO. **9.8**

920 datapoints plotted per complete transducer record

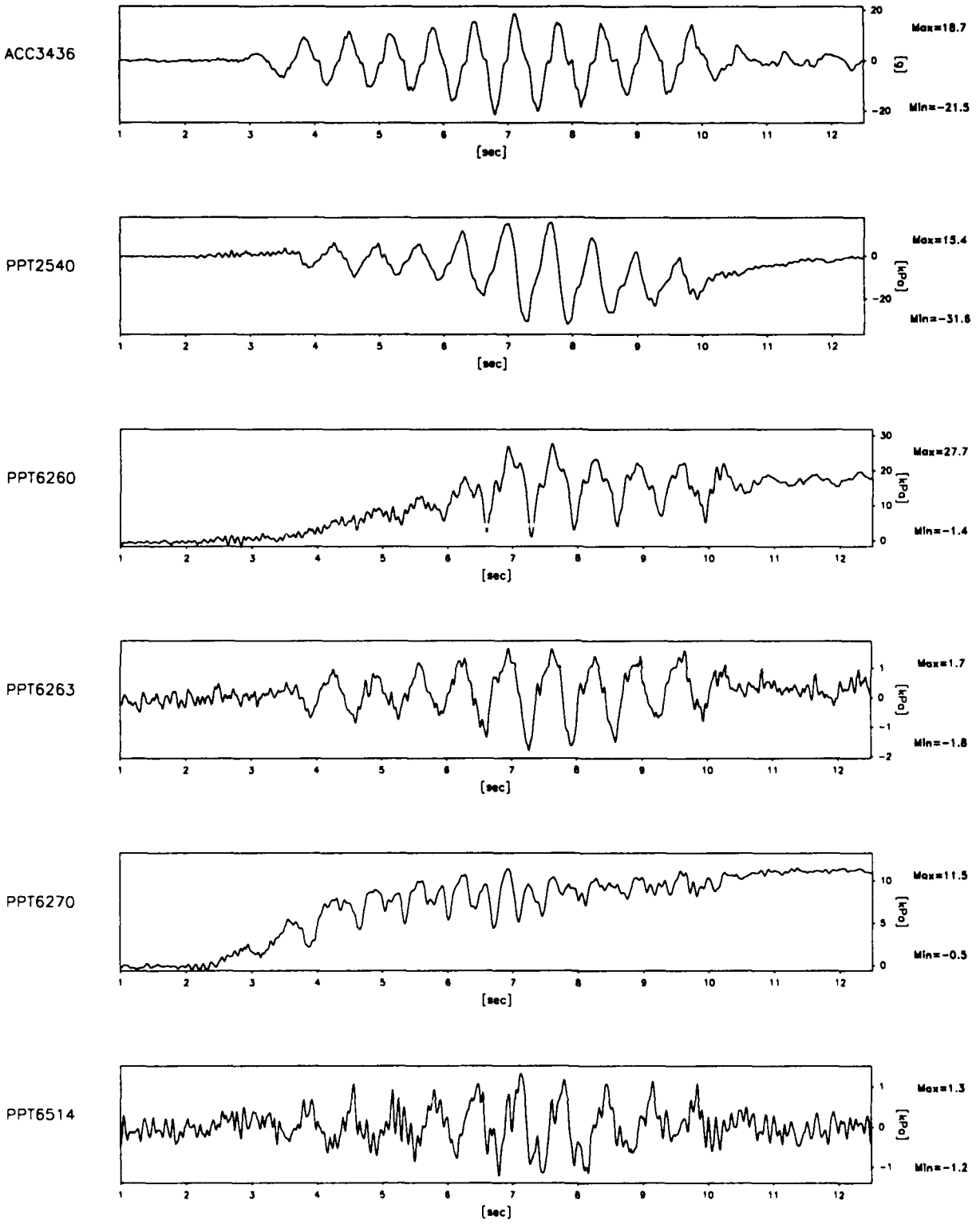

Scales : Prototype

TEST LEG-2 MODEL SAT FLIGHT -1	EQ-2	SHORT TERM TIME RECORDS	G Level 80	FIG.NO. **9.9**

921 datapoints plotted per complete transducer record

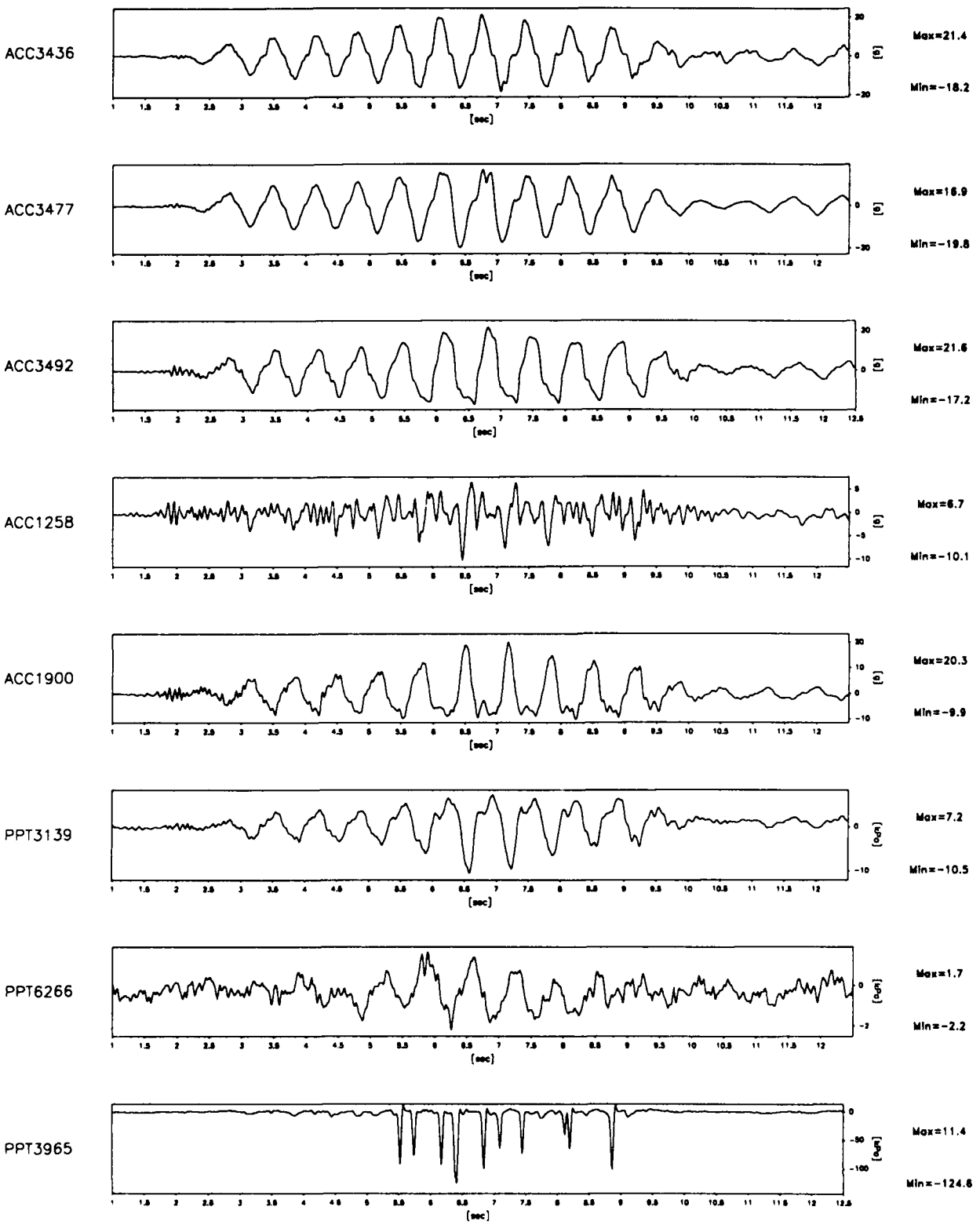

Scales : Prototype

TEST LEG-2 MODEL SAT FLIGHT -1	EQ-2	SHORT TERM TIME RECORDS	G Level 80	FIG.NO. **9.10**

930 datapoints plotted per complete transducer record

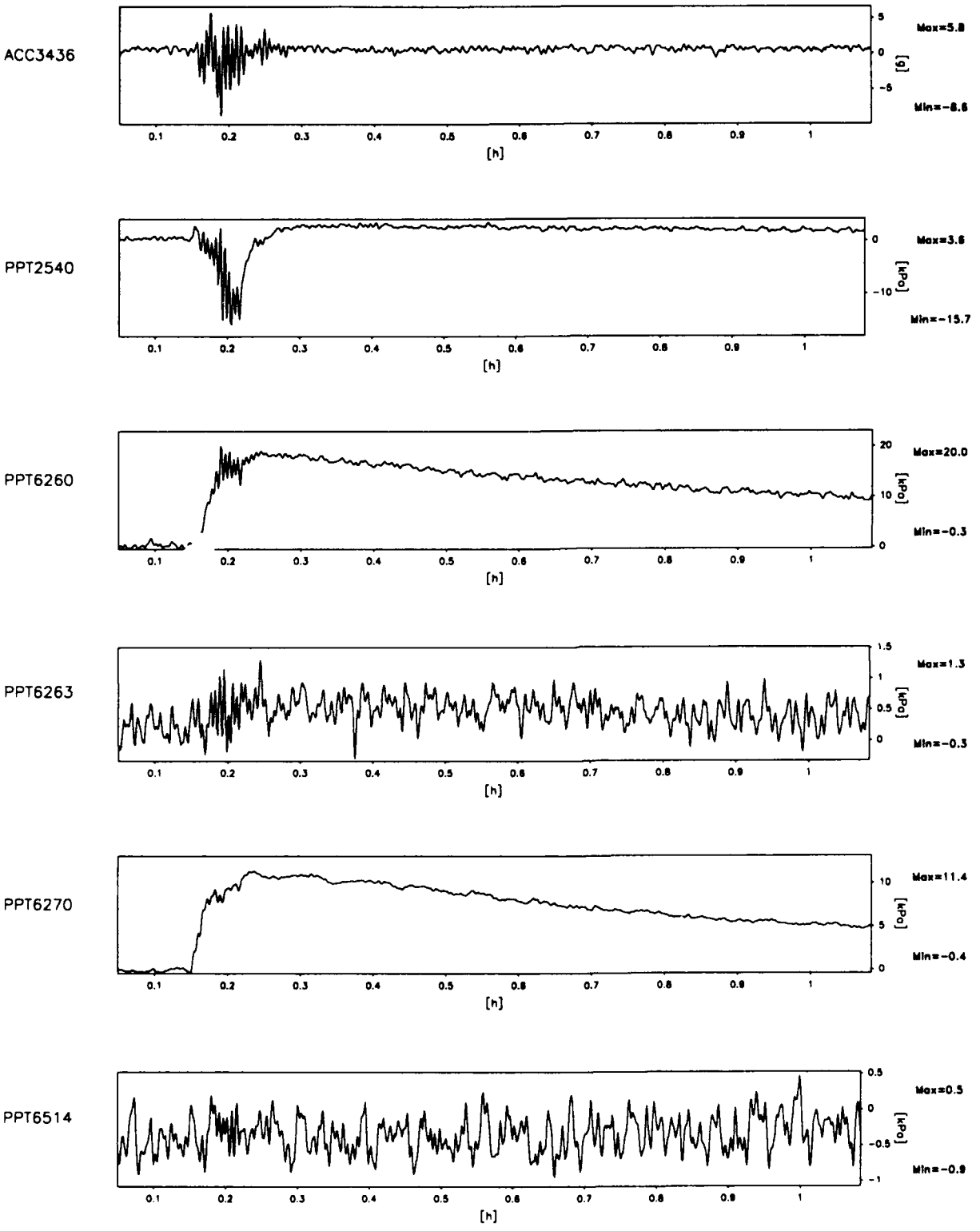

Scales : Prototype

TEST LEG-2 MODEL SAT FLIGHT -1	EQ-2	LONG TERM TIME RECORDS	G Level 80	FIG.NO. **9.11**

931 datapoints plotted per complete transducer record

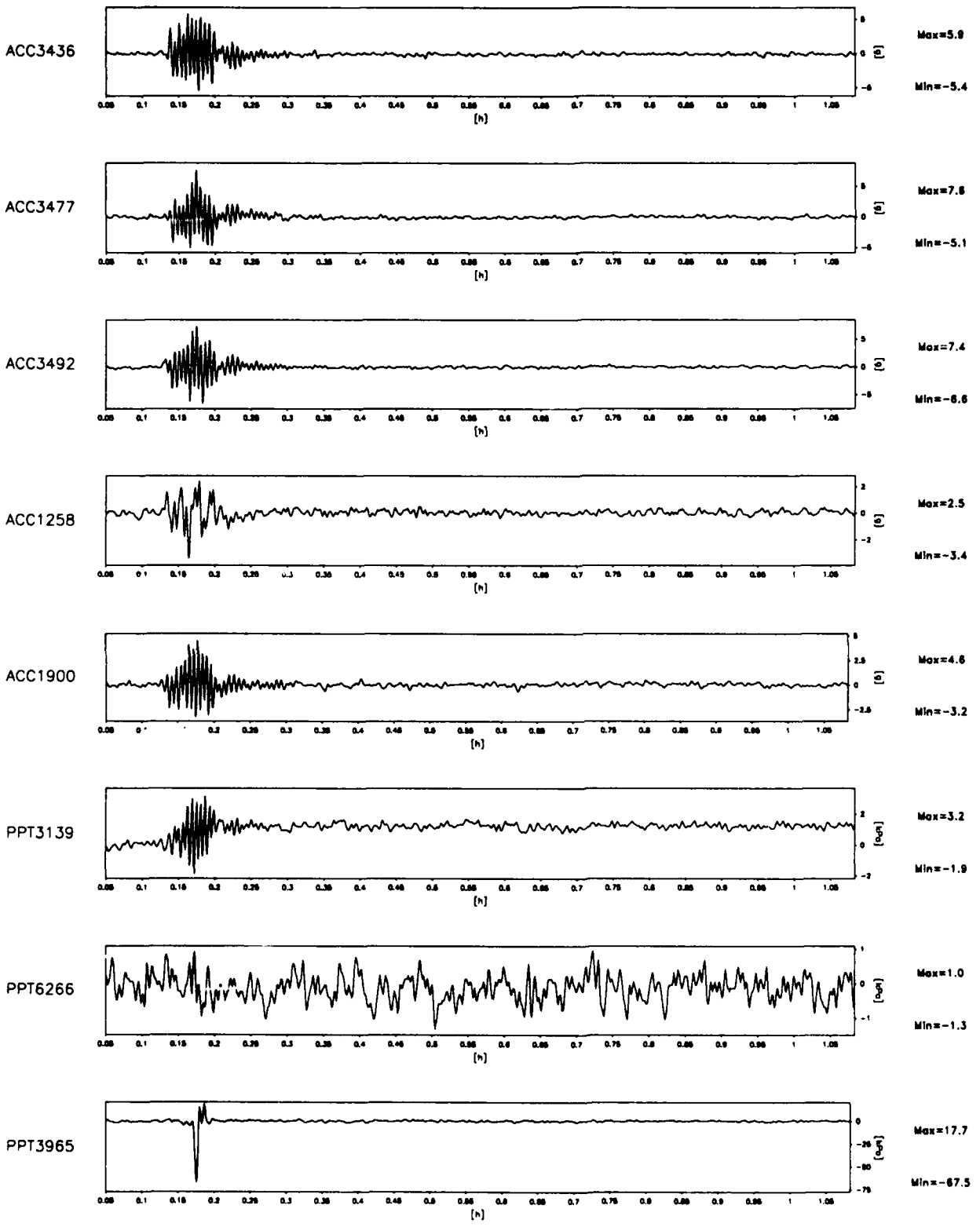

Scales : Prototype

TEST LEG-2 MODEL SAT FLIGHT -1	EQ-2	LONG TERM TIME RECORDS	G Level 80	FIG.NO. **9.12**

920 datapoints plotted per complete transducer record

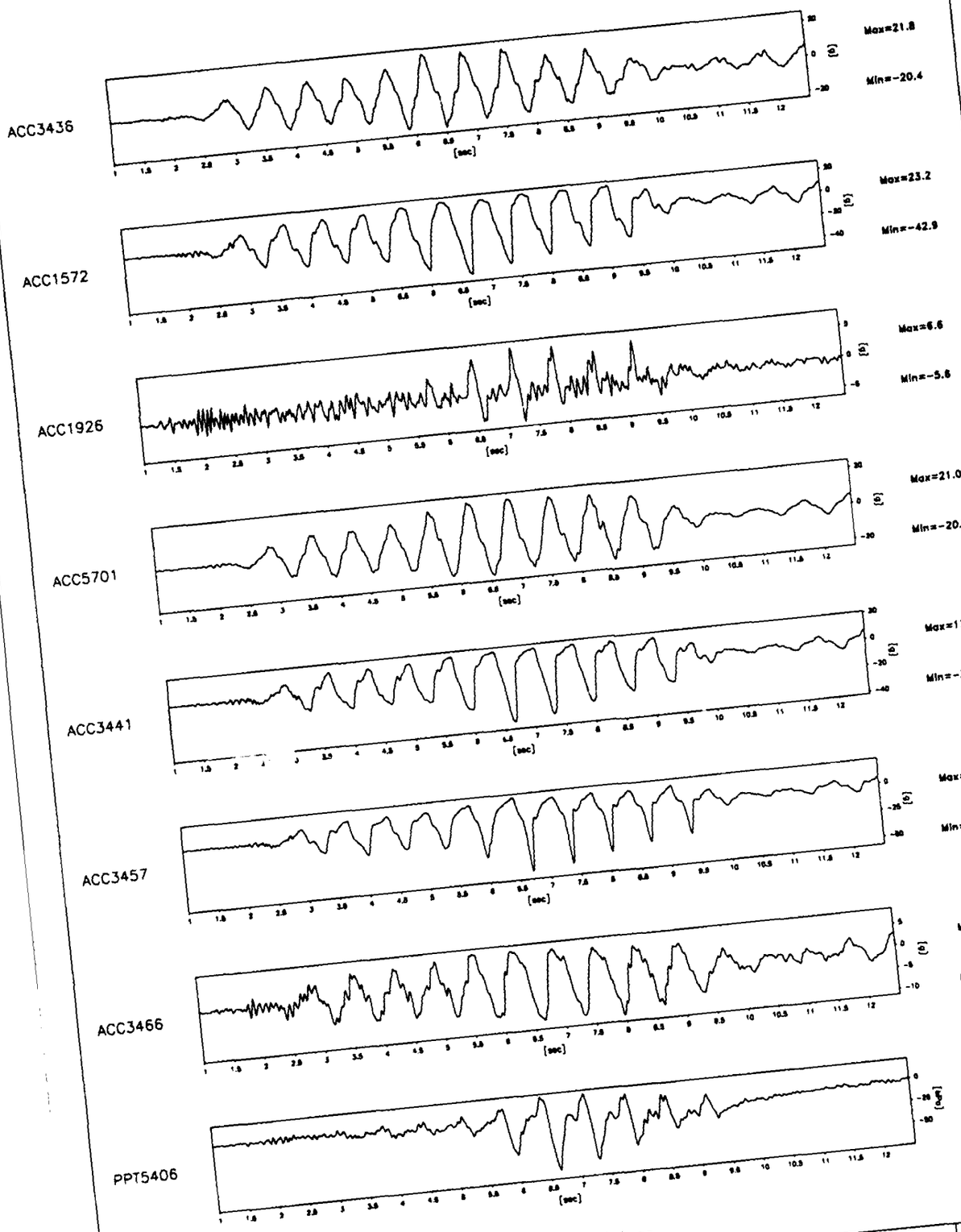

Scales : Prototype

TEST LEG-2 MODEL SAT FLIGHT -1	EQ-3	SHORT TERM TIME RECORDS	G Level 80	FIG.NO. 9.13

920 datapoints plotted per complete transducer record

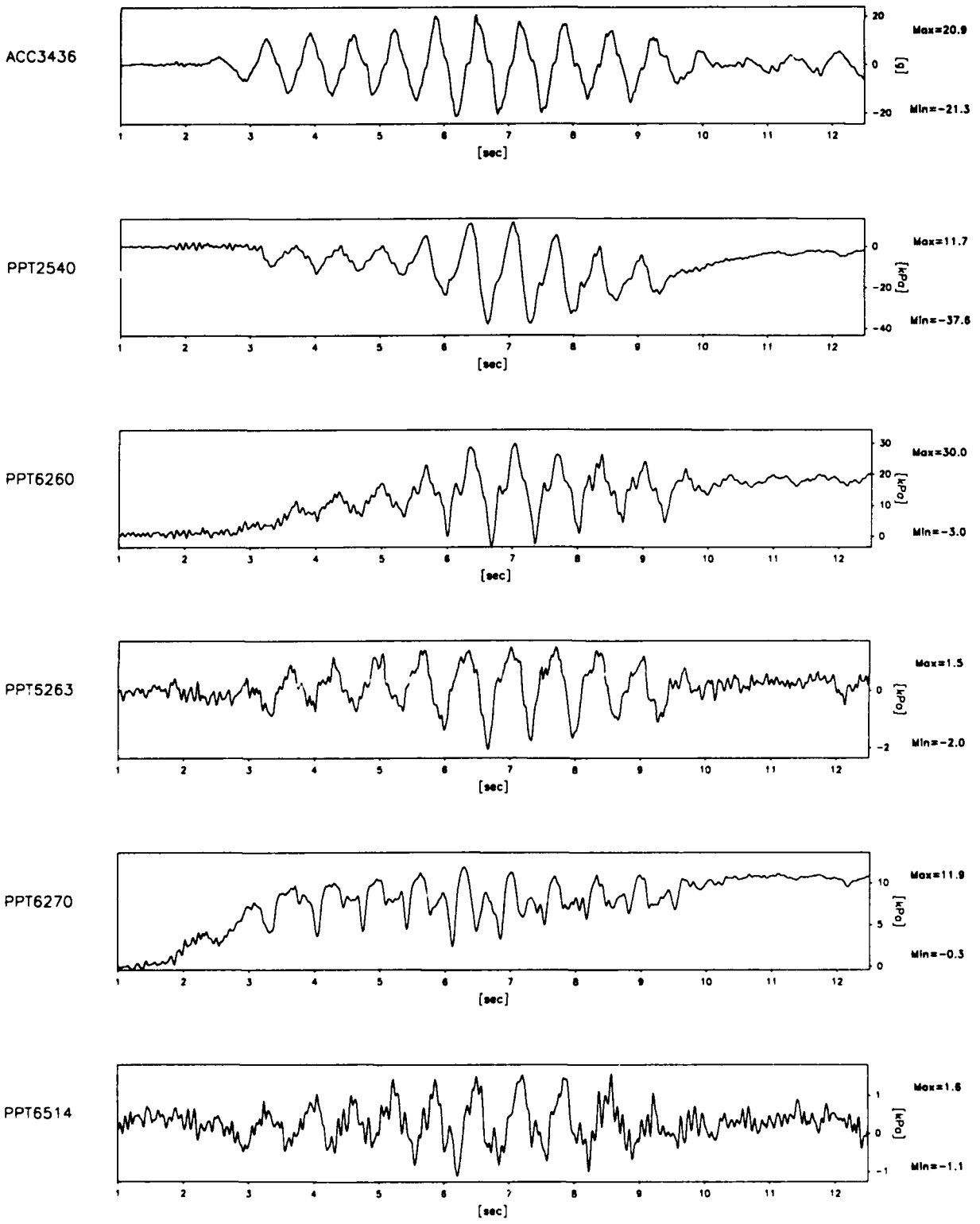

Scales : Prototype

TEST LEG-2 MODEL SAT FLIGHT -1	EQ-3	SHORT TERM TIME RECORDS	G Level 80	FIG.NO. 9.14

921 datapoints plotted per complete transducer record

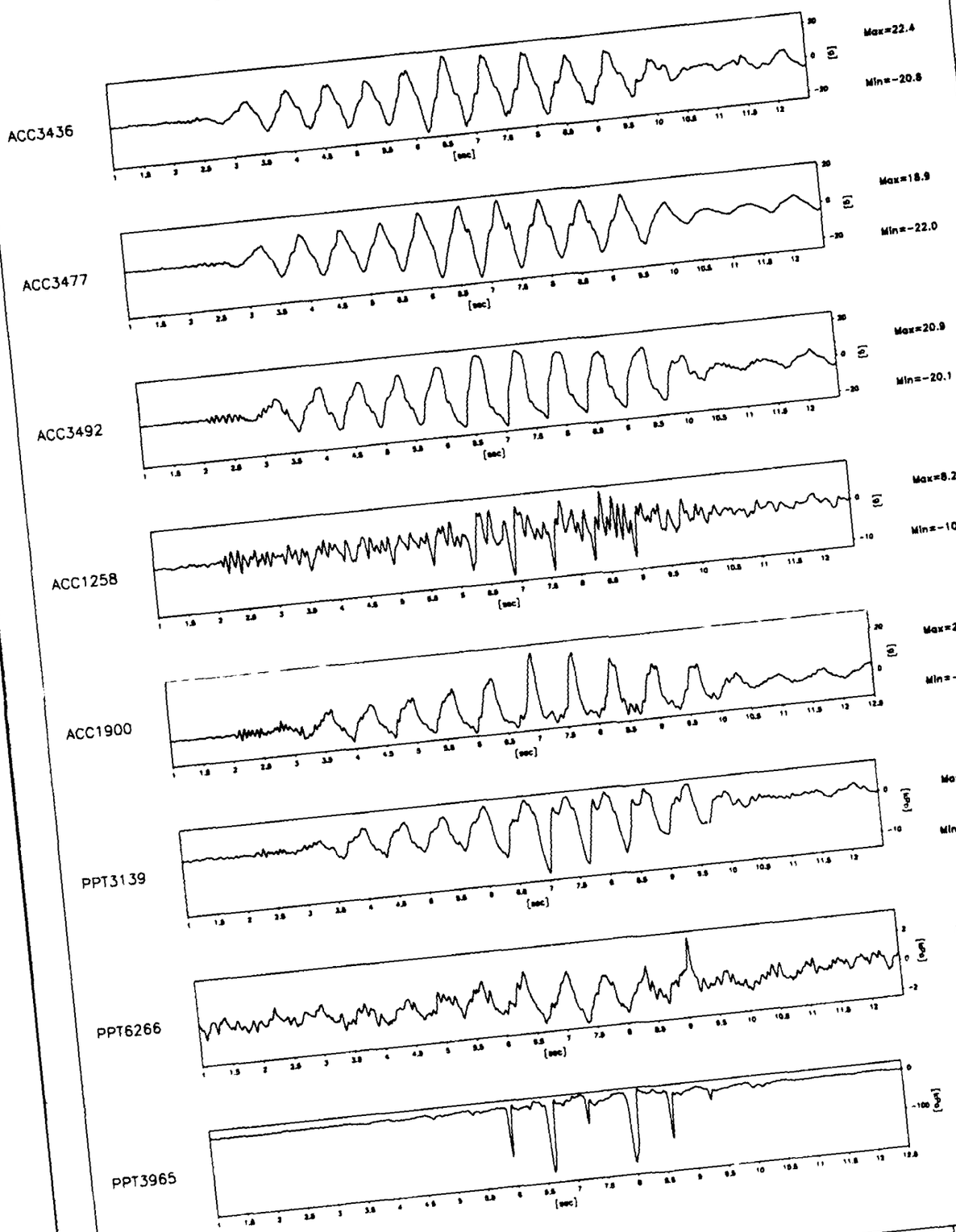

Scales : Prototype

TEST LEG-2 MODEL SAT FLIGHT -1	EQ-3	SHORT TERM TIME RECORDS	G Level 80	FIG.NO. 9.15

930 datapoints plotted per complete transducer record

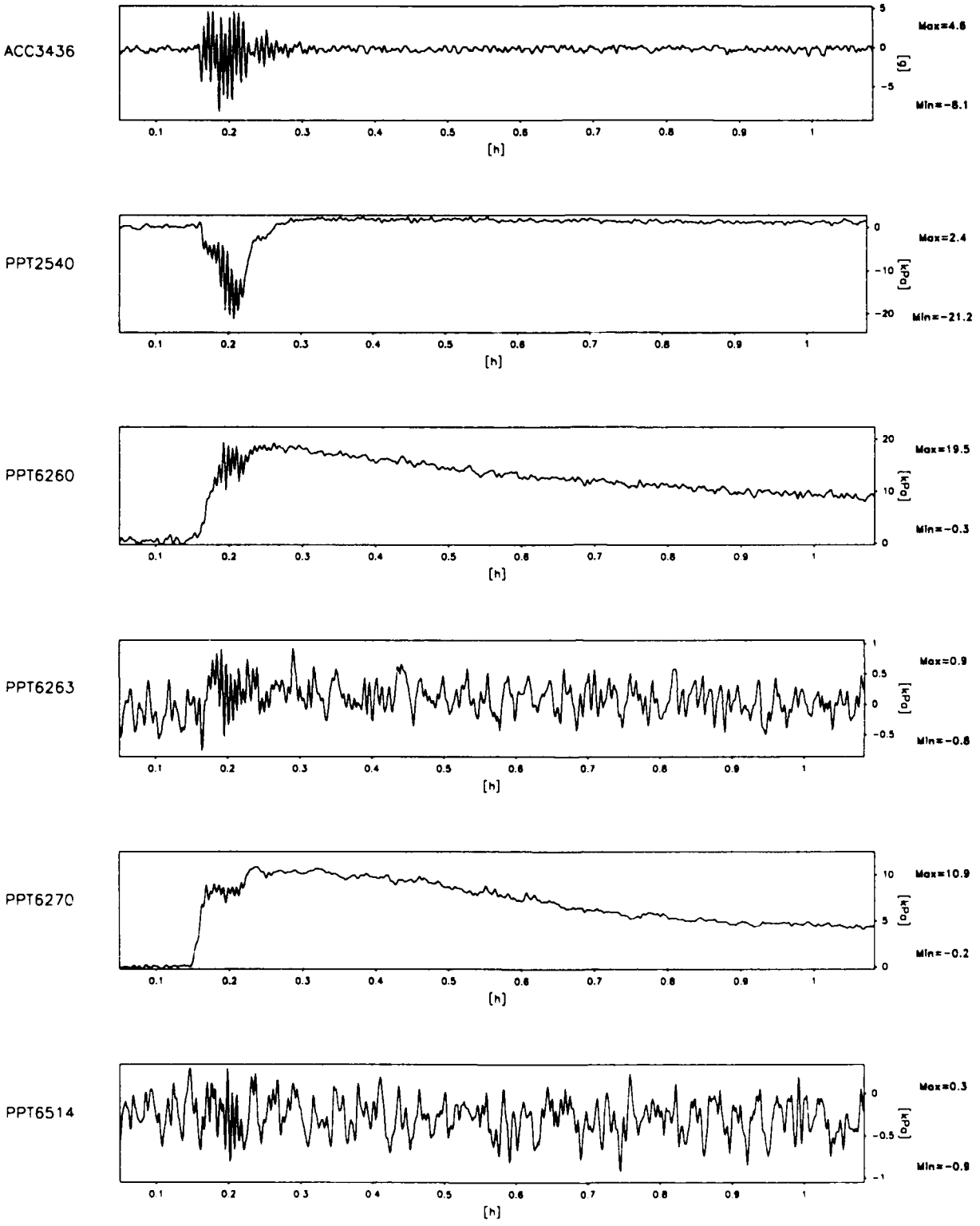

Scales : Prototype

TEST LEG-2 MODEL SAT FLIGHT -1	EQ-3	LONG TERM TIME RECORDS	G Level 80	FIG.NO. 9.16

931 datapoints plotted per complete transducer record

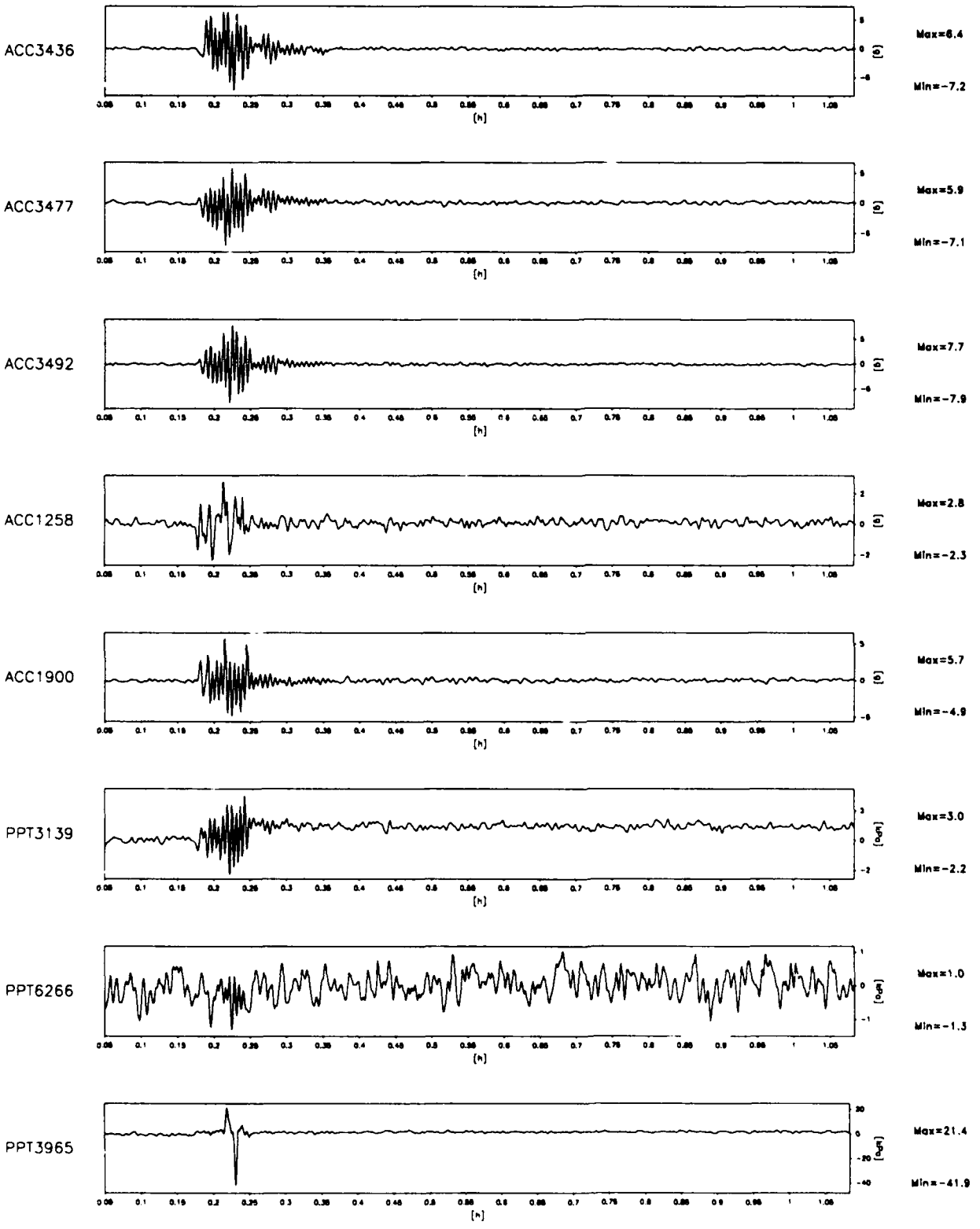

Scales : Prototype

TEST LEG-2 MODEL SAT FLIGHT -1	EQ-3	LONG TERM TIME RECORDS	G Level 80	FIG.NO. 9.17

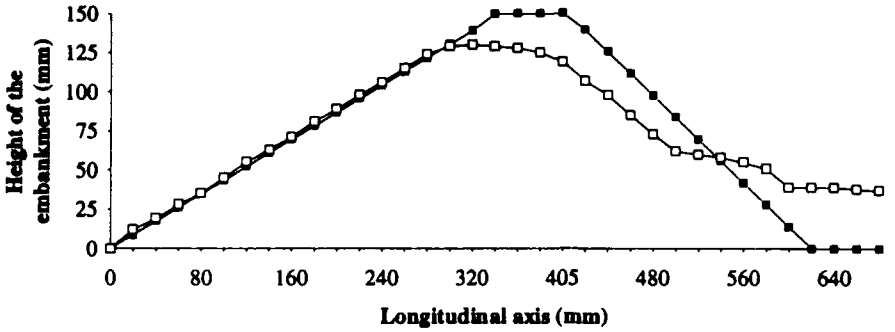

Fig.9.18 Post test profile of centrifuge model LEG-2

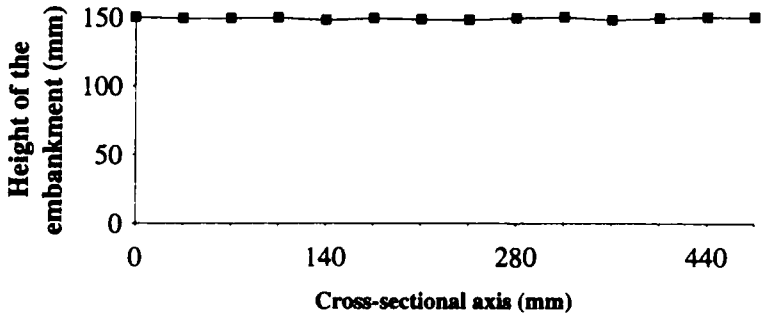

Fig.9.19 Post test profile along the cross section of centrifuge model

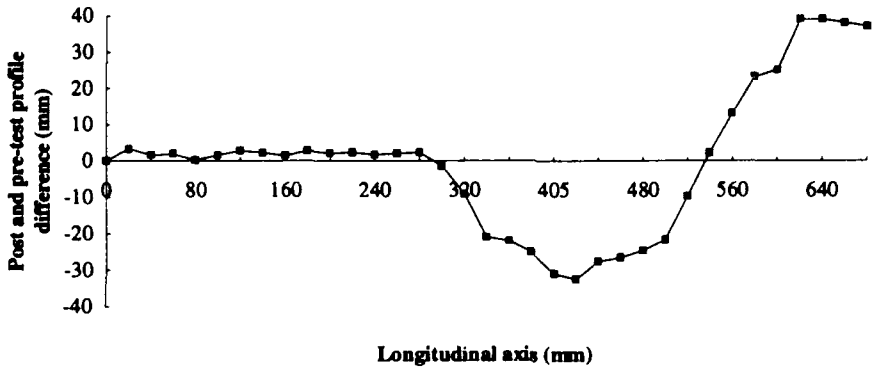

Fig.9.20 Post and Pre-test profile difference along the longitudinal axis in centrifuge test LEG-2

10.0 Centrifuge Test LEG-3

10.1 Configuration of the test

In the third centrifuge test LEG-3 the down stream slope was 35^{o} and the up stream slope was 21^{o} . The loose layer of sand was inclined at an angle of 15^{o} and had a thickness of 15 mm. This slope is much flatter than in the previous two tests. Also the location of the loose section was much more deeper than in the other tests. The reason for this is to try and mobilise a deeper failure mechanism of the down stream slope. The dense section of the embankment was constructed using coarse Leighton Buzzard 14/25 sand. The loose section of the embankment was constructed using fine Leighton Buzzard 100/170 sand as explained in section 6.0. The schematic diagram showing the cross section of the model is presented in Fig.10.1. The placement of transducers is shown in Fig.10.2. In this test it was decided to confine the loose section of the embankment using very fine rock flour to sustain the excess pore pressure built up during the earthquake loading for a longer time. Accordingly a thin layer of rock flour was introduced at the top and bottom interfaces between the loose section and the dense sections of the embankment as in the second test.

10.2 Test data

In this test the down stream slope suffered a slip resulting in the movement of the crest towards the down stream toe of the embankment. The slip surface was along the loose section of the sand as shown in Fig.10.1 (zone B). The dry densities of each of the zones in Fig.10.1 together with the void ratio and relative densities for this centrifuge model are presented in Table 10.1. The hydrostatic pore pressures recorded during the swing up of the centrifuge and increase of the centrifugal acceleration to 80g and after each earthquake are presented in Table 10.2. The data recorded during this test are presented in Figs.10.3 to 10.30. Also the slip plane was nearer to the loose zone resulting in a deeper failure mechanism as anticipated. The accelerometer 1926 placed in the crest of the embankment registered strong acceleration in one direction suggesting the slipping of the crest in one direction. This is supported by the accelerometer traces 3477 and 3466 which are also in this region. ACC 3441 and 3492 have flat top peaks suggesting the slipping of the down stream slope. The traces recorded by the accelerometers in the up stream slope were more or less uniform

suggesting no movement of this slope. The post test profile measured after the test confirmed this.

The pore pressure traces recorded in the crest section by PPT 3139 showed strong suctions. Similarly the pore pressures recorded in the lower dense section (shown in Fig.1) by PPT 5406 and 6266 showed strong suction pressures. This shows that the dense zones were dilating and under the suction pressures they would behave almost like rigid blocks. In the loose section there was a much larger excess pore pressure which was retained for a very long time due to the impermeable rock flour interface between the loose and dense sections. During the model earthquake the loose section was the slip plane available for the down stream slope as there were excess pore pressures in this zone and it was at a higher pore pressure than the other two zones. The slow dissipation of the excess pore pressure in the loose zone is revealed in the long term traces. During this test PPT 6260 has floated partially and PPT 6514 moved by about 18 mm towards the down stream slope side. Pore pressure transducer 6514 can be seen in Plate 10.1.

10.3 Post test profile

The post test profile measured after the centrifuge test is presented in Fig.10.31 together with the original profile of the embankment. The post test profile is measured at various longitudinal sections and the average profile is shown in this figure. Also the cross sectional profile is shown in Fig.10.32 which suggests that the slip is more or less uniform across the model embankment. From the post test profiles it can be clearly seen that there is a slip on the down stream slope side of the embankment. The up stream slope is relatively unchanged before and after the earthquakes. This can be observed by comparing the up stream and down stream slopes in Plate 10.2. It is possible to estimate the quantity of the soil movement resulting when the model embankment is subjected to the earthquake loading. In order to estimate the quantity of soil moved during the earthquakes, the difference of the embankment profiles before and after the earthquakes is plotted. This graph is presented in Fig.10.33. Using the numerical integration procedure given by Simpson's rule, the area under the curve shown in Fig.10.33 is estimated. Using this area the volume of the soil movement resulting from the earthquake loading is estimated. The quantity of soil which slipped from the crest of the embankment was 2.2805×10^{-3} m^3 and the quantity of soil deposited at the toe of the embankment is 1.614×10^{-3} m^3. In prototype terms these

quantities are 1167.6 m^3 and 826.8 m^3 respectively. The differential volume which may indicate the error in measurement of the post test profile is 2.72 % of the total volume of the embankment.

Table 10.1 Dry density of sand in different zones of the embankment in centrifuge test LEG-3

Zone*	γ_d (kg/m^3)	void ratio (e)	Relative Density (%)
A	1620.5	0.635	61.10
B	1341.0	0.976	11.14
C	1598.7	0.658	56.90

* see Fig.10.1 for zone specification

Table 10.2 Hydrostatic pore pressures recorded in centrifuge test LEG-3

Device	kPa/V	20-G kPa	40-G kPa	60-G kPa	80-G kPa	EQ-1 kPa	EQ-2 kPa	EQ-3 kPa	EQ-4 kPa
PPT2540	361.77	16.88	34.30	51.02	69.71	67.36	67.09	66.91	2.33
PPT3139	379.53	3.82	8.08	12.20	16.63	20.56	18.51	19.27	0.16
PPT6514	350.88	1.38	2.80	4.17	5.76	5.58	5.47	5.51	0.02
PPT6260	365.88	23.17	47.74	71.37	96.40	93.51	91.57	90.84	89.92
PPT6263	365.27	1.89	3.92	5.81	7.82	7.71	7.71	7.75	0.03
PPT6270	385.84	10.63	21.98	32.47	43.58	42.81	41.53	41.15	0.82
PPT6266	440.55	1.84	3.73	5.43	7.28	7.28	7.46	7.50	0.02
PPT3965	405.50	19.77	41.37	44.25	34.52	8.97	-22.86	-23.27	-27.04
PPT5406	393.98	23.66	30.99	ERR	ERR	91.54	91.47	92.69	93.00
PPT3112	4030.97	22.54	46.14	67.95	90.52	90.12	89.72	90.12	90.12

Plate 2a — Partial floatation of PPT 6514 during the centrifuge test LEG 3

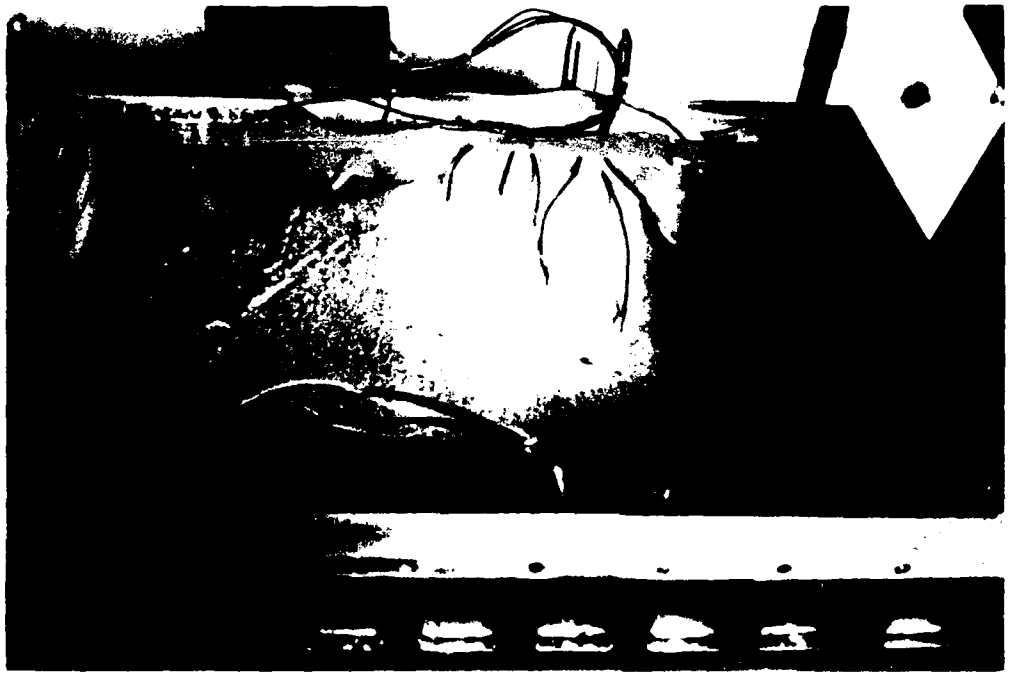

Plate 2b — View of model embankment after centrifuge test LEG
Note that the upstream slope
The downstream slope

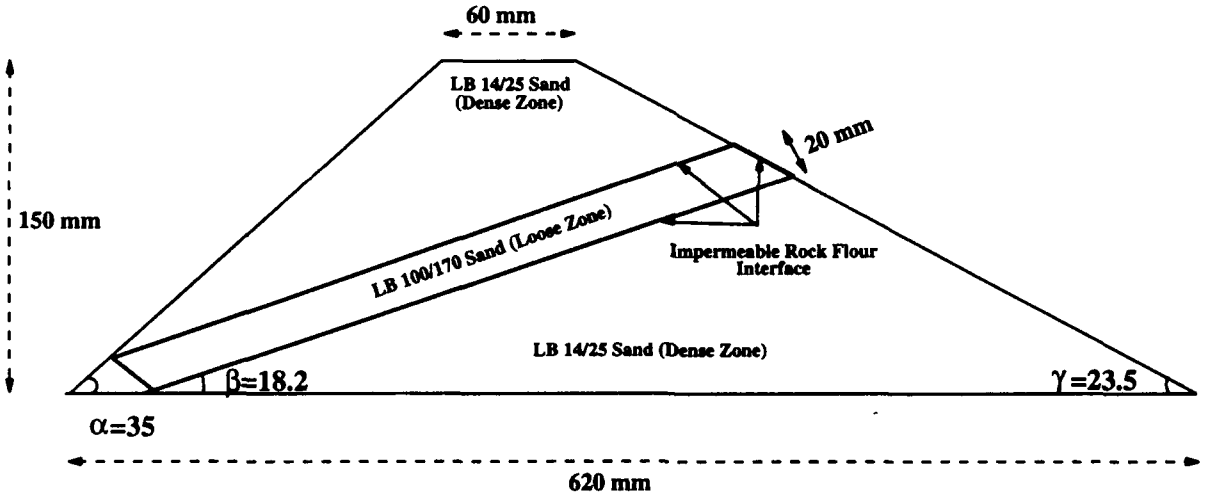

Fig.10.1 Cross section of the centrifuge model LEG-3

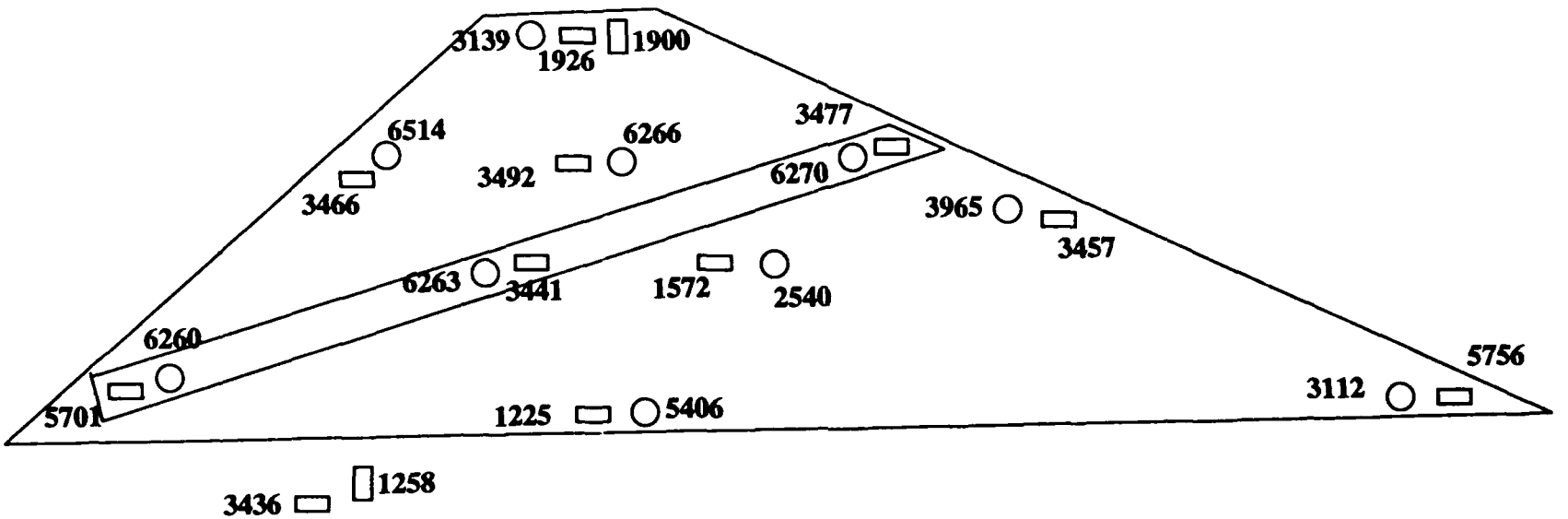

Fig.10.2 Placement of transducers in centrifuge test LEG-3

920 datapoints plotted per complete transducer record

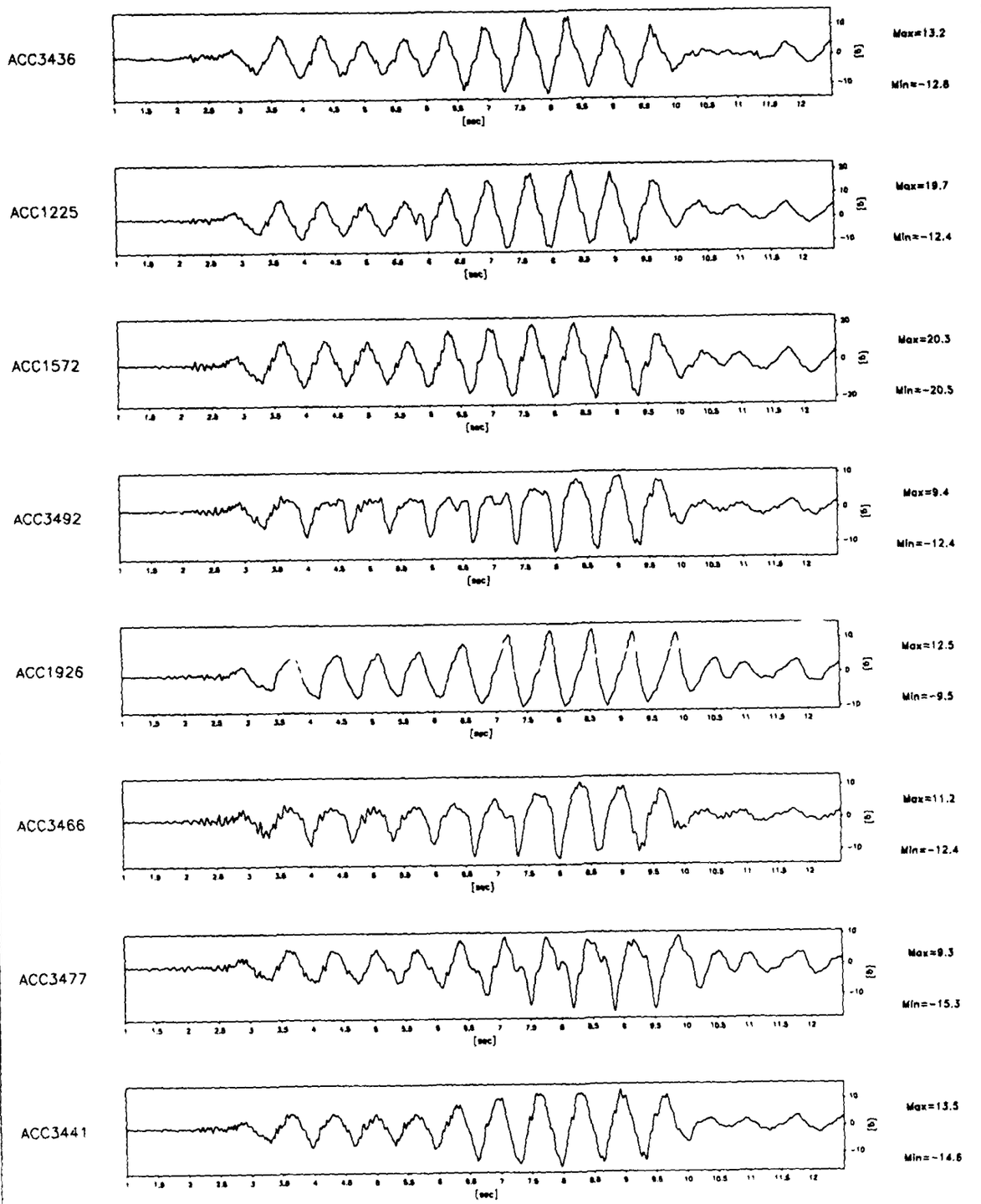

Scales : Prototype

TEST LEG-3 MODEL SAT FLIGHT -1	EQ-1	SHORT TERM TIME RECORDS	G Level 80	FIG.NO. 10.3

920 datapoints plotted per complete transducer record

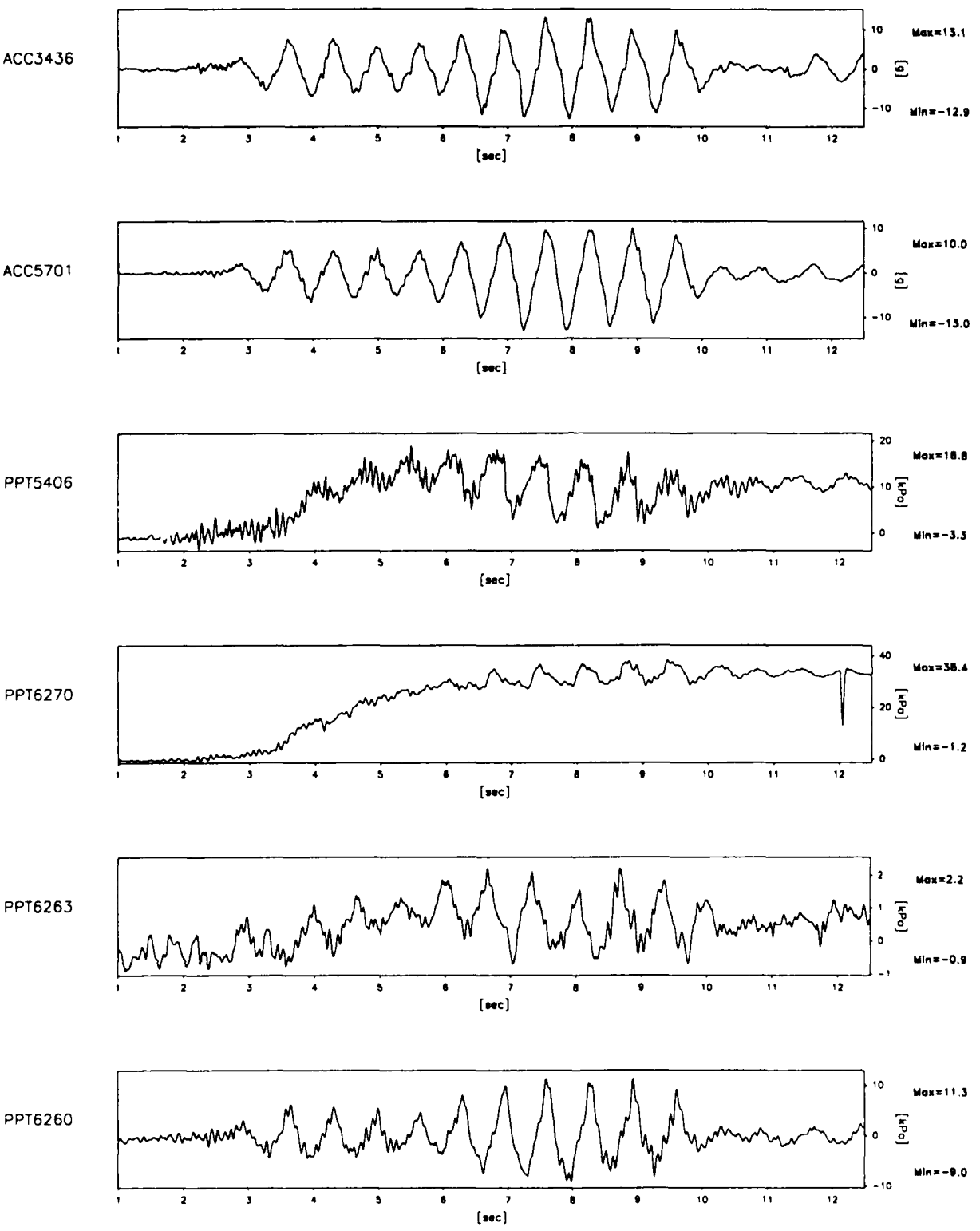

Scales : Prototype

TEST LEG-3 MODEL SAT FLIGHT -1	EQ-1	SHORT TERM TIME RECORDS	G Level 80	FIG.NO. **10.4**

841 datapoints plotted per complete transducer record

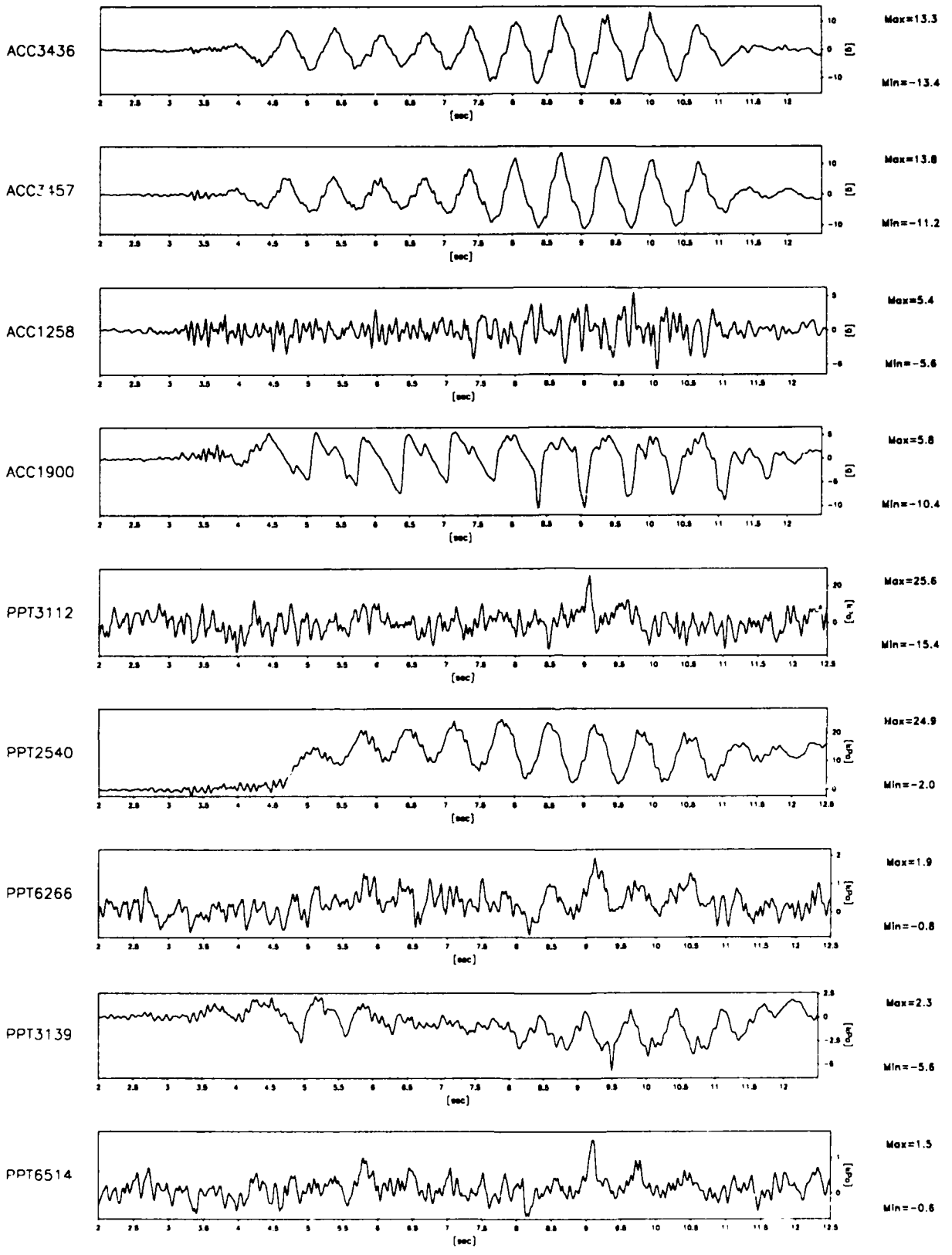

Scales : Prototype

TEST LEG-3 MODEL SAT FLIGHT -1	EQ-1	SHORT TERM TIME RECORDS	G Level 80	FIG.NO. 10.5

841 datapoints plotted per complete transducer record

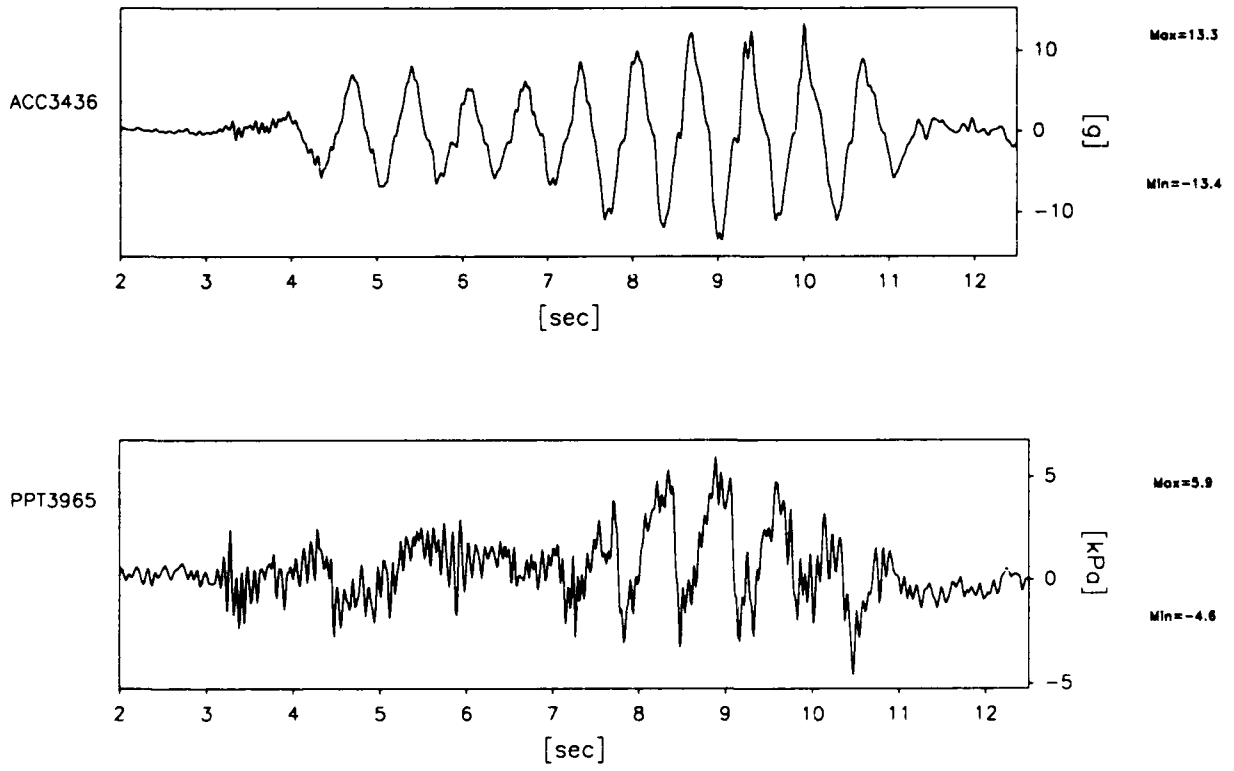

Scales : Prototype

TEST LEG-3 MODEL SAT FLIGHT -1	EQ-1	SHORT TERM TIME RECORDS	G Level 80	FIG.NO. **10.6**

930 datapoints plotted per complete transducer record

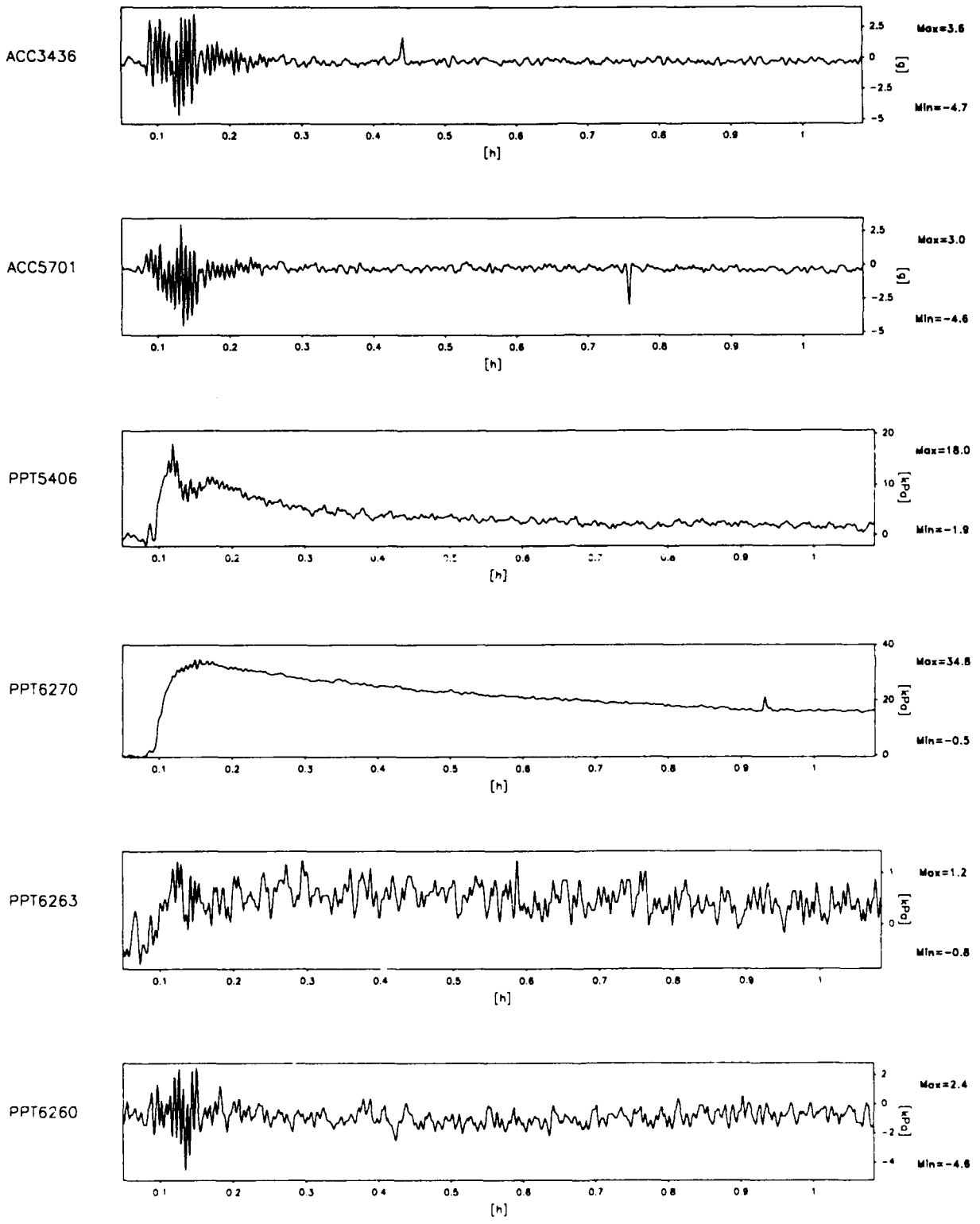

Scales : Prototype

TEST LEG-3 MODEL SAT FLIGHT -1	EQ-1	LONG TERM TIME RECORDS	G Level 80	FIG.NO. **10.7**

931 datapoints plotted per complete transducer record

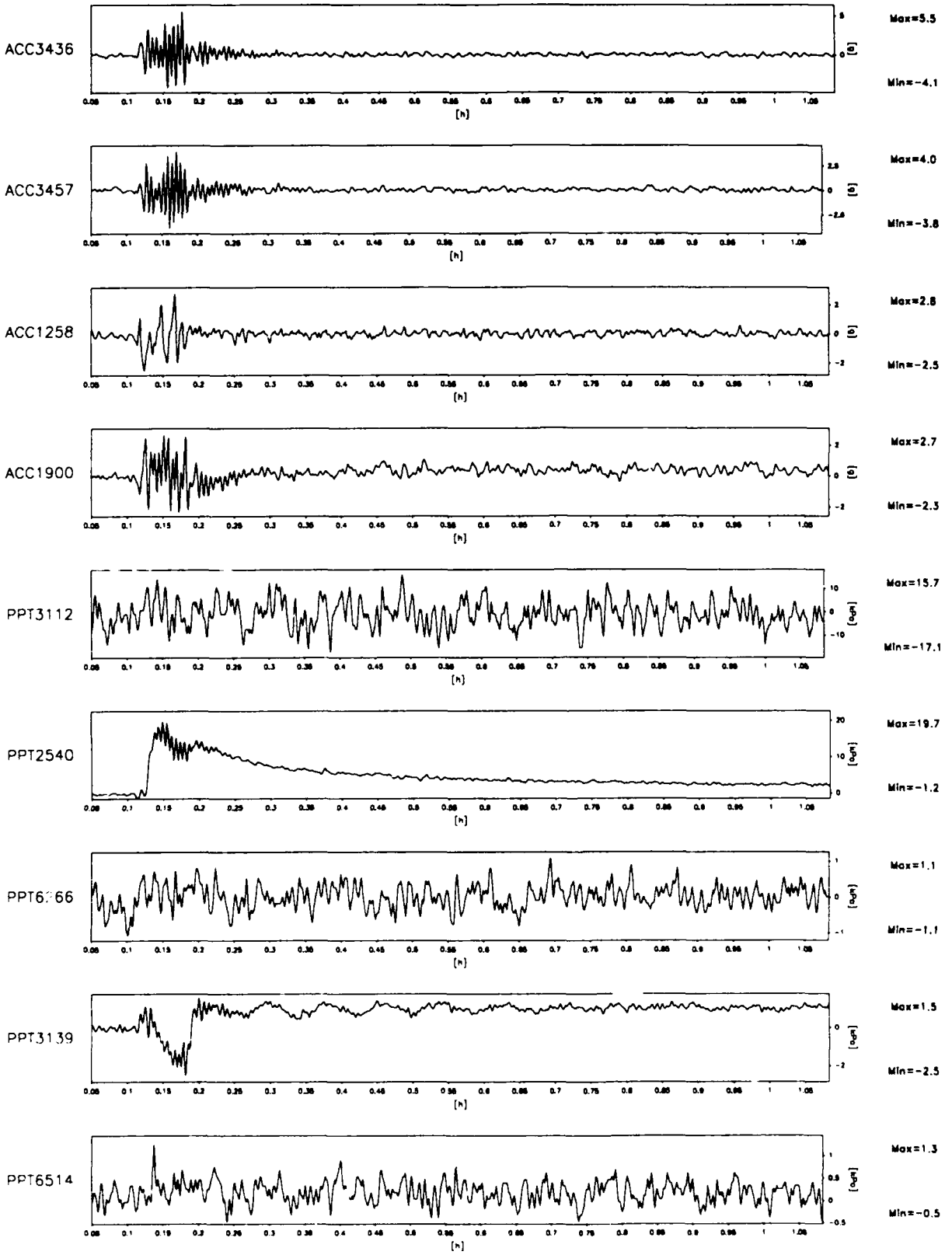

Scales : Prototype

TEST LEG-3 MODEL SAT FLIGHT -1	EQ-1	LONG TERM TIME RECORDS	G Level 80	FIG.NO. 10.8

956 datapoints plotted per complete transducer record

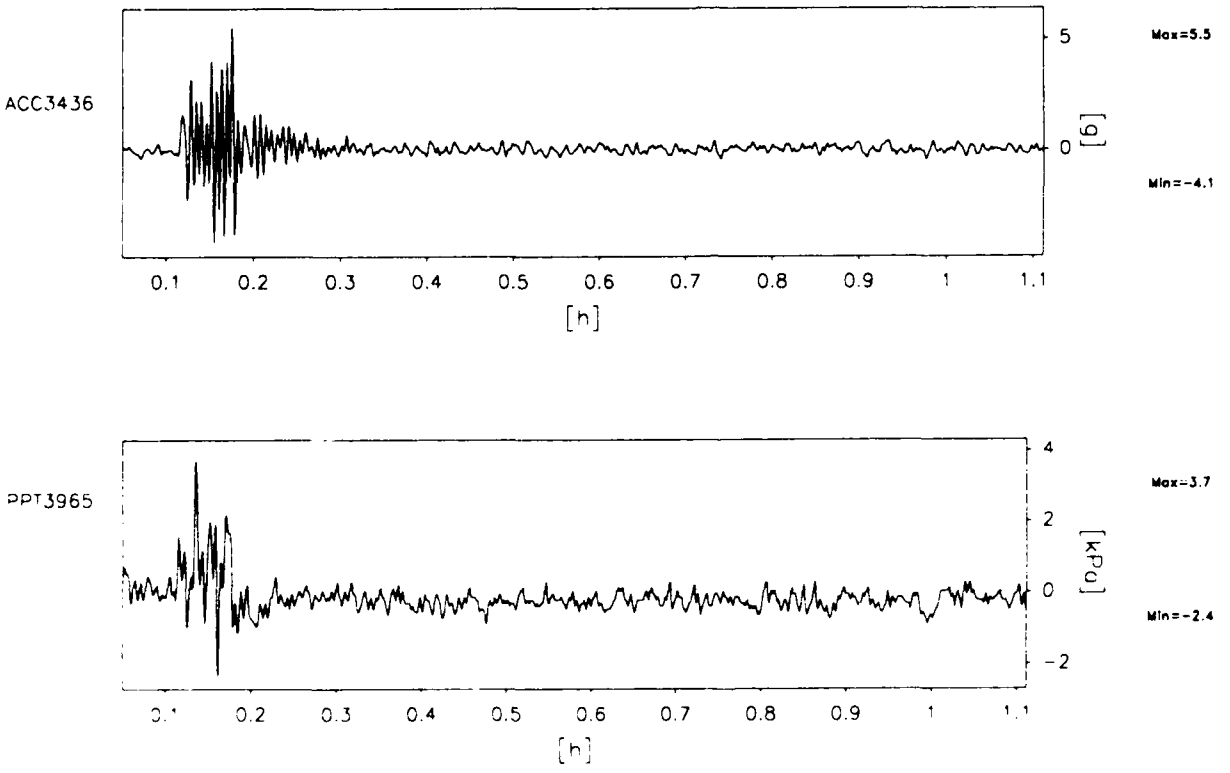

Scales : Prototype

920 datapoints plotted per complete transducer record

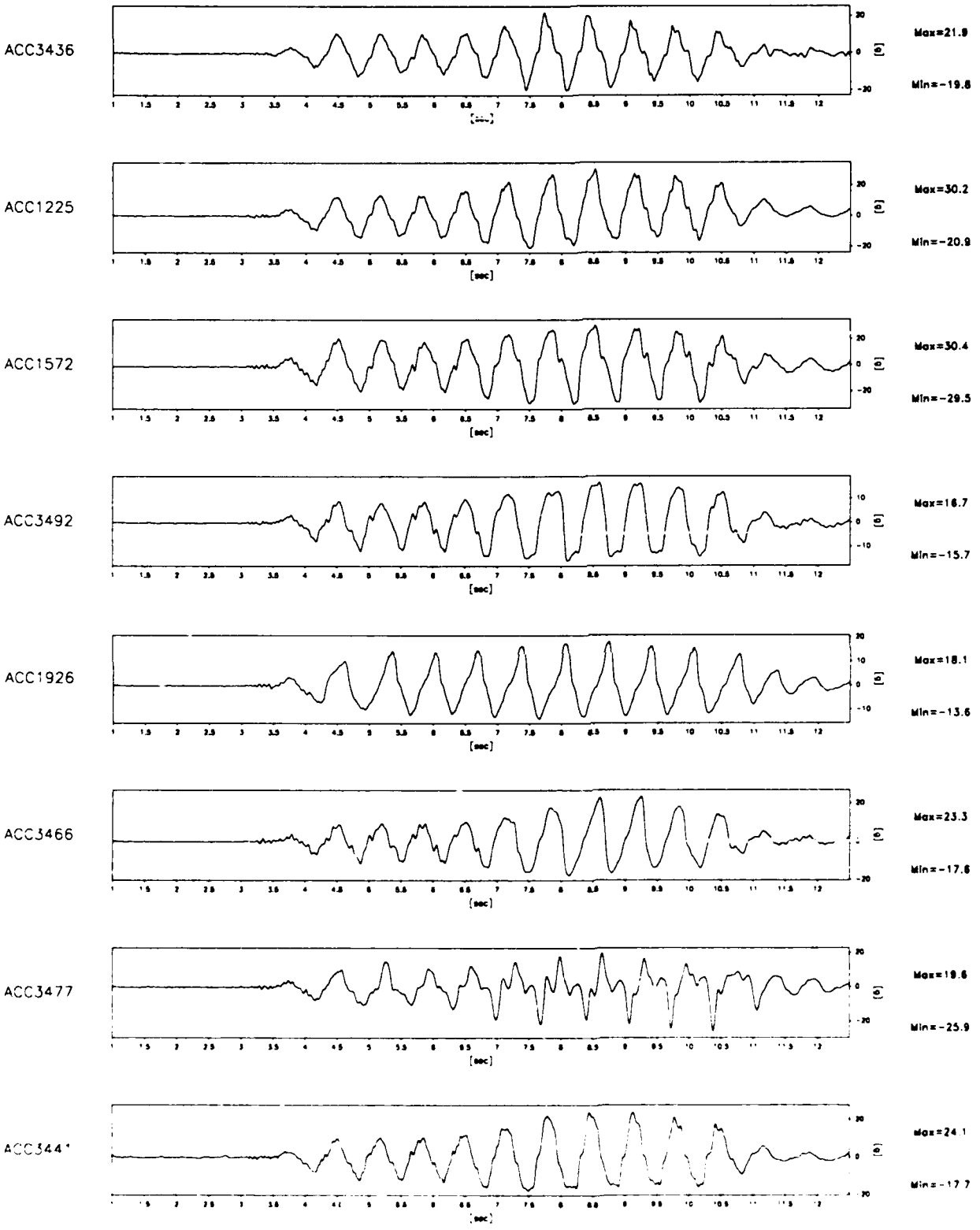

Scales : Prototype

TEST FG-3 MODEL SAT EQ-2 FLIGHT -1	SHORT TERM TIME RECORDS	G Level 80	FIG.NO. 10.10

920 datapoints plotted per complete transducer record

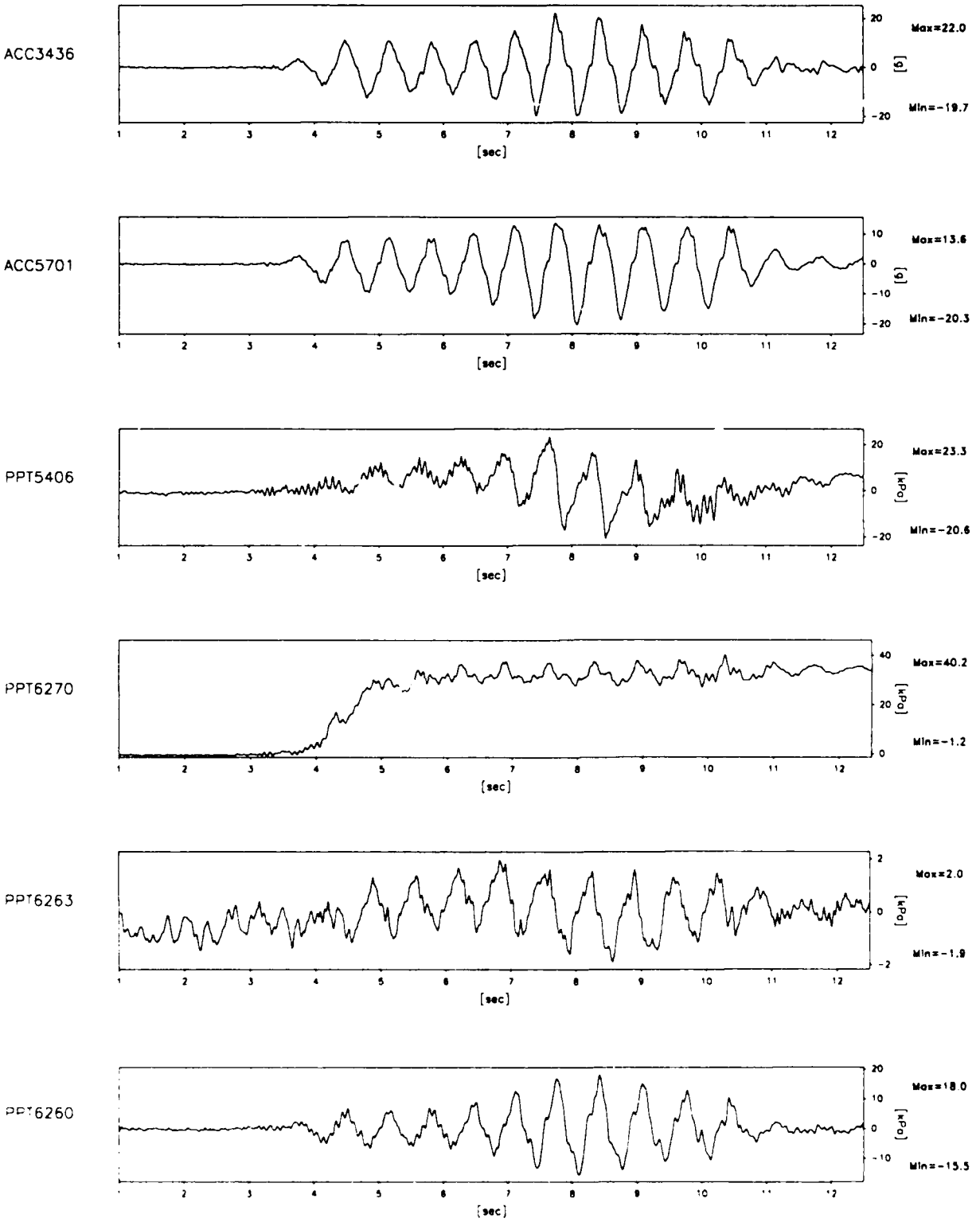

Scales : Prototype

TEST FG-3 MODEL SAT FG-2	SHORT TERM TIME RECORDS	G Level 80	FIG.NO. 10.11

841 datapoints plotted per complete transducer record

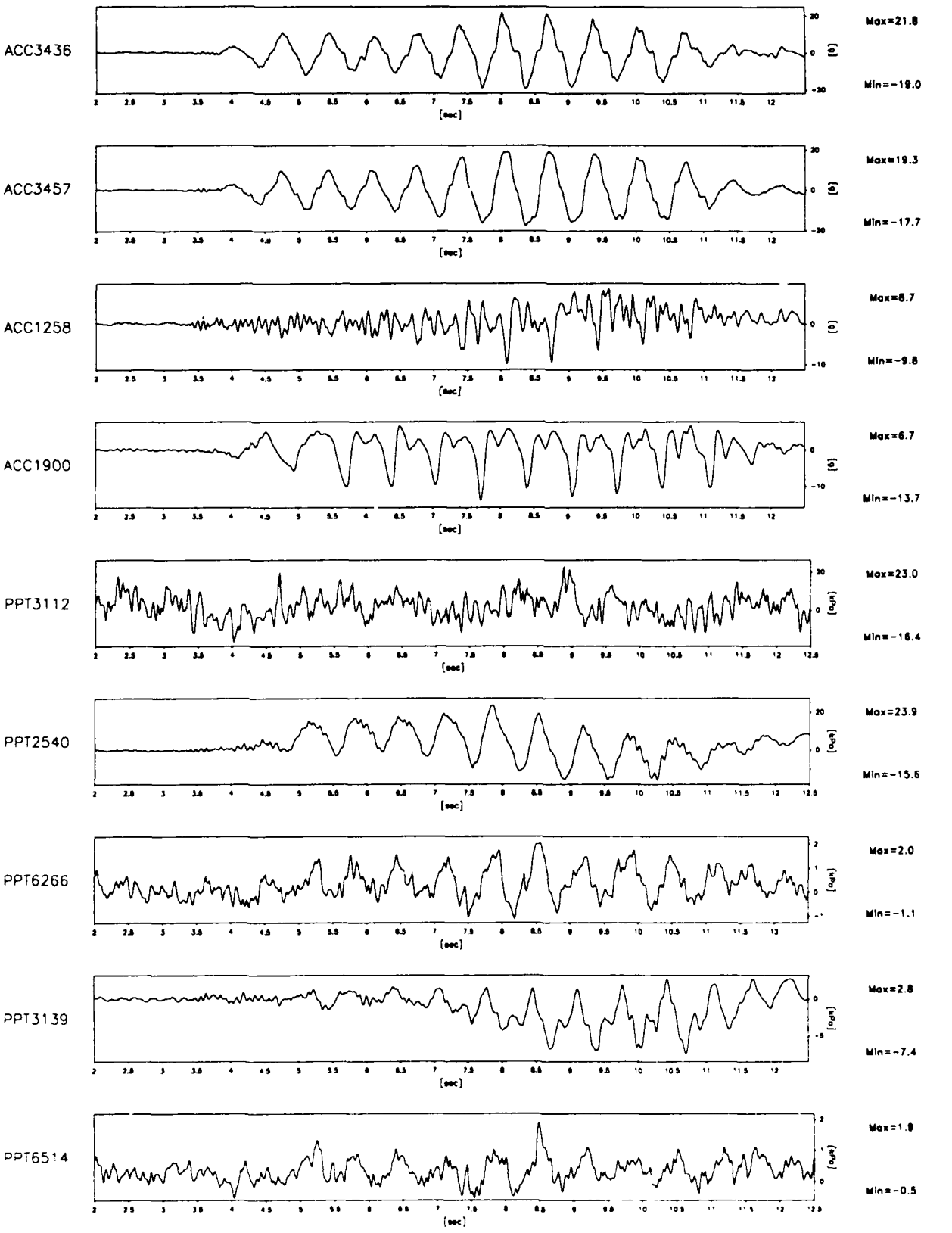

Scales : Prototype

TEST LEG-3 MODEL SAT FLIGHT -1	EQ-2	SHORT TERM TIME RECORDS	G Level 80	FIG.NO. 10.12

841 datapoints plotted per complete transducer record

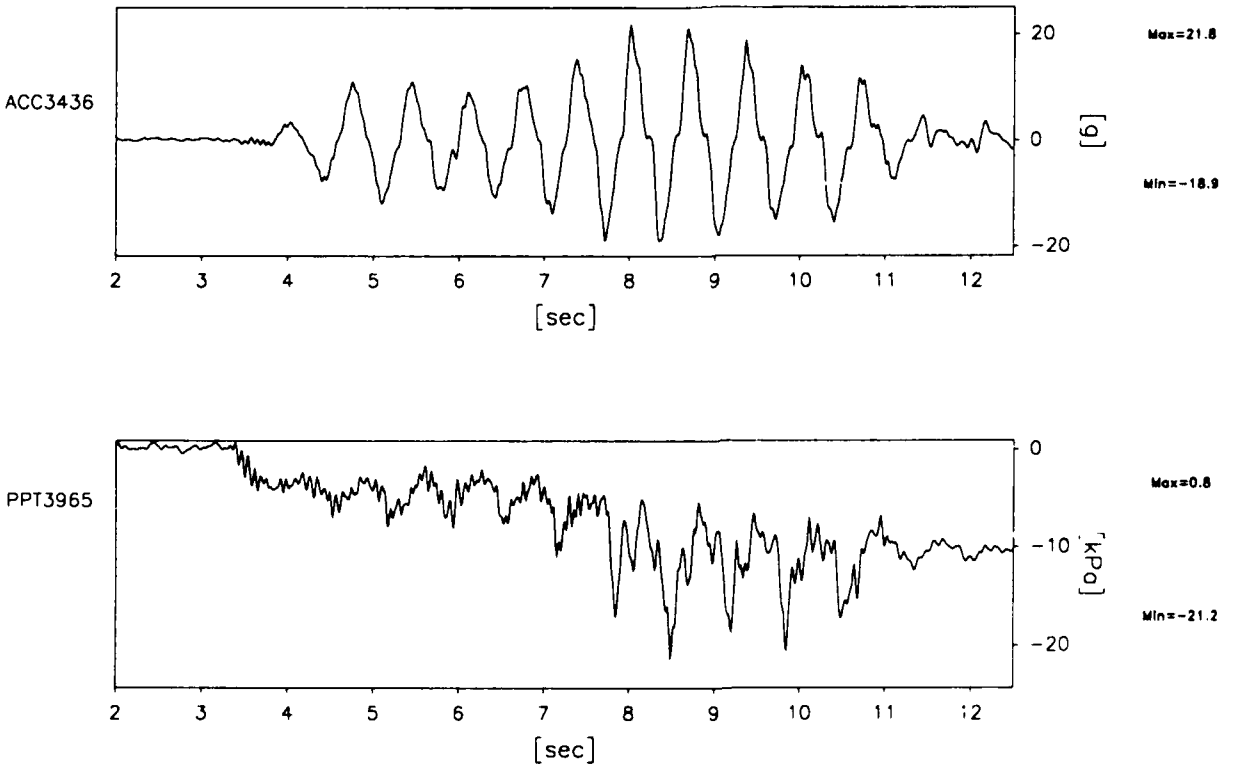

Scales : Prototype

TEST LEG-3 MODEL SAT FLIGHT -1	EQ-2	SHORT TERM TIME RECORDS	G Level 80	FIG.NO. **10.13**

930 datapoints plotted per complete transducer record

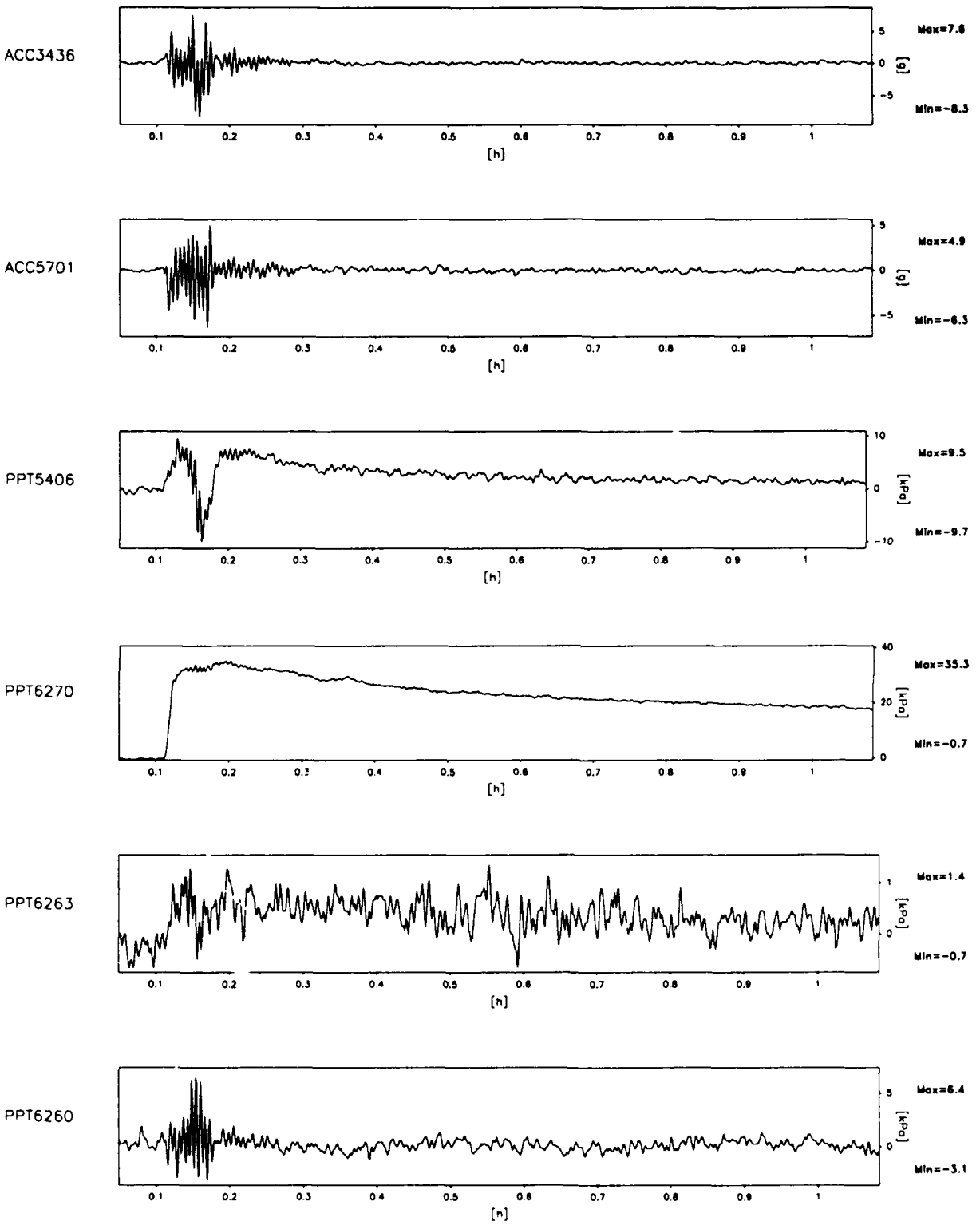

Scales : Prototype

TEST LEG-3 MODEL SAT FLIGHT -1	EQ-2	LONG TERM TIME RECORDS	G Level 80	FIG.NO. 10.14

931 datapoints plotted per complete transducer record

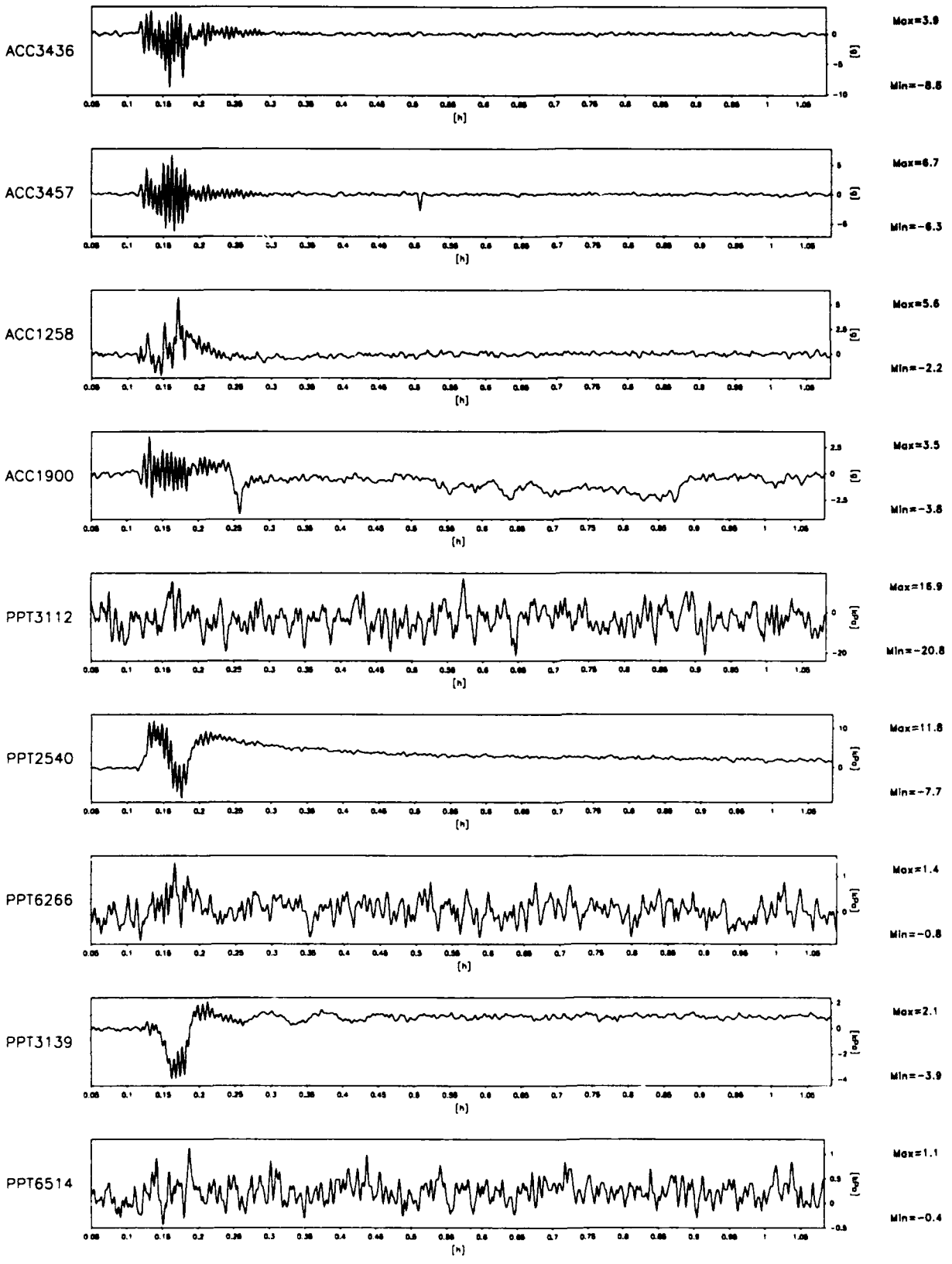

Scales : Prototype

TEST LEC-3 MODEL SAT FLIGHT -1	EQ-2	LONG TERM TIME RECORDS	G Level 80	FIG.NO. **10.15**

956 datapoints plotted per complete transducer record

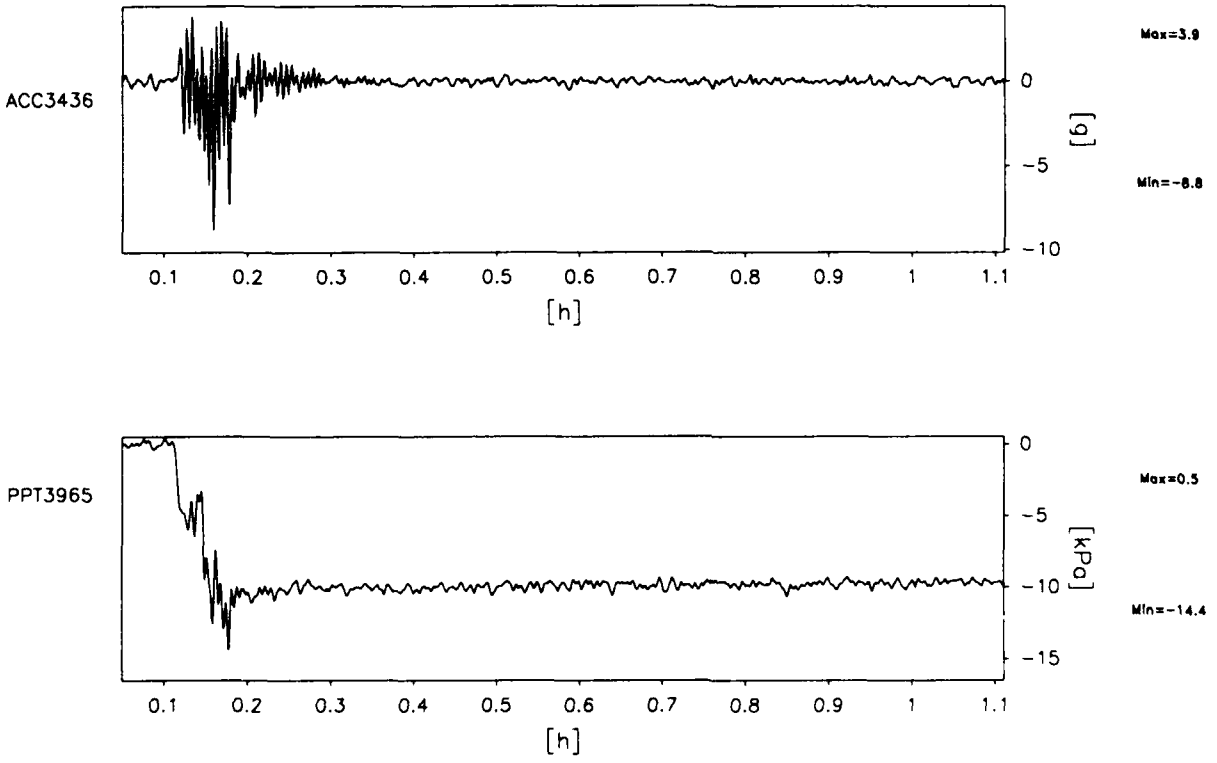

Scales : Prototype

TEST LEG-3 MODEL SAT FLIGHT -1	EQ-2	LONG TERM TIME RECORDS	G Level 80	FIG.NO. **10.16**

920 datapoints plotted per complete transducer record

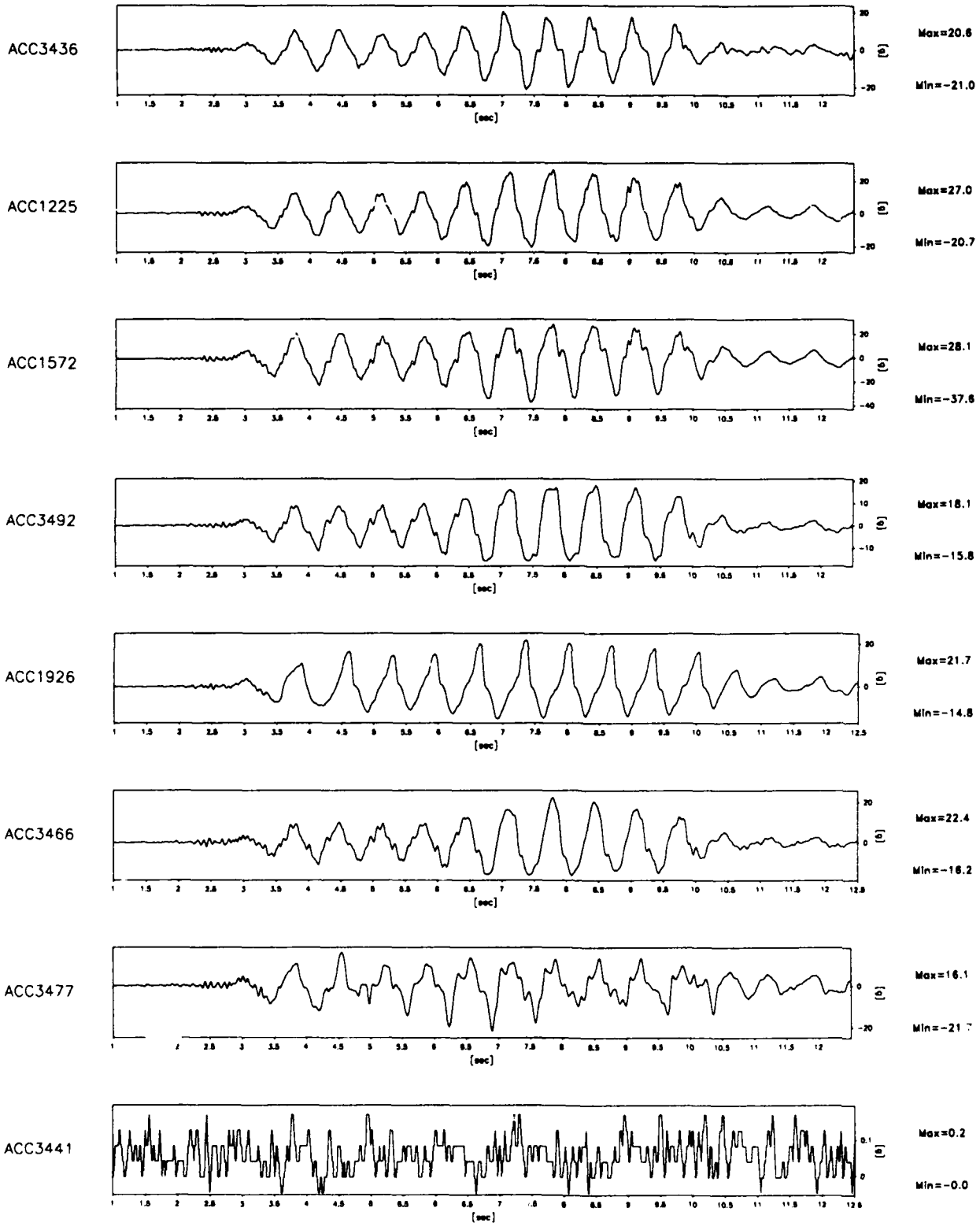

Scales : Prototype

TEST LEG-3 MODEL SAT FLIGHT -1	EQ-3	SHORT TERM TIME RECORDS	G Level 80	FIG.NO. 10.17

920 datapoints plotted per complete transducer record

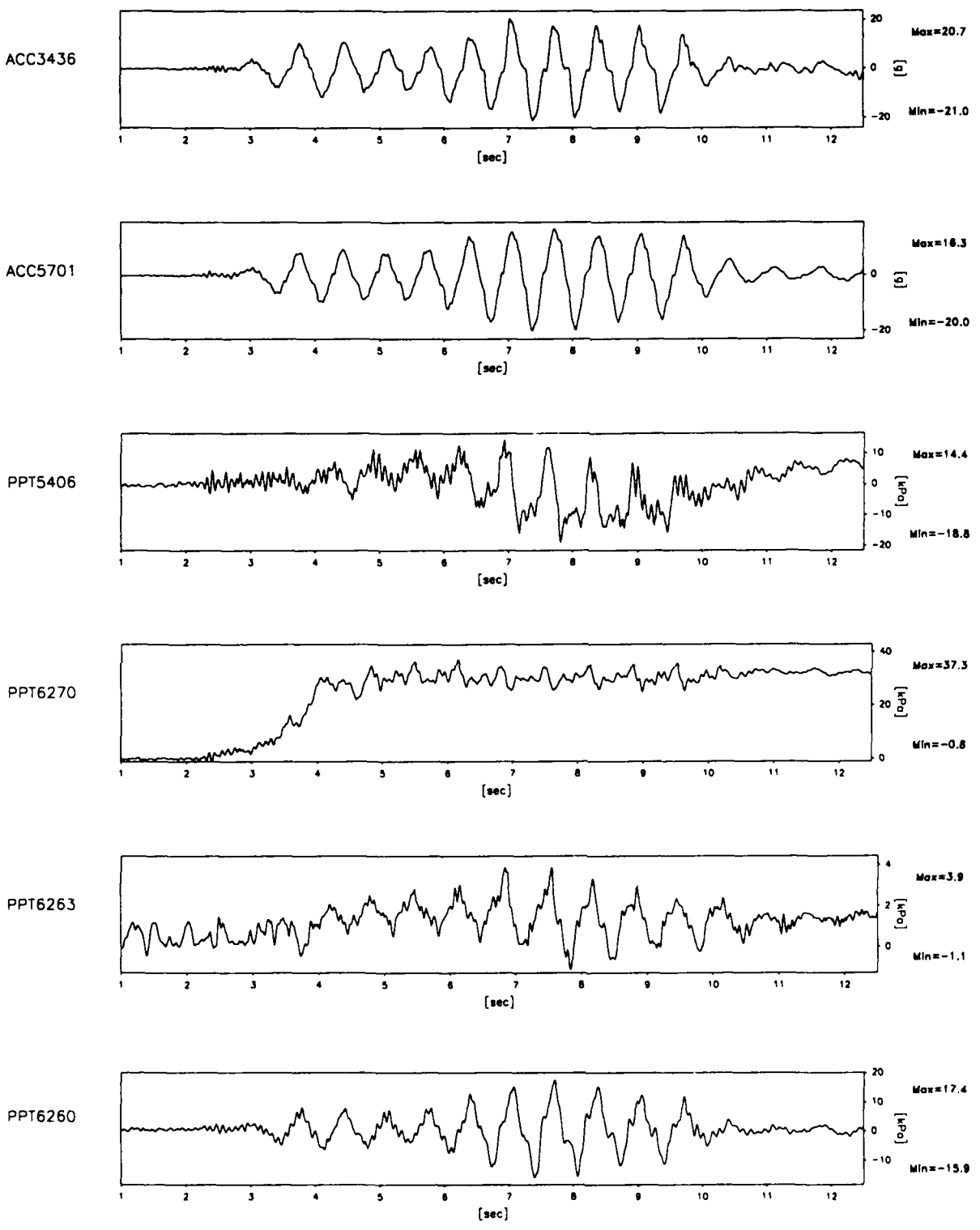

Scales : Prototype

TEST LEG-3 MODEL SAT FLIGHT -1	EQ-3	SHORT TERM TIME RECORDS	G Level 80	FIG.NO. **10.18**

841 datapoints plotted per complete transducer record

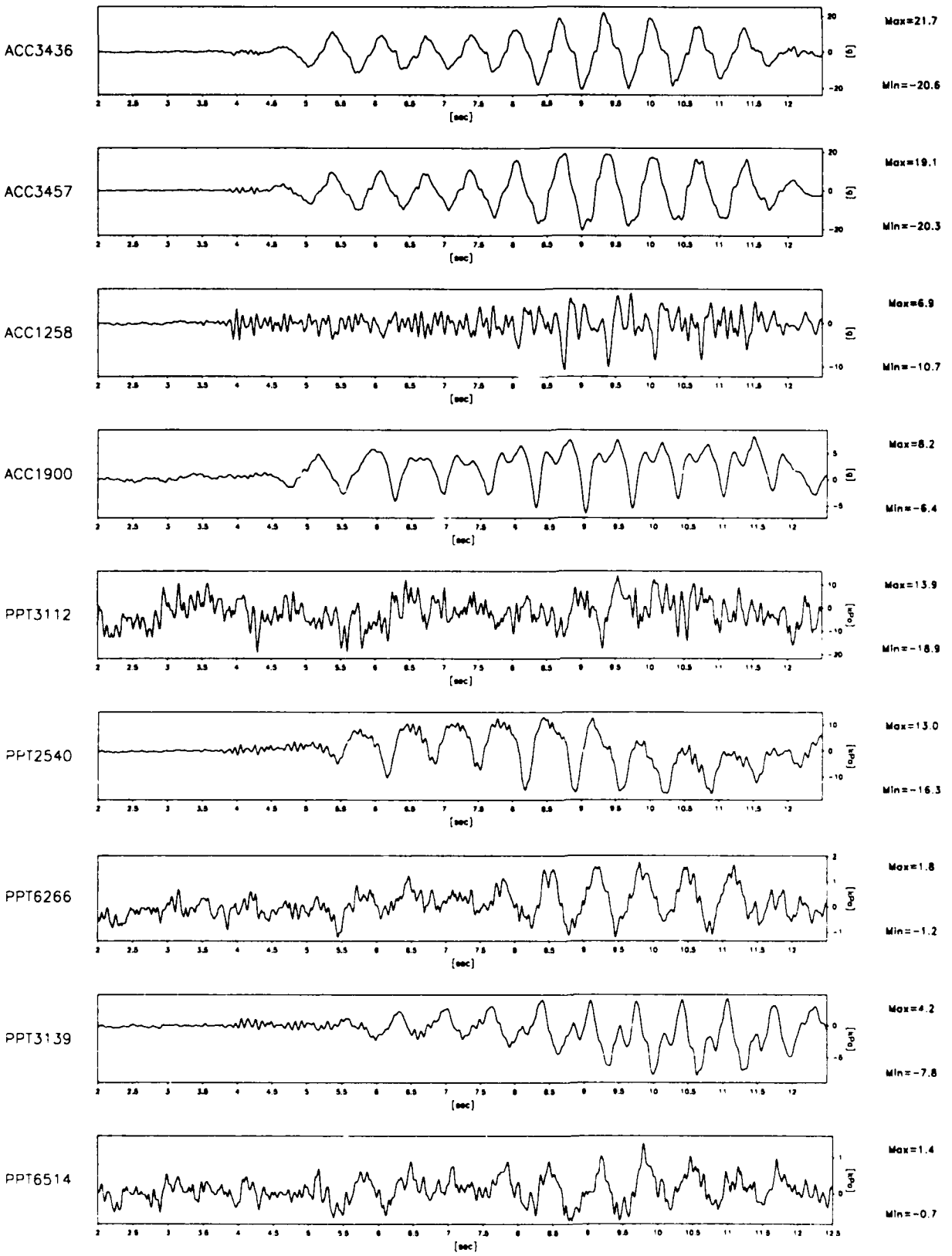

Scales : Prototype

TEST LEG-3 MODEL SAT FLIGHT -1	EQ-3	SHORT TERM TIME RECORDS	G Level 80	FIG.NO. 10.19

841 datapoints plotted per complete transducer record

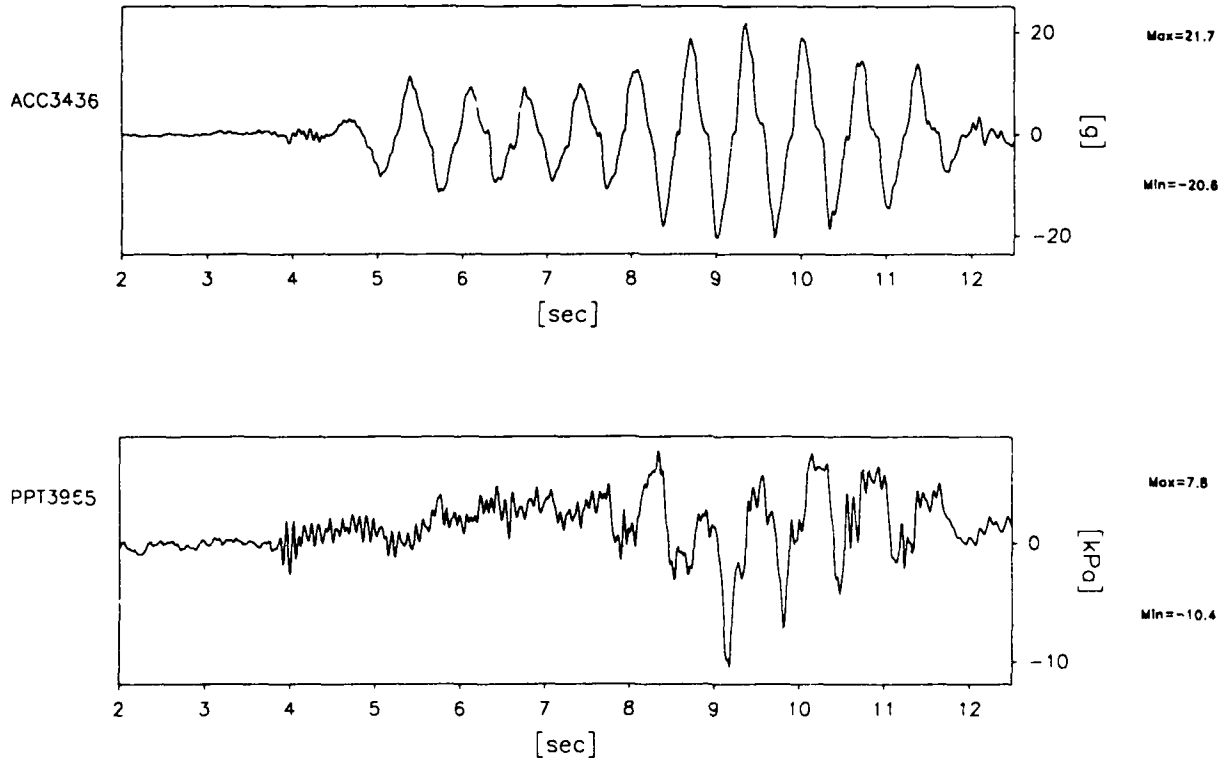

Scales : Prototype

TEST LEG-3 MODEL SAT FLIGHT -1	EQ-3	SHORT TERM TIME RECORDS	G Level 80	FIG.NO. **10.20**

930 datapoints plotted per complete transducer record

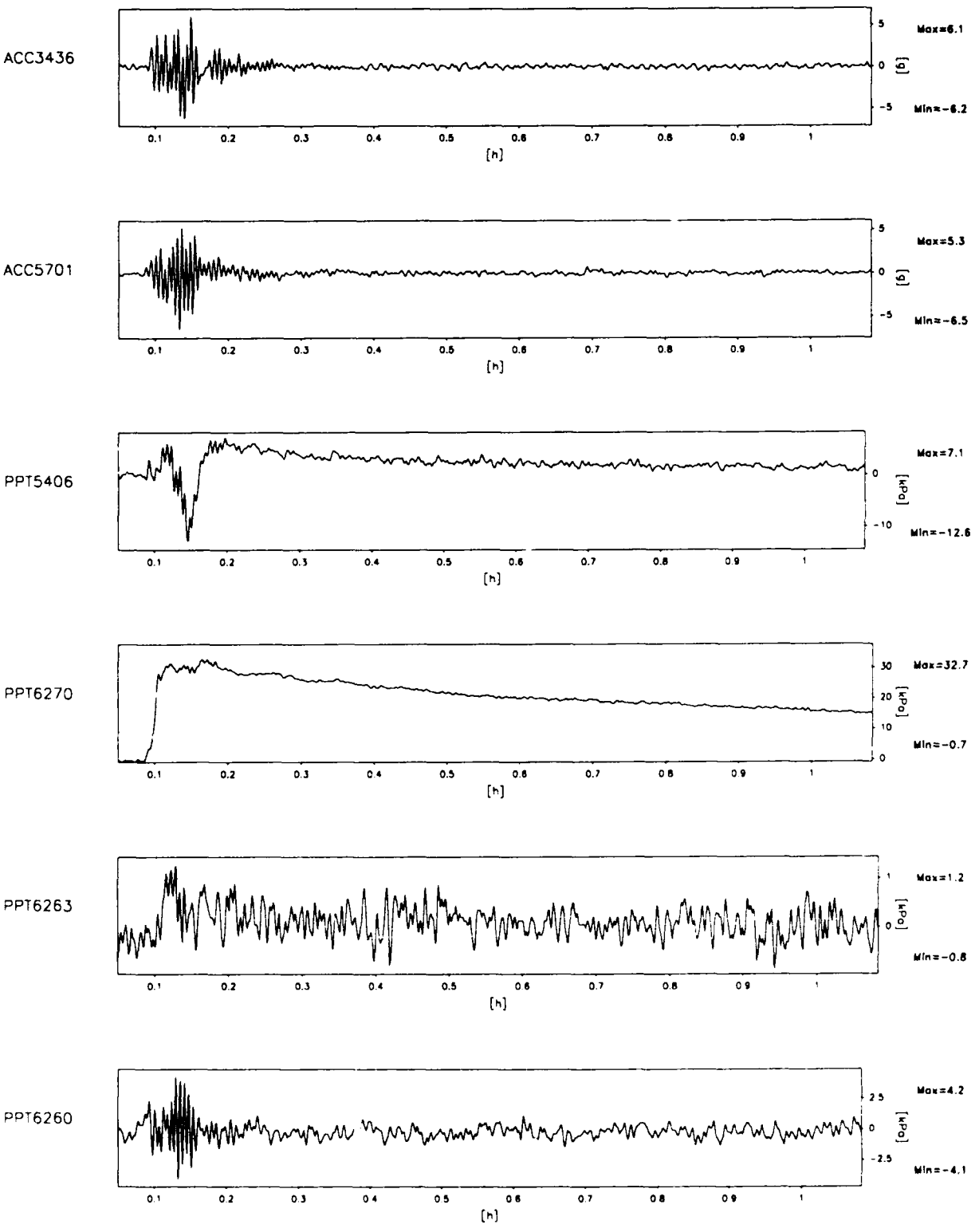

Scales : Prototype

TEST LEG-3 MODEL SAT FLIGHT -1	EQ-3	LONG TERM TIME RECORDS	G Level 80	FIG.NO. 10.21

931 datapoints plotted per complete transducer record

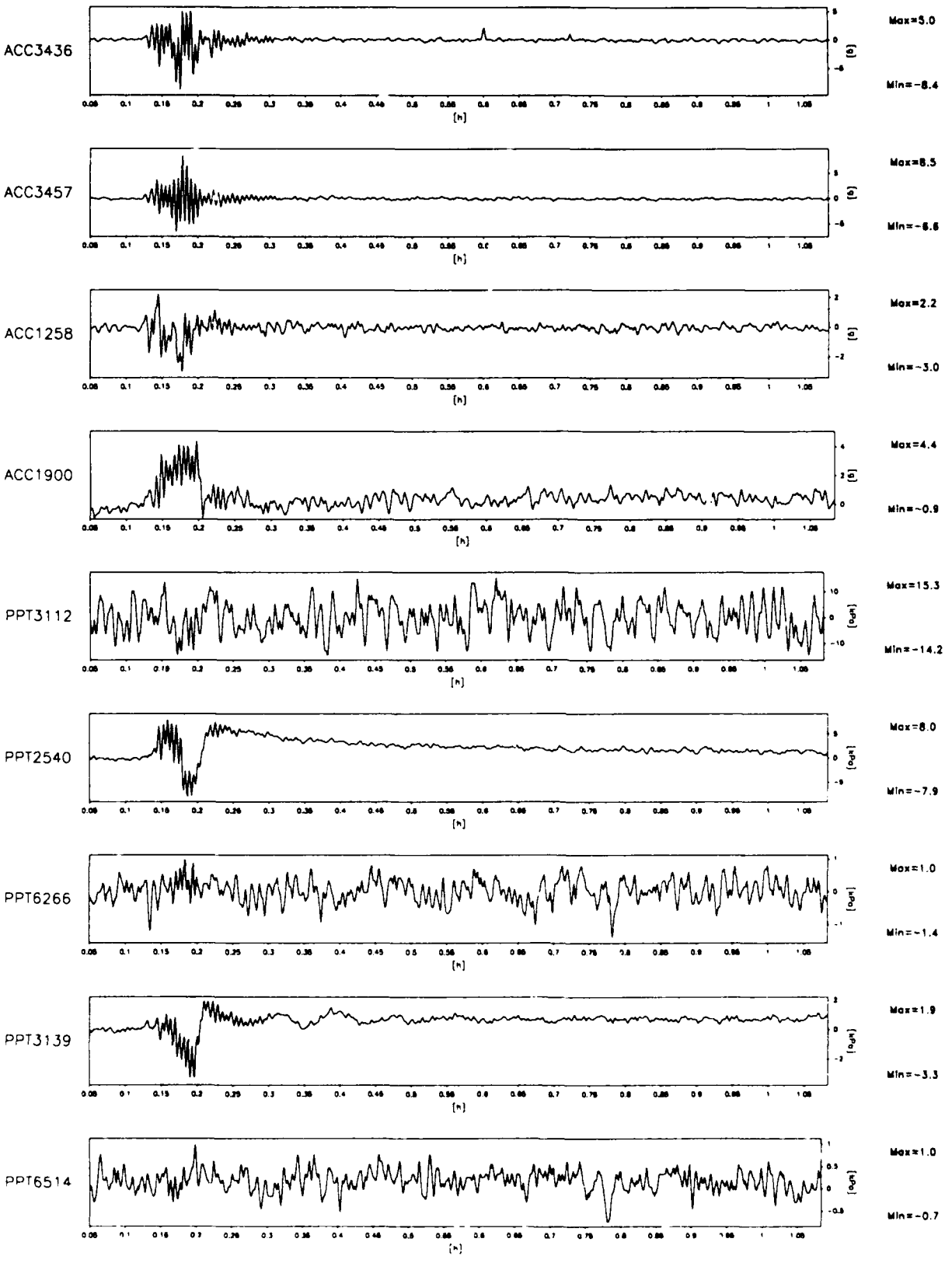

Scales : Prototype

TEST LEG-3 MODEL SAT FLIGHT -1	EQ-3	LONG TERM TIME RECORDS	G Level 80	FIG.NO. 10.22

956 datapoints plotted per complete transducer record

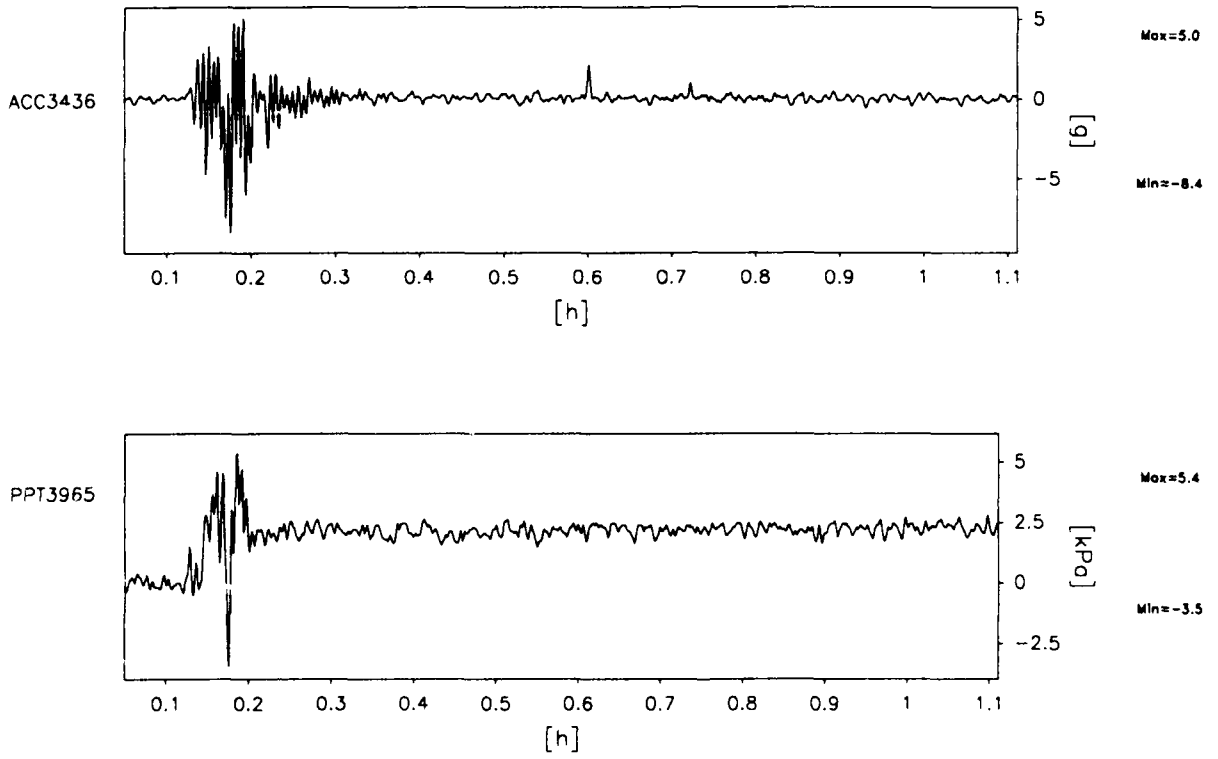

Scales : Prototype

TEST LEG−3 MODEL SAT FLIGHT −1	EQ−3	LONG TERM TIME RECORDS	G Level 80	FIG.NO. **10.23**

920 datapoints plotted per complete transducer record

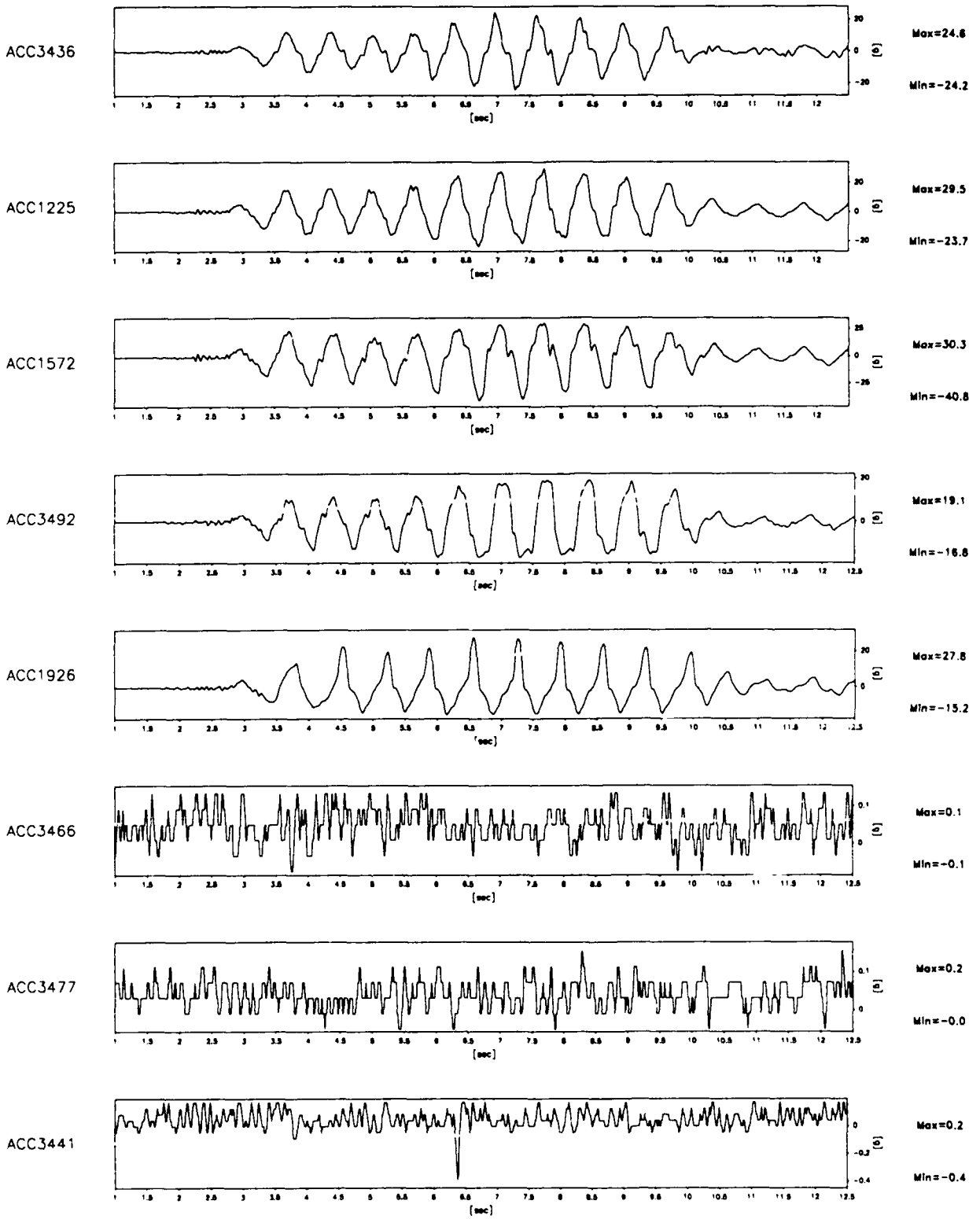

Scales : Prototype

TEST LEG-3 MODEL SAT FLIGHT -1	EQ-4	SHORT TERM TIME RECORDS	G Level 80	FIG.NO. 10.24

920 datapoints plotted per complete transducer record

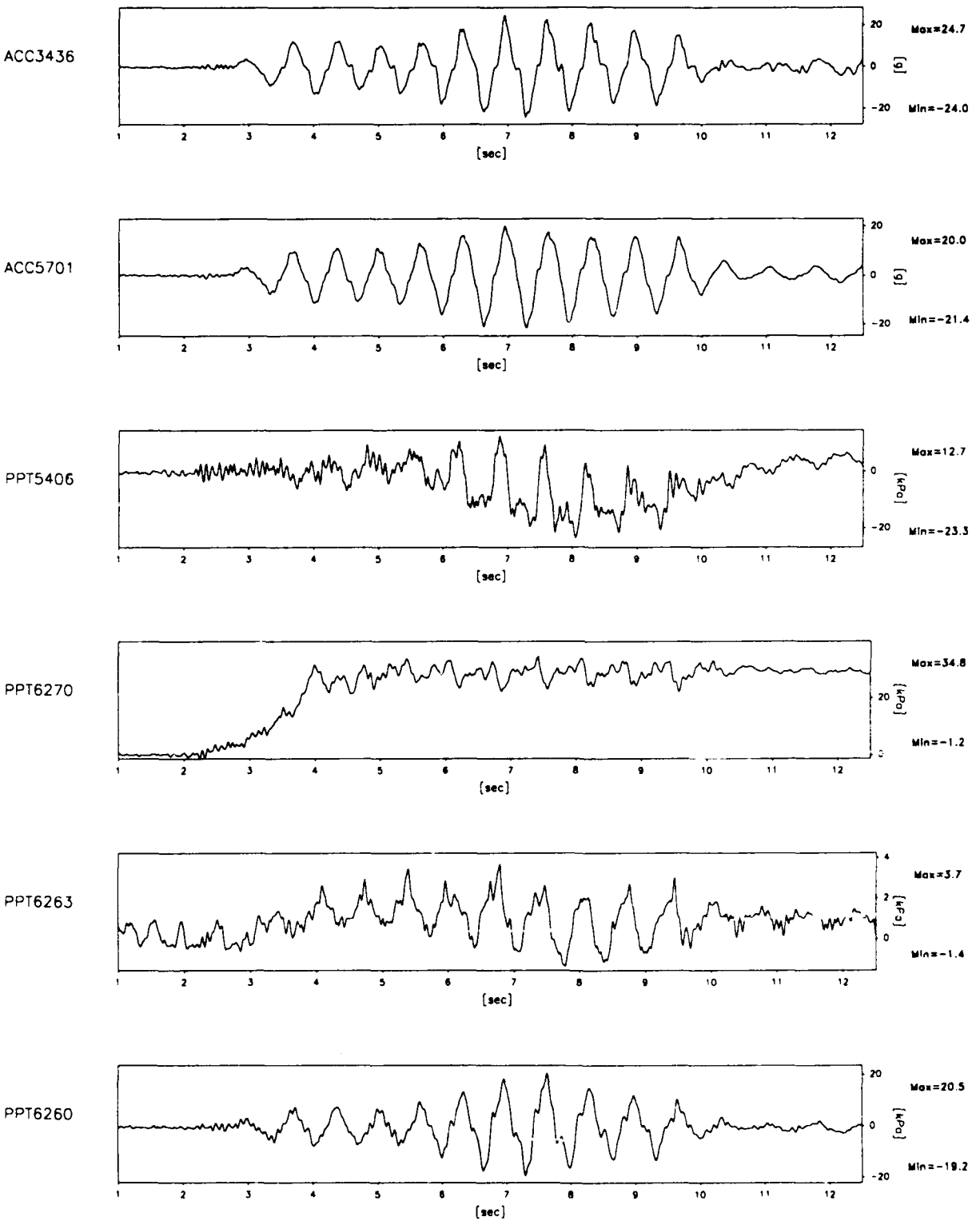

Scales : Prototype

TEST LEG-3 MODEL SAT FLIGHT -1	EQ-4	SHORT TERM TIME RECORDS	G Level 80	FIG.NO. **10.25**

841 datapoints plotted per complete transducer record

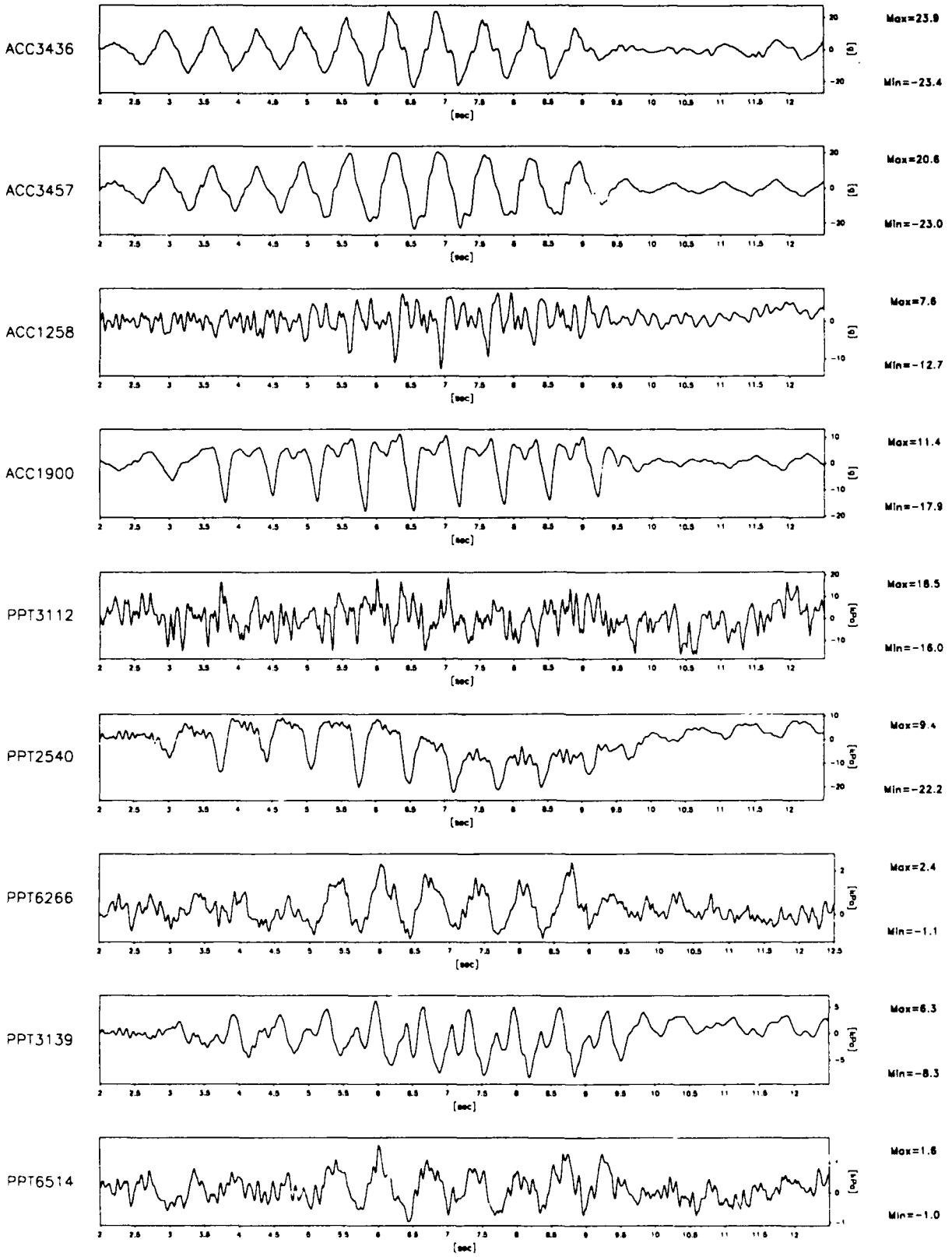

Scales : Prototype

TEST LEG-3 MODEL SAT FLIGHT -1	EQ-4	SHORT TERM TIME RECORDS	G Level 80	FIG.NO. 10.26

841 datapoints plotted per complete transducer record

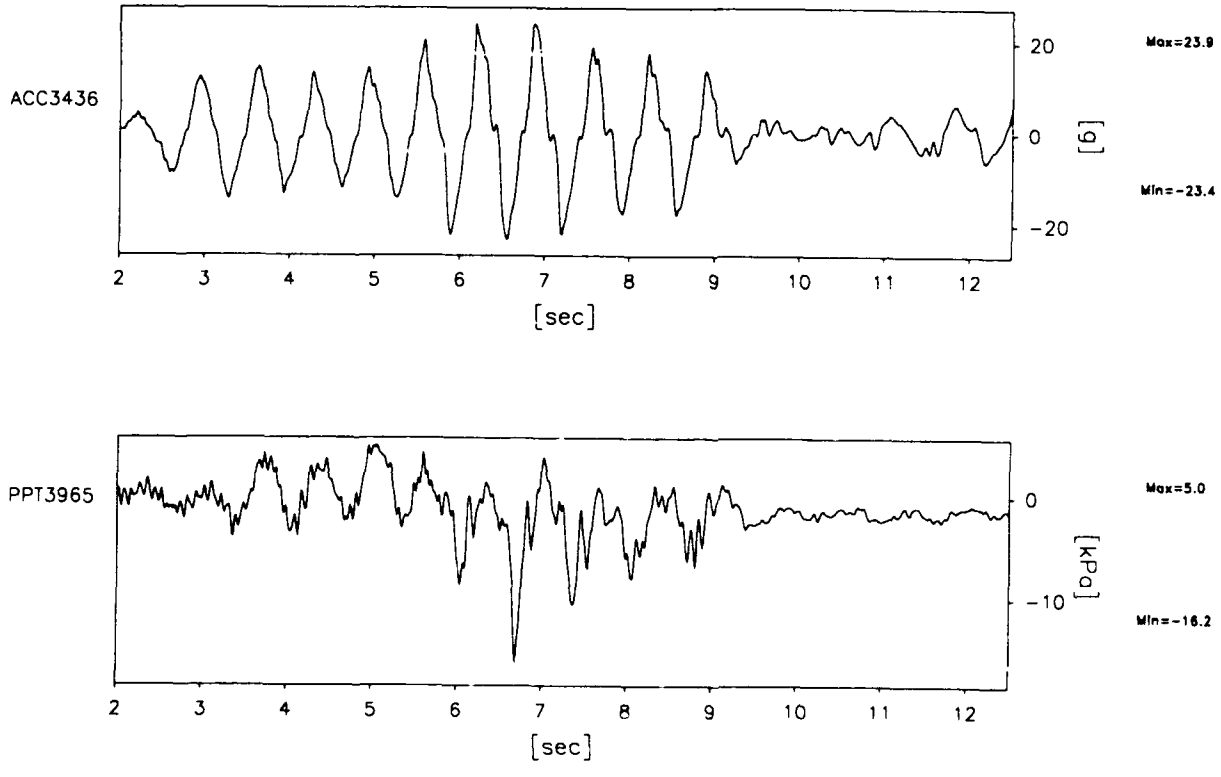

Scales : Prototype

TEST LEG-3 MODEL SAT FLIGHT ... 1	EQ-4	SHORT TERM TIME RECORDS	G Level 80	FIG.NO. 10.27

930 datapoints plotted per complete transducer record

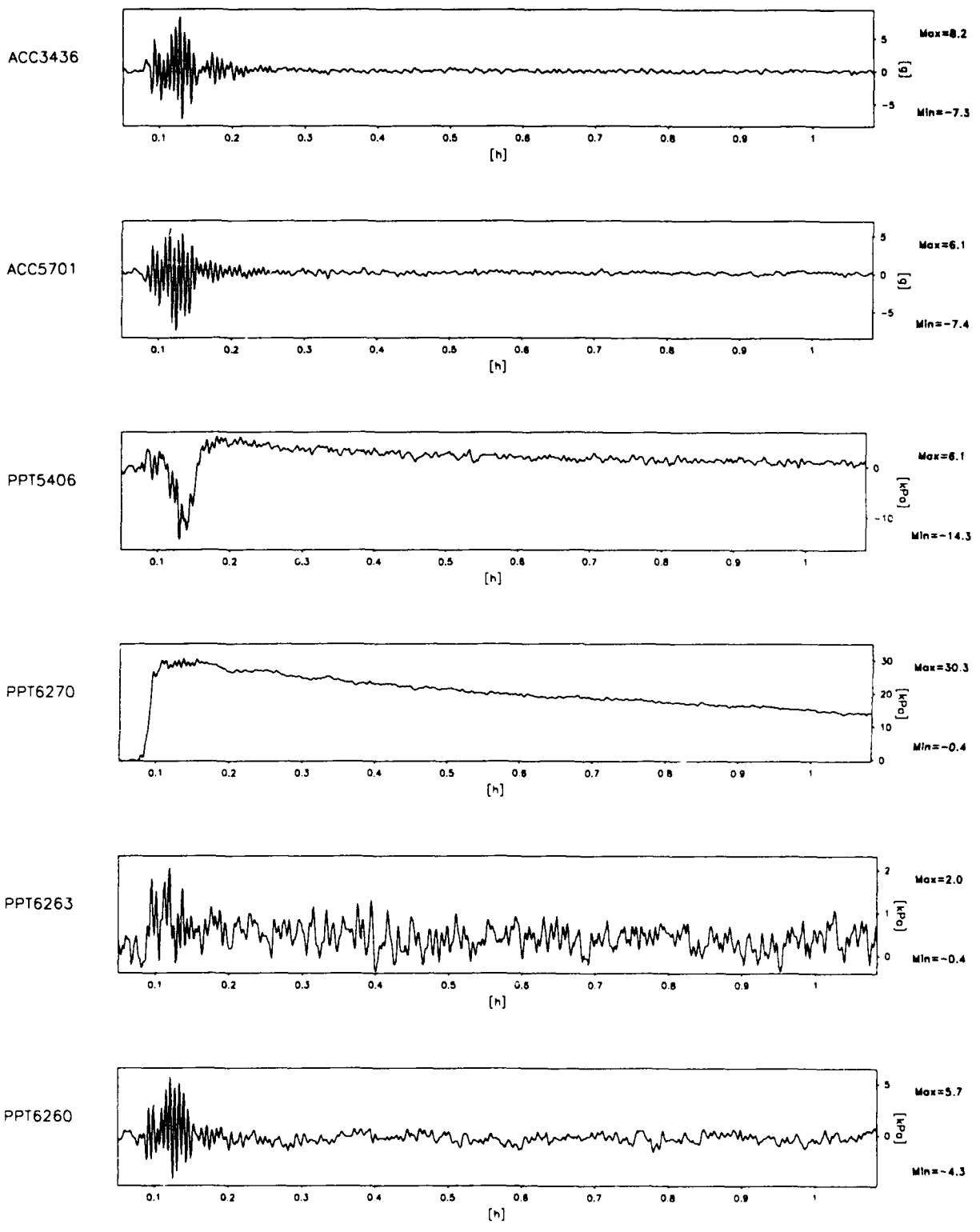

Scales : Prototype

TEST LEG-3 MODEL SAT FLIGHT -1	EQ-4	LONG TERM TIME RECORDS	G Level 80	FIG.NO. 10.28

931 datapoints plotted per complete transducer record

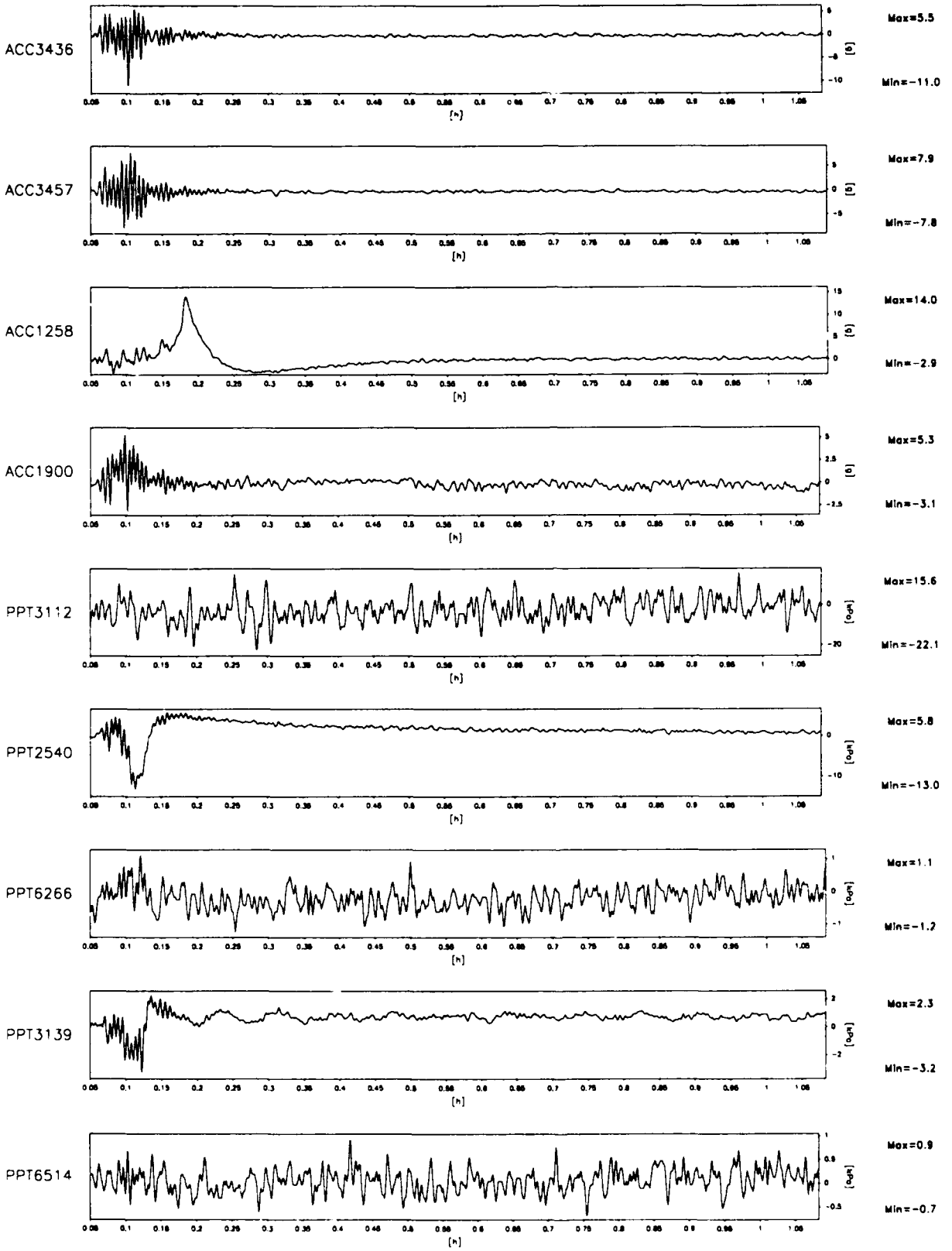

Scales : Prototype

TEST LEG-3 MODEL SAT FLIGHT -1	EQ-4	LONG TERM TIME RECORDS	G Level 80	FIG.NO. **10.29**

956 datapoints plotted per complete transducer record

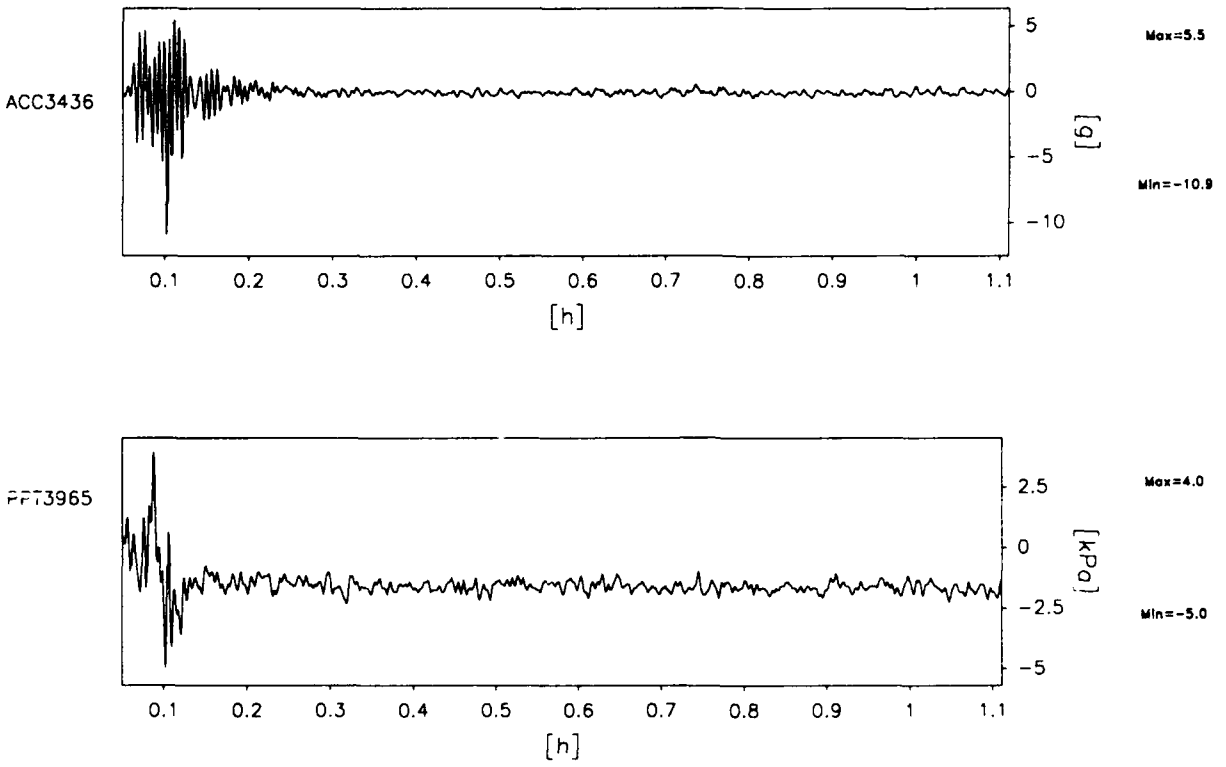

Scales : Prototype

TEST LEG−3 MODEL SAT FLIGHT −1	EQ−4	LONG TERM TIME RECORDS	G Level 80	FIG.NO. **10.30**

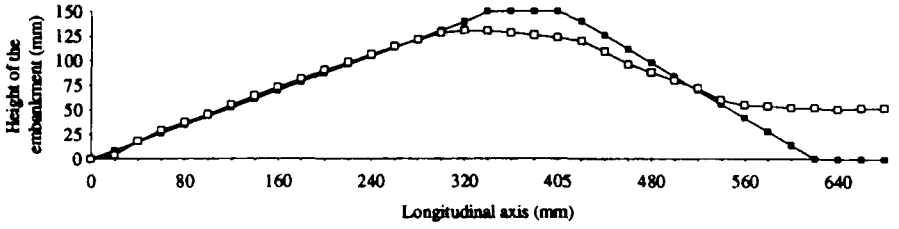

Fig.10.31 Post test profile of centrifuge model LEG-3

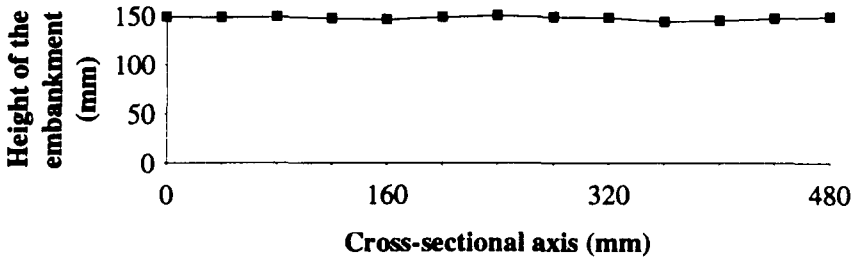

Fig.10.32 Post test profile alont the cross section of centrifuge model LEG-3

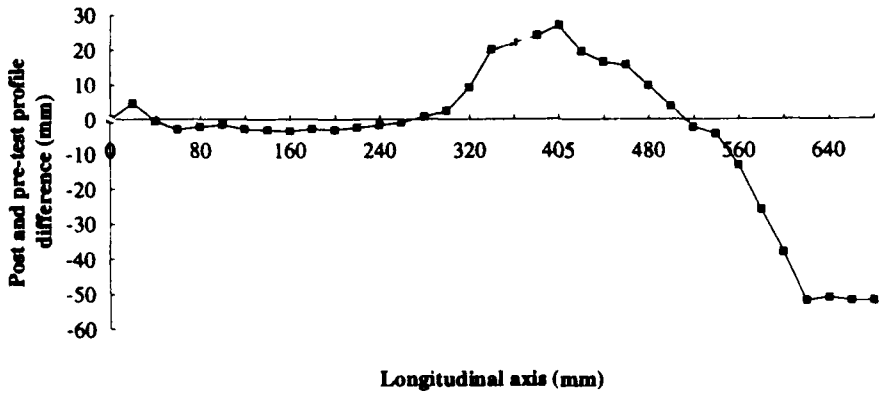

Fig.10.33 Post and pre-test profile difference along the longitudinal axis in centrifuge test LEG-3

11.0 Centrifuge Test LEG-4

11.1 Configuration of the test

In the third centrifuge test LEG-4 the down stream slope was 35^{o} and the up stream slope was 21^{o} . The loose layer of sand was inclined at an angle of 10.3^{o} and had a thickness of 10 mm. This slope is much flatter than in the previous two tests. Also the location of the loose section was much more deeper than in the other tests. The reason for this is to establish that the liquefied loose zone will mobilise a deeper failure mechanism of the down stream slope. The dense section of the embankment was constructed using coarse Leighton Buzzard 14/25 sand. The loose section of the embankment was constructed using fine Leighton Buzzard 100/170 sand as explained in section 6.0. The schematic diagram showing the cross section of the model is presented in Fig.11.1. The placement of transducers is shown in Fig.11.2. In this test it was decided to confine the loose section of the embankment using very fine rock flour to sustain the excess pore pressure built up during the earthquake loading for a longer time. Accordingly a thin layer of rock flour was introduced at the top and bottom interfaces between the loose section and the dense sections of the embankment as in the second and third tests.

11.2 Test data

In this test the down stream slope suffered a slip resulting in the movement of the crest towards the down stream toe of the embankment. The slip surface was along the loose section of the sand as shown in Fig.11.1 (zone B). The dry densities of each of the zones in Fig.11.1 together with the void ratio and relative densities for this centrifuge model are presented in Table 11.1. The hydrostatic pore pressures recorded during the swing up of the centrifuge and increase of the centrifugal acceleration to 80g and after each earthquake are presented in Table 11.2. The data recorded during this test are presented in Figs.11.3 to 11.34. Also the slip plane was nearer to the loose zone resulting in a deeper failure mechanism. However in this test the slip plane is not coincident with the loose zone. The accelerometer 1926 placed in the crest of the embankment registered strong acceleration in one direction suggesting the slipping of the crest in one direction. This is supported by the accelerometer traces 3477 and 3466 which are also in this region. ACC 3441 and 3492 have uniform response with equal peaks in positive and negative direction suggesting that the slip plane is above the location of these accelerometers. The traces recorded by the accelerometers in the up

stream slope were more or 'ess uniform suggesting no movement of this slope. The post test profile measured after the test confirmed this.

The pore pressure traces recorded in the crest section by PPT 3139 showed strong suctions. However the pore pressures recorded in the lower dense section (shown in Fig.1) by PPT 5406 and 6266 showed positive pore pressures. This shows that the upper dense zone was dilating. In the loose section there was a much larger excess pore pressure which was retained for a very long time due to the impermeable rock flour interface between the loose and dense sections. During the model earthquake the loose section was the slip plane available for the down stream slope as there were excess pore pressures in this zone and it was at a higher pore pressure than the other two zones. The slow dissipation of the excess pore pressure in the loose zone is revealed in the long term traces. In this test no transducer has floated during the earthquakes. A view of the down stream slope of this model embankment after the centrifuge test is shown in Plate 11.1.

11.3 Post test profile

The post test profile measured after the centrifuge test is presented in Fig.11.35 together with the original profile of the embankment. The post test profile is measured at various longitudinal sections and the average profile is shown in this figure. Also the cross sectional profile is shown in Fig.11.36 which suggests that the slip is more or less uniform across the model embankment. From the post test profiles it can be clearly seen that there is a slip on the down stream slope side of the embankment. The up stream slope is relatively unchanged before and after the earthquakes. It is possible to estimate the quantity of the soil movement resulting when the model embankment is subjected to the earthquake loading. In order to estimate the quantity of soil moved during the earthquakes, the difference of the embankment profiles before and after the earthquakes is plotted. This graph is presented in Fig.11.37. Using the numerical integration procedure given by Simpson's rule, the area under the curve shown in Fig.11.37 is estimated. Using this area the volume of the soil movement resulting from the earthquake loading is estimated. The quantity of oil which slipped from the crest of the embankment was 1.930×10^{-3} m^3 and the quantity of soil deposited at the toe of the embankment is 1.674×10^{-3} m^3. In prototype terms these quantities are 988.2 m^3 and 857.1 m^3 respectively. The differential volume which may indicate the error in measurement of the post test profile is 1.05 % of the total volume of the embankment.

Table 11.1 Dry density of sand in different zones of the embankment in centrifuge test LEG-4

Zone*	γ_d (kg/m^3)	void ratio (e)	Relative Density (%)
A	1611.42	0.645	59.35
B	1388.6	0.908	26.50
C	1703.8	0.555	75.87

* see Fig.11.1 for zone specification

Table 11.2 Hydrostatic pore pressures recorded in centrifuge test LEG-4

Device	kPa/V	20-G kPa	40-G kPa	60-G kPa	80-G kPa	EQ-1 kPa	EQ-2 kPa	EQ-3 kPa	EQ-4 kPa
PPT2540	361.77	22.11	47.46	66.80	93.83	90.46	90.17	90.17	90.10
PPT3139	379.53	5.30	11.39	15.91	22.48	22.67	23.42	24.26	25.06
PPT6514	350.88	2.09	3.89	5.26	7.16	7.02	7.02	7.09	7.02
PPT6260	365.88	30.33	59.19	81.44	111.33	107.93	107.12	106.14	105.33
PPT6263	365.27	2.00	4.53	6.07	8.41	8.26	8.34	8.30	8.34
PPT6270	385.84	19.41	34.57	46.77	61.66	60.35	59.92	59.46	59.08
PPT6266	440.55	1.23	2.37	3.20	4.17	3.86	3.64	3.60	2.37
PPT3965	405.50	30.66	45.70	56.77	65.20	58.55	52.07	44.85	38.20
PPT5406	393.98	25.48	54.05	78.08	105.54	103.89	103.77	103.45	102.31
PPT3112	4030.97	27.67	56.72	81.30	109.52	108.31	107.91	107.51	107.10

Plate 11.1 A view of the model embankment after centrifuge test LEG-4

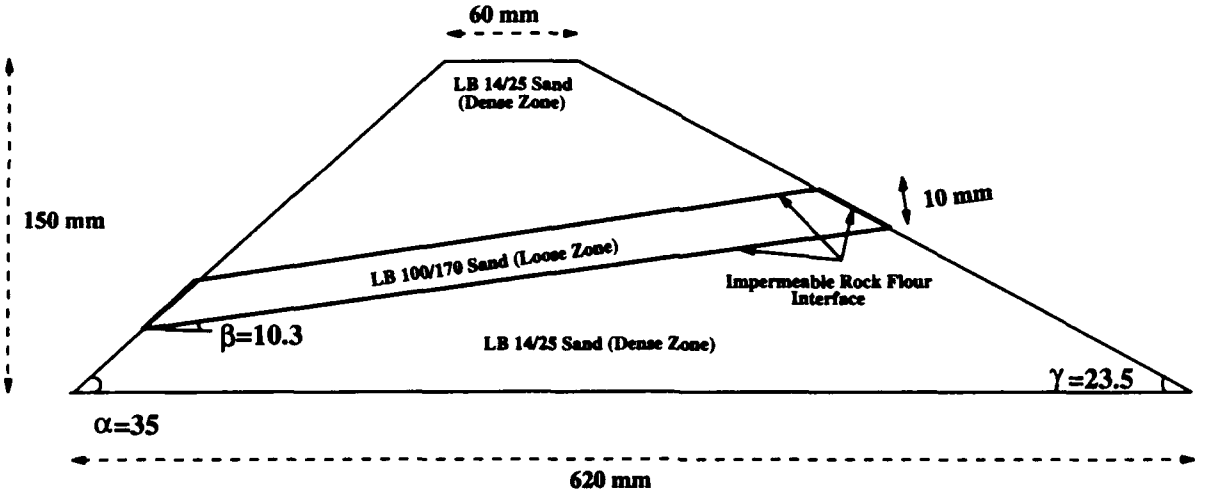

Fig.11.1 Cross section of the centrifuge model LEG-4

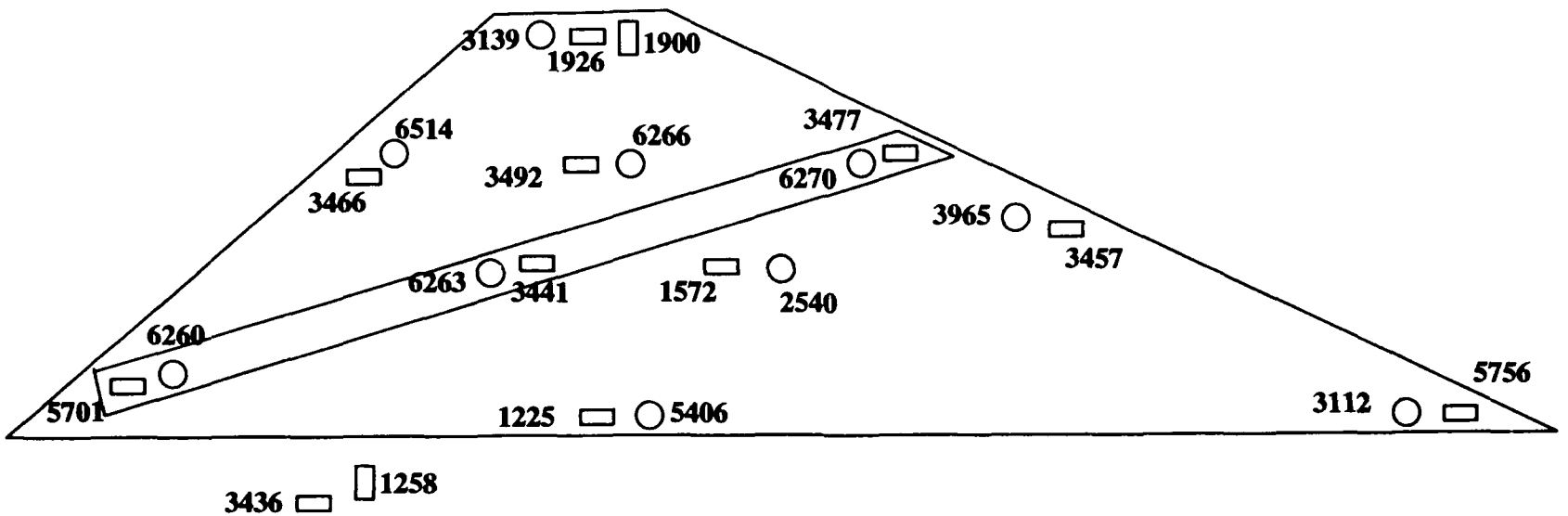

Fig.11.2 Placement of transducers in centrifuge test LEG-4

920 datapoints plotted per complete transducer record

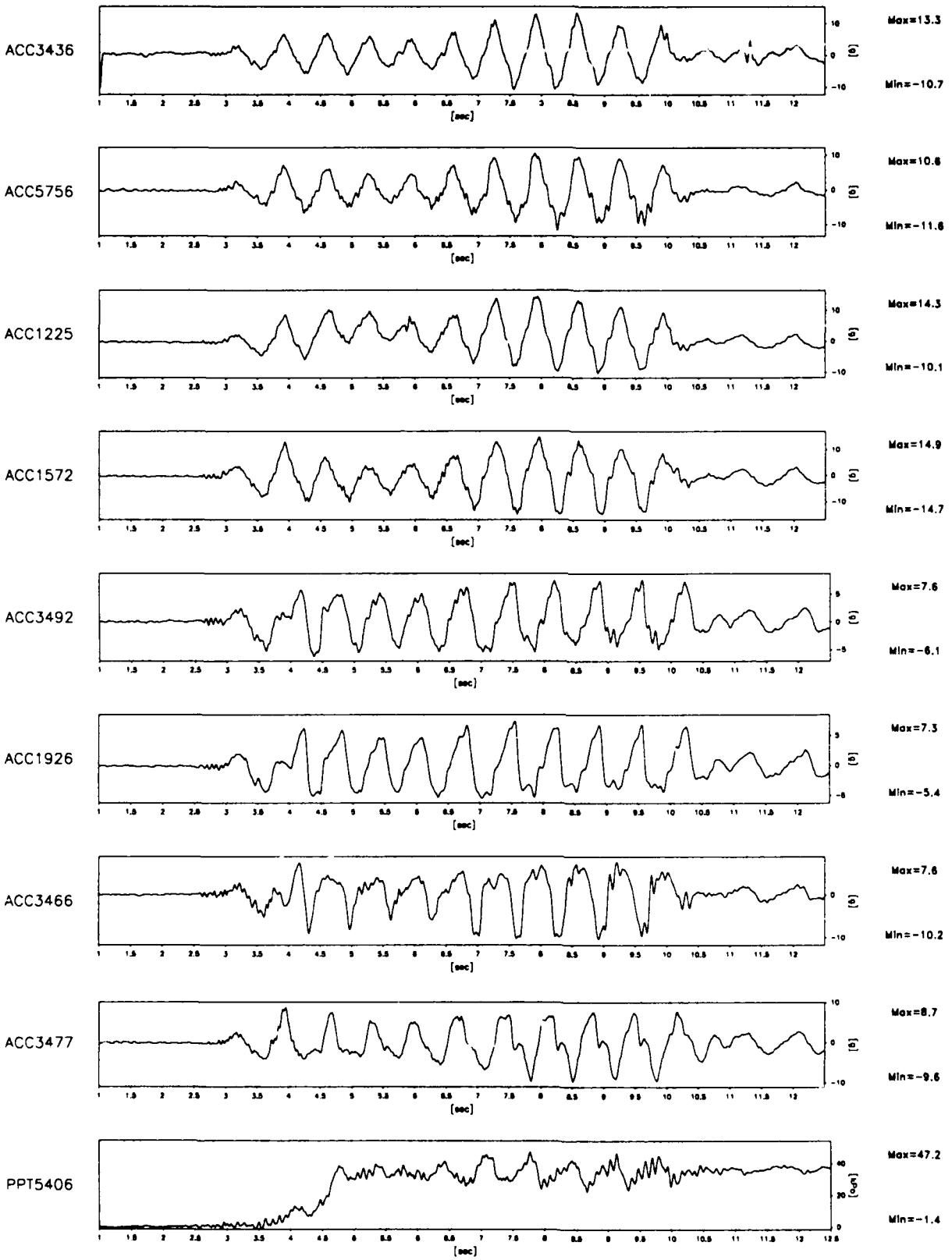

Scales : Prototype

TEST LEG-4 MODEL SAT FLIGHT -1	EQ-1	SHORT TERM TIME RECORDS	G Level 80	FIG.NO. 11.3

920 datapoints plotted per complete transducer record

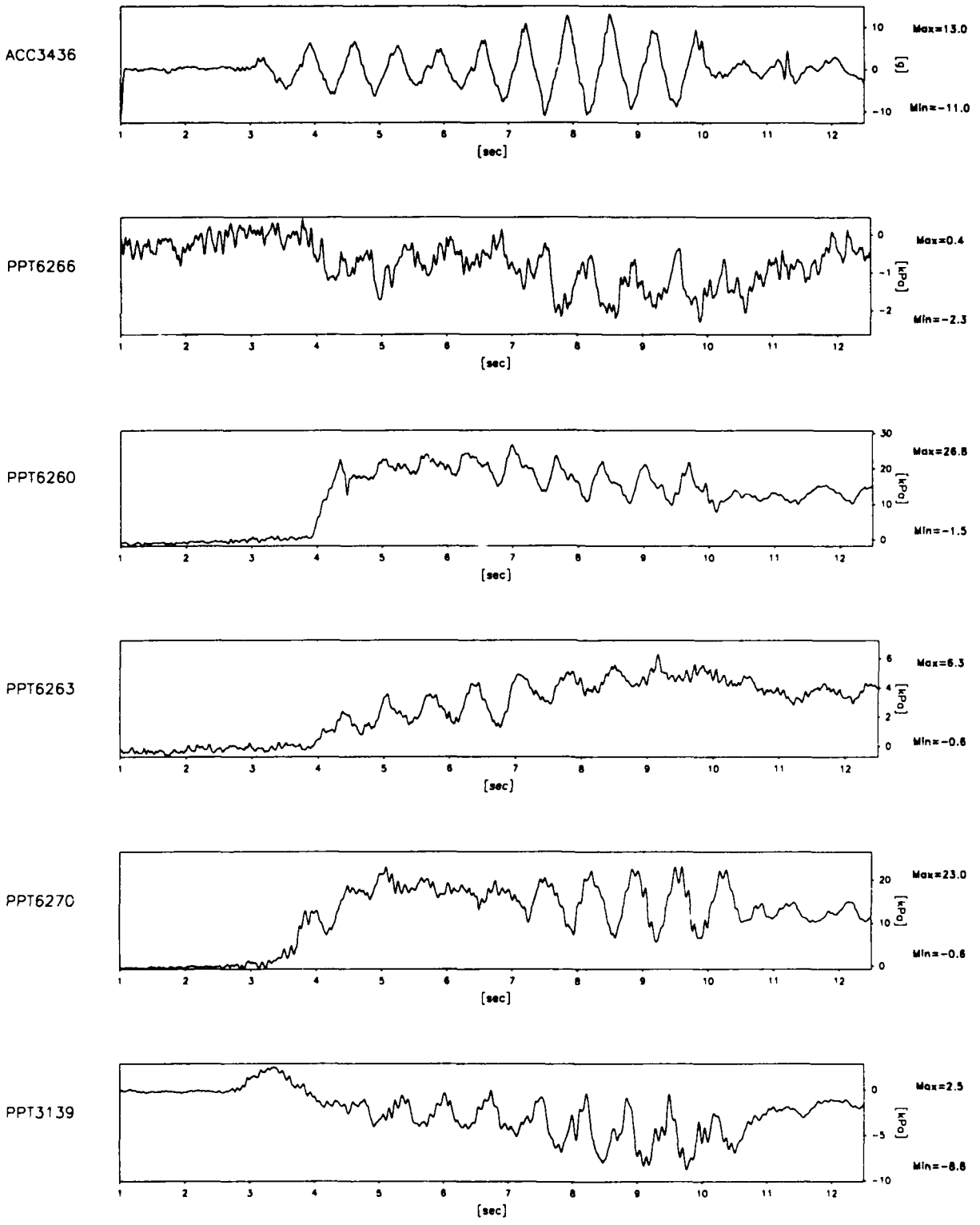

Scales : Prototype

TEST LEG--4 MODEL SAT FLIGHT -1	EQ-1	SHORT TERM TIME RECORDS	G Level 80	FIG.NO. **11.4**

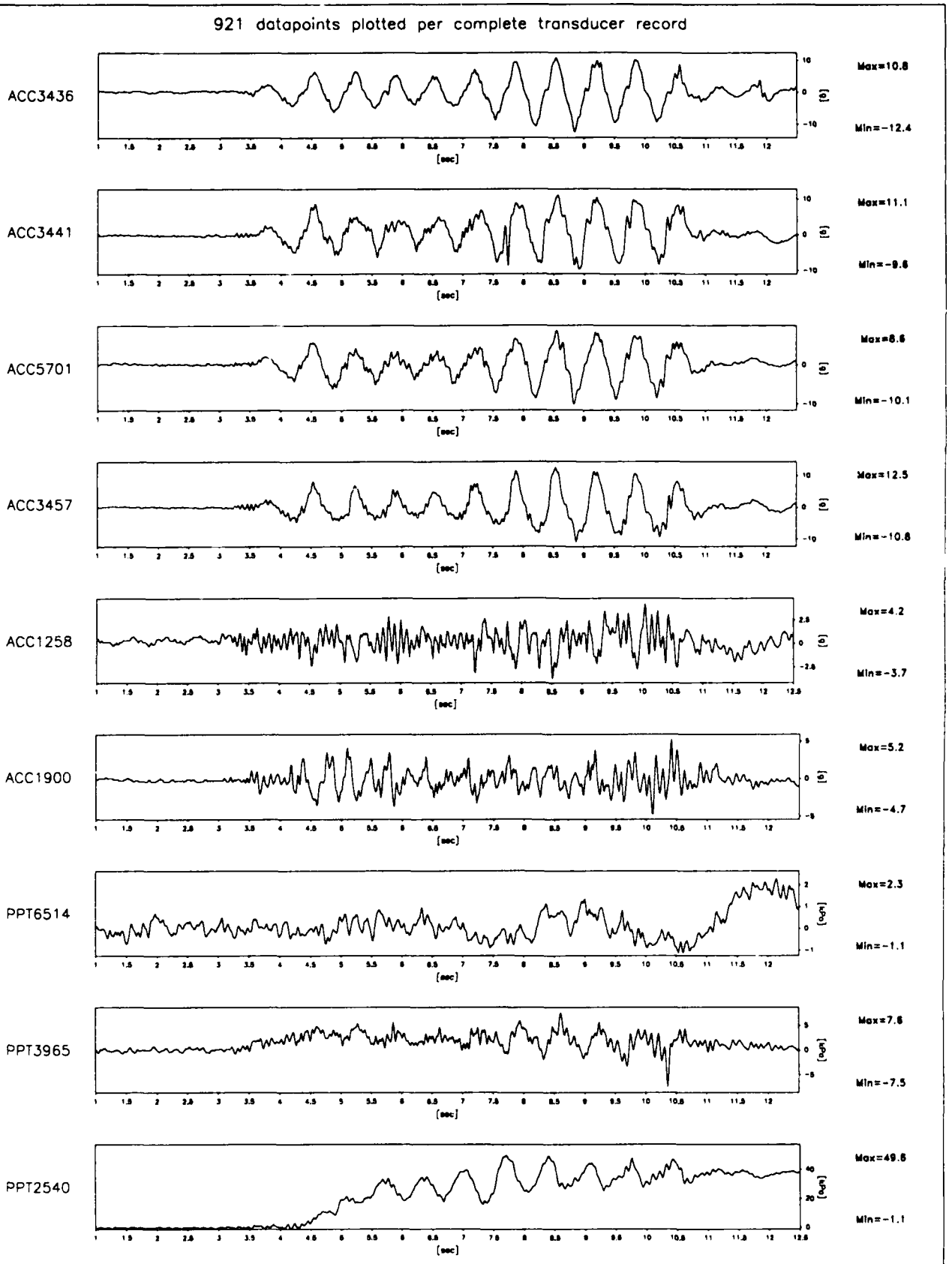

TEST LEG-4 MODEL SAT FLIGHT -1	EQ-1	SHORT TERM TIME RECORDS	G Level 80	FIG.NO. 11.5

921 datapoints plotted per complete transducer record

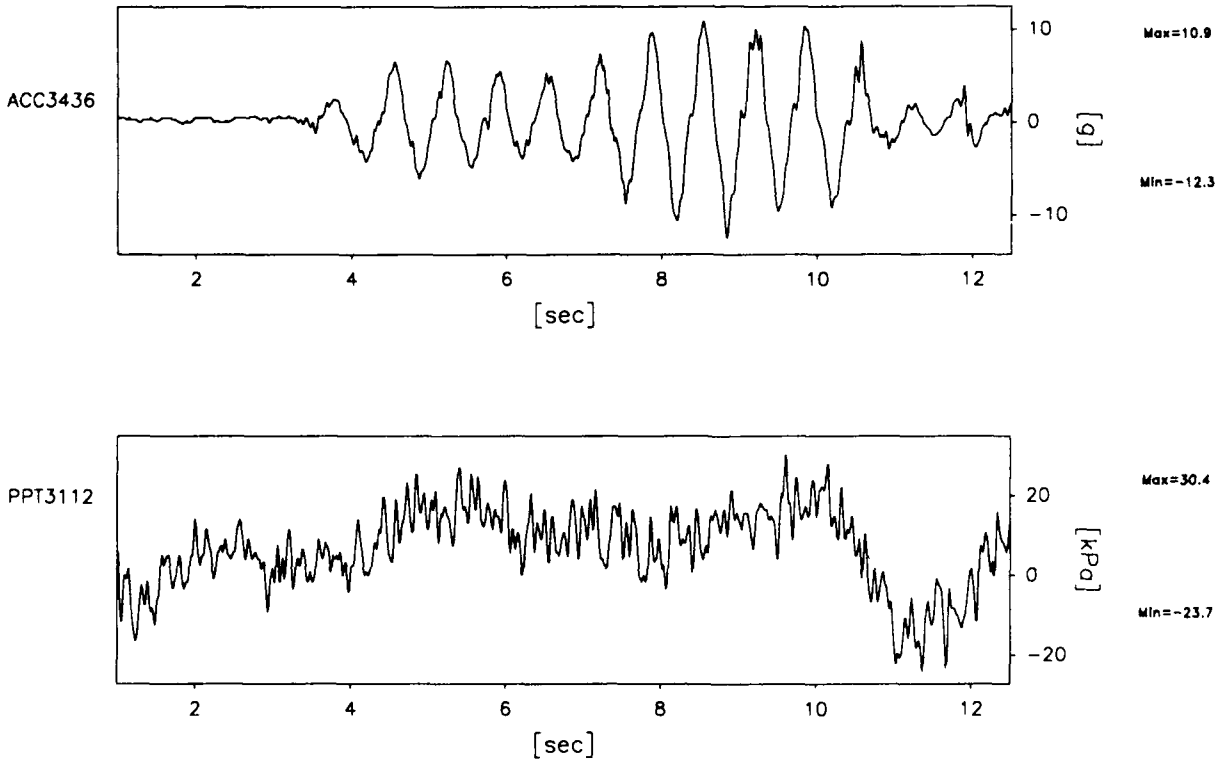

Scales : Prototype

TEST LEG-4 MODEL SAT FLIGHT -1	EQ-1	SHORT TERM TIME RECORDS	G Level 80	FIG.NO. **11.6**

930 datapoints plotted per complete transducer record

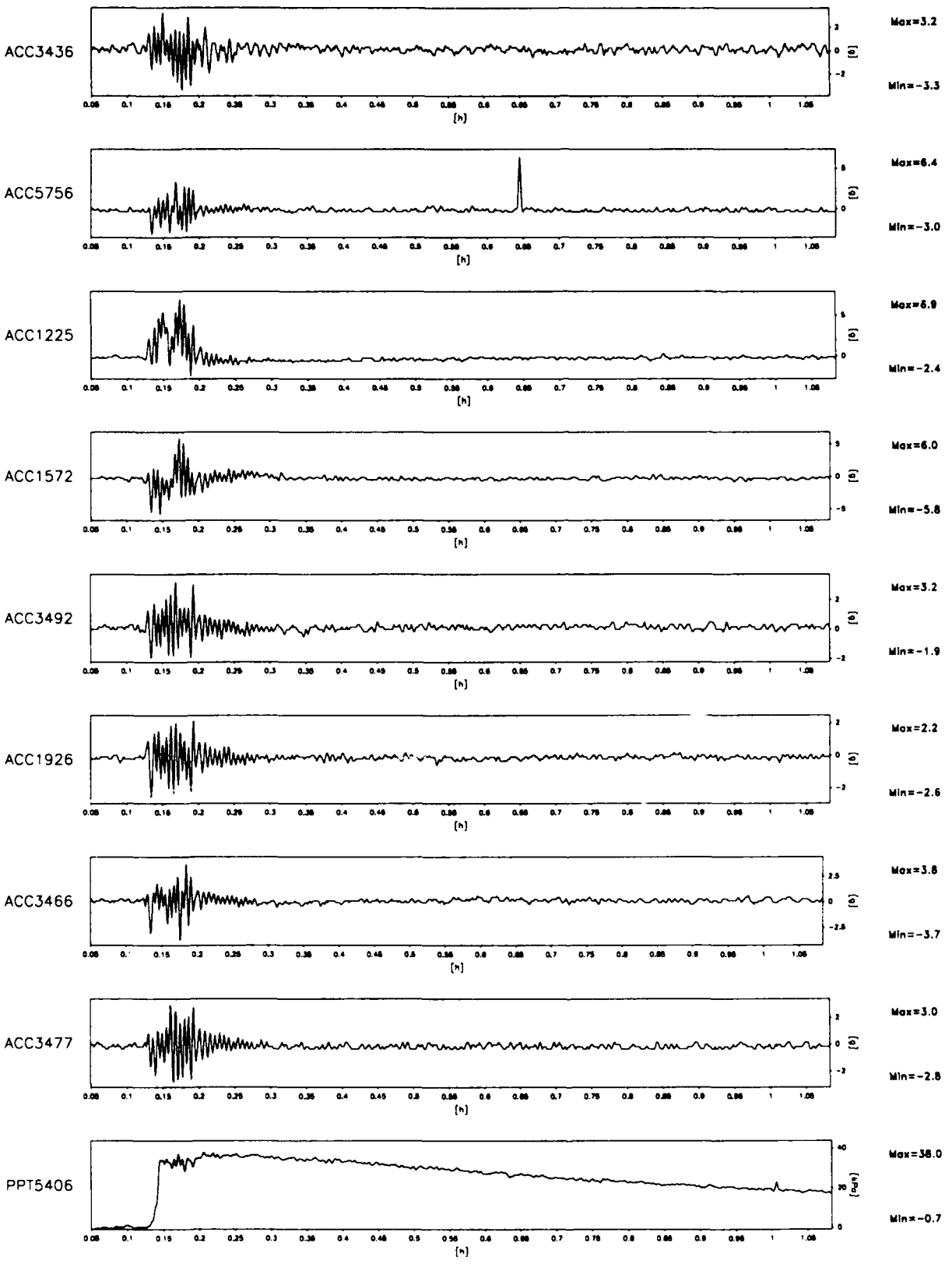

Scales : Prototype

TEST LEG-4 MODEL SAT FLIGHT -1	EQ-1	LONG TERM TIME RECORDS	G Level 80	FIG.NO. **11.7**

930 datapoints plotted per complete transducer record

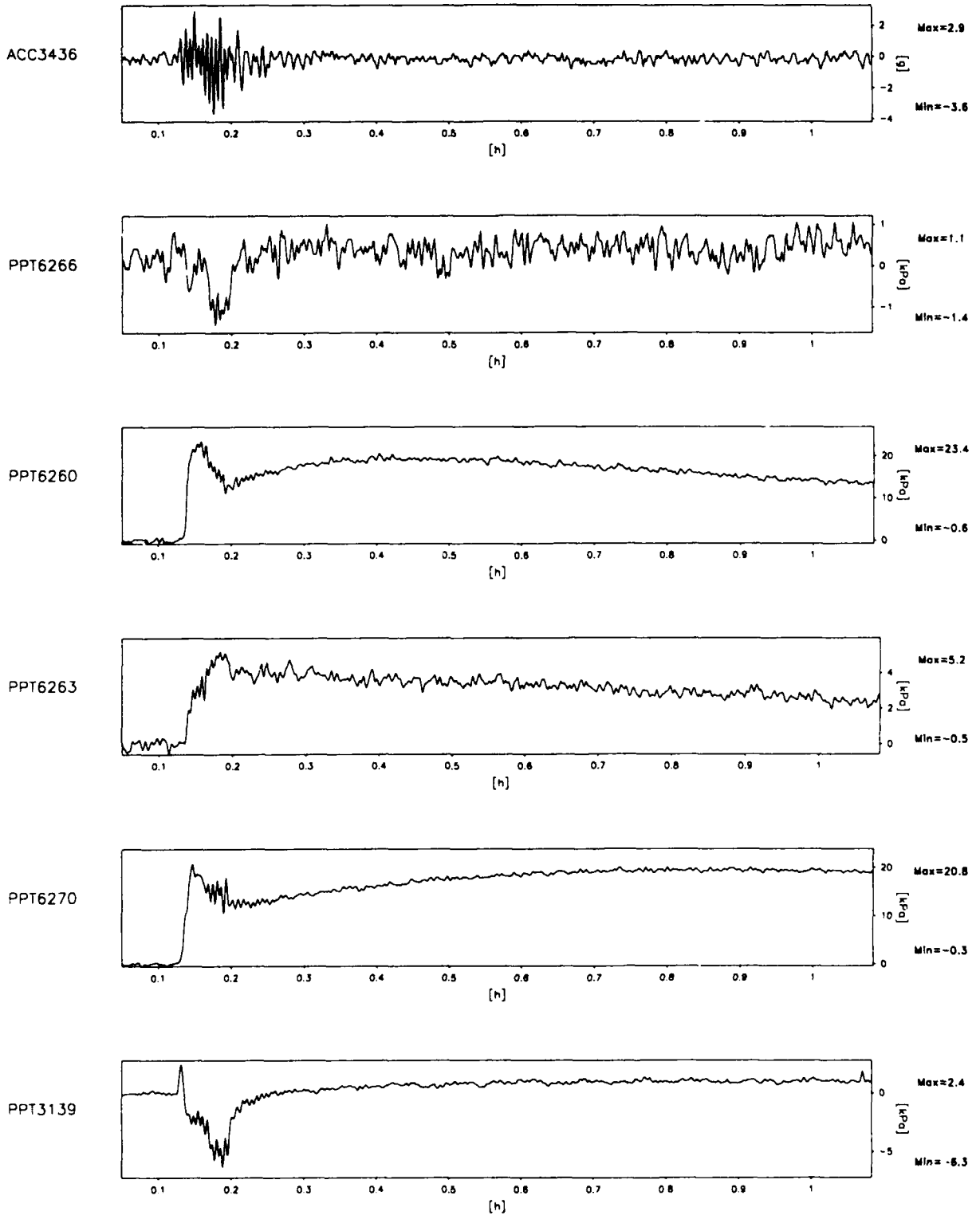

Scales : Prototype

TEST LEG-4 MODEL SAT FLIGHT -1	EQ-1	LONG TERM TIME RECORDS	G Level 80	FIG.NO. 11.8

931 datapoints plotted per complete transducer record

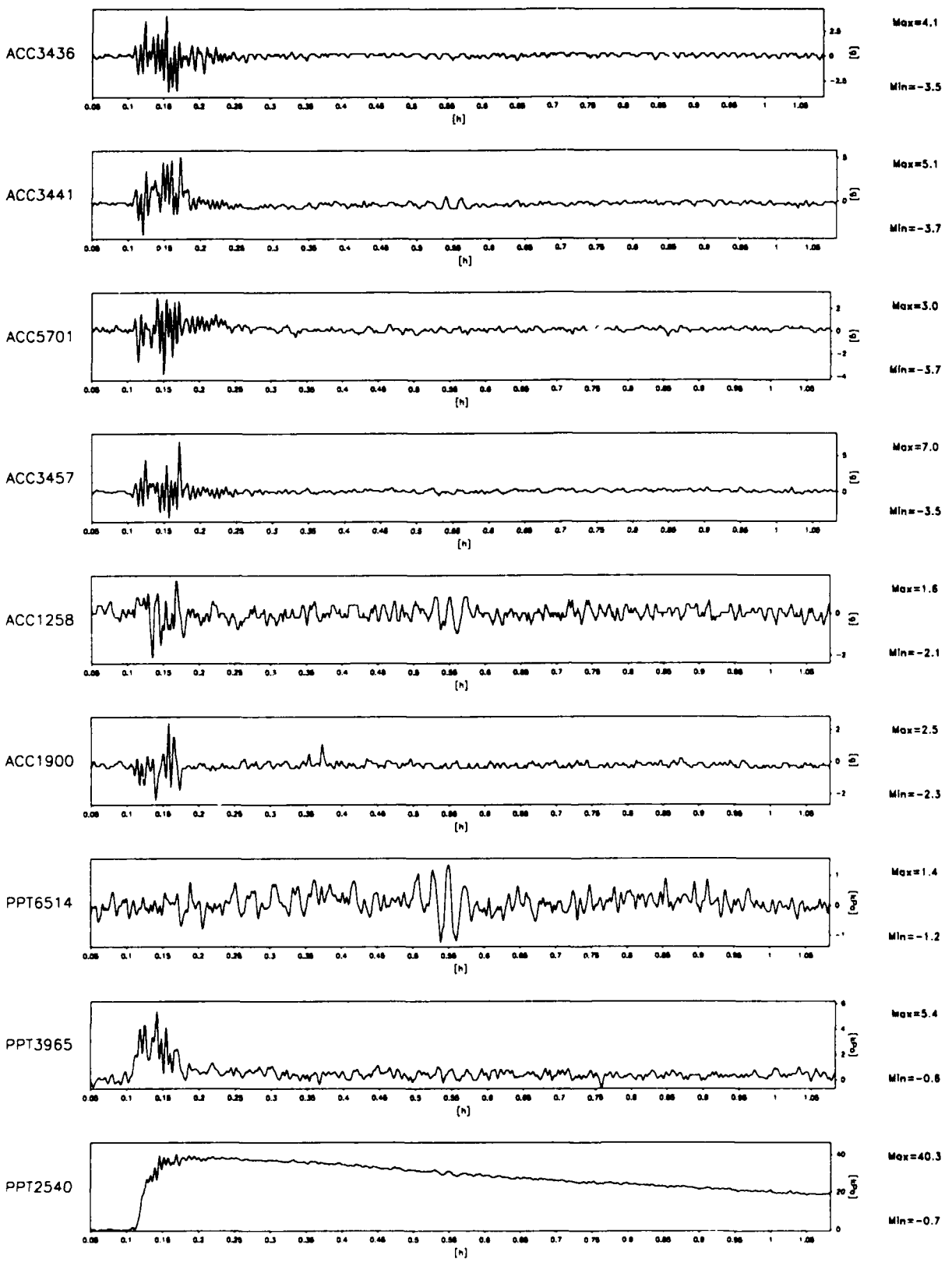

Scales : Prototype

TEST LEG-4 MODEL SAT FLIGHT -1	EQ-1	LONG TERM TIME RECORDS	G Level 80	FIG.NO. **11.9**

931 datapoints plotted per complete transducer record

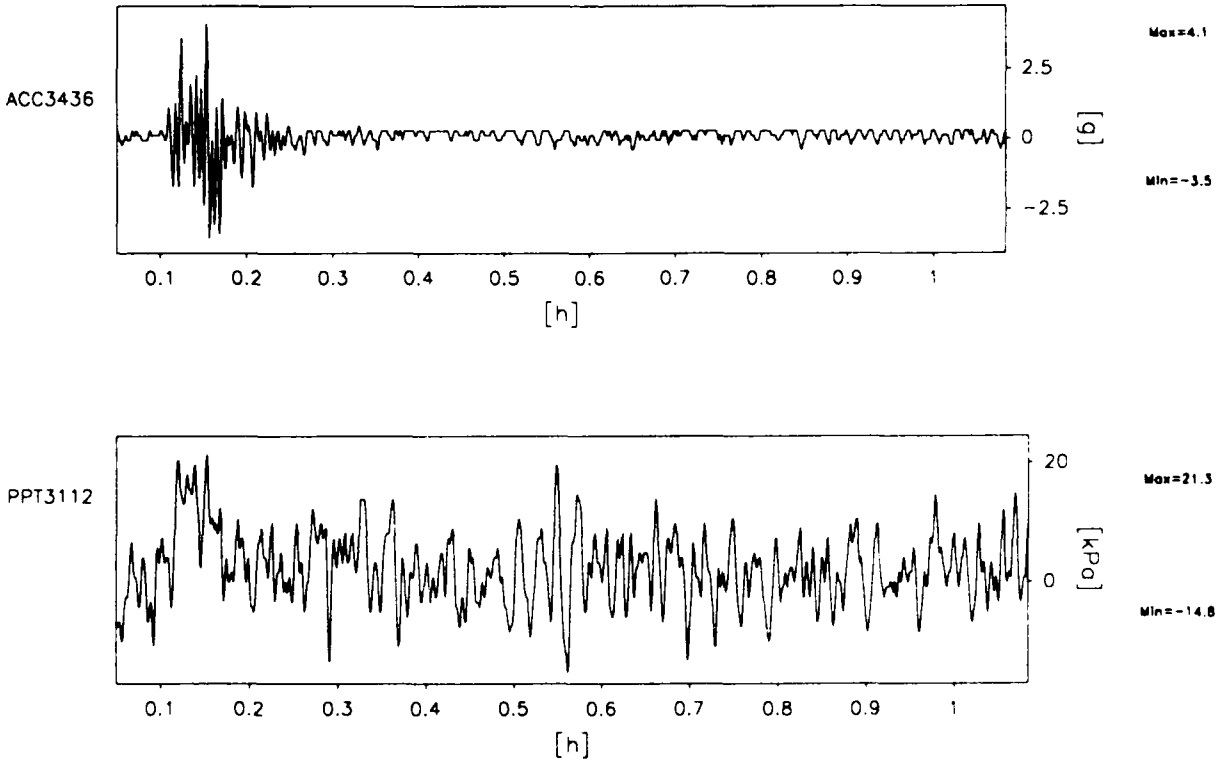

Scales : Prototype

TEST LEG-4 MODEL SAT FLIGHT -1	EQ-1	LONG TERM TIME RECORDS	G Level 80	FIG.NO. **11.10**

1202 datapoints plotted per complete transducer record

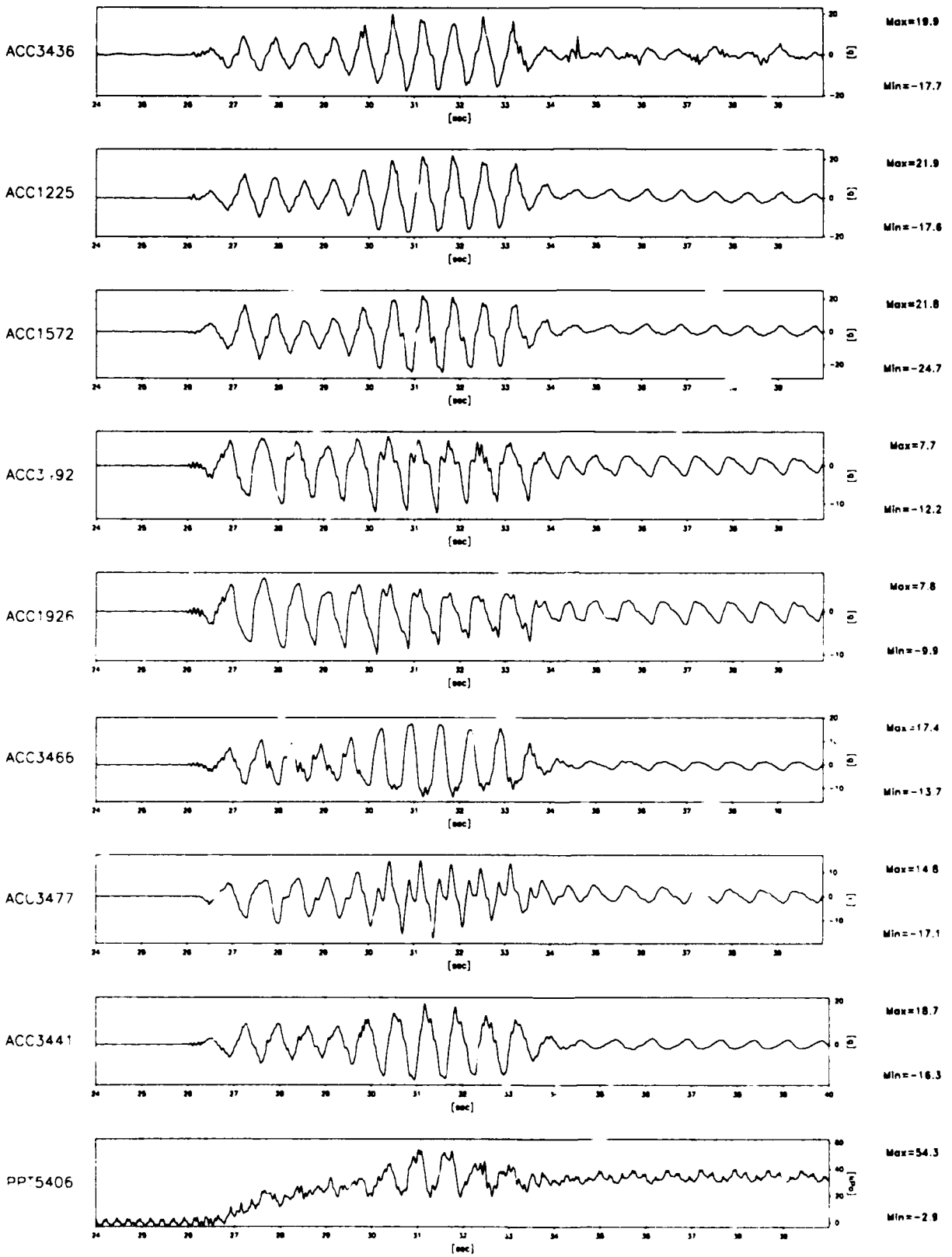

Scales : Prototype

TEST LEG-4 MODEL SAT FLIGHT -1	EQ-2	SHORT TERM TIME RECORDS	G Level 80	FIG.NO. 11.11

1202 datapoints plotted per complete transducer record

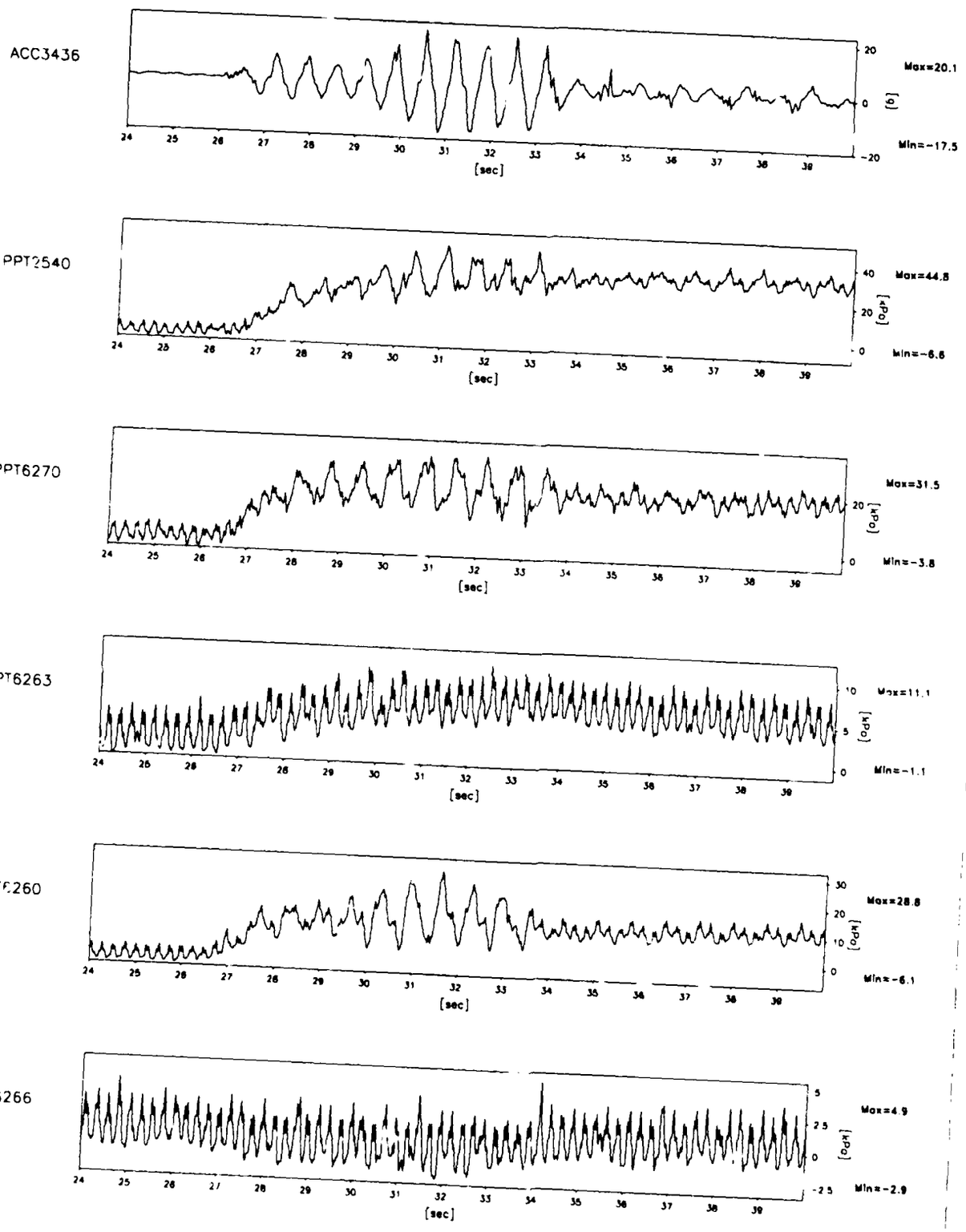

Scales : Prototype

TEST LEG-4 MODEL SAT FLIGHT - 1	EQ-2	SHORT TERM TIME RECORDS	G Level 80	FIG.NO 11.12

921 datapoints plotted per complete transducer record

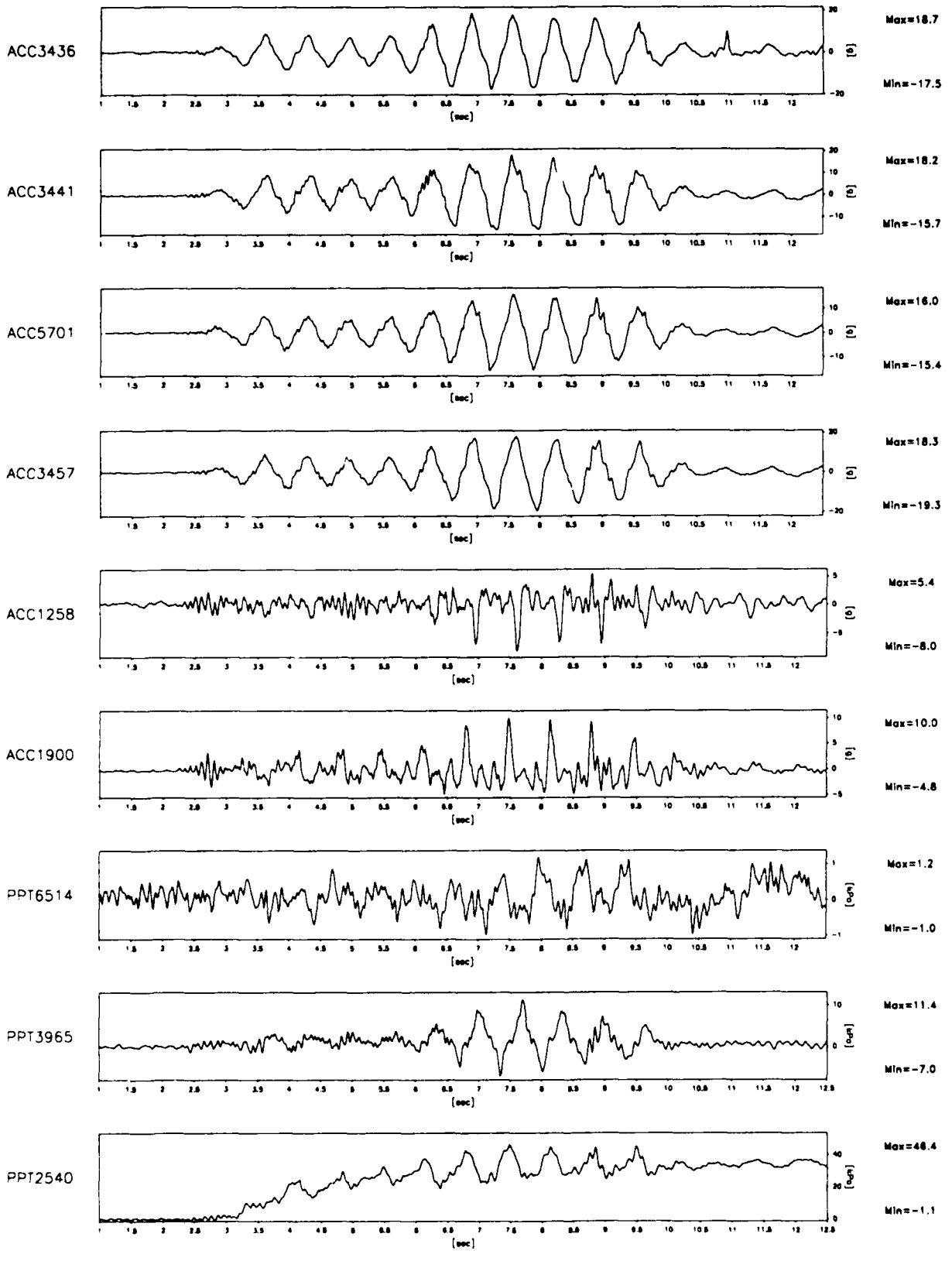

Scales : Prototype

TEST LEG-4 MODEL SAT FLIGHT -1	EQ-2	SHORT TERM TIME RECORDS	G Level 80	FIG.NO. 11.13

921 datapoints plotted per complete transducer record

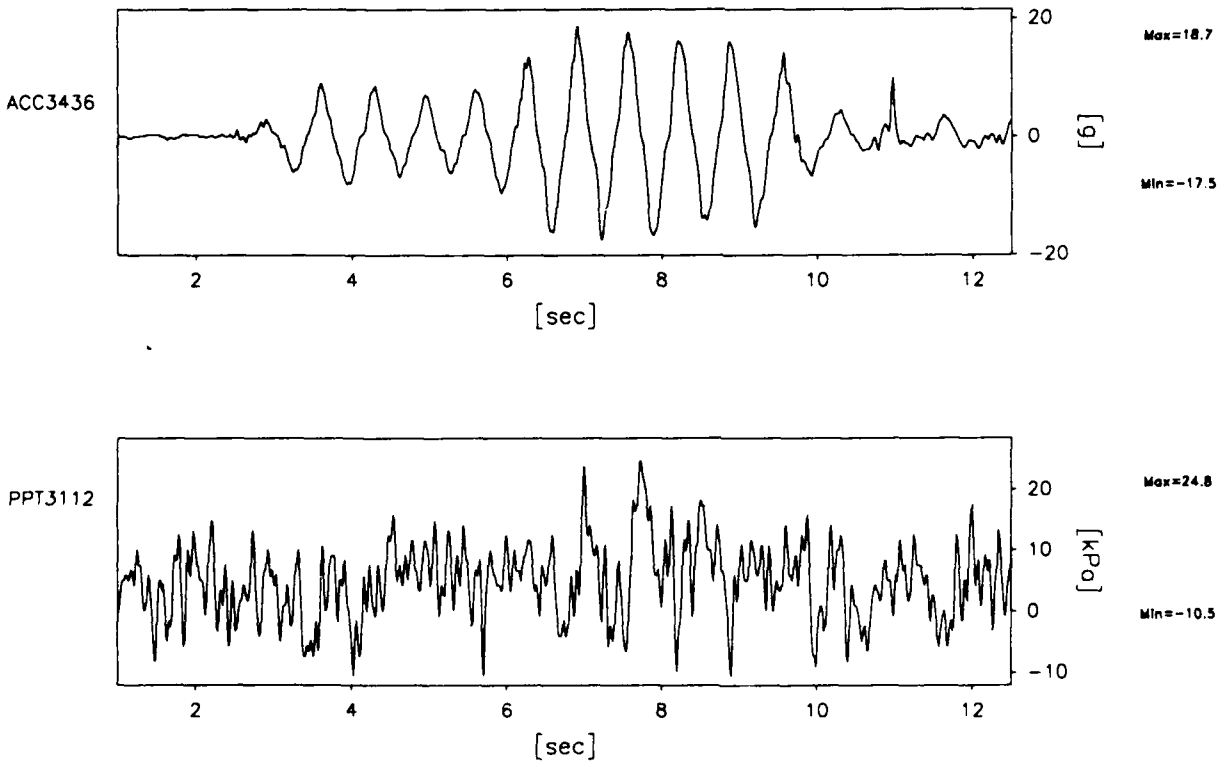

Scales : Prototype

TEST LEG-4 MODEL SAT FLIGHT -1	EQ-2	SHORT TERM TIME RECORDS	G Level 80	FIG.NO. **11.14**

930 datapoints plotted per complete transducer record

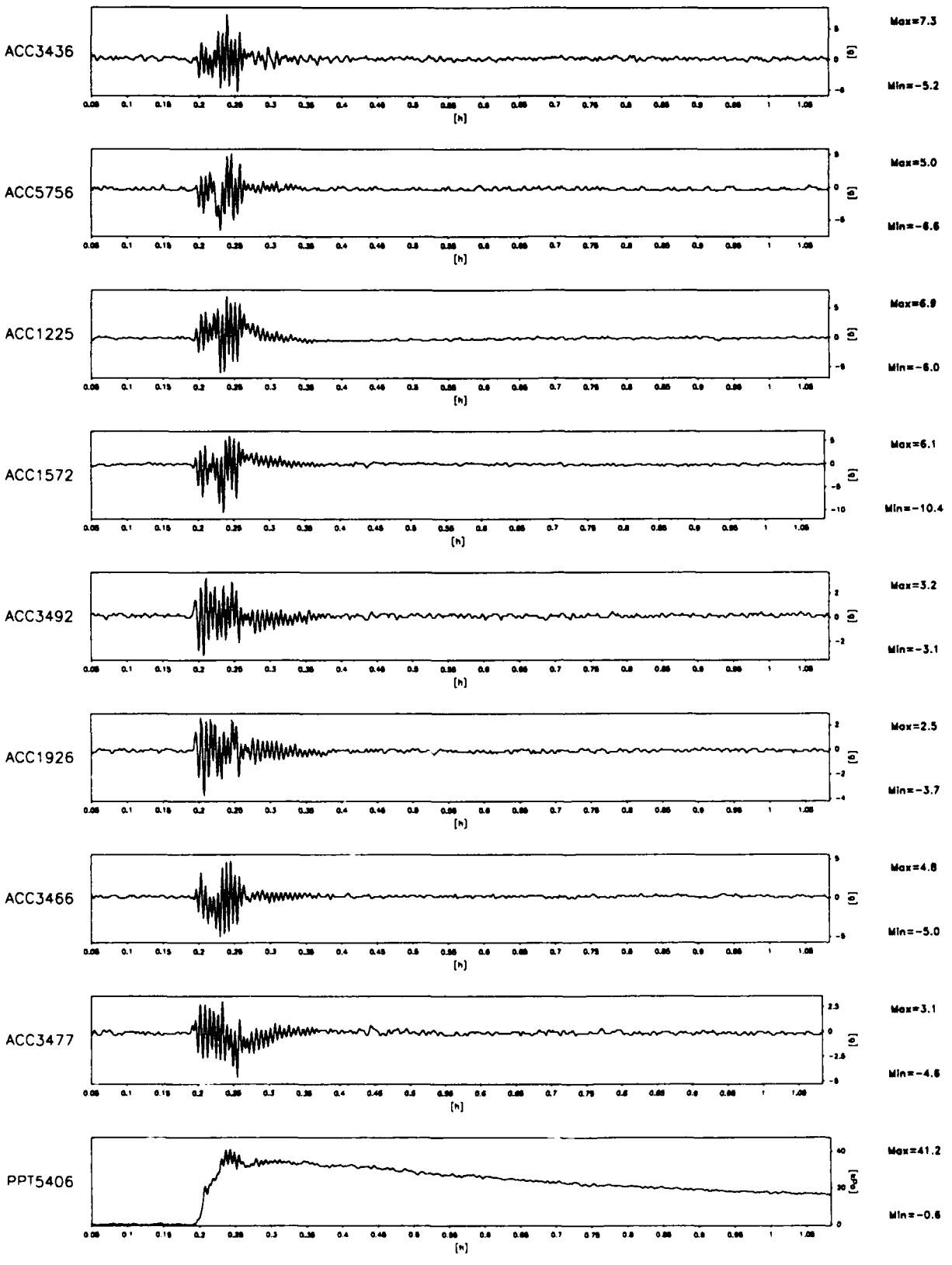

Scales : Prototype

TEST LEG-4 MODEL SAT FLIGHT -1	EQ-2	LONG TERM TIME RECORDS	G Level 80	FIG.NO. 11.15

930 datapoints plotted per complete transducer record

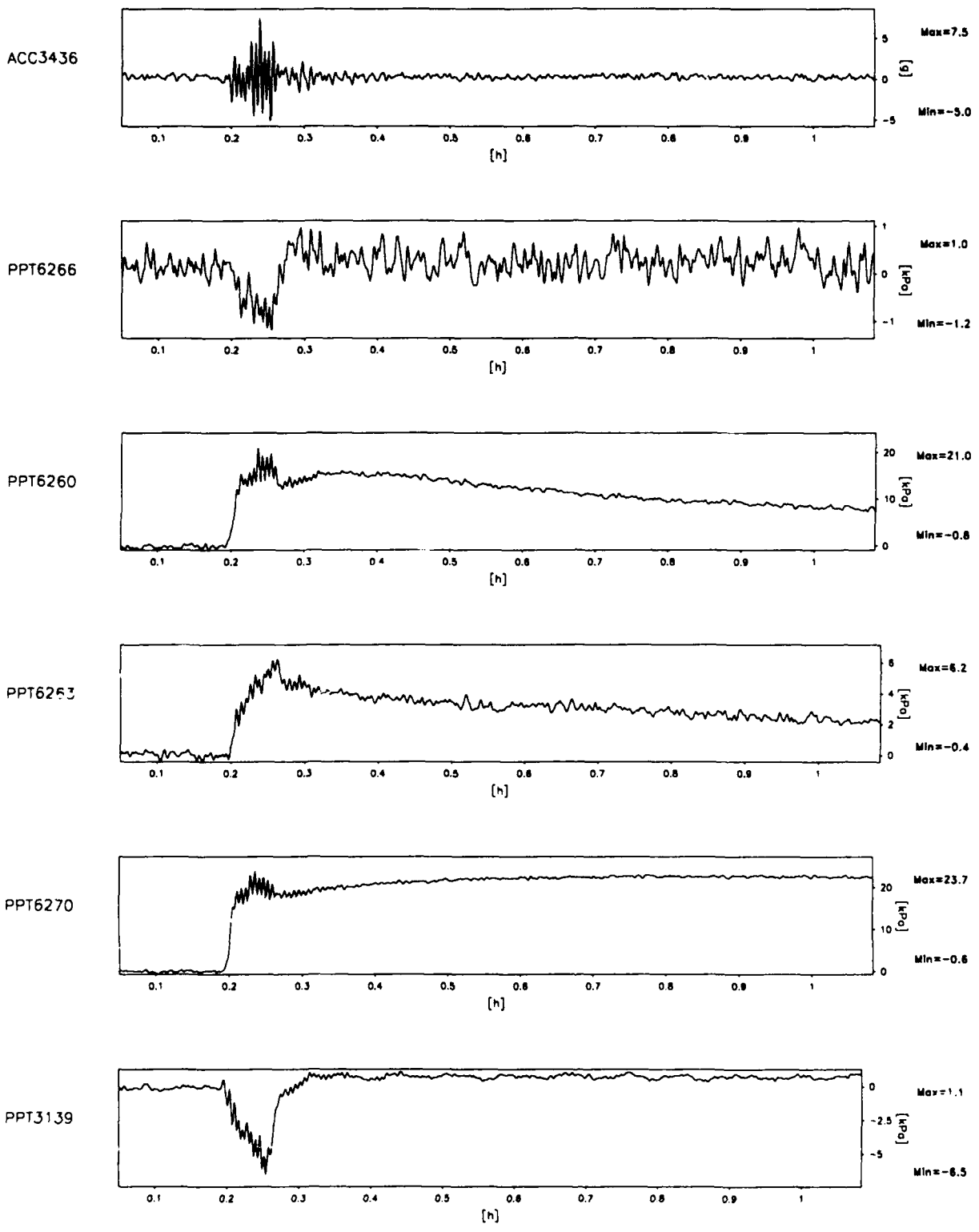

Scales : Prototype

TEST LEG-4 MODEL SAT FLIGHT -1	EQ-2	LONG TERM TIME RECORDS	G Level 80	FIG.NO. 11.16

931 datapoints plotted per complete transducer record

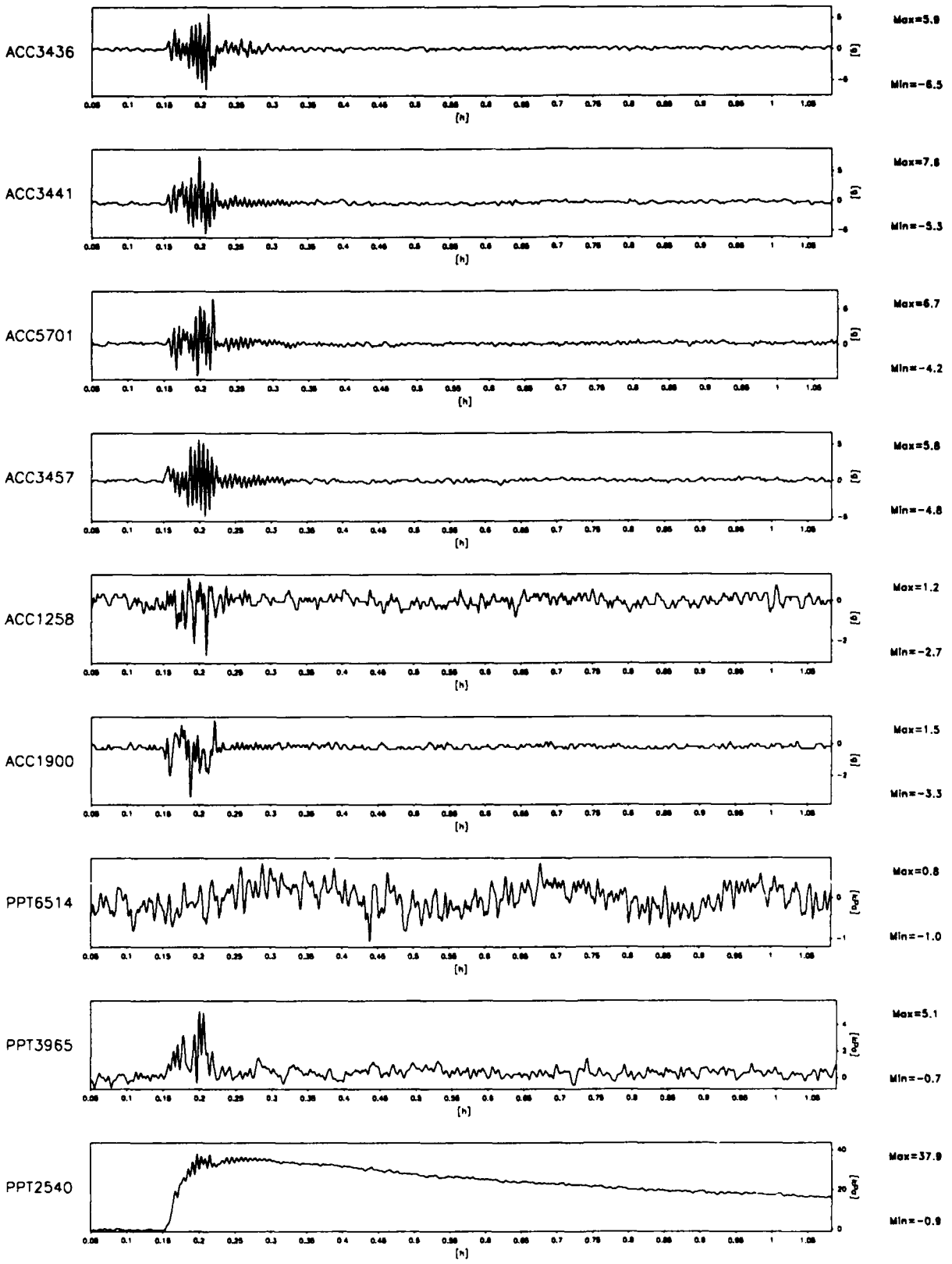

Scales : Prototype

TEST LEG-4 MODEL SAT FLIGHT -1	EQ-2	LONG TERM TIME RECORDS	G Level 80	FIG.NO. 11.17

931 datapoints plotted per complete transducer record

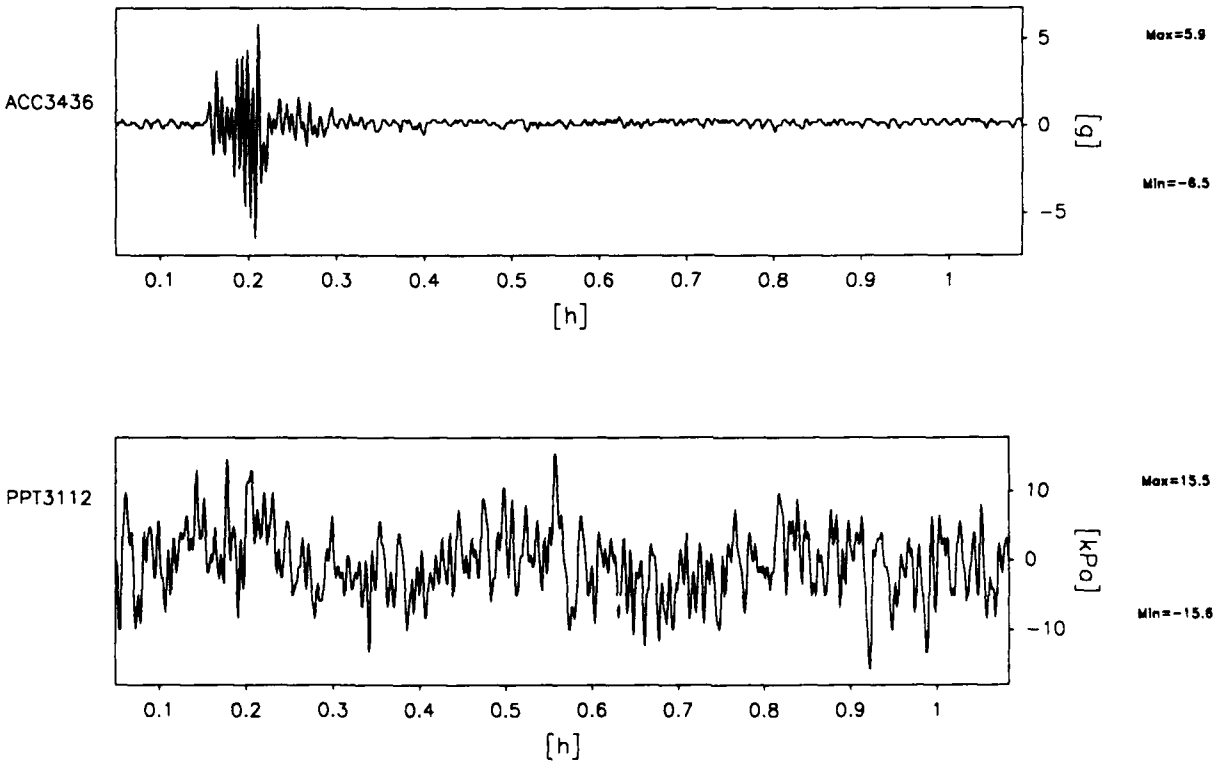

Scales : Prototype

TEST LEG-4 MODEL SAT FLIGHT -1	EQ-2	LONG TERM TIME RECORDS	G Level 80	FIG.NO. **11.18**

920 datapoints plotted per complete transducer record

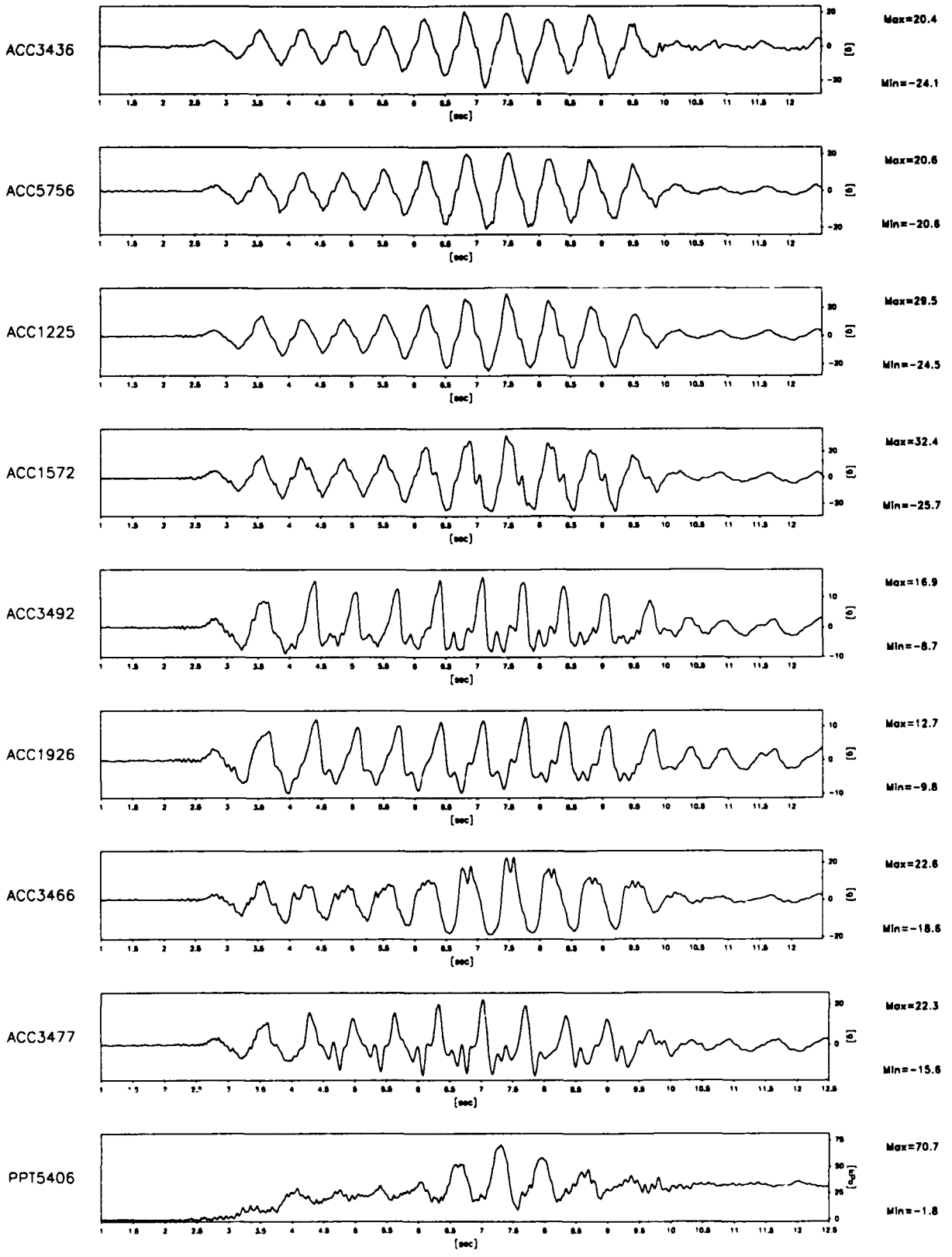

Scales : Prototype

TEST LEG-4 MODEL SAT FLIGHT -1	EQ-3	SHORT TERM TIME RECORDS	G Level 80	FIG.NO. **11.19**

920 datapoints plotted per complete transducer record

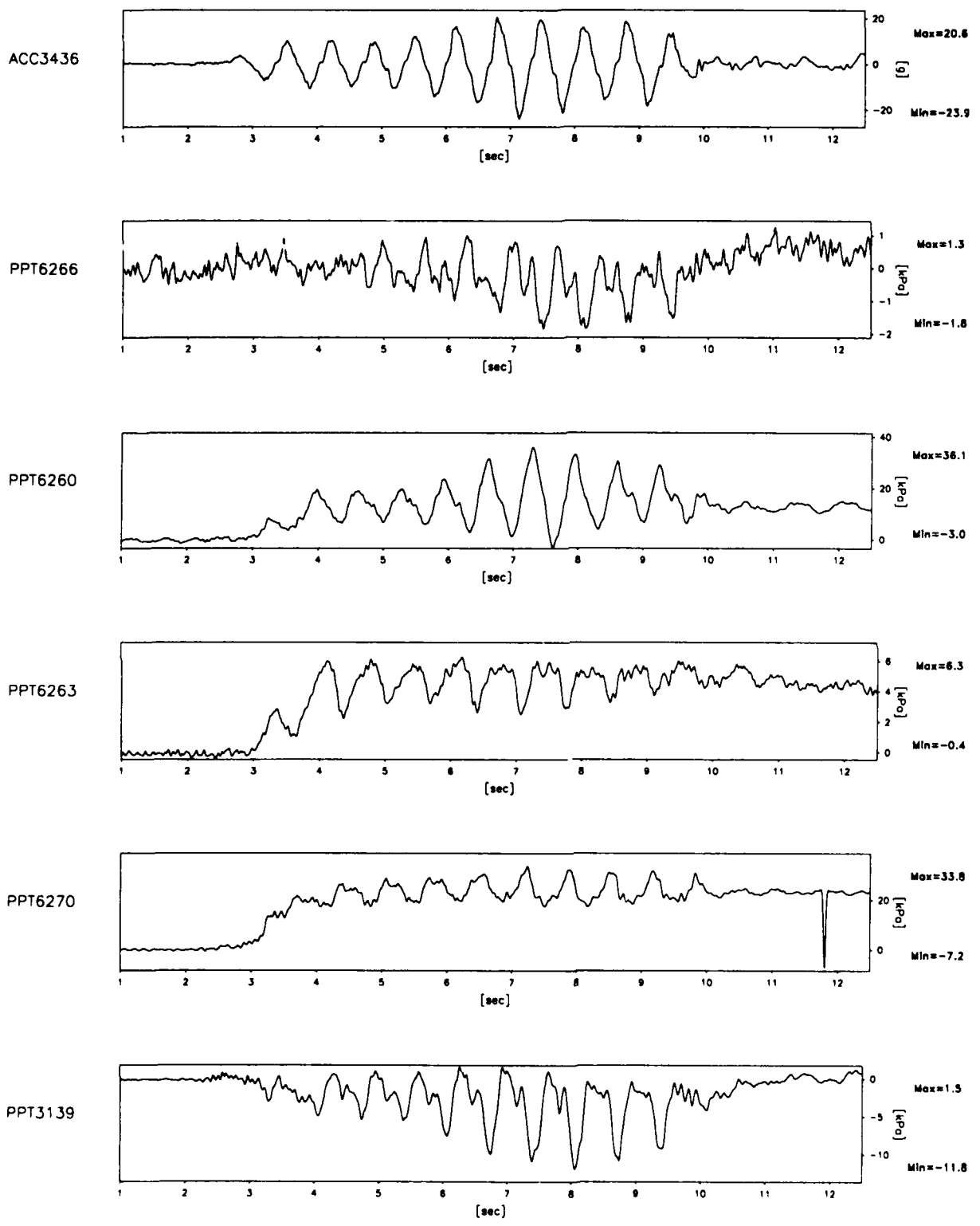

Scales : Prototype

TEST LEG-4 MODEL SAT FLIGHT -1	EQ-3	SHORT TERM TIME RECORDS	G Level 80	FIG.NO. **11.20**

921 datapoints plotted per complete transducer record

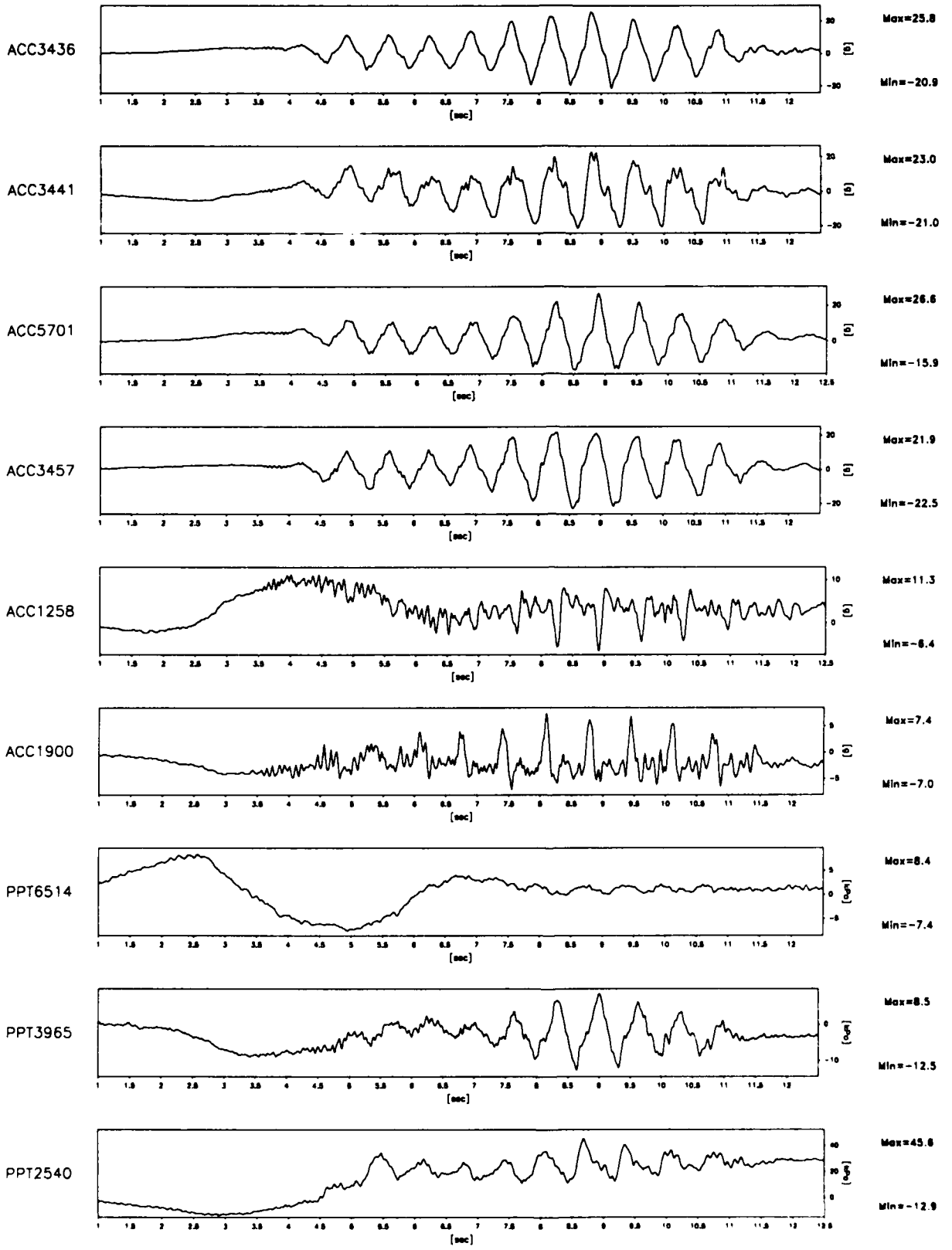

Scales : Prototype

TEST LEG-4 MODEL SAT FLIGHT -1	EQ-3	SHORT TERM TIME RECORDS	G Leve 80	FIG.NO. 11.21

921 datapoints plotted per complete transducer record

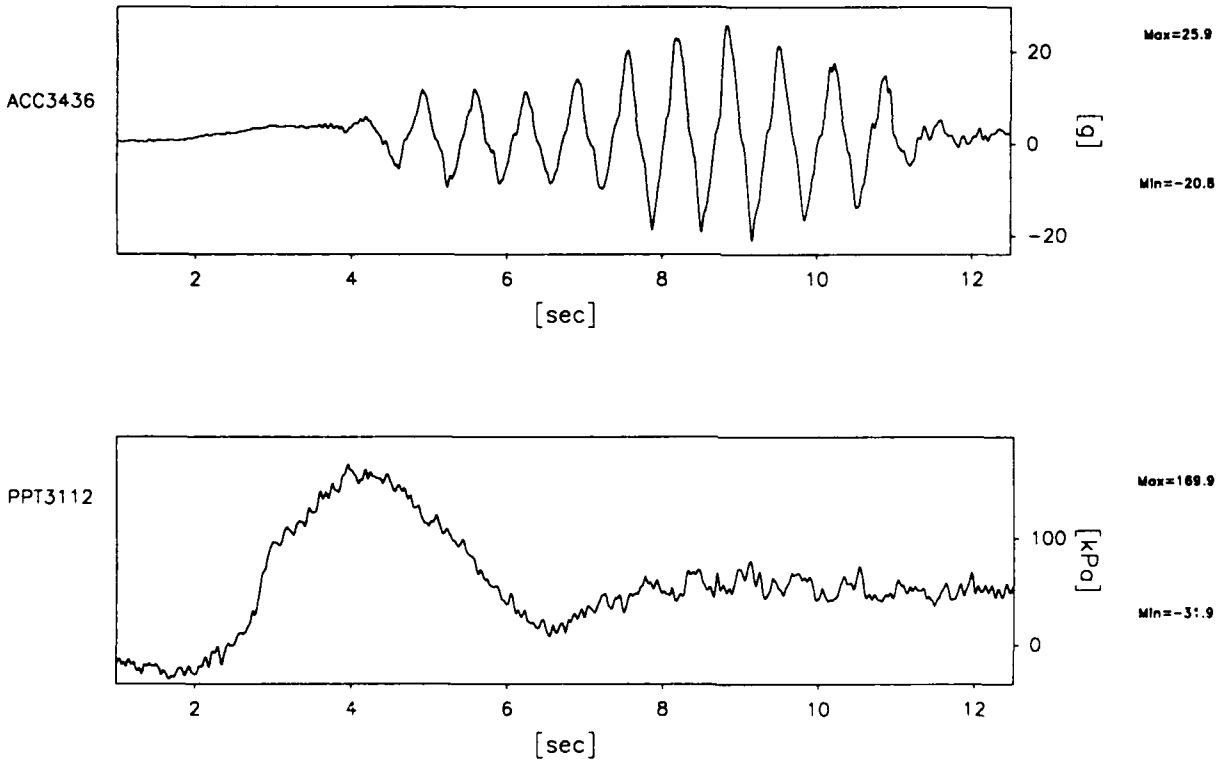

Scales : Prototype

TEST LEG-4 MODEL SAT FLIGHT -1	EQ-3	SHORT TERM TIME RECORDS	G Level 80	FIG.NO. 11.22

930 datapoints plotted per complete transducer record

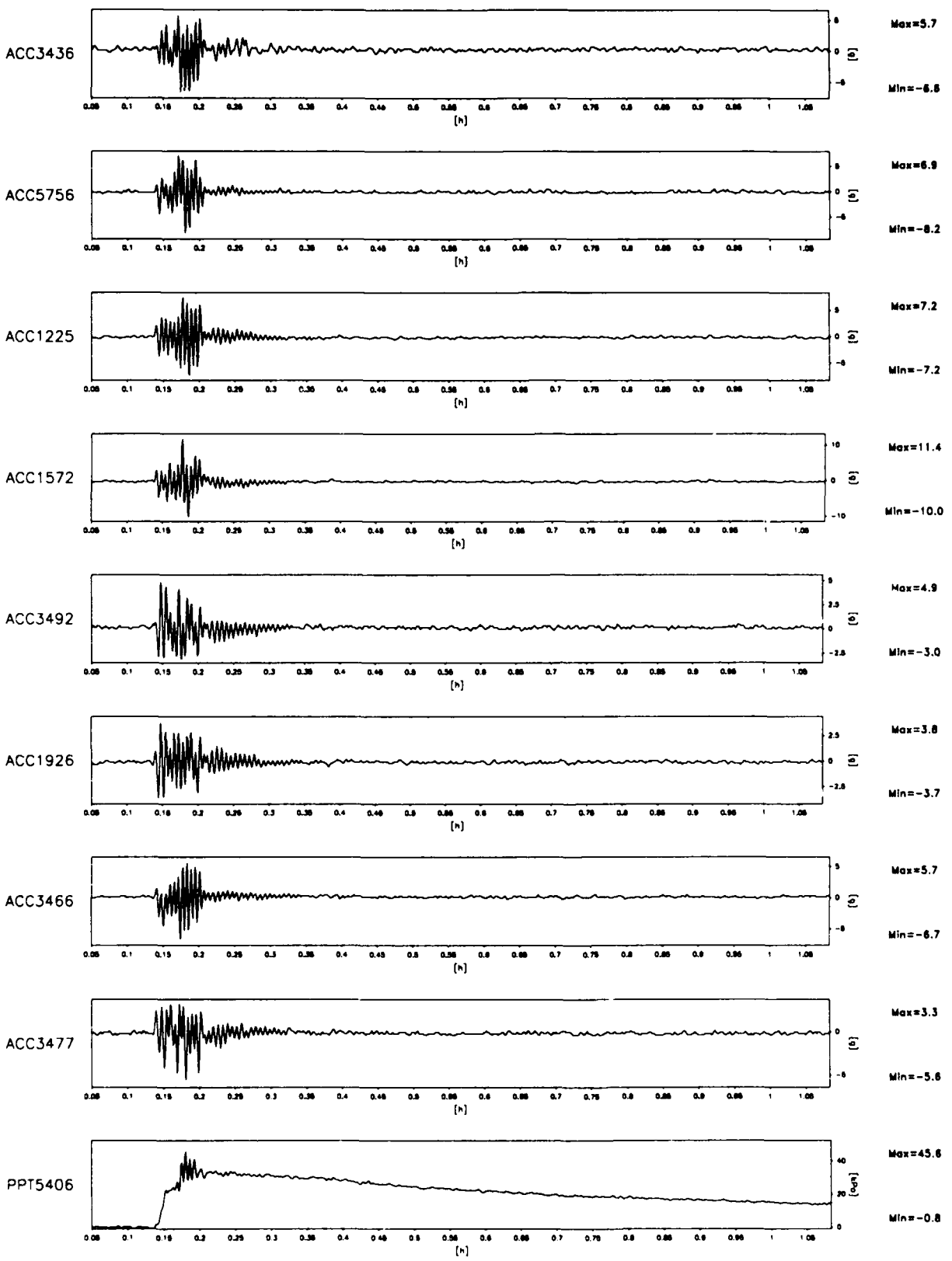

Scales : Prototype

TEST LEG-4 MODEL SAT FLIGHT -1	EQ-3	LONG TERM TIME RECORDS	G Level 80	FIG.NO. 11.23

930 datapoints plotted per complete transducer record

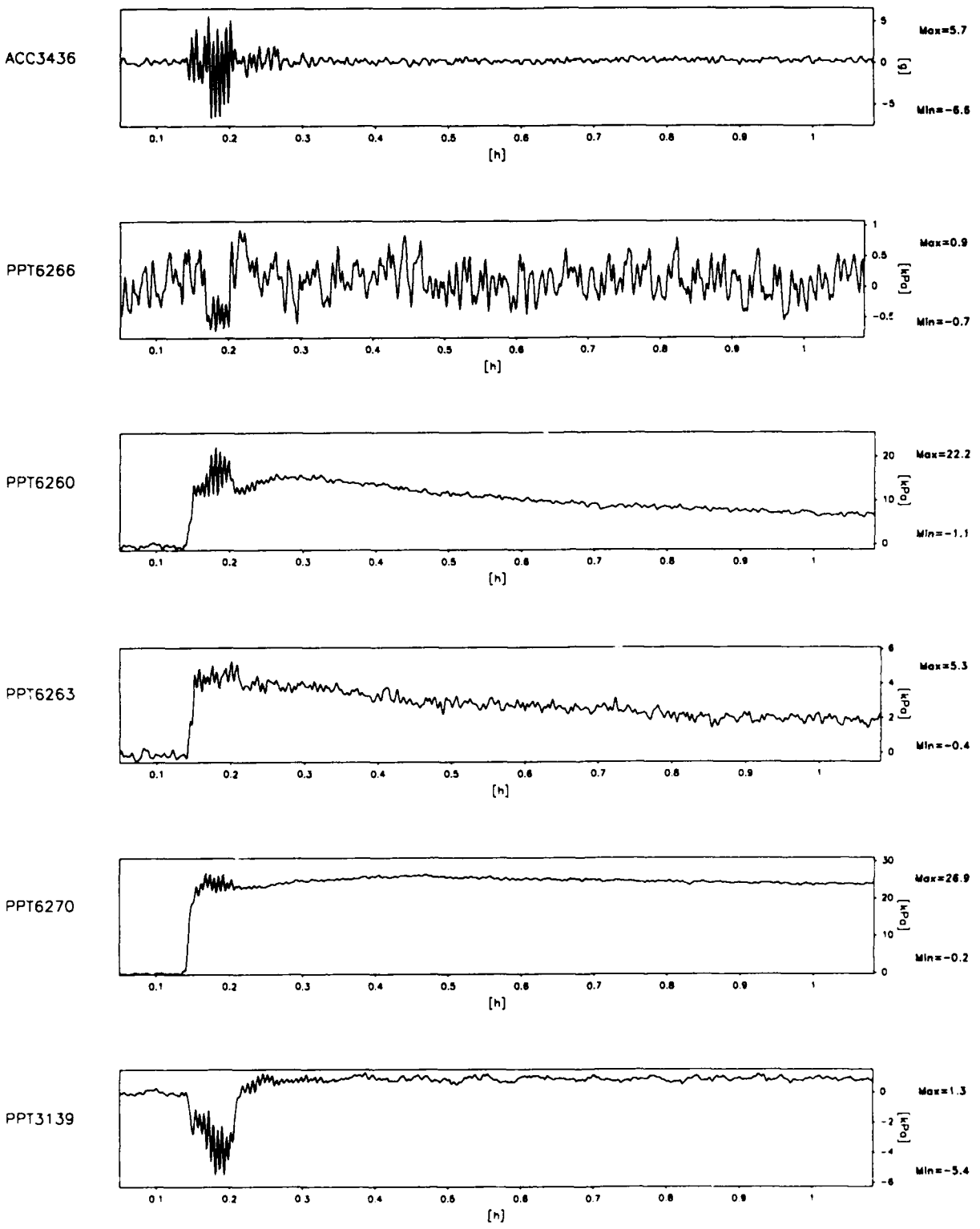

Scales : Prototype

TEST LEG-4 MODEL SAT FLIGHT -1	EQ-3	LONG TERM TIME RECORDS	G Level 80	FIG.NO. **11.24**

931 datapoints plotted per complete transducer record

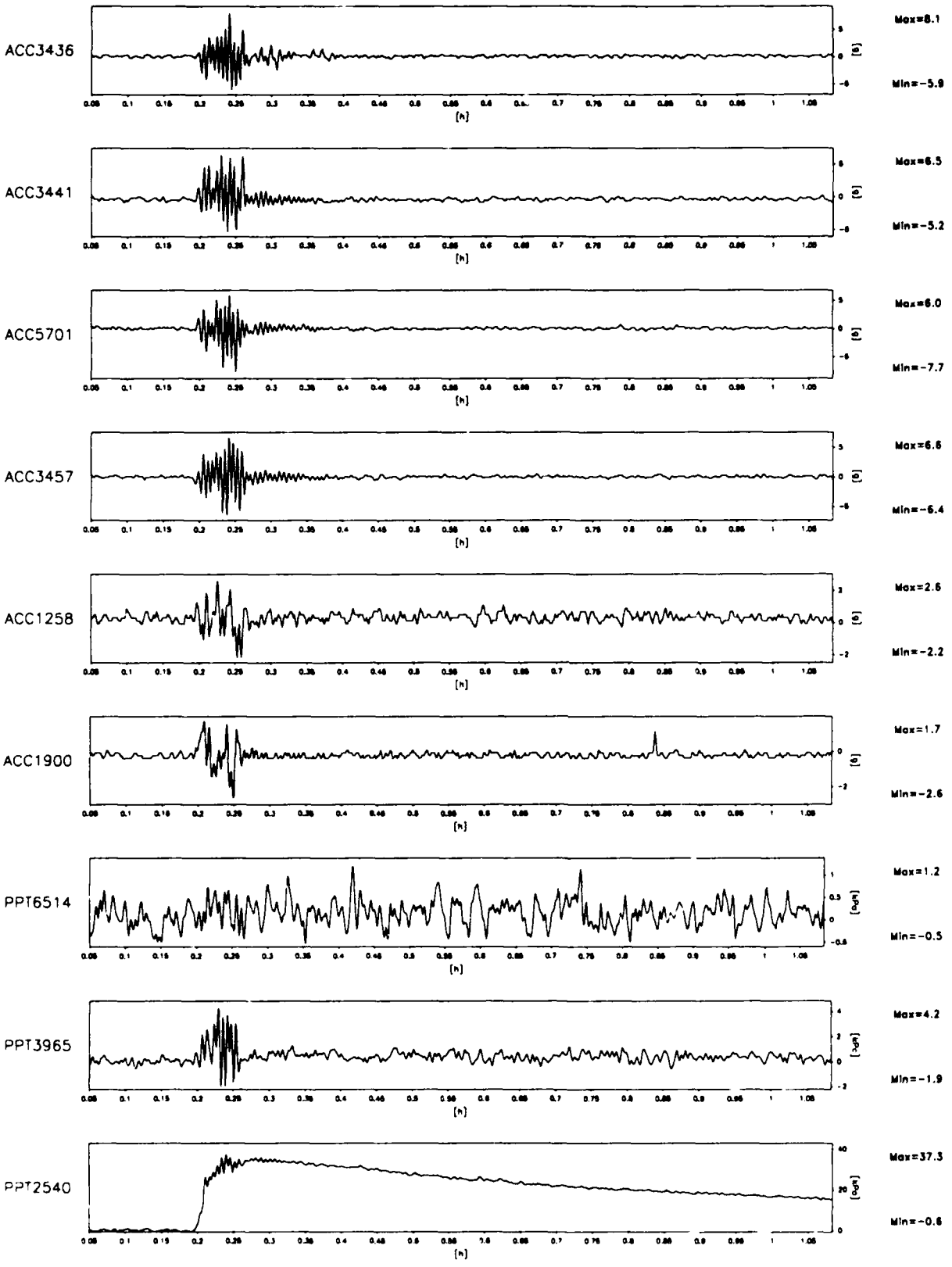

Scales : Prototype

TEST LEG-4 MODEL SAT FLIGHT -1	EQ-3	LONG TERM TIME RECORDS	G Level 80	FIG.NO. 11.25

931 datapoints plotted per complete transducer record

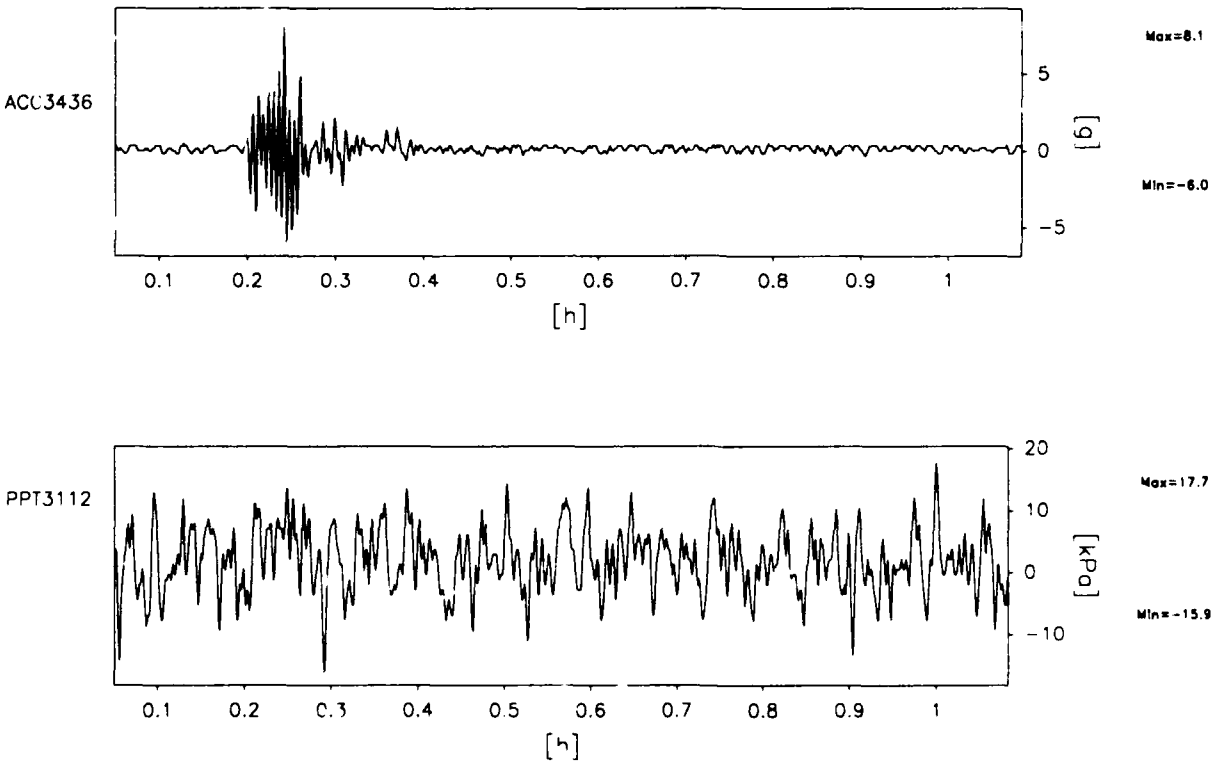

Scales : Prototype

TEST LEG-4 MODEL SAT FLIGHT -1	EQ-3	LONG TERM TIME RECORDS	G Level 80	FIG.NO. 11.26

920 datapoints plotted per complete transducer record

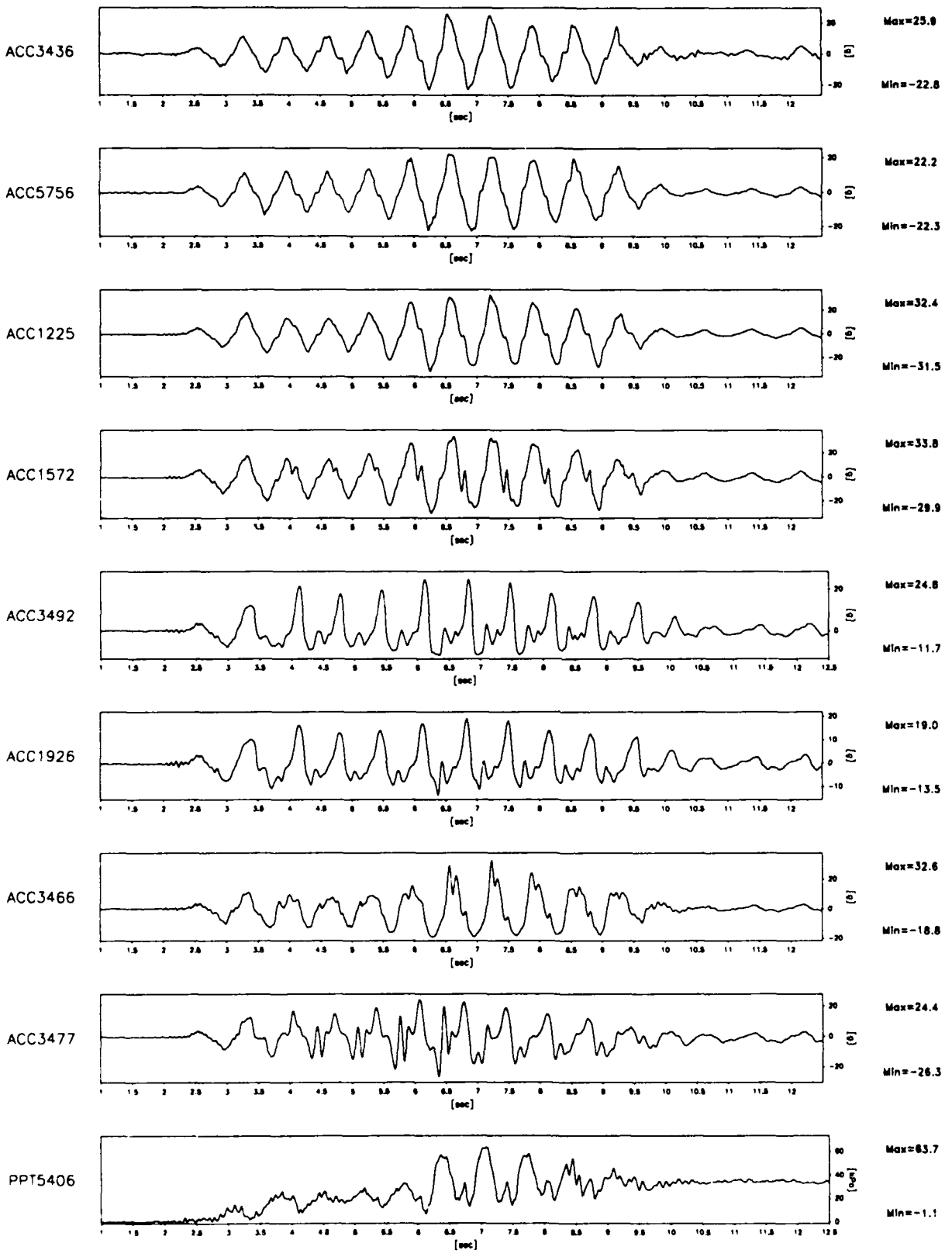

Scales : Prototype

TEST LEG-4 MODEL SAT FLIGHT -1	EQ-4	SHORT TERM TIME RECORDS	G Level 80	FIG.NO. 11.27

920 datapoints plotted per complete transducer record

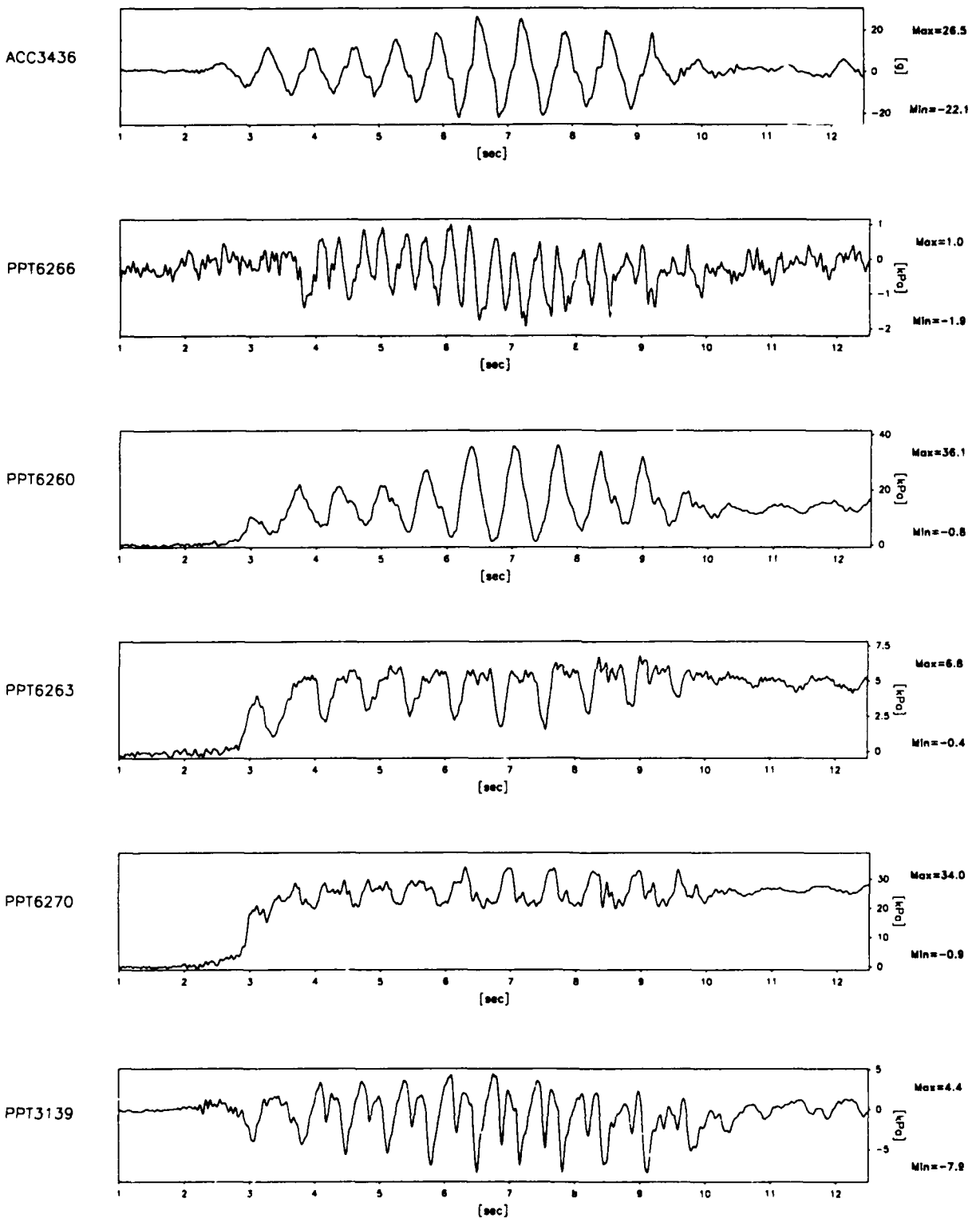

Scales : Prototype

TEST LEG-4 MODEL SAT FLIGHT -1	EQ-4	SHORT TERM TIME RECORDS	G Level 80	FIG.NO. **11.28**

921 datapoints plotted per complete transducer record

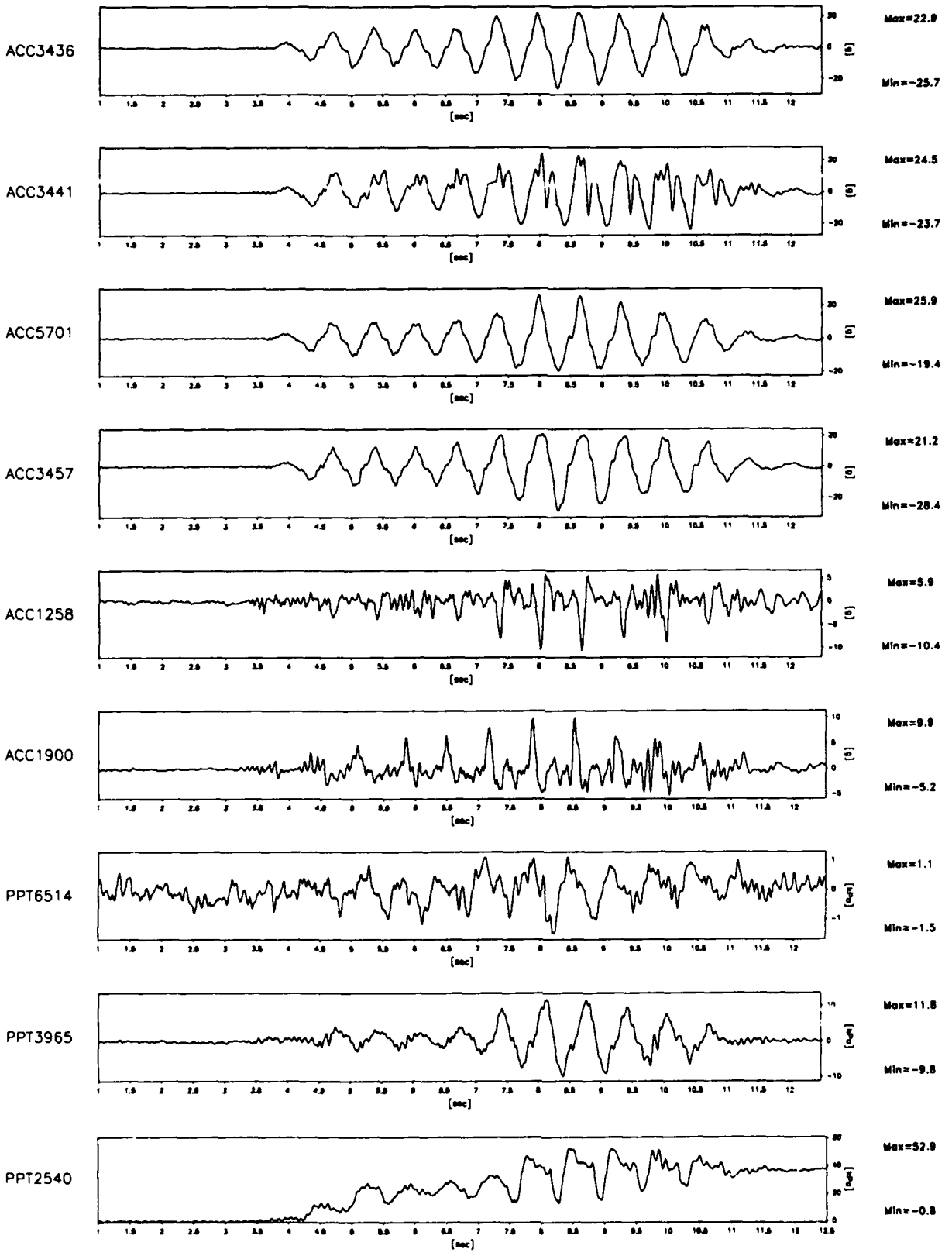

Scales : Prototype

TEST LEG-4 MODEL SAT FLIGHT -1	EQ-4	SHORT TERM TIME RECORDS	G Level 80	FIG.NO. 11.29

921 datapoints plotted per complete transducer record

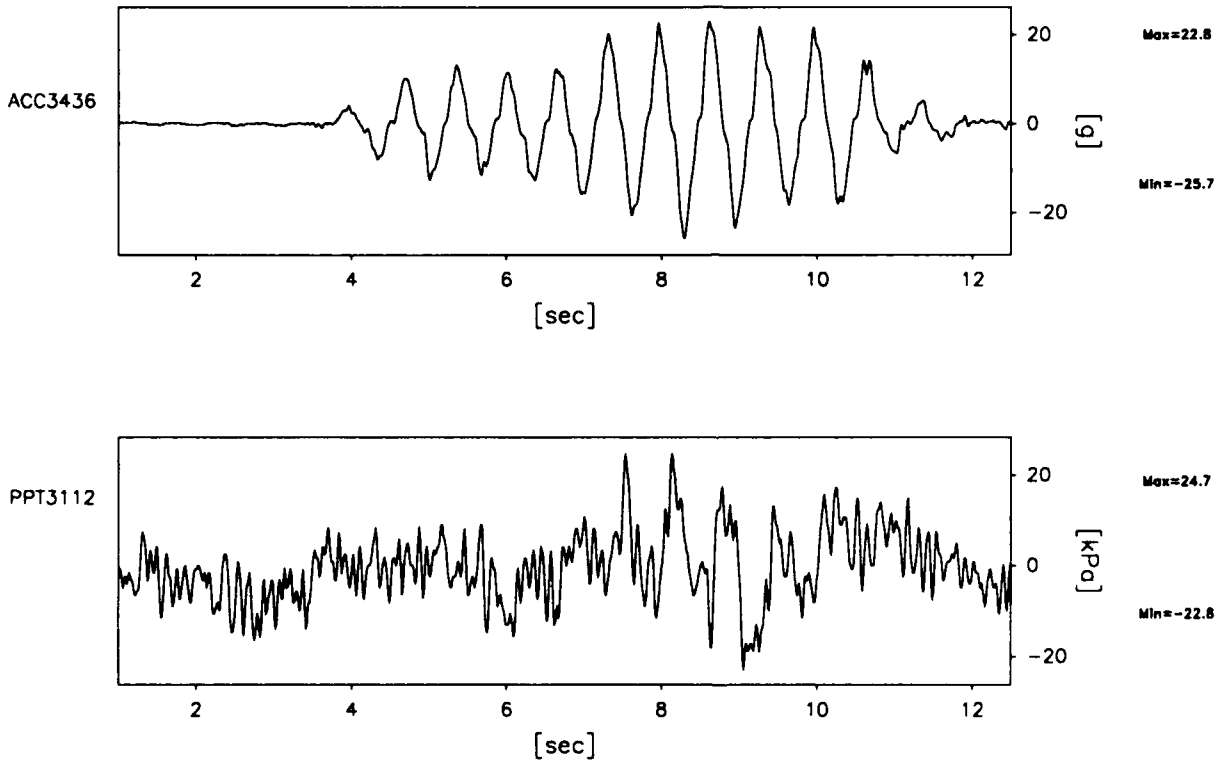

Scales : Prototype

TEST LEG-4 MODEL SAT FLIGHT -1	EQ-4	SHORT TERM TIME RECORDS	G Level 80	FIG.NO. 11.30

930 datapoints plotted per complete transducer record

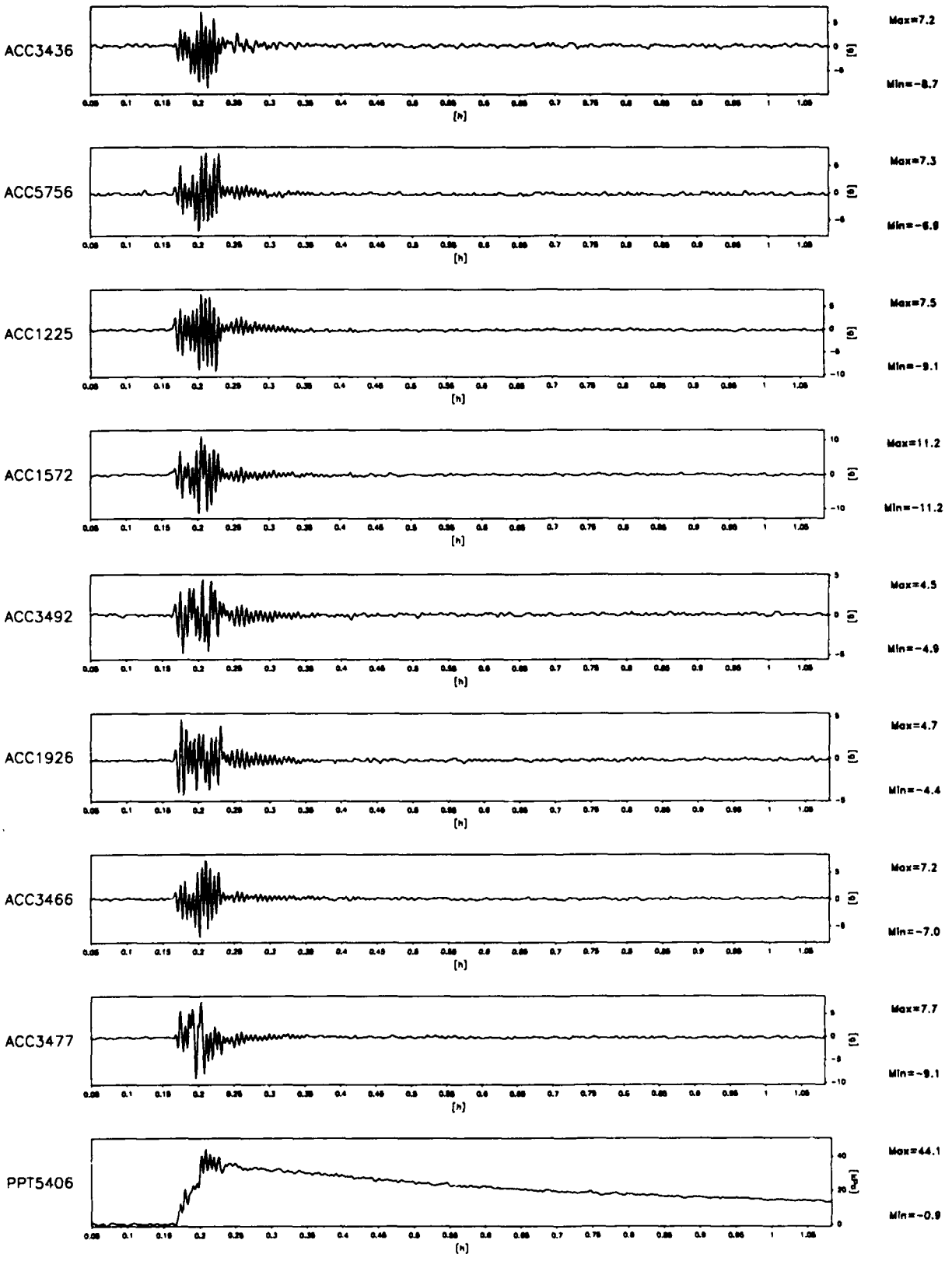

Scales : Prototype

TEST LEG-4 MODEL SAT FLIGHT -1	EQ-4	LONG TERM TIME RECORDS	G Level 80	FIG.NO. 11.31

930 datapoints plotted per complete transducer record

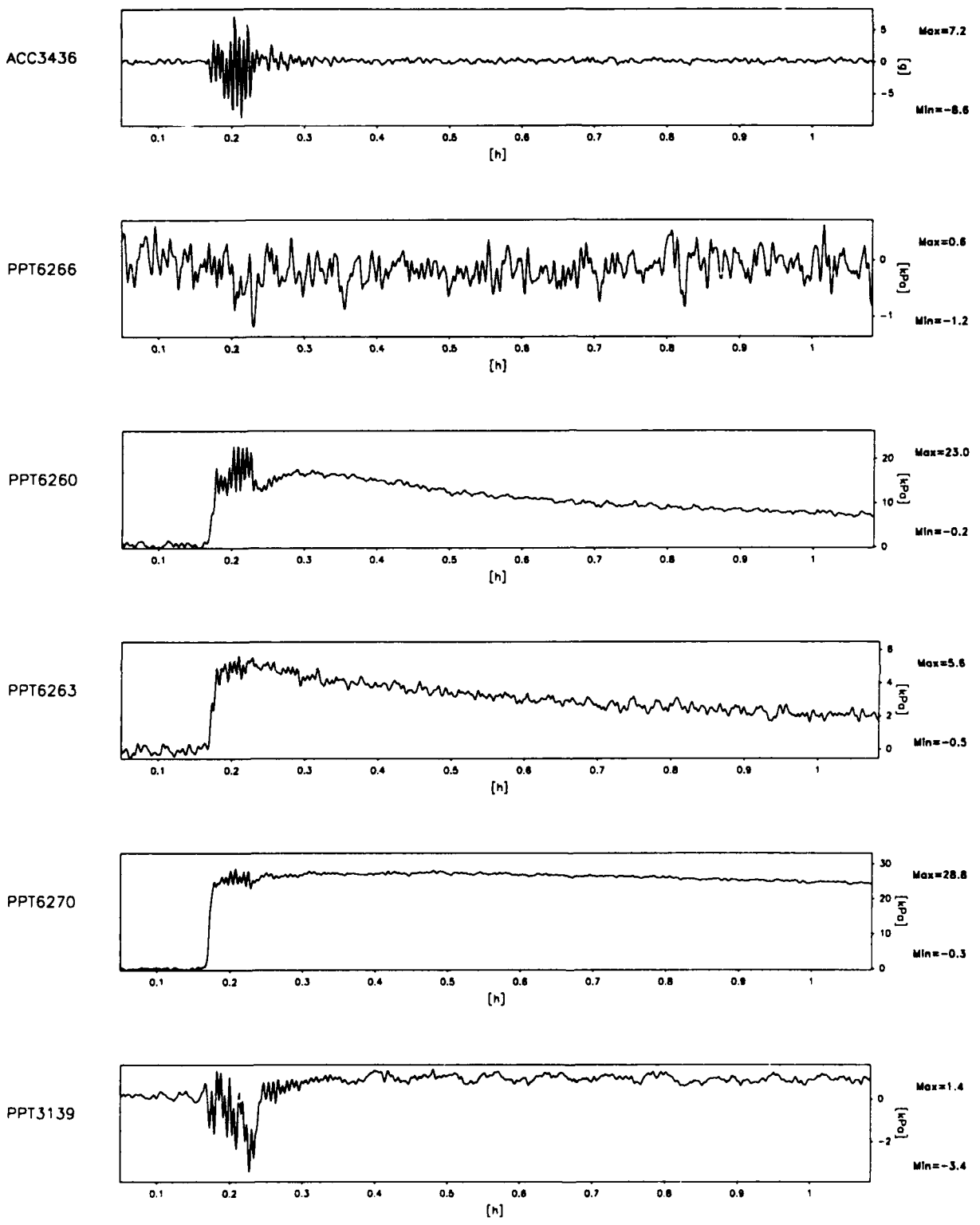

Scales : Prototype

TEST LEG-4 MODEL SAT FLIGHT -1	EQ-4	LONG TERM TIME RECORDS	G Level 80	FIG.NO. **11.32**

931 datapoints plotted per complete transducer record

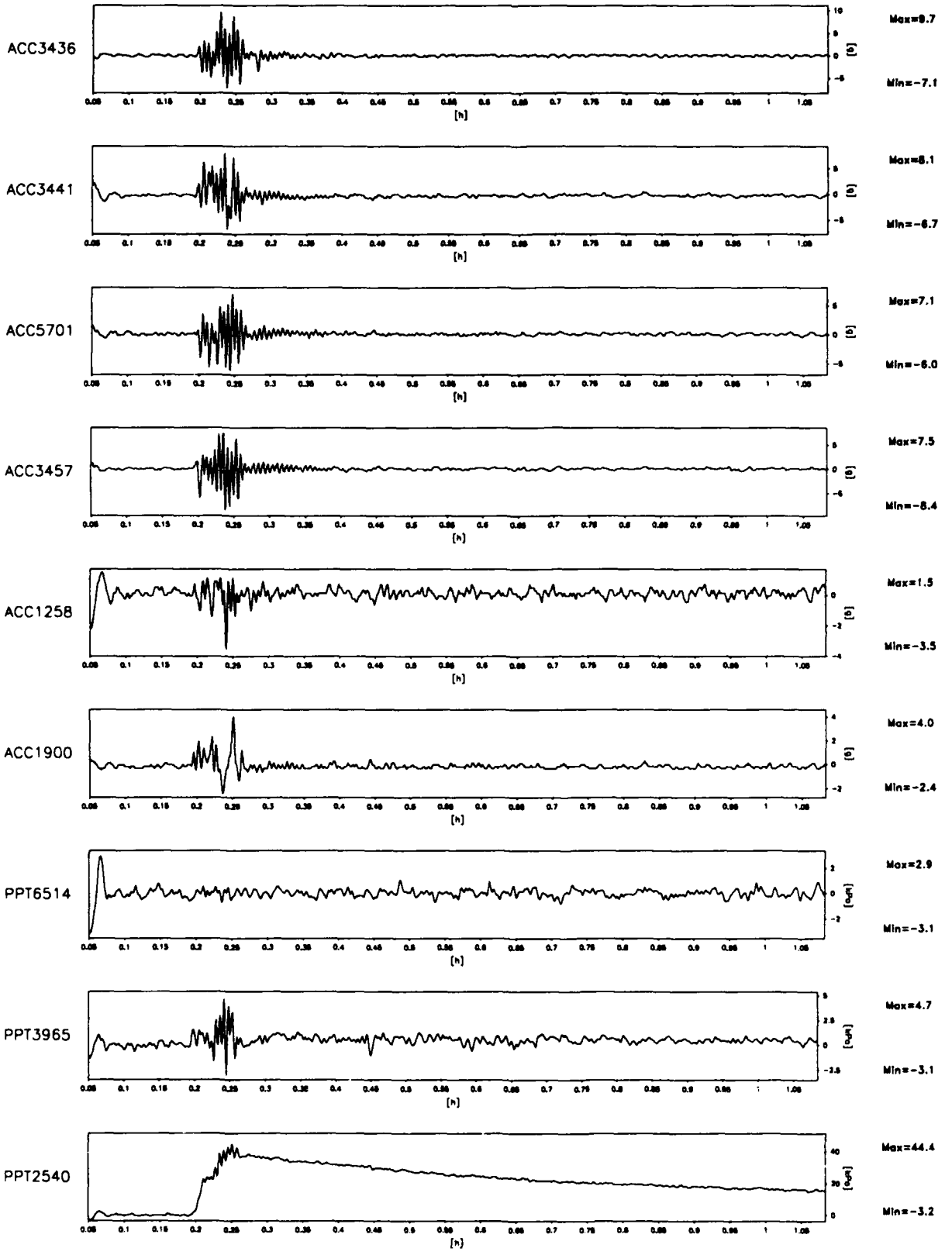

Scales : Prototype

TEST LEG-4 MODEL SAT FLIGHT -1	EQ-4	LONG TERM TIME RECORDS	G Level 80	FIG.NO. 11.33

931 datapoints plotted per complete transducer record

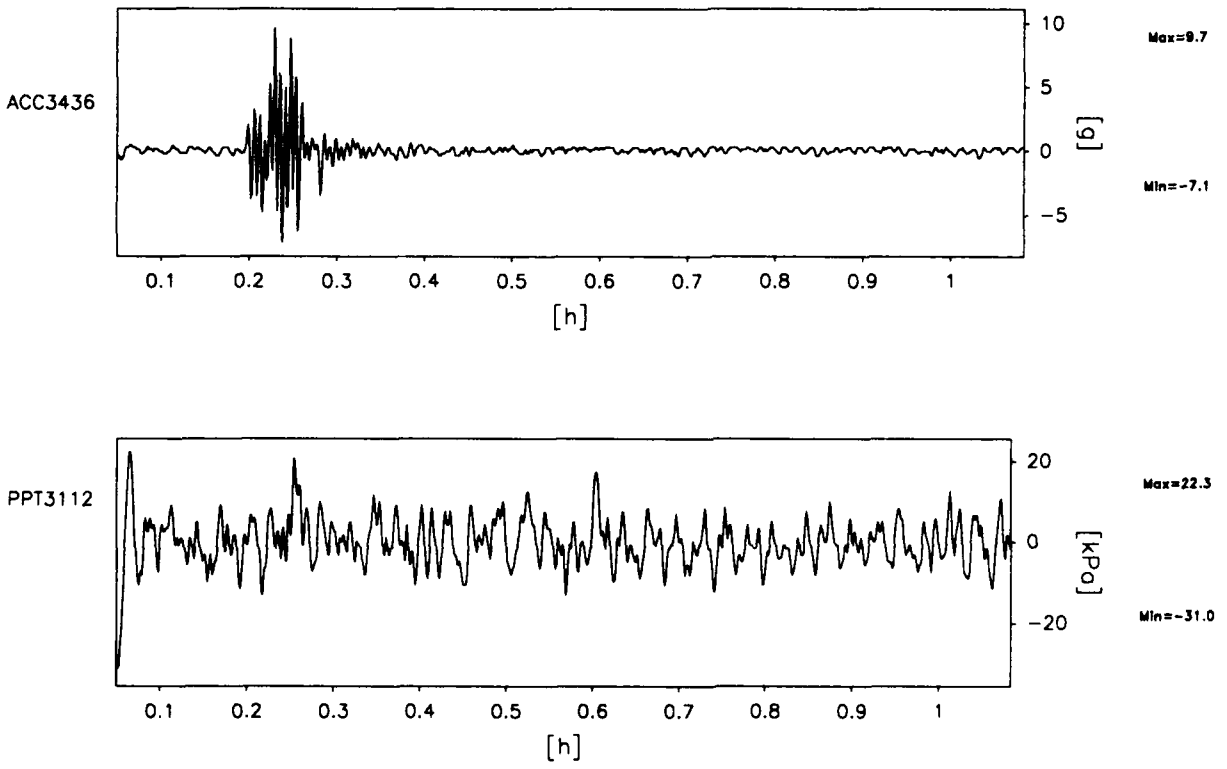

Scales : Prototype

TEST LEG−4 MODEL SAT FLIGHT −1	EQ−4	LONG TERM TIME RECORDS	G Level 80	FIG.NO. 11.34

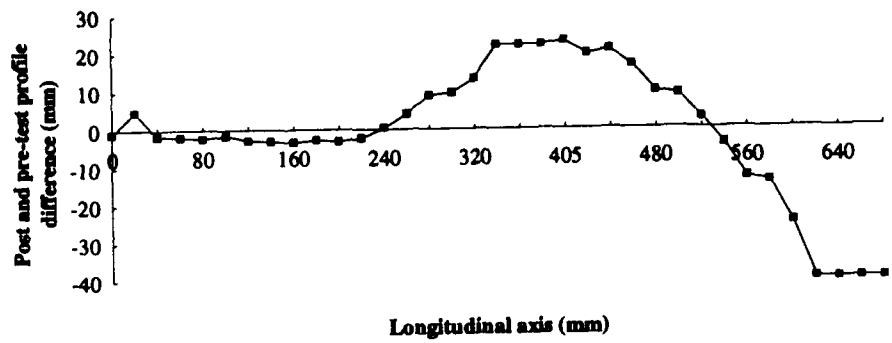

Fig.11.37 Post and pre-test profile difference along the longitudinal axis in centrifuge test LEG-4

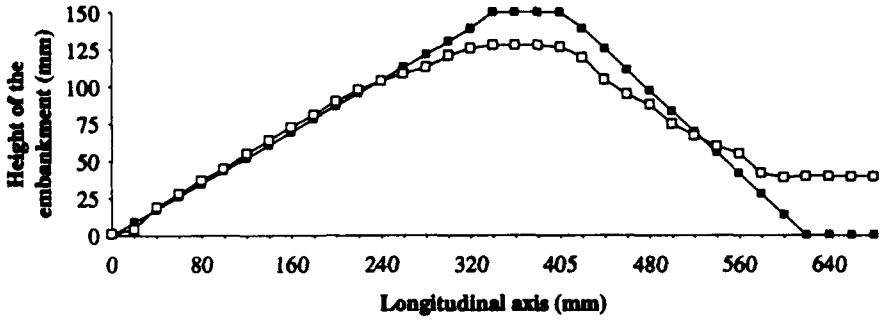

Fig.11.35 Post test profile of centrifuge model LEG-4

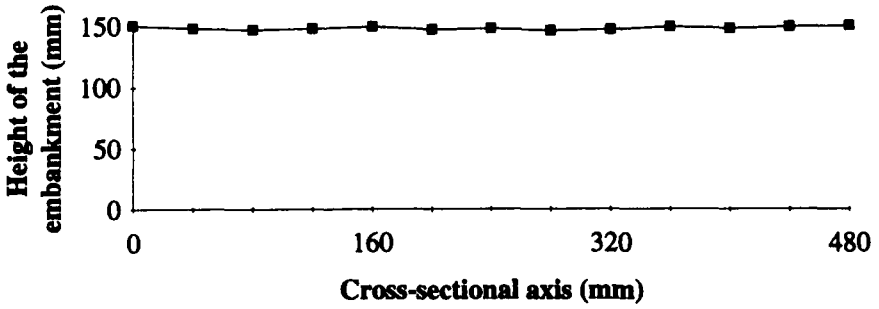

Fig.11.36 Post test profile along the cross section of centrifuge model LEG-4

12 Summary

Four dynamic centrifuge tests were conducted on model embankments with confined loose soil zones. In this series of centrifuge tests the loose confined layer was inclined and was located on the steeper slope side of the embankment. The steeper slope of the embankment was used to give a factor of safety similar to that of the flatter down stream slope of an equivalent prototype embankment with outward seepage. In the first centrifuge test LEG-1 the loose layer was inclined but the excess pore pressures generated during the earthquake loading dissipated rapidly. There was some settlement of the crest of the embankment and slipping of the down stream slope. In the subsequent centrifuge tests the inclined loose layer was confined by placing impermeable rock flour layer at the top and bottom interfaces. As a result of this the excess pore pressures were sustained for a much longer duration. In all the centrifuge tests the down stream slope suffered slipping while the up stream slope was more or less intact. The acceleration traces recorded by the accelerometers on the down stream slope confirmed this and showed a strong peak acceleration in one direction. The accelerometers on the up stream slope recorded uniform peaks in both +ve and -ve directions indicating that this side of the embankment did not suffer any slipping. The pore pressures recorded in the crest and base of the embankment showed strong suction pressures indicating the dilation of these zones. In the loose zone excess pore pressures were registered by the PPT's. The post test profiles measured after the test revealed a slip surface almost always originating from the top point of the loose layer.

The profile of the embankment was measured before and after each centrifuge test. Using this data the volume of soil suffering slipping was estimated. By comparing these results for the first two centrifuge tests which had similar geometry but with unconfined and confined loose layers it may be observed that the presence of confined loose layer resulted in a larger volume of soil movement. The third and fourth tests had a soil movement larger than the first test but smaller than the second test. This may be expected as the angle of inclination of the confined layer was flatter in these two tests compared with the second test.

Acknowledgements

The author wishes to acknowledge the advice given by Dr.Malcolm Bolton at various stages of this work. The excellent technical support given by Mr.Chris Collison, Mr.Neil Baker and Mr.Paul Ford are gratefully acknowledged.

References

Global Lab User Manual, (1991), Data Translation Inc., Marlboro, MA 01752-1192, USA.

Kutter, B.L., (1982),'Centrifugal modelling of the response of clay embankments to earthquakes', Ph.D. thesis, Cambridge University, England.

Schofield, A.N., (1980), 'Cambridge Geotechnical Centrifuge Operations', Geotechnique, Vol.25.,No.4, pp 743-761.

Steedman,R.S. and Madabhushi,S.P.G., (1992), Earthquake-induced liquefaction of confined soil zones: A centrifuge study (I series), ANS&A report No: 26-04-R-03.